

Some pages of this thesis may have been removed for copyright restrictions.

If you have discovered material in Aston Research Explorer which is unlawful e.g. breaches copyright, (either yours or that of a third party) or any other law, including but not limited to those relating to patent, trademark, confidentiality, data protection, obscenity, defamation, libel, then please read our [Takedown policy](#) and contact the service immediately (openaccess@aston.ac.uk)

**BIOMATERIAL INTERACTIONS WITH
COMPROMISED TISSUE SURFACES**

Manpreet Kaur Cooner

Doctor of Philosophy

ASTON UNIVERSITY

September 2014

© Manpreet Kaur Cooner, 2014

Manpreet Kaur Cooner asserts her moral right to be identified as the author of this thesis

This copy of this thesis has been supplied on condition that anyone who consults it is understood to recognise that its copyright rests with its author and that no quotation from this thesis and no information derived from it may be published without proper acknowledgement.

ASTON UNIVERSITY

Biomaterial Interactions with Compromised Tissue Surfaces

Manpreet Kaur Cooner

Doctor of Philosophy, September 2014

This thesis is concerned with the nature of biomaterial interactions with compromised host tissue sites. Both ocular and dermal tissues can be wounded, following injury, disease or surgery, and consequently require the use of a biomaterial. Clear analogies exist between the cornea/tear film/contact lens and the dermal wound bed/wound fluid/skin adhesive wound dressing. The work described in this thesis builds upon established biochemistry to examine specific aspects of the interaction of biomaterials with compromised ocular and dermal tissue sites, with a particular focus on the role of vitronectin.

Vitronectin is a prominent cell adhesion glycoprotein present in both tear fluid and wound fluid, and has a role in the regulation and upregulation of plasmin. The interaction of contact lenses with the cornea was assessed by a novel on-lens cell-based vitronectin assay technique. Vitronectin mapping showed that vitronectin-mediated cell adhesion to contact lens surfaces was due to the contact lens-corneal mechanical interaction rather than deposition out of the tear film. This deposition is associated predominantly with the peripheral region of the posterior contact lens surface. The locus of vitronectin deposition on the contact lens surface, which is affected by material modulus, is potentially an important factor in the generation of plasmin in the posterior tear film.

Use of the vitronectin mapping technique on *ex vivo* bandage contact lenses revealed greater vitronectin-mediated cell adhesion to the contact lens surfaces in comparison to lenses worn in the healthy eye. The results suggest that vitronectin is more readily deposited from the impaired corneal tissue bed than the intact healthy tissue bed. Significantly, subjects with a deficient tear film were found to deposit high vitronectin-mediated cell adhesion levels to the BCL surface, thus highlighting the influence of the contact lens-tissue interaction upon deposition.

Biomimetic principles imply that adhesive materials for wound applications, including hydrogels and hydrocolloids, should closely match the surface energy parameters of skin. The surface properties of hydrocolloid adhesives were found to be easily modified by contact with siliconised plastic release liners. In contrast, paper release liners did not significantly affect the adhesive surface properties. In order to characterise such materials in the actual wound environment, which is an extremely challenging task, preliminary considerations for the design of an artificial wound fluid model from an animal serum base were addressed.

Key phrases: bandage contact lens; hydrocolloid; hydrogel; skin adhesive wound dressings; vitronectin; wound healing.

For my Mum

ACKNOWLEDGEMENTS

I would first and foremost like to express my gratitude to my supervisor Professor Brian Tighe. Without his constant guidance, patience, enthusiasm and encouragement, this research would not have been possible. I am extremely grateful for the many opportunities to attend conferences, particularly in Madrid, and numerous retreats with the group.

I thank EPSRC and Salts Healthcare for their financial support during the duration of my work. In particular, I would like to thank Richard Darwood for supplying the adhesive materials used for testing within this work. I must also extend my gratitude to Professor Martin Rubinstein for supplying bandage contact lenses and for the many useful and interesting discussions centring ocular healing and treatment.

I am grateful to all members of the Biomaterials Research Unit, past and present, who have made my time with the group a really happy one. I would especially like to thank Dr Aisling Mann for always guiding me along the way and for digging me out of more holes than I can remember!

A big thank you to all the office family for the belly laughs, food and fun... who could forget the abseil! Thanks to my good friends Aman, Mani, Sukhi and Sukh for the moral support and always providing entertainment.

Last, but by no means least, I thank my brothers, Sandeep and Amar, Sabrina, my granddad and my mum. I am lucky to have friends who are such an amazing support system and a loving family at home.

LIST OF CONTENTS

Content	Page Number
TITLE PAGE	1
SUMMARY	2
DEDICATION	3
ACKNOWLEDGEMENTS	4
LIST OF CONTENTS	5
LIST OF TABLES	13
LIST OF FIGURES	16
ABBREVIATIONS AND NOTATIONS	21
Chapter One - Introduction	23
1.1 Introduction	24
1.2 The Ocular/Dermal Wound Healing Analogy	25
1.3 Dermal Wound Healing	26
1.3.1 Anatomy of Skin	26
1.3.1.1 The Hypodermis	27
1.3.1.2 The Dermis	27
1.3.1.3 The Epidermis	28
1.3.2 Aging Skin	29
1.3.3 The Dermal Wound Healing Process	31
1.3.4 Wound Chronicity	33
1.3.5 Cell Adhesion Molecules in Wound Healing	34
1.3.5.1 The Importance of Cell Adhesion Molecules	34
1.3.5.2 Vitronectin – Structure, Roles and Functions	35
1.3.5.3 The Interaction of Vitronectin with Synthetic Materials	36
1.4 Dermal Wound Dressings	37
1.4.1 The Ideal Wound Dressing	37
1.4.2 Skin Adhesive Hydrogels	39
1.4.3 Skin Adhesive Hydrocolloids	40
1.4.3.1 Hydrocolloids for Wound Dressings	40
1.4.3.2 Hydrocolloids for Ostomy Devices	42

1.4.4	Adhesion in Relation to Skin Adhesive Hydrogels and Hydrocolloids	43
1.4.4.1	Adhesion Mechanism	43
1.4.4.2	Properties of Adhesives	44
1.5	Ocular Wound Healing	45
1.5.1	Anatomy of the Eye	45
1.5.1.1	The Cornea	45
1.5.2	Wounding of Ocular Tissue	48
1.5.3	The Corneal Wound Healing Process	49
1.5.3.1	Corneal Epithelium Wound Healing	49
1.5.3.2	Corneal Stromal Epithelium Wound Healing	52
1.6	Ocular Wound Dressings	53
1.6.1	The Role of Bandage Contact Lenses	53
1.6.2	Advances in Contact Lens Materials for Therapeutic Use	53
1.6.3	Protein Adsorption	55
1.6.3.1	General Structure of Proteins	55
1.6.3.2	Principles of Protein Adsorption to Biomaterial Substrates	56
1.6.3.3	Protein Adsorption to Bandage Contact Lenses	59
1.7	Aims of Research	60
Chapter Two – Materials and Experimental Technique		62
2.1	Materials	63
2.1.1	Contact Lens Materials	63
2.1.2	Skin Adhesive Wound Dressing Materials	66
2.1.2.1	Hydrocolloid Materials Supplied by Salts Healthcare	66
2.1.2.2	Other Skin Adhesive Materials	69
2.2	Experimental Techniques	70
2.2.1	Cell Culture	70
2.2.1.1	Materials	70
2.2.1.2	Isolation and Culture	71
2.2.1.3	Determination of Cell Viability	71
2.2.1.4	Passage of Cells	71
2.2.1.5	In Vitro Doping of Contact Lenses	72
2.2.1.6	Ex Vivo Contact Lenses	72

2.2.1.7	On-Lens Cell Attachment Assay Procedure	72
2.2.2	Schirmer Test	74
2.2.3	Preparation of Skin Adhesive Hydrogels	75
2.2.3.1	Materials	75
2.2.3.2	Preparation of Skin Adhesive Hydrogels Method	76
2.2.4	Surface Energy Measurements	77
2.2.4.1	Materials	78
2.2.4.2	The Sessile Drop Technique	78
2.2.5	X-ray Photoelectron Spectroscopy	80
2.2.6	Peel Strength	81
2.2.7	Tensile Strength	83
2.2.8	Dynamic Testing	85
2.2.9	Total Protein Method	86
2.2.9.1	Materials	86
2.2.9.2	Preparation of Diluted Albumin Standards	86
2.2.9.3	Preparation of the Micro BCA Working Reagent (WR)	86
2.2.9.4	Total Protein Determination	87
2.2.10	Osmolarity Measurements	87
 Chapter Three – The Nature and Consequences of Vitronectin Interactions in the Non-Compromised Contact Lens-Wearing Eye		88
3.1	Aim	89
3.2	Introduction	89
3.2.1	Introduction	89
3.2.2	Vitronectin in Tears	90
3.3	Method Validation - <i>In Vitro</i> Demonstration of the On-Lens Cell Attachment Assay for the Detection of Vitronectin-Mediated Cell Adhesion	91
3.3.1	Assessment of the Contributory Role of Vitronectin	91
3.3.2	Assessment of the Contributory Role of Fibronectin	92
3.3.3	Discussion	94
3.3.4	Key Points for Cell Assay Method Validation	94
3.4	The Effect of Protein Concentration on Vitronectin-Mediated Cell Adhesion	94
3.4.1	<i>In Vitro</i> Doping Experiments – Varying Protein Concentration	94

3.4.2	Discussion	95
3.4.3	Key Points for the Effect of Protein Concentration on Vitronectin-Mediated Cell Adhesion	96
3.5	The Influence of Contact Lens Water Content and Ionicity on Vitronectin-Mediated Cell Adhesion	96
3.5.1	<i>In Vitro</i> Doping Experiments – Varying Contact Lens Water Content and Ionicity	96
3.5.2	Discussion	98
3.5.3	Key Points for the Influence of Contact Lens Water Content and Ionicity on Vitronectin-Mediated Cell Adhesion	98
3.6	Vitronectin-Mediated Cell Adhesion to Anterior and Posterior Surfaces of <i>ex vivo</i> Contact Lenses in Daily Wear and Extended Wear Modalities	99
3.6.1	<i>Ex vivo</i> Contact Lenses - Anterior versus Posterior and Daily Wear versus Extended Wear	99
3.6.2	Discussion	100
3.6.3	Key Points for the Analysis of Anterior versus Posterior and for Daily Wear versus Extended Wear on <i>Ex Vivo</i> Contact Lenses	100
3.7	Vitronectin-Mediated Cell Adhesion to <i>ex vivo</i> Daily Wear Contact Lenses - Centre versus Edge	101
3.7.1	<i>Ex Vivo</i> Contact Lenses – Centre versus Edge	101
3.7.2	Discussion	102
3.7.3	Key Points for Vitronectin-Mediated Cell Adhesion to the Contact Lens Centre versus the Lens Edge	103
3.8	Investigating Contact Lens Material Variation	103
3.8.1	The Effect of Contact Lens Modulus on Vitronectin-Mediated Cell Adhesion	103
3.8.2	Discussion	105
3.8.3	Key Points for the Influence of Contact Lens Modulus on Vitronectin-Mediated Cell Adhesion	106
3.9	Concluding Discussion	106
3.9.1	Vitronectin-Mediated Cell Adhesion Due to Contact Lens-Tissue Interaction	106
3.9.2	Vitronectin and Tear Plasmin Activity	107
3.9.3	Potential for Further Work	108

3.10	Chapter Summary	109
Chapter Four – The Investigation of the Locus and Extent of Vitronectin Deposition on Bandage Contact Lenses		110
4.1	Aim	111
4.2	Introduction	111
4.3	Methods	112
4.3.1	Contact Lens Materials	112
4.3.2	Study Population for Bandage Contact Lens Wearers	112
4.3.3	Assay Procedure	115
4.4	A Comparison between Vitronectin-Mediated Cell Adhesion to <i>ex vivo</i> Contact Lenses Worn in the Healthy Contact Lens-Wearing Eye and the Bandage Contact Lens-Wearing Eye	115
4.4.1	Non-Compromised versus Compromised Eye	115
4.4.2	Discussion	116
4.5	The Influence of Wear Duration on Vitronectin-Mediated Cell Adhesion	117
4.5.1	The Effect of Wear Duration on Vitronectin-Mediated Cell Adhesion to <i>ex vivo</i> Contact Lenses Worn in the Healthy Contact Lens-Wearing Eye	117
4.5.2	The Effect of Wear Duration on Vitronectin-Mediated Cell Adhesion to <i>ex vivo</i> Contact Lenses Worn in the Bandage Contact Lens-Wearing Eye	118
4.5.2.1	Discussion	121
4.5.3	The Effect of Wear Duration on Vitronectin-Mediated Cell Adhesion: One Day Healthy CL-wearing Non-Compromised Eye versus One Day BCL-wearing Compromised Eye	122
4.5.3.1	Discussion	123
4.5.4	The Effect of Wear Duration on Vitronectin-Mediated Cell Adhesion: Four Week Wear Duration	123
4.5.4.1	Discussion	124
4.5.5	Key Points for the Influence of Wear Duration on Vitronectin-Mediated Cell Adhesion	125
4.6	The Influence of Contact Lens Material on Vitronectin-Mediated	125

Cell Adhesion in the Bandage Contact Lens-Wearing Eye	
4.6.1 Biofinity versus UltraWave SiH	125
4.6.2 Discussion	127
4.6.3 Key Points for the Influence of Contact Lens material Type on Vitronectin-Mediated Cell Adhesion	129
4.7 A Comparison Between Vitronectin-Mediated Cell Adhesion to <i>ex vivo</i> Biofinity Contact Lenses Worn for the Management of Bullous Keratopathy or Sjögren’s Syndrome	129
4.7.1 Bullous Keratopathy versus Sjögren’s Syndrome	129
4.7.2 Discussion	138
4.7.3 Key Points – Bullous Keratopathy versus Sjögren’s Syndrome	139
4.8 Concluding Discussion	140
4.9 Chapter Summary	143
Chapter Five – Surface and Mechanical Properties of Skin Adhesive Wound Healing Materials	144
5.1 Aim	145
5.2 Introduction	145
5.3 Materials	146
5.3.1 Skin Adhesive Materials	146
5.3.1.1 Overview of Skin Adhesive Materials	146
5.3.1.2 Hydrocolloids	147
5.3.1.3 Hydrogels	149
5.3.1.4 Medical Tapes	150
5.3.2 Release Liner Materials	150
5.4 Surface Properties of Skin Adhesive Materials	151
5.4.1 Surface Energy Measurements for a Range of Skin Adhesive Materials	151
5.4.1.1 Discussion	152
5.4.2 A Comparison Between Release Liners and Their Effect on Hydrocolloid Adhesive Surface Properties – Paper versus Plastic	154
5.4.2.1 Discussion	155
5.4.3 Quantifying Silicon on the Adhesive Surface – X-Ray Photoelectron Spectroscopy	156

5.4.3.1	Discussion	159
5.4.4	Removal of Silicone from the Adhesive Surface	160
5.4.4.1	Discussion	161
5.4.5	Key Points for the Surface Properties of Skin Adhesive Materials	161
5.5	Peel Strength Analysis of Skin Adhesive Materials	163
5.5.1	Peel Strength Measurements of Skin Adhesive Wound Dressing and Medical Tape Materials	163
5.5.1.1	Discussion	166
5.5.2	Pain Scores for Skin Adhesive Wound Dressing and Medical Tape Materials	167
5.5.3	Correlations Between Adhesive Peel Strengths, Pain Scores and Surface Energies	168
5.5.3.1	Discussion	169
5.5.4	Key Points for the Peel Strength Analysis of Skin Adhesive Materials	170
5.6	Tensile Strength Analysis of Skin Adhesive Materials	170
5.6.1	Tensile Strength Measurements of Skin Adhesive Wound Dressing and Medical Tape Materials	170
5.6.1.1	Discussion	171
5.6.2	Key Points for the Tensile Analysis of Skin Adhesive Materials	172
5.7	Dynamic Testing of Skin Adhesive Materials	172
5.7.1	Rheology Measurements of Skin Adhesive Wound Dressing and Medical Tape Materials	172
5.7.1.1	Discussion	174
5.7.2	Key Points for the Dynamic Testing of Skin Adhesive Materials	175
5.8	Concluding Discussion	175
5.8	Chapter Summary	177
Chapter Six – Towards the Design of an Artificial Wound Fluid Model		179
6.1	Aim	180
6.2	Introduction	180
6.3	Tear Fluid Models	182
6.3.1	The Tear Film – Function and Composition	182
6.3.2	Artificial Tear Fluid Models	184
6.3.2.1	Tear Substitutes	184

6.3.2.2 The Need for Artificial Tear Fluid Models to Study in vitro	186
Biomaterial Interactions with Biological Fluids	
6.4 Artificial Wound Fluid Models	188
6.4.1 Wound Fluid – Function and Composition	188
6.4.1.1 Acute Wound Fluid versus Chronic Wound Fluid	189
6.4.2 An Overview of Artificial Wound Fluid Models in Literature for	193
Biomaterial Design and Investigations	
6.4.3 Fetal Bovine Serum for Preliminary Considerations of an Artificial	196
Chronic Wound Fluid Model	
6.5 Proposals for the Design of Standard Artificial Wound Fluid Models	198
6.6 Overall Discussion	201
Chapter Seven – Conclusions and Suggestions for Further Work	204
7.1 Introduction	205
7.2 Interactions of Vitronectin with the Non-Compromised Eye	205
7.3 Interactions of Vitronectin with the Compromised Bandage	207
Contact Lens-Wearing Eye	
7.4 Investigation of the Surface and Mechanical Properties of Skin Adhesive	209
Materials	
7.5 Considerations for the Design of an Artificial Wound Fluid Model	212
7.6 Suggestions for Further Work	213
References	216
Appendices	229
APPENDIX 1 – Fetal Bovine Serum Specification	230

LIST OF TABLES

Table		Page Number
Table 1.1	A summary of the changes that occur with aging in human skin (adapted from Gosain and DiPietro [14]).	30
Table 1.2	A summary of the diverse functions of vitronectin.	35
Table 1.3	FDA approved silicone hydrogel contact lenses for bandage lens use.	55
Table 1.4	The effect of substrate surface functional group on preferential protein adsorption (adapted from Thevenot <i>et al</i> [93]).	58
Table 2.1	Daily disposable conventional hydrogel contact lenses and their properties.	63
Table 2.2	Silicone hydrogel contact lenses and their properties.	64
Table 2.3	Monomer structures of the principle components of contact lens materials.	65
Table 2.4	Skin adhesive wound dressing materials supplied by Salts Healthcare.	66
Table 2.5	Commercial skin adhesive ostomy, hydrocolloid and medical tapes, and hydrogels prepared in the laboratory.	69
Table 2.6	Chemicals and immunochemicals used with name, abbreviation and supplier.	70
Table 2.7	Compositions of skin adhesive hydrogels – Hydrogel 1 and Hydrogel 2.	77
Table 2.8	The surface free energy data for water and diiodomethane.	78
Table 2.9	Preparation of bovine serum albumin (BSA) standards.	86
Table 3.1	The relationship between edge:centre ratio and contact lens modulus.	104
Table 4.1	Properties and characteristics of the two contact lens materials studied; Biofinity and UltraWave SiH.	112
Table 4.2	Patient information for the subject population of bandage contact lens wearers (n=15).	114
Table 4.3	Patient information for subjects requiring Biofinity bandage contact lenses for the management of bullous keratopathy.	132

Table 4.4	Patient information for subjects requiring Biofinity bandage contact lenses for the management of Sjögren’s syndrome (SS).	133
Table 5.1	Five skin adhesive material groups used for investigations.	147
Table 5.2	Compositions of the Salts Hydrocolloid Adhesives group for wound dressings.	148
Table 5.3	Compositions of skin adhesive hydrogels synthesised in-house: Hydrogel 1 and Hydrogel 2.	150
Table 5.4	Average surface energy measurements (derived from contact angle measurements with water and diiodomethane probe liquids) for a range of commercial and non-commercial skin adhesive materials.	152
Table 5.5	Surface energy values for the contact side and non-contact side of release liners RL1-paper and RL2-plastic before application to adhesives.	155
Table 5.6	A comparison between surface energy values of two Salts Hydrocolloid Adhesives with the same composition, but different release liner materials: S1 and S3.	155
Table 5.7	Photoelectron spectroscopy results for the detection of silicon on the surface of Salts Hydrocolloid Adhesives (S1-S4) after the release liners are removed. Values for the paper (RL1) and plastic (RL2) release liners are also provided.	157
Table 5.8	Surface energy values for Salts Hydrocolloid Adhesives S1 and S3, before and after the treatment of acetone to remove silicone from the adhesive surfaces	161
Table 5.9	Peel strength measurements of skin adhesive wound dressings and medical tapes at 90° and 180° on steel and skin test substrates.	164
Table 5.10	Pain scores for skin adhesive wound dressing and medical tape materials	167
Table 5.11	The correlation between adhesive peel strengths on skin at 90°, corresponding pain scores and surface energy data.	168
Table 5.12	Tensile strength measurements for a range of skin adhesive materials.	171

Table 5.13	Rheological measurements for skin adhesive materials tested at 0.5-25 Hz.	174
Table 5.14	Surface properties of human skin.	176
Table 6.1	Composition of the human tear fluid [135].	183
Table 6.2	The composition of the Aston Serum-based Tear Model developed by Franklin [142].	187
Table 6.3	The compositional comparison of healing wound fluid from acute wounds and non-healing wound fluid from chronic wounds [145].	190
Table 6.4	A comparison of acute wound fluid and chronic wound fluid in relation to healthy human serum [22, 143, 145-147, 152].	192
Table 6.5	The composition of artificial wound fluid produced by 3M Health Care [154].	194
Table 6.6	The composition of artificial wound fluid produced by Lutz <i>et al</i> in comparison to extracellular fluid and chronic wound fluid [155].	195
Table. 6.7	The comparison of compositions of different animal sera with human chronic wound fluid.	197

LIST OF FIGURES

Figure		Page Number
Figure 1.1	Cross section of skin morphology - the hypodermis, dermis and epidermis.	27
Figure 1.2	Phases of dermal wound healing.	32
Figure 1.3	Structures of hydrocolloid components: A) poly(isobutylene), B) carboxymethyl cellulose, C) gelatine, D) pectin.	41
Figure 1.4	Ostomy devices with hydrocolloid adhesives are available as: A) a one-piece system, B) a two-piece system.	42
Figure 1.5	Cross section of the human eye.	45
Figure 1.6	Five layers of the cornea with the recently discovered sixth layer, and the pre-corneal tear film.	46
Figure 1.7	The corneal epithelium wound healing process.	51
Figure 1.8	The corneal stromal wound healing process.	52
Figure 1.9	The general structure of an amino acid monomer.	56
Figure 2.1	The repeat structure of poly(isobutylene).	67
Figure 2.2	The repeat structure of carboxymethyl cellulose.	67
Figure 2.3	The structure of gelatine.	68
Figure 2.4	The repeat structure of pectin.	68
Figure 2.5	The on-lens cell attachment assay procedure for the location and quantification of surface-bound vitronectin on <i>ex vivo</i> or vitronectin-doped contact lenses.	73
Figure 2.6	Five defined areas on the posterior contact lens surface for recording cell counts (zones not to scale).	74
Figure 2.7	The Schirmer test for sampling of tear secretions.	75
Figure 2.8	The structure of sodium salt of 2-(acrylamido)-2-methyl propane sulfonate (NaAMPs.)	75
Figure 2.9	The structure of potassium salt of 3-sulfopropyl acrylate (SPA).	75
Figure 2.10	The structure of Irgacure 184.	76
Figure 2.11	The structure of glycerol.	76
Figure 2.12	A droplet of probe liquid forming a contact angle with a solid surface.	79

Figure 2.13	Contact angle hysteresis.	80
Figure 2.14	Photoelectron spectroscopy - excitation of electrons to emit photoelectrons by photoemission.	81
Figure 2.15	A representation of the peel test set-up at: A) 90° and B) 180°.	83
Figure 2.16	Dimensions of an adhesive samples for tensile testing.	84
Figure 2.17	A representation of the tensile strength test set-up.	84
Figure 2.18	A concentration curve for bovine serum albumin standards at 0-1000 µg/mL.	87
Figure 3.1	Cell counts on polyHEMA contact lenses doped with 20 µg/ml vitronectin in vitro.	92
Figure 3.2	Cell counts on polyHEMA contact lenses doped with 20 µg/ml fibronectin in vitro.	93
Figure 3.3	The relationship between vitronectin-mediated cell adhesion and concentration of the vitronectin doping solution.	95
Figure 3.4	The relationship between vitronectin-mediated cell adhesion and: A) contact lens water content, B) contact lens ionicity.	97
Figure 3.5	Cell counts on the anterior and posterior surfaces of etafilcon A contact lenses worn on both daily wear and extended wear basis.	99
Figure 3.6	Cell counts on the centre and edge areas of the posterior surface of <i>ex vivo</i> Group II and Group IV contact lenses worn on a daily wear basis.	101
Figure 3.7	Cells on the posterior surface of the contact lens edge of a Group IV <i>ex vivo</i> etafilcon A material. The high cell counts at the lens edge are apparent.	102
Figure 3.8	Vitronectin-mediated cell adhesion to <i>ex vivo</i> contact lenses worn on a daily wear basis averaging 8 hours over 1 day, where n=8.	104
Figure 3.9	The relationship between vitronectin-mediated cell adhesion and contact lens modulus; the lower the material modulus the greater the cell adhesion at the lens edge.	105

Figure 4.1	A flowchart to show contact lens material and clinical condition information for the study population of bandage contact lens wearers.	113
Figure 4.2	A comparison of cell counts on <i>ex vivo</i> Biofinity bandage contact lenses (BCLs) (n=11) and UltraWave SiH BCLs (n=4) worn in the compromised eye. Biofinity lenses (n=6) worn by a subgroup of healthy contact lens-wearers (CL wear) are also shown for comparison.	116
Figure 4.3	Comparative average cell count data on the posterior surface of <i>ex vivo</i> Biofinity contact lenses (1 day wear schedule, n=6) and <i>ex vivo</i> Biofinity contact lenses (5 day daily wear schedule, n=6) in the healthy contact lens-wearing eye.	118
Figure 4.4	Comparative average cell count data from 5 fields for <i>ex vivo</i> UltraWave SiH bandage contact lenses (n=4) and Biofinity bandage contact lenses (n=11). Lenses were worn for durations ranging from 1 day daily wear to 8 weeks continuous wear.	119
Figure 4.5	The effect of wear duration of bandage contact lenses on cell counts to: A) Biofinity lenses (n=11) and B) UltraWave SiH lenses (n=4). Bandage contact lenses were worn by subjects over differing wear durations ranging from 1 day to 8 weeks.	120
Figure 4.6	A comparison of average cell counts on Biofinity contact lenses worn in the non-compromised eye (n=6) with a Biofinity bandage contact lens worn in the compromised eye (n=1). All contact lenses were worn for 8 hours.	122
Figure 4.7	Cell count data for <i>ex vivo</i> Biofinity bandage contact lenses worn by five subjects for the management of bullous keratopathy (n=5). All lenses were worn for four weeks.	124
Figure 4.8	The effect of contact lens material type on the locus of vitronectin mediated-cell adhesion. The locus of cell adhesion (contact lens centre and lens edge) is shown for <i>ex vivo</i> Group II Biofinity bandage contact lenses (n=11) and for <i>ex vivo</i> Group IV UltraWave SiH bandage contact lenses (n=4).	126

Figure 4.9	The relationship between bandage contact lens (BCL) wear duration and the edge:centre cell count ratio. Data is provided for Biofinity contact lenses (n=11) and UltraWave SiH contact lenses (n=4).	127
Figure 4.10	Corneal oedema and the formation of bullae in bullous keratopathy [126].	130
Figure 4.11	Possible symptoms of Sjögren's Syndrome.	131
Figure 4.12	A comparison of the locus of cell adhesion on <i>ex vivo</i> Biofinity bandage contact lenses worn for the management of Sjögren's Syndrome (n=3, contact lens wear duration: 3-6 weeks) and for the management of bullous keratopathy (n=6,contact lens wear duration: 2-4 weeks).	134
Figure 4.13	The locus of cell adhesion (contact lens centre and lens edge) on <i>ex vivo</i> Biofinity bandage contact lenses worn for the management of bullous keratopathy (n=6). Lenses were worn from 2-6 weeks.	136
Figure 4.14	The relationship between vitronectin-mediated cell adhesion and the edge:centre cell count ratio for <i>ex vivo</i> Biofinity bandage contact lenses worn for the management of bullous keratopathy (n=6).	136
Figure 4.15	The locus of cell adhesion (contact lens centre and lens edge) on <i>ex vivo</i> Biofinity bandage contact lenses worn for the management of Sjögren's Syndrome (n=3). Lenses were worn from 3-6 weeks.	137
Figure 5.1	The structure of poly(dimethylsiloxane).	151
Figure 5.2	A representation of the hydrocolloid system.	152
Figure 5.3	Silicon detected on the surface of adhesives S1 and S2 that had paper release liners and of Salts Hydrocolloid Adhesives S3 and S4 that had plastic release liners.	158
Figure 5.4	Silicon detected on the surface of paper and plastic release liners removed from Salts Hydrocolloid Adhesives.	158
Figure 5.5	The peel strength trace for Coloplast Ostomy at 90° on a skin test substrate, showing the maximum force of peel strength at	165

	1.6 N.	
Figure 5.6	Average maximum forces of peel strength (N) for various skin adhesive materials for three substrates - 90° skin, 90° steel and 180° steel.	166
Figure 5.7	The relationship between maximum force of peel strength (N) and pain scores.	169
Figure 5.8	The relationship between $\tan \delta$ and the maximum force of peel strength (N).	173
Figure 6.1	Cross-section of the tear film.	181
Figure 6.2.	A comparison between proteins concentrations of tear fluid and blood plasma of healthy subjects. Protein concentrations range from pg/ml to mg/l. (Adapted from Zhou <i>et al</i> [136]).	184
Figure 6.3	Changes in total protein concentration after material interaction with the fetal bovine serum-based artificial chronic wound fluid model.	199
Figure 6.4	Changes in osmolarity after material interaction with the fetal bovine serum-based artificial chronic wound fluid model.	200

ABBREVIATIONS AND NOTATIONS

Anti-Fn	anti-fibronectin	PIB	poly(isobutylene)
Anti-Vn	anti-vitronectin	PMCs	post mitotic cells
AWF	acute wound fluid	PMMA	poly(methyl methacrylate)
BCL	bandage contact lens	PRK	photorefractive keratectomy
BE	binding energy	PSA	pressure sensitive adhesive
BK	bullous keratopathy	PTK	phototherapeutic keratectomy
BSA	bovine serum albumin	RL1	release liner 1
CL	contact lens	RL2	release liner 2
CMC	carboxymethyl cellulose	S1-S4	Salts Hydrocolloid Adhesives 1-4
CWF	chronic wound fluid	SE	surface energy
ECM	extracellular matrix	SiHy	silicone hydrogel
EGF	epidermal growth factor	SS	Sjögren's syndrome
ESCA	electron spectroscopy for chemical analysis	TACs	transient amplifying cells
EWC	equilibrium water content	TDCs	terminally differentiated cells
FBS	fetal bovine serum	TGF-β	transforming growth factor-beta
FDA	Food and Drug Administration	TIMPs	tissue inhibitors of metalloproteinases
Fn	fibronectin	tPA	tissue plasminogen activator
KE	kinetic energy	UV	ultraviolet
LASIK	laser-assisted <i>in situ</i> keratomileusis	VEGF	vascular endothelial growth factor
LRI	Leicester Royal Infirmary	Vn	vitronectin
MMPs	matrix metalloproteinases	WK	Warwick Hospital
PAI-1	plasminogen activator inhibitor-1	WR	working reagent
PBS	phosphate buffered saline	XPS	X-ray photoelectron spectroscopy
PDGF	platelet-derived growth factor		

%	percent	mg/ml	milligram per millilitre
°	degree	mm	millimetre
°C	degrees Celcius	mM	millimolar
bn	billion	mm/minute	millimetre per minute
cm	centimetre	mmol/l	millimoles per litre
cm²	centimetre squared	mNm⁻¹	milliNewtons per metre
cm³	centimetre cubed	mOsm/kg	milliosmoles per kg
g	gram	MPa	megaPascal
g/l	grams per litre	N	Newton
Hz	Hertz	N/25mm	Newtons per 25 millimetres
kDa	kiloDalton	N/m²	Newton per metre squared
kg	kilogram	nm	nanometre
m	metre	pg/ml	pictogram per millilitre
m/min	metre per minute	rpm	rotations per minute
mEq/l	milliequivalent per litre	µg/ml	microgram per millilitre
mg/l	milligram per litre	µl	microlitre
		µm	micrometre
eΦ	spectrometer work function		
G'	elastic modulus		
G''	viscous modulus		
h	Planck's constant		
pI	isoelectric point		
pH	power of the concentration of hydrogen ions		
tan δ	tan δ		
v	photon frequency		
w/e	weight equivalent		

Please refer to Section 2.1.1 for the following monomers:

DMA, HEMA, MA, NCVE, NVP, PBVC, TPVC, TRIS

and Section 2.2.1 for the following chemicals and immunochemicals:

DMEM, EDTA, HBS, IgG, L-glu, MgCl₂

CHAPTER ONE

Introduction

1.1 Introduction

The aim of this work is to investigate the nature of biomaterial interactions with compromised ocular and dermal tissue sites.

Both the cornea and skin can become wounded, following injury, disease or surgery. It is desirable for these compromised tissue sites to return to a 'normal' healthy state by a natural sequence of events. This is typical of acute wounds which heal in a stepwise process of partially overlapping phases. The healing cascade does not, however, always occur in an orderly process. Wounds may become trapped in a phase of non-healing, otherwise identified as chronic wounds. Synthetic biomaterial devices serve many important purposes and protection of the tissue is a primary function; both the wounded cornea and wounded skin require protection from the external environment. Biomaterials are designed to replace some natural function of the compromised tissue site. The presence of a material, however, creates a new interface at the wound surface and consequently new interfacial events can occur. The work described in this thesis builds upon established biochemistry to examine the consequences of specific aspects of the interaction of biomaterials with compromised ocular and dermal tissue sites.

Ocular wounds, including rapidly healing superficial injuries and more severe chronic conditions, are often managed by the use of therapeutic bandage contact lenses. Hydrogels, which are water-swollen polymer networks, are used to produce conventional soft contact lenses and silicone hydrogel contact lenses (SiHy lenses). Similarly, hydrogels are also used for skin adhesive wound dressing materials to manage acute and chronic dermal wounds. Another important material type of wound dressings is hydrocolloids; these do not contain water as the name suggests, but are capable of absorbing water to form a hydrophilic gel. The interaction of a biomaterial, whether it is a hydrogel bandage contact lens or a hydrogel/hydrocolloid skin adhesive wound dressing, with the compromised tissue site brings about physicochemical and biochemical changes in the wound environment.

This first area of study in this thesis is concerned with the investigation of contact lens interactions with the cornea by the use of a novel on-lens cell-based assay technique. Vitronectin is a multifunctional adhesion molecule present in both tear fluid and wound fluid. As a pro-healing glycoprotein that promotes cell adhesion and spreading,

vitronectin possesses a high affinity for surface interaction. Consequently, vitronectin was chosen as an important biomarker for interfacial biomaterial studies in order to investigate tissue-material interactions. The second main area of study was the investigation of the influence of surface and mechanical properties of skin adhesive hydrogel and hydrocolloid biomaterials at the skin-biomaterial interface.

This introduction discusses the unusual similarities between the ocular and dermal tissue sites. A background to dermal wound healing is provided. This includes a description of the anatomy of skin and the aging skin, the stages of the dermal healing process, the role of cell adhesion proteins in the healing process and a comparison of acute and chronic wounds. Similarly, background information for ocular wound healing is provided with a discussion of the anatomy of the eye and ocular wound healing process. Lastly, an overview of key biomaterials relevant to this work for the use in both dermal and ocular applications is presented.

1.2 The Ocular/Dermal Wound Healing Analogy

The central theme of this thesis lies in the similarities between ocular and dermal wound sites. More specifically, both corneal and skin surfaces act to protect the body from the external environment. However, both surfaces can become wounded and it is the comparison of these two compromised surfaces which are of particular interest in this work. Firstly, the healthy intact cornea with the overlying tear film is comparable to the chronic dermal wound; both are surfaces with a rapid cell turnover. The tear film of the eye coats the cornea with optical, lubricant and protective functions [1]. Should, however, the tear film begin to fail, as in the severe case of chronic dry eye, the cornea keratinises to give a dry skin-like structure. It is this damaged corneal surface which is physically similar to healthy unbreached skin. Secondly, when considering the biointeractions of materials with their respective host site, a contact lens over the surface of the cornea may be likened to a wound dressing protecting an injury. Comparisons may also be drawn between tear fluid and wound exudate, with the two fluids containing many of the same proteins, lipids and mucins.

1.3 Dermal Wound Healing

Dermal wound healing is a dynamic biological process involving the repair of disruptions or breaches in the structure of skin. Ordinarily the body is capable of achieving closure of acute wounds without major complications. However, patients who suffer with conditions, such as poor blood circulation and diabetes mellitus for example, often experience impaired healing resulting in the formation of chronic wounds [2]. There is no set definition for a chronic wound, but it is generally accepted that a wound falls under this category if it fails to heal within 3-4 months. In the UK it is estimated that around 200,000 patients have a chronic wound, such as foot ulcers, pressure ulcers and venous leg ulcers, with a cost to the National Health Service of between £2.3bn-3.1bn per annum [3]. The occurrence of foot ulcerations alone has been reported at 64,000 cases per annum, with 2,600 amputations taking place annually [4].

1.3.1 Anatomy of Skin

Skin is the largest organ of the body, accounting for over 10% of the total body mass [5]. Knowledge of the physiology of skin is essential in order to understand wound healing. The broad functions of skin are threefold [6]. Firstly, it acts to provide a protective permeable barrier against exposure to water and fluids, microorganisms, electrolytes, ultraviolet radiation, and mechanical and thermal insults. Secondly, skin is involved in the regulation of body temperature and vitamin D synthesis. Finally, skin acts as a sensory organ. It contains nerve receptors that detect changes or pain encountered in the external environment, such as changes in temperature and pressure to skin. Superficial, acute or chronic wounding affects all three functions of skin. The structural arrangement of skin consists of three layers; the innermost hypodermis, the overlying dermis, and the uppermost epidermis, as shown in Figure 1.1.

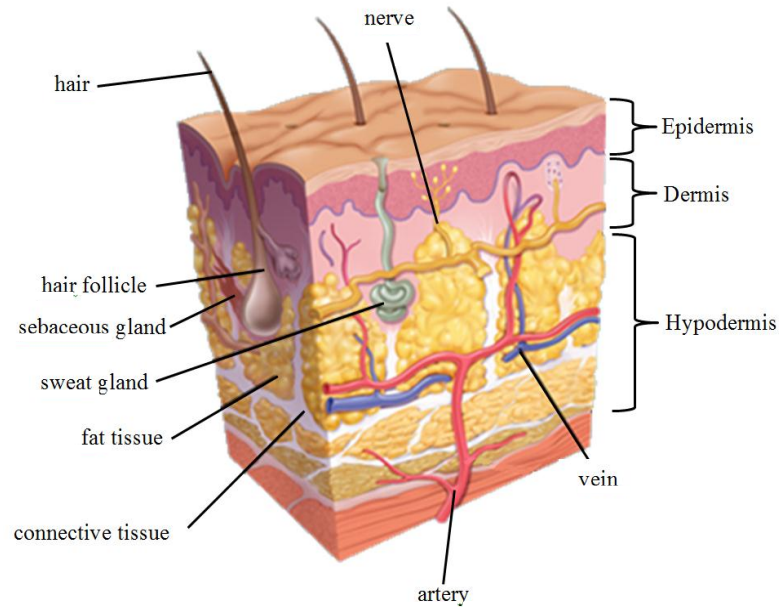


Figure 1.1 Cross section of skin morphology - the hypodermis, dermis and epidermis.

1.3.1.1 The Hypodermis

The hypodermis, also referred to as subcutaneous tissue or the subcutis, is the innermost thickest layer of skin. In addition to a network of blood vessels, lymphatics and nerves, this layer is abundant in adipose tissue and loose connective tissue. Round adipocyte cells are arranged in lobules separated by bands of fibrous connective tissue, which compose the interlobular space. Functions of the hypodermis include heat insulation, energy store and release, shock absorption, in addition to visually and cosmetically contouring the body. It also anchors the skin to underlying tissue and muscles, allowing moderate mobility of the skin. Distribution of the hypodermis across the body is not uniform, with low abundance at the eyelids for example, in comparison to greater tissue at the hips and buttocks [7]. Appendages of skin, including hair follicles and sweat glands, extend into the hypodermis layer.

1.3.1.2 The Dermis

Immediately above the hypodermis lies the dermis; the two layers are connected by interconnecting collagen and elastin fibres. The thickness of the dermis layer varies with anatomic location, ranging from 0.3 mm at the eyelids to 3 mm at the palms and soles [8], and contains blood vessels, lymphatic vessels, hair follicles, eccrine glands, apocrine glands and small quantities of striated muscles. The dermis is itself divided

into two subcategories; the upper papillary layer, which anchors to the epidermis, and the deeper reticular layer, which connects to the underlying hypodermis. The two layers are separated by the subpapillary plexus boundary. Loosely organised collagen fibres and elastin fibres constitute the thin superficial papillary layer in a perpendicular arrangement to the dermal-epidermal junction. Coarser bundles of collagen fibres and elastin fibres form the thicker reticular layer to give the bulk of the dermal tissue.

Fibroblasts are the primary cell type of the dermis, which synthesise collagen, elastin, ground substance, proteoglycans and glycosaminoglycans (GAGs). Collagen is a major structural protein which accounts for approximately 75% of the dry weight of skin [9] and is, therefore, responsible for tensile strength and mechanical resistance. Elastin makes up approximately 4% of the dermis [9] and provides elasticity in order to recoil the skin to its normal configuration following any disorder. Intracellular ground substance consists of water, electrolytes, GAGs and plasma proteins such as fibronectin and vitronectin. The transdifferentiation of fibroblast cells to myofibroblast cells is central to the wound healing process, as myofibroblasts possess contractile properties, thereby allowing wound closure.

1.3.1.3 The Epidermis

The epidermis, a stratified squamous epithelium, is the continually renewing uppermost layer of skin. It functions to provide a physical barrier, maintain skin integrity and hydration, and prevent excessive loss of internal bodily fluids. Keratinocytes are the fundamental cells of the epidermis, which synthesise the fibrous keratin protein. The epidermis is divided into four further layers;

- *The stratum basale layer* consists of a single cell layer of keratinocytes. Langerhans cells, Merkel cells and melanocytes form approximately 5-10% of this layer. The keratinocyte cells may be categorised as two types. Firstly, keratinocytic stem cells undergo mitotic divisions to produce daughter cells, which become flatter and lose their nuclei as they migrate towards the uppermost layer of skin. The second type of keratinocytic cells connect to the basement membrane, thus anchoring the epidermis to the papillary layer of the dermis.

- *The stratus spinosum*, also referred to as the spinous or prickle layer, contains keratinocytes that are larger and flatter than cells found in the basale layer. These prickly-shaped cells, with intact nuclei, are connected by an intracellular network of desmosomes.
- *The stratus granulosum*, or the granular layer, is so-called as the keratinocyte cells continue to flatten as they mature and migrate further. The nuclei disappear to leave the cytoplasm containing granular lamella.
- *The stratus corneum* is the uppermost layer of the epidermis, more commonly referred to as the horny layer. All nuclei and cell organelles are lost at this stage of the cell maturation, and the now hexagonal shaped cells are closely packed and adhere together by intracellular lipids and desmosomes. This layer undergoes continuous desquamation.

Additionally, a fifth layer of the epidermis, identified as the stratus lucidum, is often only present in regions of thick skin, such as the soles and palms, and is absent from thinner skin. This narrow layer of closely packed cells is found between the granulosum and corneum.

1.3.2 Aging Skin

A large proportion of individuals suffering with non-healing chronic wounds, such as pressure ulcers and venous leg ulcers, are elderly patients [10-12]. The continuing growth of the elderly population means that the prevalence of chronic wounds is escalating. The elderly population is more susceptible to developing chronic wounds because of underlying chronic medical conditions, such as diabetes mellitus, and because of mobility issues. It is estimated by the NHS that 1 in 50 people aged over 80 in the UK suffer with a venous leg ulcer [13].

As skin ages over time, structural changes result in a decrease of maximal function and resiliency, increased vulnerability to the external environment, in addition to reduced vascular and glandular response [14, 15]. Intrinsic changes occur due to chronological aging, which are independent of environmental effects. Conversely, extrinsic changes are a result of long term exposure to the environment, predominantly UV radiation

exposure [14]. Collectively, both types of aging may cause skin to appear atrophic, wrinkled, sagged, dehydrated, pale and with altered pigmentation [14, 16]. Loss of elasticity means that skin is less able to respond to natural stress [16]. A summary of the changes that take place with aging in human skin is provided in Table 1.1.

Table 1.1 A summary of the changes that occur with aging in human skin (adapted from Gosain and DiPietro [14]).

Clinical Changes	Histological Changes
Atrophy	Flattening of the dermal-epidermal junction
Drying	Increased turnover time
Roughness	Decreased fibroblasts, mast cells and macrophages
Alterations in pigmentation	
Sagging	Decreased collagen content
Wrinkling	Disorganised collagen and elastin
Benign and malignant tumours	Impaired microcirculation

Although the cell turnover rate of the epidermis decreases as skin ages, little change is seen within its structure. The epidermal thickness tends to remain fairly consistent with age [17]. The dermis layer, however, is largely affected by aging, particularly at the dermal-epidermal junction. The cells here flatten to give decreased contact between the dermis and the epidermis. Collagen and elastin depletion occurs due to decreased synthesis coinciding with increased degradation, leading to thinning of skin. In the hypodermis, migration of the keratinocyte daughter cells decreases by about 50% in aged skin, thereby diminishing the volume of subcutaneous fat tissue, and resulting in atrophy. As a result, the fragility of aged skin increases and it is more susceptible to trauma caused by tearing, which can lead to chronic wounding.

1.3.3 The Dermal Wound Healing Process

The complicated yet dynamic process of wound healing is divided into the four overlapping phases of haemostasis and inflammation, tissue granulation or cell proliferation, and tissue remodelling, as demonstrated in Figure 1.2.

The first phase of inflammation occurs immediately after injury and rupturing of blood vessels, with the primary vascular response inducing vasoconstriction [18]. The proceeding inflammatory response involves platelet adhesion and blood coagulation to facilitate the formation of a thrombus. This haemostatic plug consists of a matrix of platelets, fibrin, fibronectin and vitronectin. As the principal means of protecting the wound from bacterial exposure, the plug also functions as a scaffold for the recruitment and migration of many various cell types. Inflammatory host cells, including neutrophils and monocytes, rapidly infiltrate the wounded tissue. Neutrophils debride the area of bacteria and pathogenic microorganisms by phagocytosis, whilst monocytes metamorphosise to macrophages. The debriding macrophages scavenge tissue debris, but serve a dual purpose to the healing process by stimulating various growth factors and chemotactic mediators; these are essential for the initiation of the subsequent repair steps.

Cell proliferation occurs approximately one day after the initial wounding and may last up to several weeks. Macrophages migrate to the open wounded tissue site to provide growth factors essential for fibroplasia. Additionally, macrophages and platelets stimulate the migration of fibroblasts to the wound. The fibroblasts synthesise and deposit a provisional extracellular matrix, thereby providing a platform for cell migration. The complex matrix, which initially consists of type III collagen, fibrin, fibronectin, vitronectin, tenascin and hyaluronic acid, resembles pebbled granules of red/pink tissue. Although the immature collagen is greatly unorganised at this stage, it forms a major component of the matrix, and synthesis by fibroblasts is only stopped when a sufficient collagenous matrix is developed. Angiogenesis, the process of forming new blood vessels from existing vessels, then occurs. These new vessels function to sustain cell metabolism by supplying oxygen and nutrients. Fibroblasts then undergo a phenotypic change to myofibroblasts, which are responsible for wound contraction.

The final phase of tissue remodelling aims to recover the normal tissue structure of the affected area. As the matrix undergoes maturation, the composition of the granulation tissue changes – a decrease in the amount of fibronectin and hyaluronic acid is seen, whereas there is an increase in collagen fibres. Type III collagen is eventually replaced with type 1 collagen in a careful process of new collagen synthesis and old collagen degradation. This degradation is controlled by the action of matrix metalloproteinases (MMPs) and tissue inhibitors of metalloproteinases (TIMPs). The newly remodelled scar tissue gradually increases in strength due to the reorganisation and realignment of the collagen fibres, in a process that can take up to two years. This healed tissue, however, loses approximately 20% of its original strength [19] and is consequently at greater risk of breach than ordinary tissue.

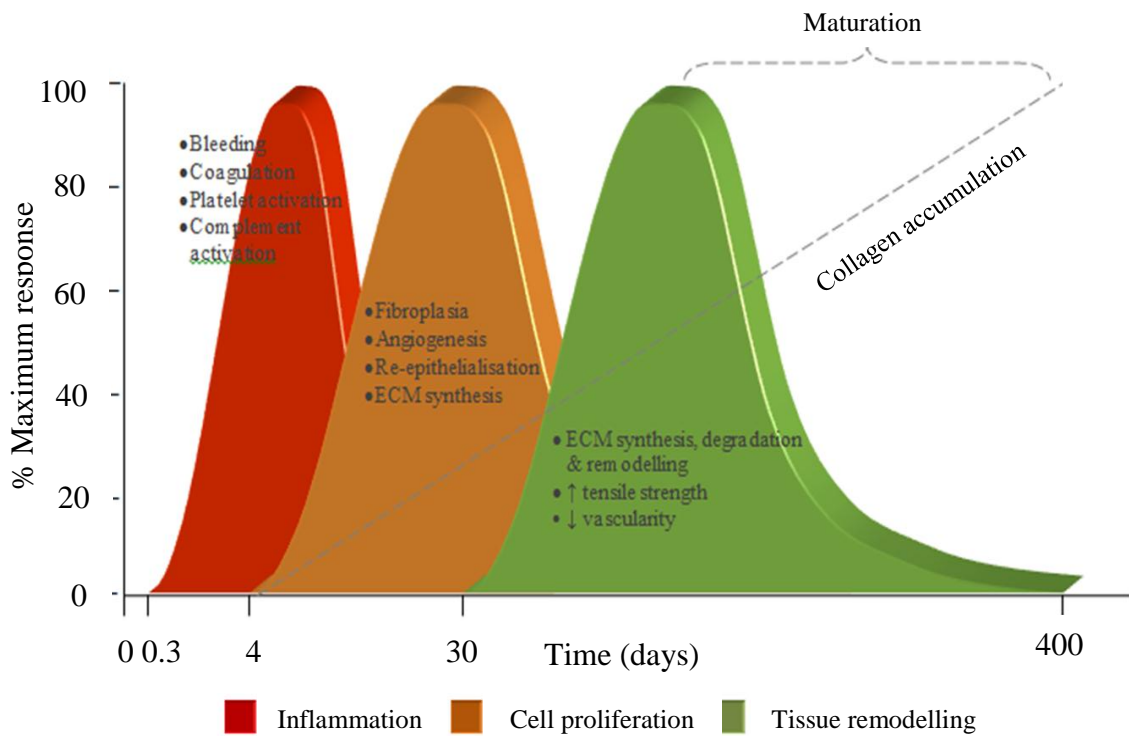


Figure 1.2 Phases of dermal wound healing.

1.3.4 Wound Chronicity

Whilst the healing mechanism for acute wounds occurs in a linear progression of overlapping events, the process for chronic wounds is highly disordered and non-linear, with some areas of the wound in different stages of healing to others. As stated in section 1.3 there is no agreed definition for chronic wounds, but they may be described as “wounds which have failed to proceed through an orderly and timely reparative process to produce anatomic and functional integrity over a period of 3 months” [20]. Chronic wounds are primarily characterised as foot ulcers, venous leg ulcers and pressure ulcers, where patients often suffer from an additional underlying condition or disease [2]. Low oxygen pressure, tissue hypoxia, nutritional deficiencies or malnutrition, infection and repetitive trauma can contribute towards wound chronicity [21]. Ischemia results in tissue necrosis and greater susceptibility to bacterial colonisation, which therefore increases the risk of serious infection. It is now well recognised that the chronic wound microenvironment exhibits increased matrix metalloproteinase expression coinciding with decreased tissue inhibitors of metalloproteinases expression, in addition to an imbalance between levels of growth factors, proteases and cytokines [22]. Together, these factors lead to a state of persistent inflammation, whereby the wound is prevented from re-epithelialisation and progression onto the proliferation phase of healing. Chronic wounds are, therefore, identified by the decrease or complete absence of granulation tissue.

Many theories regarding the causes of wound chronicity have been formed. Two principal theories for the cause of venous ulcers in the lower extremities were proposed. Firstly, in 1917 Homans [23] postulated that venous stasis leading to anoxia was a cause of tissue necrosis, findings which were later criticised due to the experimental technique implemented. Secondly, in 1947 Pratt [24] suggested that the raised oxygen tension of blood in legs with venous insufficiency was due to arteriovenous shunts, findings which were also later challenged. In 1982, Browse and Burnard [25] then proposed a series of events termed the ‘fibrin-cuff’ hypothesis for the cause of venous ulceration, suggesting that high venous pressure results in the widening of endothelial pores. It was suggested that this may allow the escape of large molecules, in particular fibrinogen with an approximate molecular weight of 340 kDa, which form around the capillaries in a ‘cuff.’ The cuff prevents the diffusion of oxygen and essential nutrients,

leading to tissue death and ulceration. Falanga and Eaglstein [26] expanded this theory in 1993 by proposing the 'trap' hypothesis. Macromolecules, including albumin, α -2-macroglobulin and fibrinogen, may leak into the dermis where they trap growth factors and matrix proteins. The impedence of normal metabolic activity then results in ulceration. Furthermore, the 'white cell trapping' hypothesis describes a theory by which a reduction in venous blood flow results in the margination of white blood cells [27]. This can lead to tissue necrosis by two means; firstly capillary plugging may give areas of localised ischaemia, and secondly activation of the cells may release free radicals, cytokines and proteolytic enzymes. A study by Bjarnsholt [28] suggested that the presence of *Pseudomonas aeruginosa* in biofilms, together with the lack of elimination by polymorphonuclear neutrophils, contribute towards chronicity. Despite the numerous hypotheses, there is no single theory that can be attributed to impaired wound healing and the development of chronic wounds.

1.3.5 Cell Adhesion Molecules in Wound Healing

1.3.5.1 The Importance of Cell Adhesion Molecules

Cell adhesion is important in many different phases of the wound healing process and cell adhesion molecules are an integral component of this process. Adhesion molecules may be categorised into several classes. Integrins are a large family of adhesion receptors consisting of α and β sub-units. Integrins may be further classified as molecules that mediate cell-cell interactions or molecules that are involved in adhesion to the extracellular matrix (ECM).

Additionally, glycoproteins play an important role in cell adhesion to ECM components. Glycoproteins are essential to many phases of wound healing such as the regulation of haemostasis, cell adhesion, migration and proliferation. One such protein is vitronectin, which is a multifunctional protein present in the ECM, plasma and other bodily fluids such as the amniotic fluid and urine. Vitronectin is involved in numerous physiological processes crucial to successful wound healing. It has been shown that its absence from the provisional ECM leads to increased fibrinolysis, which consequently delays the healing process [29]. Vitronectin is a key component of the wound healing process and thus its structure and functions are discussed in greater detail.

1.3.5.2 Vitronectin – Structure, Roles and Functions

Vitronectin, also known previously as ‘S-protein’ or ‘epibolin’, was first discovered in 1967 [30]. The protein is present in plasma under normal conditions at 200 to 400 µg/ml, which constitutes approximately 0.2–0.5% of the total protein in plasma [31, 32]. Vitronectin is a relatively small glycoprotein of 459 amino acid residues [33] and is commonly detected in two forms; a single 75 kDa polypeptide chain and a 65 kDa subunit linked to a 10 kDa fragment by a disulfide bond [34]. This glycoprotein is involved in many physiological processes, a number of which are summarised in Table 1.2. Its role and functions are dependent on its binding to various matrix and cellular components, which in turn stabilises or activates a variety of biological macromolecules.

Table 1.2 A summary of the diverse functions of vitronectin.

Process	Description	Consequences
Fibrinolysis	Stabilises PAI-1	Anti-proteolytic activity
Complement regulation	Inhibition of MAC (C5b-9)	Protection of bystander cells
T-cell cytotoxicity	Inhibition of cell lysis by perforin	Protection of bystander cells
Cellular adhesion	Integrin binding	Migration, attachment and aids healing
Thrombosis	Binds thrombin-antithrombin III	Inhibits thrombin inactivation, regulating blood coagulation
Inflammation	Binds β-endorphin	Pain suppressor
Binds structural macromolecules	Heparin, collagen, heparin sulphate	For activation or adhesion to surfaces. Healing?
Growth factor interaction	Vitronectin-GF complexes	Promote wounding healing and cell regulation
Anti-bacterial	Binds to various strains of bacteria	Inhibition in the initial phase of bacterial infections

One of the primary functions of vitronectin is to regulate the spreading and attachment of a wide variety and range of cells [35, 36]. An Arg-Gly-Asp (RGD; residues 45-47) cell binding sequence enables vitronectin to bind integrins. The integrin family of heterodimeric proteins recognise the RGD sequence on many extracellular components,

including vitronectin, fibronectin and fibrinogen [37]. This cell-matrix interaction - which directly regulates cellular differentiation, proliferation, and migration - can influence processes such as wound healing and inflammation. Vitronectin also minimises the unnecessary lysis of host cells [38], protecting these nearby bystander cells. Regulation of the complement system through the inhibition of the action of membrane attack complex is controlled by a number of regulating proteins including vitronectin. By binding to the hydrophobic domains of the C5b-7 protein complex to form SC5b-7,[39] the SC5b-7 complex is prevented from penetrating into cell membranes.

1.3.5.3 The Interaction of Vitronectin with Synthetic Materials

Vitronectin is an adhesive protein which is recognised for its adhesion to synthetic biomaterials. The affinity of vitronectin for various polymeric biomaterials has been noted by many workers including: commercial and laboratory synthesised materials [40, 41], cell culture substrates such as tissue culture polystyrene [42] and Primaria™ [43], poly(methyl methacrylate) (PMMA) intraocular lenses [44], silicone [44, 45] and conventional hydrogel contact lenses [46]. Due to the fact that vitronectin is such an adhesive protein, it is highly likely to interact with biomaterials at the wound interface, which includes both dermal and ocular tissue sites.

One important role of vitronectin is the regulation of fibrinolysis, as highlighted in Table 1.2. The conversion of plasminogen to plasmin is kept in equilibrium by the antagonistic actions of plasminogen activator inhibitor-1 (PAI-1) and tissue plasminogen activator (tPA). Vitronectin binds PAI-1 and thus modulates the conversion of plasminogen to plasmin. If vitronectin is adhered to a synthetic biomaterial at a compromised tissue site, it may bind PAI-1 to create an imbalance of plasminogen activator and thus resulting in the upregulation of active plasmin.

1.4 Dermal Wound Dressings

1.4.1 The Ideal Wound Dressing

The history of wound dressings originates from the earliest known record of dressings in the form of a clay tablet around 2100/3000 BC. This tablet is considered to be the first medical manuscript of ancient medical practice, with concepts of washing the wound, applying dressings and bandaging the wound being conveyed. The Egyptians in 1550BC produced the Ebers Papyrus - a 20 m papyrus stating that the basic constituents of a dressing should include lint to absorb exudates, grease to act as a barrier to contamination from external sources, and honey as an anti-bacterial component. It was not until the 19th century, however, that a breakthrough in the use of antiseptics for wound healing and surgical practice to reduce infections was made. James Lister in 1865 observed that soaking dressings in carbolic acid (phenol) prior to wound application successfully reduced the rate of wound infection. Following from this discovery, Robert Johnson in the 1870s began producing gauze dressings pre-treated with iodine for its anti-microbial properties. However, it was the concept of moist wound healing, demonstrated by George Winter in 1962, that revolutionised the field of wound healing. Winter demonstrated that the epithelialisation of porcine wounds occurred at a faster rate under occlusive dressings that promoted a moist wound environment, rather than wounds which were exposed to air and allowed to dry out [47]. This finding led to an evolution of materials used for wound dressing purposes, and thus the requirements of materials also expanded.

The current perception of an ideal biocompatible wound dressing is based upon a combination of various functions and properties:

- *Biocompatibility*: The primary requirement of a dressing material is that it must be biocompatible with the host tissue site. It must be non-toxic, non-allergenic and non-sensitising, and ideally interact with the wound without causing any adverse reactions.
- *Fluid/exudate absorption*: A dressing must be able to absorb excess exudate without leakage to the surface of the dressing. Suitable fluid handling capabilities, whilst maintaining a moist wound environment, are essential.

- *Humidity*: Due to the fact that chronic wounds benefit from a moist environment, a high stable humidity prevents scar formation which thereby accelerates wound healing. It has been reported, however, that exudate trapped within the wound bed increases the wound humidity beyond acceptable levels, causing other complications such as an imbalance of the wound pH [48].
- *pH maintenance*: Although the pH of chronic wound exudate varies from wound to wound, the fluid is relatively highly alkaline and has been recorded within the range of 7.5-8.9 [49]. The absorbency property of a dressing should remove surplus exudates to maintain a natural wound bed pH.
- *Impermeability*: The dressing must act as an effective “barrier” against all external contaminants, including water and bacteria, to protect from secondary infections. Occlusive dressings must, however, allow for moisture vapour and gaseous exchange between the wound and the external environment.
- *Thermal insulation*: Wounds heal effectively at body temperature. It has been suggested that a wound bed temperature of 36-38°C is optimal for a reduction of the wound surface area, whereas temperatures below 35°C and above 42°C may hinder healing [50]. A dressing which can provide thermal insulation to the wound site, such as foam dressings, or provide a cooling effect, such as hydrogel dressings, are suitable for different wound types.
- *Structural integrity*: The structural integrity of a dressing has the potential to cause an inflammatory response, infection and damage to newly re-epithelialised tissue. Fibres from the dressing may become incorporated into the wound itself. This is a downfall of traditional fabric dressings, such as the cotton gauze. In order to prevent an inflammatory response, a dressing must not leave foreign particles in the wound.
- *Adherence*: Many wound dressing materials have an adhesive system to keep them secure at the wound site. The adhesive may either be separate to the dressing, such as adhesive tapes/strips and supplementary adhesives, or the adhesive may be a component of the wound dressing. Pressure sensitive adhesive (PSA) materials form a large element of biomaterials for wound

healing management. PSA materials are designed to provide instantaneous adhesion to a substrate upon the application of slight pressure. In this case the substrate is skin.

Numerous types of dressings are available which vary in absorptive and adhesive capacities, including hydrogels, hydrocolloids, alginates, foam dressings, collagen dressings and amorphous gels. Although individual manufacturers undoubtedly use testing techniques for quality control of dressing materials within their own industries, the academic literature is lacking in the assessment of the biophysical properties of skin and the corresponding properties of wound dressing materials. Little is known regarding suitable characterisation techniques that may attempt to match or relate the properties of materials to the behaviour of the natural tissue. This is in great contrast to the ocular area where the clinical relevance of physicochemical properties, such as wetting, modulus and permeability behaviour, is well-advanced in both industrial and academic settings. One aspect of the work described in this thesis involves the examination of the surface and mechanical properties of materials in relation to the biophysics of skin. This work is concerned with skin adhesive wound dressing materials and, therefore, skin adhesive hydrogels and hydrocolloids shall be discussed in further depth.

1.4.2 Skin Adhesive Hydrogels

Hydrogels may be described as cross-linked, water-swollen polymer networks [51]. They are able to swell due to their hydrophilic nature, without dissolving in water. The water content on a fully hydrated hydrogel may range from 20-98% and is expressed as the equilibrium water content (EWC):

$$\text{Equation 1} \quad \text{EWC} = [\text{Weight of water in gel} / \text{Weight of gel}] * 100$$

Hydrogel wound dressings are generally available as either sheet or amorphous formulations. Sheet hydrogels are firm sheets that uphold their structural integrity when swollen, whereas amorphous hydrogels are soft shapeless gels that decrease in viscosity with increasing fluid absorption.

A distinct advantage of hydrogel dressings is the ability to donate moisture to dehydrated tissue and, therefore, maintain a moist wound healing environment. This property allows hydrogels to promote autolytic debridement of slough and wound

debris. Additionally, hydrogel dressings are able to absorb fluid from an exuding wound; the rate of which is dependent upon the EWC. This can, however, lead to over-hydration of the wound and peri-wound area, particularly for highly exuding wounds. Hydrogels have also been reported to relieve pain by providing a cooling effect for wounds producing a burning sensation [52]. Amorphous hydrogels have been shown to reduce the temperature of a wound by up to 5°C [53]. In general, these properties indicate that hydrogel dressings are best suited for dry painful wounds exuding low levels of fluid.

Hydrogel dressings are typically non-adherent materials and thus minimise localised trauma caused by removal – this is important for cases where frequent dressing changes of every 1-3 days are required. A secondary dressing may be necessary to hold the hydrogel in place, although many hydrogel dressings are available with an adhesive border or entire adhesive surface.

1.4.3 Skin Adhesive Hydrocolloids

1.4.3.1 Hydrocolloids for Wound Dressings

A hydrocolloid forms a colloid system as a result of interaction with water. Hydrocolloids may be classified as either natural (formed from natural proteins and carbohydrates), semi-synthetic (modification of natural hydrocolloids) or synthetic (synthesised from petroleum-based materials). The name “hydrocolloid” is somewhat inaccurate, as the material does not contain any water in its formulation. Rather, the distinctive feature of hydrocolloid materials is the ability to form a hydrophilic gel when in the presence of water, through hydrogen bonding.

Hydrocolloid dressings are absorptive, occlusive and generally adhesive dressings. They are typically formulated of: sodium carboxymethyl cellulose (NaCMC) for absorption and exudate management; poly(isobutylene) (PIB) for the provision of an adhesive matrix; and gelatine and pectin which act as ‘gum-like’ gel forming agents [54]. The structures for each component are provided in Figure 1.3. Hydrocolloids are able to absorb low to moderate levels of exudate by undergoing a phase inversion to form a hydrophilic gel. This yellow/brown gel, which is responsible for maintaining a moist wound healing environment, remains on the wound tissue after dressing removal,

1.4.3.2 Hydrocolloids for Ostomy Devices

In addition to wound dressings, hydrocolloid technology has been applied to medical ostomy devices. It is estimated that 13,500 people per annum undergo stoma formation in the UK following colostomy, ileostomy or urostomy surgery [55]. Ostomy devices are designed to collect waste products through a surgically created ostomy. The device consists of a discharge collecting pouch or bag attached to an adhesive component (also referred to as a skin barrier or wafer). Devices are available as either a one-piece appliance where the pouch is attached to the adhesive (Figure 1.4A), or as a two-piece appliance where the pouch is a separate component to the adhesive and does not come into direct contact with skin (Figure 1.4B). The adhesive forms an integral element of an ostomy device and is generally formed of a hydrocolloid adhesive. For ostomy devices, the hydrocolloid adhesive must not only provide a protective seal around the stoma in order to prevent leakage of stomal effluent, it must also absorb moisture to avoid maceration of the peristomal skin. It is not uncommon for ostomy devices to be changed up to three times a day. Therefore, the adhesive must adhere easily to skin, without causing any trauma, irritation, soreness or residue deposition upon removal.

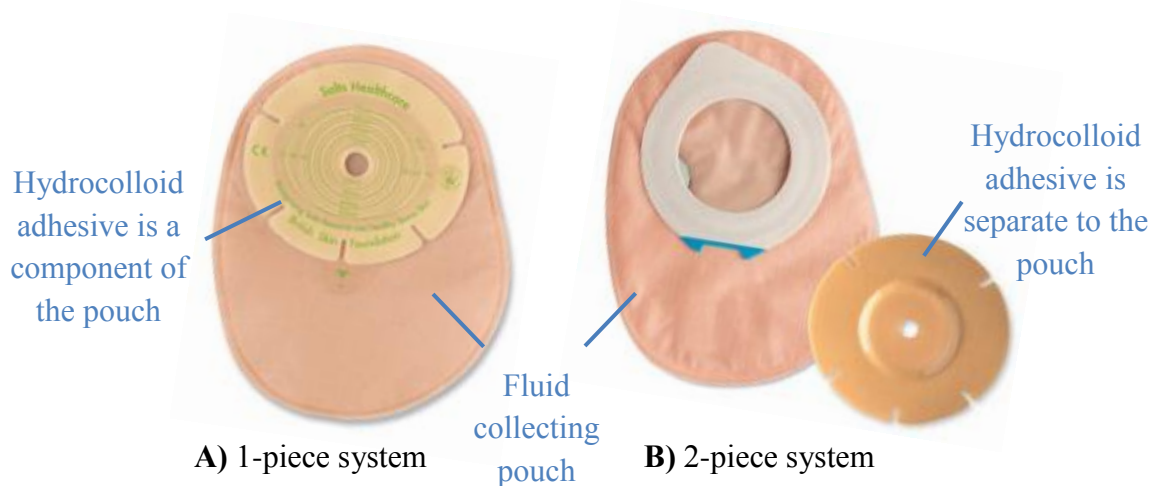


Figure 1.4 Ostomy devices with hydrocolloid adhesives are available as: A) a one-piece system, B) a two-piece system.

Adhesion is a central component of skin adhesive hydrogels and hydrocolloids studied within this thesis and therefore the mechanism of adhesion and properties of the adhesive itself must be considered.

1.4.4 Adhesion in Relation to Skin Adhesive Hydrogels and Hydrocolloids

1.4.4.1 Adhesion Mechanism

Adhesion may be defined as the state in which two surfaces are held together by interfacial forces. The mechanisms of adhesion may be classified as four theories;

- *Chemical adhesion* refers to formation of covalent, ionic or hydrogen bonds between the adhesive-substrate interface.
- *Mechanical adhesion* first described by McBain [56] in 1925 refers to the adhesive material interlocking into the pores of the solid surface.
- *Diffusive adhesion* describes the interdiffusion of one component across the interface to create an interphase. This theory of adhesion requires sufficient mobility of one component in order for interfacial penetration to occur.
- *Electrostatic adhesion* creates an electrostatic force of attraction between two components. This theory was originally described for metal materials, and thus is difficult to apply to polymeric wound dressings.

Additionally, in order for measurable tack, the Dahlquist criterion states that the elastic modulus of the material must be below 10^5 N/m².

Bioadhesion is defined as the adhesion of two surfaces, of which at least one has a biological nature. Three types of bioadhesion have been identified. Firstly, type I describes the adhesion between biological substrates, such as cell-to-cell adhesion within wound healing. Secondly, type II describes the adhesion of a biological substrate to an artificial substrate, such as cells to cell culture flasks or proteins from the tear film to contact lenses. Thirdly, the adhesion of an artificial component to a biological substrate is known as type III, for example a synthetic wound dressing to skin tissue or dental sealant to tooth enamel. The locus of adhesive failure within any of these systems may be categorised as follows:

- *Adhesive failure* refers to interfacial bond failure between the adhesive and substrate.

- *Cohesive failure of the adhesive* arises from the failure of the adhesive to maintain the bond between the substrate due to insufficient cohesive strength.
- *Cohesive failure of the substrate* involves failure within the substrate, independent of the bond with the adhesive.

1.4.4.2 Properties of Adhesives

The properties of an ‘ideal’ wound dressing were discussed in section 1.4.1. The adhesive system itself, however, has separate functions and requirements, firstly in terms of adhesion and then secondly for removal.

For successful and safe adherence to skin, the primary requirement for any adhesive is to meet appropriate toxicological standards. It must also secure the dressing at the wound site for the intended wear duration, and should not cause maceration to peri-wound skin. Adhesives are generally required to have good tack, peel and cohesive strength at room temperature. Tack describes the measure of initial adhesion or grab to the substrate. The force required to remove the adhesive from the substrate under defined conditions is termed the peel adhesion; an adhesive that is easily removed with a light peel force is desirable. Cohesive strength is the force of attraction between molecules of the same substance, the adhesive, which is indicative of the internal strength. This is evaluated by the measure of shear strength. It is desirable for an adhesive material to retain sufficient cohesive strength throughout its wear duration.

The adhesive should also allow safe removal from the wound, with minimal risk of trauma inflicted to the tissue. Traumatic removal of adhesives can have damaging consequences for the wound, such as increased wound size and increased healing time, in addition to undue pain and trauma to the patient [57]. Furthermore, the adhesive should not leave any residue upon removal and should ideally be repositionable if necessary. Quite often a dressing may be improperly placed on the first attempt and must be reapplied. Therefore, removal and reapplication must not cause any further trauma, transfer any adhesive residue upon removal or cause loss of adhesion once reapplied.

1.5 Ocular Wound Healing

1.5.1 Anatomy of the Eye

The eyeball consists of an inner globe encased by an outer globe (Figure 1.5). Vitreous humour forms more than two-thirds of the volume of the eye to provide structural support [58], and largely fills the inner globe which consists of three concentric layers; the retina, choroid, and sclera [59]. The innermost retina contains photoreceptor neurons, namely rods and cones, and is supported by the nutrient supplying choroid layer. The outer sclera is tough, opaque, fibrous tissue which protects the inner layers. The inner globe also houses the pupil, crystalline lens and gelatinous vitreous humour, whilst the outer globe consists of the conjunctiva, cornea and tear film.

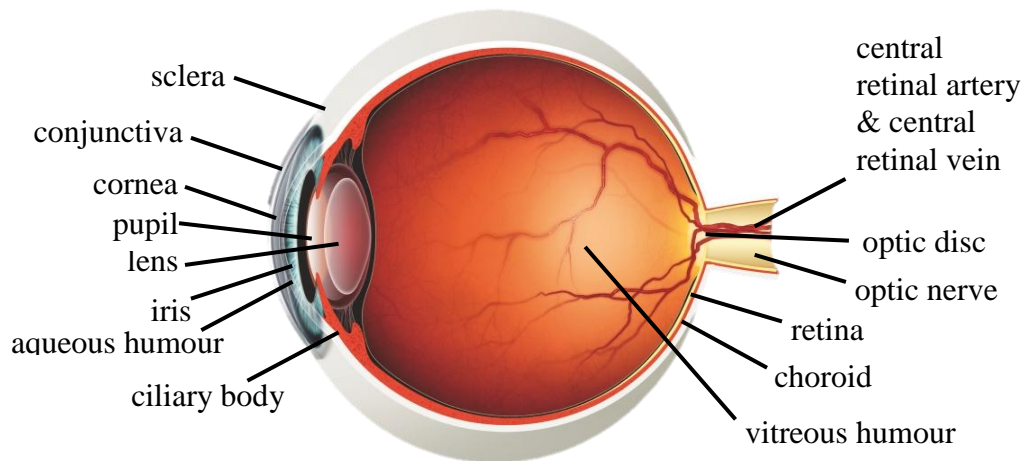


Figure 1.5 Cross section of the human eye.

1.5.1.1 The Cornea

The cornea is a transparent avascular tissue that forms part of the outermost layer of the eye (Figure 1.6). The typical human anterior corneal radius is 7.5 mm [60] with the thickness across the structure varying from 0.5 mm at the centre to 0.69 mm at the periphery [61]. Corneal thickness has also been shown to change throughout the course of the day, and is at its thickest upon wakening [62]. The cornea consists of five layers; the underlying endothelium, Descemet's membrane, the stroma, Bowman's membrane and the epithelium [63]. A sixth layer termed the Dua's layer has recently been reported to lie sandwiched between the Descemet's membrane and the stroma [64]. The structure

of the cornea bears similarity to that of skin because cells in both tissue sites are generated at the base and migrate towards the surface of the tissue. Acting as a transparent window, the cornea enables refracted light to be transmitted further towards the lens. Because of the fact that the cornea is an avascular tissue, the presence of blood vessels due to irritation or infection would interfere with this process [65].

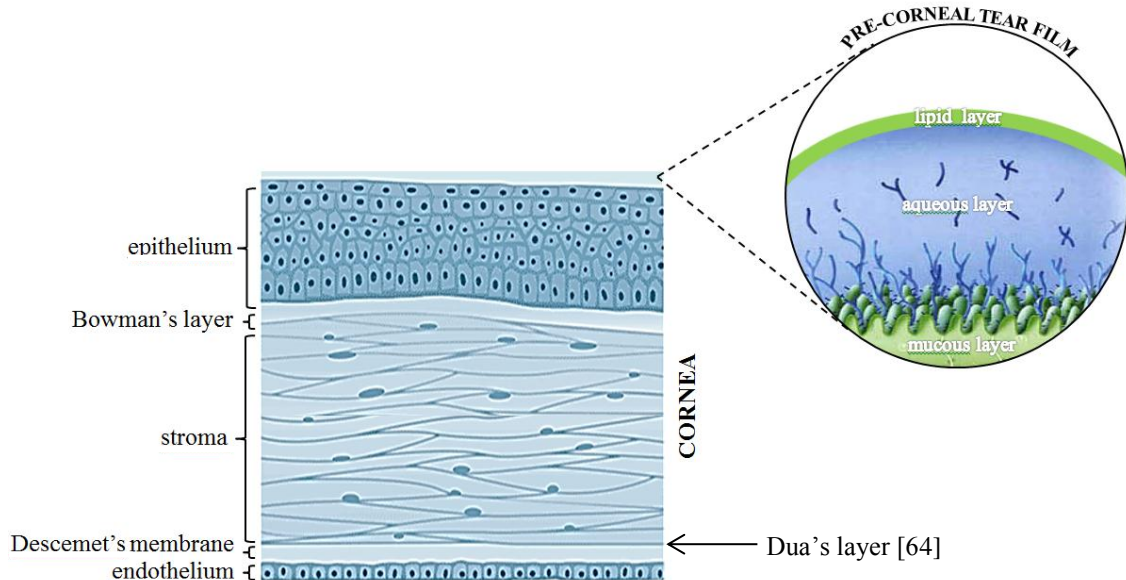


Figure 1.6 Five layers of the cornea with the recently discovered sixth layer, and the pre-corneal tear film.

The endothelium is a monolayer of cells that lies between the aqueous humor and stroma. It functions to maintain corneal hydration and transparency. Damage to the endothelium can result in oedema and, therefore, visual impairment. Fuch's dystrophy and bullous keratopathy are the two most common causes of endothelial disruption. The endothelium underlies the basement membrane, termed the Descemet's membrane, which connects to the stroma. Consisting largely of collagen, the membrane coils upon injury, but is unable to readily regenerate.

The stroma forms 90% of the cornea [61]. Collagen fibrils are organised in highly ordered parallel sheets of lamellae, with keratocytes forming an interlinking network between the sheets. This provides the cornea with high tensile resistance and mechanical strength. The anterior portion of the stroma is separated from the overlying epithelium by Bowman's membrane; this membrane is a layer of closely packed

collagen fibres without the presence of keratocytes. Although highly resistant, Bowman's membrane is wholly unable to regenerate following injury and heals by scarring [66].

The epithelium connects to Bowman's membrane via the basement membrane. The epithelium is a stratified squamous epithelium bathed in the tear film, and is dependent upon the tear film and aqueous humor for nutrition. As a layer of 5-7 cells thick, they progress to basal, wing and squamous cells at different stages. The epithelium provides a barrier to fluid loss and pathogen exposure. Additionally, the epithelium prevents the tear film from diffusing into the stroma.

1.5.1.2 The Tear Film

The pre-corneal tear film coats the anterior surface of the eye (Figure 1.6). The tear film is a multi-functional liquid layer that is responsible for spreading over and maintaining the health of the cornea and conjunctiva. Firstly, the tear film establishes a smooth optical surface over the eye, and increases the optical resolution as it fills any irregularities of the corneal surface. Secondly, it has a largely lubricious role as it sustains a moist surface. This lubricity provides comfort and ease of blinking. Thirdly, the tear film has a protective barrier role, which not only is fulfilled by protecting the eye from ocular surface infection, but also by removing cellular debris and foreign material which are moved by the blinking mechanism. Fourthly, the tear film has an antibacterial role and contains antibacterial tear proteins such as lysozyme. Lastly, the tear film acts as a transport medium, providing oxygen from the external environment and nutritional elements to the underlying cornea, and removing waste products.

The configuration of the tear film consists of three layers; the overlying lipid layer (0.1-0.2 μm), the intermediate aqueous layer (6.5-7.5 μm) and the underlying mucous layer (0.2-1 μm) [67]. Although the thinnest component of the tear film, the lipid layer has an important role in preventing or retarding evaporation of the aqueous layer, in addition to preventing overflow of tears. It has been shown that the rate of tear evaporation increases by a factor of four when the lipid layer is absent from the tear film [68]. The aqueous layer forms 98% of the tear film composition, and contains proteins and growth factors, electrolytes, and metabolites. Electrolytes provide osmolarity to the fluid, whilst growth factors are essential for cell proliferation during healing. The

mucous layer predominantly consists of mucin glycoproteins and adheres to the underlying epithelial cells. This layer is responsible for anchoring the tear film to the cornea.

1.5.2 Wounding of Ocular Tissue

The ocular tissue may become wounded by three means. Firstly, the eye may suffer injury due to accidental trauma. The robust ocular surface has the propensity to heal rapidly following superficial injuries or abrasions [69]. A minor scratch to the corneal surface is normally self-healing with epithelial cells undergoing complete regeneration within a few days of the trauma. However, deeper wounds that penetrate the cornea can result in corneal scarring, therefore inflicting severe pain and affecting normal visual acuity.

Secondly, surgery to correct common medical conditions, such as cataracts and glaucoma, require an incision to be made. Such incisional wounds tend to heal successfully. However, underlying and undetected causes often prevent an ocular wound from healing successfully. These include disorders of the corneal epithelium, conjunctival epithelium and of the tear film. Recurrent corneal erosions, for example, may initially occur as a result of corneal trauma, but then persist due to underlying corneal epithelial dystrophy. In severe cases of irreversible corneal damage, corneal grafts may be necessary; it is estimated that over 52,000 grafts have taken place since the UK Corneal Transplant Service was founded in 1983 [70].

Thirdly, the ocular surface can be wounded following elective surgery to correct vision. The relatively new phenomena of vision correction procedures, such as laser *in situ* keratomileusis (LASIK), have become increasingly popular. Approximately 100,000 cases of LASIK are performed per year in the UK [71]. This type of surgery has opened up a new area of ocular healing. The procedure involves creating a hinged corneal flap using a blade or laser in order to expose the underlying corneal tissue. An excimer laser is then used to reshape the cornea. At the end of the procedure, the flap is repositioned over the cornea without the use of sutures, where it adheres to the corneal stroma.

1.5.3 The Corneal Wound Healing Process

As is the case with dermal wound healing, the objective for healing in the ocular environment is the successful repair and restoration of damaged tissue to the previous unwounded structure. The formation of scar tissue in dermal sites is the target for successful healing. However, the corneal healing process must restore visual clarity and corneal transparency. The formation of scar tissue must be minimised to prevent impaired vision.

Wounds that disrupt the corneal epithelium, but do not penetrate the basement membrane, tend to heal fairly rapidly due to the self-renewing capacity of the epithelium. Conversely, wounds that do penetrate the basement membrane and extend into the corneal stroma require a lengthier healing time [72]. Both corneal epithelium and corneal stromal healing processes shall be discussed in further detail.

It should be noted that considerable information regarding corneal wound healing is resultant from studies involving animal models such as rabbits and monkeys. Anatomical differences, however, exist between species. For instance, Bowman's layer is absent from rabbit corneas. Therefore, consideration should be given when extending animal studies to human findings [73].

1.5.3.1 Corneal Epithelium Wound Healing

Corneal wound healing normally begins immediately after an injury or an incision. The process includes three overlapping phases as part of a continuous process: the lag/latent phase, the cellular migration phase and the proliferation phase. Figure 1.7 provides an overview of the three phases.

The initial lag phase involves the movement of basal epithelial cells at the corneal wound margin. Within an hour of injury for smaller wounds, or 4-6 hours for larger wounds, polymorphonuclear leukocyte white blood cells are released from the disrupted epithelium. These remove necrotic cells and cellular debris by phagocytosis, which initially causes an enlargement of the epithelial wound. This action by the polymorphonuclear cells is stopped once a monolayer of epithelial cells has formed over the wound site. Newly synthesised desmosomes anchor the epithelial monolayer to

the basement membrane. Finally, cell membrane extensions, such as lamellipodia, filopodia, and ruffles, develop at the wound margin. This increased mitotic activity begins the next phase of cell migration.

The subsequent cell migration phase occurs approximately 24 hours after an injury for small to medium wounds or as long as 96 hours for larger severe wounds. This phase, whereby epithelial cells migrate across the wound area to cover the defect before mitosis ensues, may last up to 2-3 days. The cell migration phase begins with the formation of actin filaments, which accumulate at the edges of the developed lamellipodial and filopodial cell extensions. This accumulation of actin filaments provides the epithelial cells with cytoskeletal support. It is thought that the lamellipodia and filopodia create temporary anchors in order to enable the epithelial cells to migrate across the wound in a cyclical process [73]. Fibronectin, which is an important cell adhesion protein, stimulates the epithelial cells to produce plasminogen activator. The action of plasminogen activator converts plasminogen to plasmin, which functions to break adhesions between the epithelial cells and the underlying sub-epithelial matrix. Thus, the lamellipodia and filopodia bind and cleave from the underlying sub-epithelial matrix during the cyclical process, enabling cells to advance over the wound area to form an epithelial monolayer. At this stage fibronectin is no longer required in the healing process and disappears. The synthesis of new hemidesmosomes and anchoring complexes enables firm attachment of the epithelial monolayer to the underlying Bowman's membrane. Anchoring fibrils consisting of collagen spread into the stroma to create strong attachment of the epithelium to the stroma.

The final phase of cell proliferation aims to restore normal epithelial thickness. Stem cells located near the limbus produce rapidly dividing transient amplifying cells. The transient amplifying cells (TACs) of the basal layer divide to produce post mitotic cells (PMCs). In turn, the post mitotic cells fully differentiate into terminally differentiated cells (TDCs), which are the final corneal epithelial cells. At this final stage of healing, the epithelium is permanently anchored to the underlying stroma by fully developed desmosomes. The corneal epithelium is restored to a regular smooth surface.

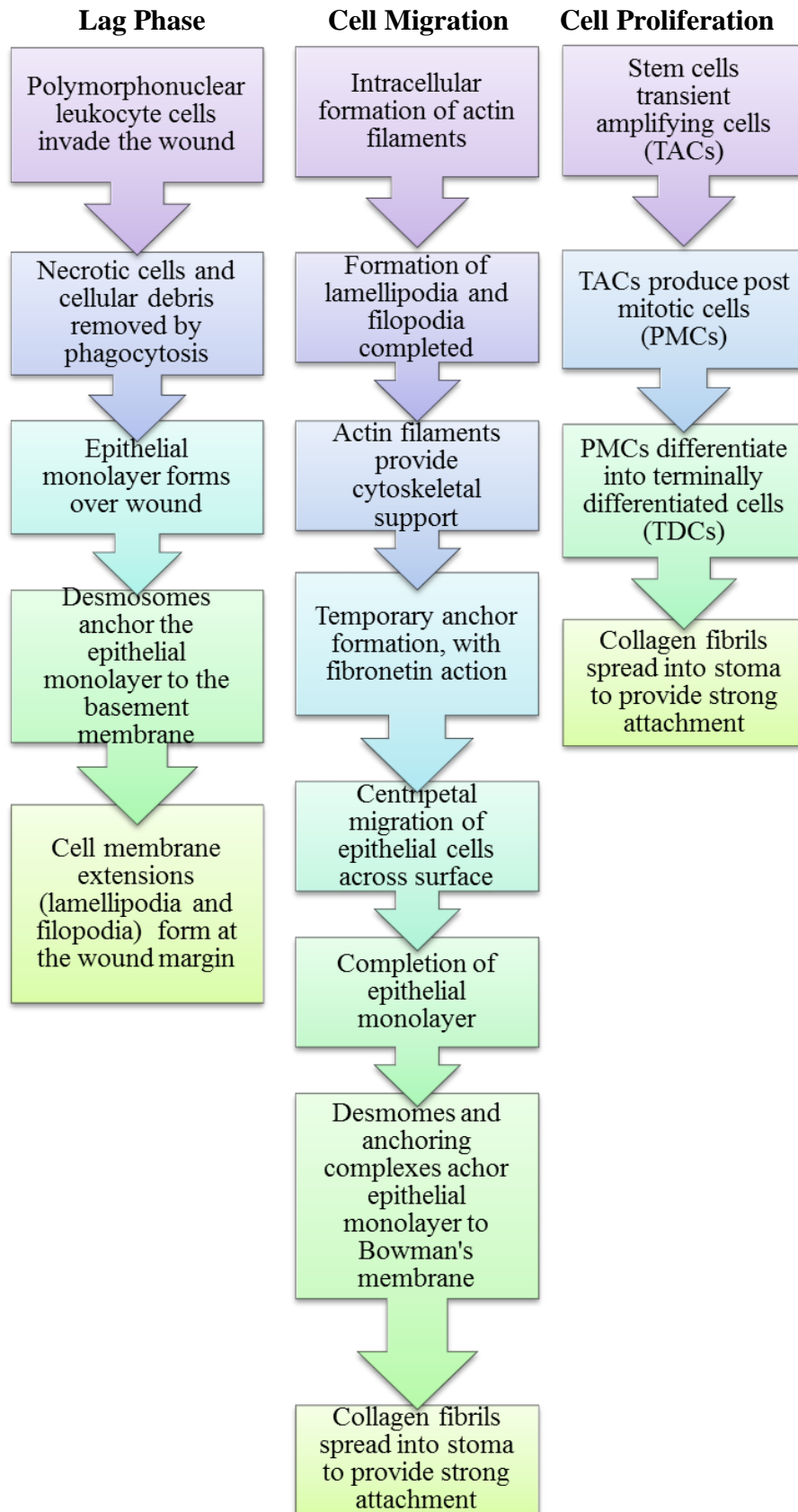


Figure 1.7 The corneal epithelium wound healing process.

1.5.3.2 Corneal Stromal Epithelium Wound Healing

Stromal wound healing progresses only once a new epithelium has formed over the corneal wound. The process commences with the apoptosis of disrupted keratocytes at the wound site. Remaining peripheral keratocytes to this newly created acellular zone differentiate into stromal repair fibroblasts, which then migrate towards the wound. These stromal repair fibroblasts are stimulated by transforming growth factor-beta (TGF- β) to undergo further differentiation to myofibroblasts. Similarly to dermal healing, the myofibroblasts are responsible for wound contraction by re-approximating the wound margins and ‘pulling’ or contracting the wound to close. Both stromal fibroblasts and myofibroblasts deposit collagens, glycoproteins and proteoglycans to initially form a rather disorganised stromal extracellular matrix (ECM). Remodelling of the stromal ECM is regulated by the fine balance between matrix metalloproteinases (MMPs) and the inhibitory action of tissue inhibitors of metalloproteinases (TIMPs). An overview of the stromal wound healing process is provided in Figure 1.8.

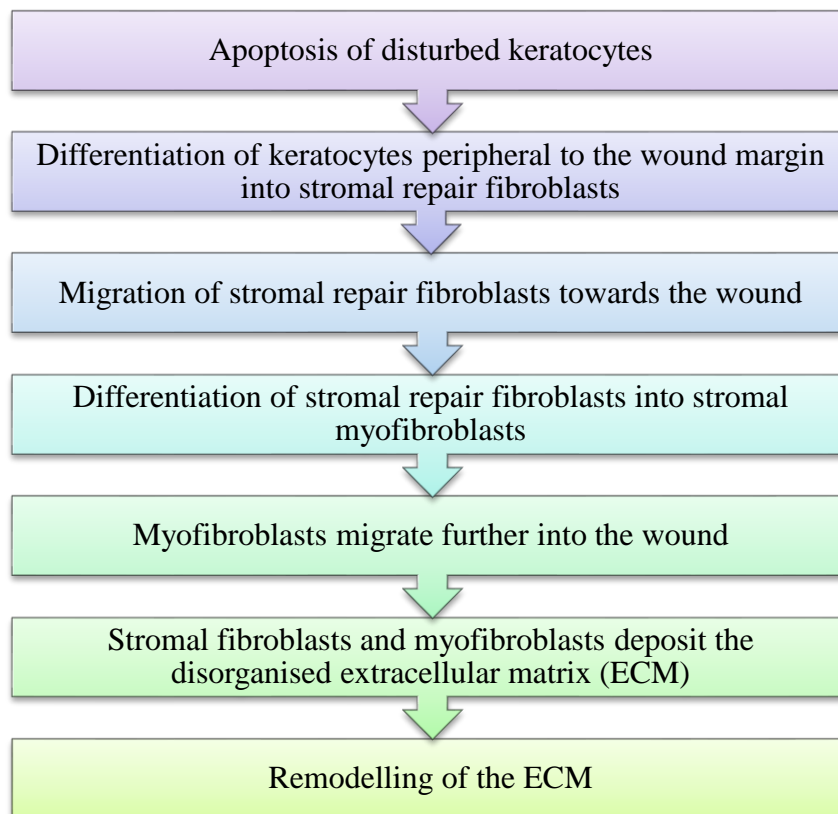


Figure 1.8 The corneal stromal wound healing process.

1.6 Ocular Wound Dressings

1.6.1 The Role of Bandage Contact Lenses

In the anterior healing eye a bandage contact lens (BCL) can be used to protect the cornea following injury, disease or surgery, thereby relieving pain and improving the ability of the corneal epithelium to heal. The roles of a BCL include; mechanical protection of the cornea from eyelid movement; protection from atmospheric exposure and further ocular insult; improving the ability of the corneal epithelium to heal; corneal hydration; and if required drug delivery [74, 75]. One of the principal indications of BCL use is for the relief of pain and to provide comfort. A study by Jackson *et al* [74] investigating the use of bandage lenses for the management of corneal pathologies found that 87% of cases fitted with a BCL were for the primary or secondary indication of pain relief. BCLs have been shown to successfully facilitate healing for different pathological treatments such as;

- bullous keratopathy [76]
- dry eye syndrome [77]
- laser-assisted *in situ* keratomileusis (LASIK) [78]
- persistent epithelial defects [79]
- photorefractive keratectomy/ phototherapeutic keratectomy (PRK/PTK) [80]
- recurrent corneal erosions [81]

1.6.2 Advances in Contact Lens Materials for Therapeutic Use

The origin of applying a bandage to the ocular surface is thought to date back to the first century A.D., when a honey-soaked linen dressing was applied to the eye. This was in an attempt to prevent symblepharon formation, a condition whereby the eyelid adheres to the bulbar conjunctiva [82]. It was not until the 1950s, however, that Ridley [83] fitted poly(methyl methacrylate) (PMMA) scleral contact lenses for the management of various ophthalmic disorders. Following Wichterle's [84] development of hydroxyethyl methacrylate (HEMA), Gasset and Kauffman [85] reported the use of hydrophilic contact lenses for therapeutic purposes in the 1970s. Conventional daily disposable hydrogel materials, such as etafilcon A, were then typically recommended

for therapeutic use [86-88] until the advent of silicone hydrogel (SiHy) contact lenses in 1998.

Although conventional hydrogel contact lenses are typically low modulus materials, which allow for a more uniform draping of the contact lens over the cornea, advances in SiHy contact lenses since the introduction of the first generation mean that SiHy lenses are no longer constrained by high moduli. The use of conventional hydrogels for continuous wear is restricted due to their inability to provide adequate oxygen permeability (Dk), therefore potentially resulting in hypoxia-related complications and corneal swelling [89]. For this reason conventional hydrogels are poorly suited for bandage lens use. Conversely, SiHy contact lenses with higher Dk values generally allow for greater oxygen transport over extended wear [90]. Accordingly, many SiHy lenses are accepted as a safe material choice for extended wear and bandage lens use, with wear times ranging from one day to four weeks of continuous wear. Advances in SiHy materials have since resulted in the availability of a wider range of BCLs that are able to successfully manage a variety of ocular conditions.

It is extremely important to note that the vast majority of contact lenses currently available for therapeutic use are designed for the correction of refractive error and for comfortable wear in the non-compromised healthy eye, rather than for purposely designed bandage lens use. SiHy contact lenses with Food and Drug Administration (FDA) approval for bandage lens usage are shown in Table 1.3.

The risks of inserting a foreign material into an eye which is already compromised should be considered. Therefore, the efficacy of various SiHy contact lenses for successful therapeutic use has been studied by different authors. Ambrosiak *et al* [91] evaluated the use of lotrafilcon A contact lenses (Air Optix Night & Day Aqua) in 70 patients with bullous keratopathy, dry eye syndrome or postoperative keratoepitheliopathy. Therapeutic improvement was reported in 91% of patients in their respective corneal defect following contact lens wear and 94% rated contact lens comfort highly. In a similar study, Arora *et al* [75] investigated balafilcon A contact lenses (PureVision) in 30 eyes of 28 patients. The contact lens was found to successfully provide pain relief in all cases. Complications occurred in 6 eyes due to predispositions to infection.

Table 1.3 FDA approved silicone hydrogel contact lenses for bandage lens use.

Commercial Contact Lens	Material	Manufacturer	Water Content (%)	Oxygen Permeability (Dk)	Modulus (MPa)
PremiO	Asmofilcon A	Menicon	40	129	0.9
PureVision	Balafilcon A	Bausch & Lomb	36	91	1.1
Biofinity	Comfilcon A	CooperVision	48	128	0.75
Avaira	Enfilcon A	CooperVision	46	100	0.5
Acuvue Advance	Galyfilcon A	Vistakon	47	60	0.43
Air Optix Night & Day Aqua	Lotrafilcon A	Ciba Vision	24	140	1.5
Air Optix Aqua	Lotrafilcon B	Ciba Vision	33	110	1.0
Acuvue Oasys	Senofilcon A	Vistakon	38	103	0.72

1.6.3 Protein Adsorption

When a biomaterial is brought into contact with a biological fluid, the first event that occurs is the adsorption of proteins onto the surface. This process of protein adsorption may be defined as “*adsorption (that is, adhesion or sticking) of protein(s) on a variety of surfaces*” [92]. In order to consider protein adsorption to contact lenses in both the non-compromised and compromised eye, it is useful to consider, firstly, general protein structure and, secondly, the fundamentals of protein adsorption to biomaterials.

1.6.3.1 General Structure of Proteins

Amino acids are the organic monomers of proteins; fundamentally peptide bonds between the amino acid monomers form the basic structure of a protein. Amino acids

contain an amino group (-NH₂) and a carboxyl group (-COOH) in addition to a side chain (R-group) that provides the amino acid with unique properties. The nature of the side chain determines the class of amino acid which may be classified as; non-polar and neutral; polar and neutral; polar and acidic; and polar and basic. Figure 1.9 illustrates the general structure of an amino acid monomer.

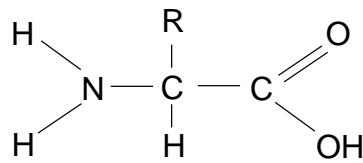


Figure 1.9 The general structure of an amino acid monomer.

Protein structure may be designated by four levels: primary, secondary, tertiary and quaternary. Firstly, the primary structure of a protein describes the linear sequence of amino acid monomers bonded by peptide bonds to give a polypeptide. Secondly, the secondary structure describes the conformational shape of the protein from hydrogen bonding between the side chains of the amino acids. Three common shapes exist which include the α -helix, β -helix and triple helix. The third level of protein structure, tertiary, describes the complex three-dimensional folding of the protein. Molecular interactions occur between the side chains which include; hydrogen bonds between polar R-groups; hydrophobic interactions between non-polar R-groups; ionic bonds between charged R-groups; and disulphide bonds between sulphur atoms on R-groups. Lastly, the quaternary structure of proteins describes the bonding between two or more polypeptides.

1.6.3.2 Principles of Protein Adsorption to Biomaterial Substrates

The affinity of a protein for a substrate surface and the overall protein adsorption to a biomaterial is influenced by the nature of the protein, substrate and fluid components of the system:

- *Protein properties*

The properties of an individual protein molecule influence its adsorption to a foreign substrate surface. Upon arrival at the substrate, the protein can interact and bind through hydrophobic interactions, ionic bonds and charge transfer interactions. These

interactions are dependent on the size, charge, and stability of the protein. Firstly, the size of the protein molecule governs the rate of diffusion through the solution; smaller molecular weight proteins are generally able to diffuse at a faster rate than larger proteins and, therefore, primarily adsorb to the substrate surface.

The net charge of a protein is governed by the amino acid monomers of the protein structure. Charged hydrophilic amino acids, which are polar in nature, are exposed at the outer parts of the protein and are able to preferentially interact with polar regions of the substrate surface. It is hypothesised that adsorption is maximised when a protein is at its isoelectric point (pI), this is the pH at which a protein does not carry a net charge. At the isoelectric point, electrostatic repulsions between other adsorbing proteins are reduced, which may favour adsorption to the substrate.

Stability of a protein is also influential upon protein adsorption. Proteins may undergo partial or substantial conformational changes during or after adsorption to a substrate. Conformational changes are determined to some extent by protein stability. When discussing protein stability, proteins are often classed as either 'soft proteins' that have a low internal stability or 'hard proteins' that have a high internal stability. Unfolding of 'soft proteins' during conformational changes may expose greater numbers of domains that are able to interact and bind to the substrate. These proteins are therefore able to interact with both hydrophilic and hydrophobic domains. Conversely, 'hard proteins,' with high thermodynamic stability, are governed by hydrophobic interactions with the substrate and will essentially adsorb to hydrophobic surfaces. Adsorption of 'hard proteins' to hydrophilic surfaces occurs when favourable electrostatic interactions exist within the system.

- *Substrate properties*

In addition to protein properties, the chemical properties of the substrate material can influence adsorption of proteins to its surface. Four selected surface functional groups (methyl $-CH_3$, hydroxyl $-OH$, amine $-NH_2$ and carboxyl $-COOH$) of substrates and their influence on protein adsorption has been studied by Thevenot *et al* [93]. Methyl (neutral and hydrophobic) functional groups were found to bind fibrinogen and IgG strongly, whereas hydroxyl groups (neutral and hydrophilic) were found to decrease the overall affinity for plasma proteins. Both amine (positive and hydrophilic) and carboxyl

(negative and hydrophilic) groups were found to increase the affinity for fibronectin. The negatively charged carboxyl functional groups were found to interact with plasma proteins over the positively charged amine groups. Table 1.4 summarises the effect of four surface functional groups on preferential protein adsorption.

Table 1.4 The effect of substrate surface functional group on preferential protein adsorption (adapted from Thevenot et al [93]).

Surface Functional Group	Effect on Protein Interaction
Methyl (-CH ₃) neutral, hydrophobic	Strongly binds fibrinogen. Binds IgG more effectively than other surface functional groups.
Hydroxyl (-OH) neutral, hydrophilic	Decreased affinity for plasma proteins.
Amine (-NH ₂) positive, hydrophilic	High affinity for fibronectin.
Carboxyl (-COOH) negative, hydrophilic	High affinity for fibronectin and albumin.

The nature of the substrate surface topography may also influence protein adsorption. In comparison to a smooth surface, a rough surface topography may provide greater surface area for protein interaction.

- *Fluid properties*

The protein concentration of a biological fluid is an important aspect that greatly influences protein adsorption. When considering a fluid that contains one single type of protein only, it can generally be stated that the higher the protein concentration in solution, the greater the protein adsorption to a substrate material. However, in complex biological fluids such as serum, blood, tear fluid and wound fluid, the presence of many competitive adsorbing proteins complicates the process. The relatively abundant plasma proteins, such as albumin and fibrinogen, typically adsorb first onto the substrate. The Vroman effect then leads to partial displacement of the primary layer of adsorbed proteins by proteins with a greater affinity for the substrate surface.

1.6.3.3 Protein Adsorption to Bandage Contact Lenses

Evidence shows that SiHy lenses have a lower susceptibility to general protein adsorption in comparison to conventional hydrogels [94-96]. Protein adsorption to contact lenses worn in the non-compromised healthy eye is a common phenomenon; relatively few adverse effects occur when protein adsorbs on the surface. Complications, such as vision affected by clouding of the contact lens and contact lens discolouration [97], can occur when protein irreversibly denatures on the lens surface. When considering contact lens materials to be worn for therapeutic purposes over extended wear periods, minimal levels of protein deposition at the surface are therefore desirable. SiHy materials, which are renowned for low protein adsorption, appear to be ideal for this purpose.

Protein adsorption is influenced greatly by material properties. Factors such as contact lens water content and ionicity have been linked to the levels of protein deposition; increasing water content and ionicity of materials increases the levels of protein deposits [98].

- FDA Group I (<50% EWC, <0.2% ionic content) materials adsorb approximately 10-20 µg/lens.
- FDA Group IV (>50% EWC, >0.2% ionic content) materials adsorb approximately 1000 µg/lens. Methacrylic acid is a principle component of Group IV contact lenses and provides the materials with a negative polymeric charge, which thereby attracts positively charged proteins.

Duration of contact lens wear can also affect the levels of protein deposits. Jones *et al* [99] investigated the differences in extractable protein between Group II contact lenses replaced monthly over a three month period with contact lenses worn for three consecutive months. This work revealed a significant increase in protein for the longer three month replacement schedule in comparison to the shorter monthly replacements. BCLs are commonly worn in long replacement schedules such as these, yet little is known regarding protein deposits in these circumstances. Protein adsorption to contact lenses is an instantaneous effect of material/host site interaction and is well reported in the non-compromised healthy eye over shorter wear periods, but far less has been

investigated in the compromised healing eye, where contact lenses are worn for extended continuous periods. Additionally, although it is well recognised that certain minimum levels of oxygen permeability are required for continuous wear [100] there is little knowledge in relation to the interactive effects of specific contact lens materials with corneas diagnosed with clinical conditions, and the way in which materials can promote or inhibit the corneal healing process.

1.7 Aims of Research

This thesis is concerned with the interaction of biomaterials with compromised ocular and dermal tissue sites. Section 1.2 of the introduction highlighted the analogies that exist between these two tissue sites. A key aspect is that in severe cases of corneal impairment and tear film dysfunction, the corneal surface will keratinise to give a pseudo-dermal surface. Conversely, distinct parallels may be drawn between the healthy functional cornea and the impaired chronic dermal wound. These analogies require further investigation and it is the exploration of these links which underpin the work in this thesis.

Chapter one addressed that both ocular and dermal tissue sites may suffer from acute and chronic injury and thus require a biomaterial to support the healing process. In the acute/chronic wound environment, skin adhesive materials serve as wound dressings at the dermal wound interface. Similarly, in the compromised ocular environment contact lenses designed for conventional use also serve as therapeutic bandage contact lenses. The material, whether it is a wound dressing or a bandage contact lens, has a substantial influence upon the biological interface. Because the eye is such an easily accessible site, and because contact lenses are particularly well-studied devices, the physical interaction of the contact lens with the cornea appears to be a logical platform for the study of material interactions with compromised tissue sites. There are three aims of this research which will enable these interactions to be studied.

- 1) The first aim is to identify biomarkers which are common to both ocular and dermal sites. One prime candidate is vitronectin, an important cell adhesion glycoprotein present in both tear fluid and wound fluid. The eye is a useful body site to study tissue-biomaterial interactions because the cornea is an easily

accessible tissue site. In order to investigate the nature of biointeractions in the non-compromised ocular environment, the potential value of a novel cell-based on-lens assay technique to detect the presence of vitronectin on the contact lens surface will be explored.

- 2) The second aim of this work is to extend investigations of biomarkers in lens-cornea interactions to bandage contact lenses worn in the compromised eye. The majority of contact lenses suitable for therapeutic use are, in fact, lenses designed for conventional wear. The potential adverse effects of vitronectin deposition on contact lenses worn by symptomatic subjects will be discussed.
- 3) Parallel work in the compromised dermal environment requires examination of the physical properties of skin adhesive wound dressing materials. A third aim is to investigate skin adhesive material properties in relation to the biophysical properties of skin, and to investigate material interactions with unbreached skin. Furthermore, because the dermal wound environment is a far more complex environment to study in comparison to the easily accessible ocular surface, the design of a standard artificial wound fluid is appealing to further tissue-biomaterial interaction studies. Thus, it would be logical to explore the potential design of artificial wound fluid models for acute and chronic wounds, which are influenced by parallel studies in the ocular environment.

CHAPTER TWO

Materials and Experimental Techniques

2.1 Materials

The following section outlines the contact lens materials and skin adhesive wound dressing materials tested within this thesis.

2.1.1 Contact Lens Materials

Table 2.1 lists all daily disposable conventional hydrogel contact lenses and Table 2.2 list all silicone hydrogel (SiHy) contact lenses used for the studies in chapters three and four. The monomer chemical structures of the contact lenses are provided in Table 2.3.

Table 2.1 Daily disposable conventional hydrogel contact lenses and their properties.

Material	Vistagel 38	Vistagel 42	Vistagel 60, 72		Precision UV	Acuvue
USAN/ISO Nomenclature	Filcon I 1	Filcon I 2	Filcon II 2		Vasurfilcon A	Etafilcon A
Manufacturer	Vista Optics	Vista Optics	Vista Optics		CIBA Vision/Alcon	Johnson & Johnson Vision Care
Principal Components	HEMA	HEMA	HEMA/NVP		PMMA, NVP	HEMA, MA
FDA Group	I	I	II		II	IV
Water Content (%)	38	42	60	72	74	58
Modulus (MPa)	0.48	0.43	0.22	0.16	0.25	0.25
Oxygen Permeability (Barrers)	9	10	20	43	39	28
Surface Treatment	No treatment	No treatment	No treatment		No treatment	No treatment

HEMA, 2-hydroxyethyl methacrylate; MA, methacrylic acid; PMMA, methyl methacrylate; NVP, N-vinyl pyrrolidone.

Table 2.2 Silicone hydrogel contact lenses and their properties.

Material	Focus Night & Day	O ₂ Optix	Pure Vision	Biofinity	UltraWave SiH*
USAN/ISO Nomenclature	Lotrafilcon A	Lotrafilcon B	Balafilcon A	Comfilcon A	Filcon II 3
Manufacturer	CIBA Vision/ Alcon	CIBA Vision/ Alcon	Bausch & Lomb	Coopervision	UltraVision
Principal Components	DMA, TRIS, Siloxane macromer	DMA, TRIS, Siloxane macromer	NVP, TPVC, NCVE, PBVC	Aquaform	NVP, Siloxane macromer
FDA Group	I	I	III	I	IV
Water Content (%)	24	33	36	48	58
Modulus (MPa)	1.5	1.0	1.1	0.75	0.5
Oxygen Permeability (Barrers)	140	110	91	128	86
Surface Treatment	25nm plasma coating	25nm plasma coating	Plasma oxidation	No treatment	No treatment

DMA, N,N-dimethylacrylamide; NCVE, N-carboxyvinyl ester; NVP, N-vinyl pyrrolidone; PBVC, poly(dimethylsiloxy) di (silylbutanol) bis(vinyl carbamate); TPVC, tris-(trimethylsiloxy silyl) propyl vinyl carbamate; TRIS, trimethylsiloxy silane.

** please note that UltraWave SiH is the correct name for this contact lens and not UltraWave SiHy*

Table 2.3 Monomer structures of the principle components of contact lens materials.

Monomer Name	Abbreviation	Structure
N,N-dimethylacrylamide	DMA	$\text{CH}_2=\text{C}(\text{H})-\text{C}(=\text{O})-\text{N}(\text{CH}_3)_2$
2-hydroxyethyl methacrylate	HEMA	$\text{CH}_2=\text{C}(\text{CH}_3)-\text{C}(=\text{O})-\text{O}-\text{CH}_2-\text{CH}_2-\text{OH}$
methacrylic acid	MA	$\text{H}_2\text{C}=\text{C}(\text{CH}_3)-\text{C}(=\text{O})-\text{OH}$
poly(methyl methacrylate)	PMMA	$\left[\text{CH}_2-\text{C}(\text{CH}_3)(\text{C}=\text{O})\text{OCH}_3 \right]_n$
N-vinyl pyrrolidone	NVP	$\text{H}_2\text{C}=\text{CH}-\text{N}(\text{CH}_2)_2-\text{CH}_2$
trimethylsiloxy silane.	TRIS	$\text{H}_3\text{C}-\text{Si}(\text{CH}_3)_2-\text{O}-\text{Si}(\text{H})(\text{O}-\text{Si}(\text{CH}_3)_2)-\text{O}-\text{Si}(\text{CH}_3)_3$
3-[Tris(trimethylsiloxy) silyl]propyl vinyl carbamate	TPVC	$\text{H}_3\text{C}-\text{Si}(\text{CH}_3)_2-\text{O}-\text{Si}(\text{CH}_3)_2-\text{O}-\text{Si}(\text{CH}_3)_2-\text{O}-\text{CH}_2-\text{CH}_2-\text{C}(=\text{O})-\text{NH}-\text{CH}_2-\text{CH}=\text{CH}_2$

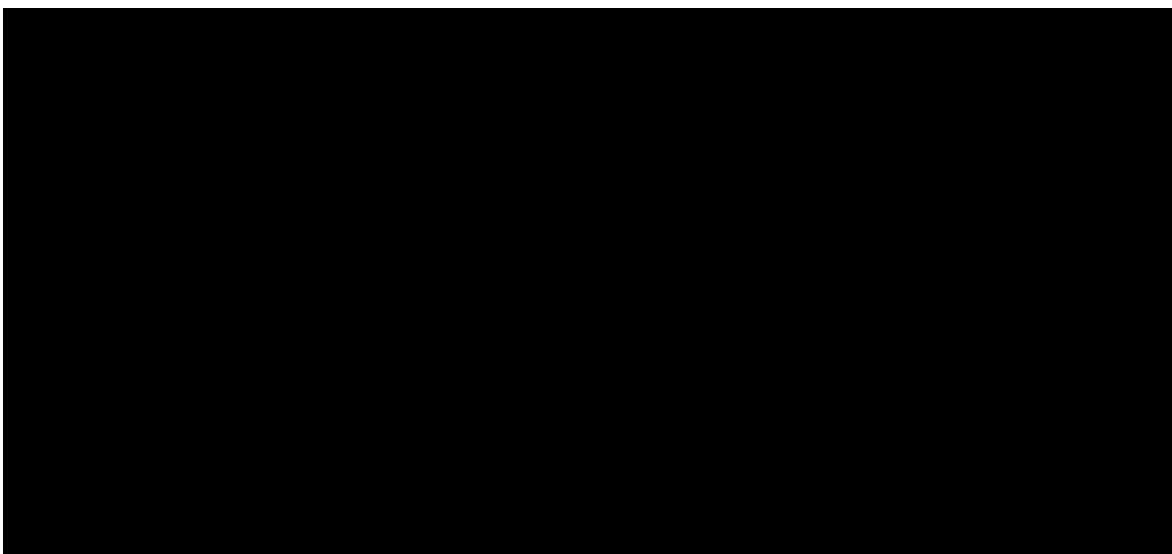
2.1.2 Skin Adhesive Wound Dressing Materials

This section outlines all skin adhesive wound dressing materials used for testing and investigation in chapters five and six.

2.1.2.1 Hydrocolloid Materials Supplied by Salts Healthcare

Much of the work carried out in this thesis was in conjunction with Salts Healthcare, a leading company that manufactures ostomy and healthcare products. Four skin adhesive hydrocolloid materials for wound dressings were supplied by Salts Healthcare. These adhesives are coded as S1, S2, S3 and S4. Table 2.4 lists each adhesive together with the composition, type of release liner (paper or plastic) and thickness without the release liner.

Table 2.4 Skin adhesive wound dressing materials supplied by Salts Healthcare.



A typical hydrocolloid adhesive consists of natural polymer particles (carboxymethyl cellulose, gelatin and pectin) dispersed within an adhesive polymer matrix [51]. These individual components, together with their chemical structures, are presented in further detail.

- Poly(isobutylene)

Poly(isobutylene) (PIB) typically forms the hydrophobic polymer matrix of a hydrocolloid adhesive. When exposed to fluid, the hydrophilic natural polymers absorb the moisture to form a gel. PIB is a hydrophobic molecule because it lacks the presence of any polar groups within its structure (Figure 2.1) and, therefore, PIB becomes dispersed in a continuous aqueous phase as the phase structure inverts.

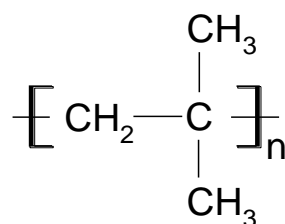


Figure 2.1 The repeat structure of poly(isobutylene).

- Carboxymethyl cellulose (CMC)

Carboxymethyl cellulose (CMC) forms the major fluid absorbing component of hydrocolloids. It is synthesised by reacting cellulose with alkali to form alkali cellulose, which is then reacted with monochloroacetic acid. CMC is an anionic, hydrophilic carbohydrate capable of forming viscous solutions. It is this gel-forming function that is ideal for its inclusion within the typical hydrocolloid composition. The repeat structure of CMC is shown in Figure 2.2.

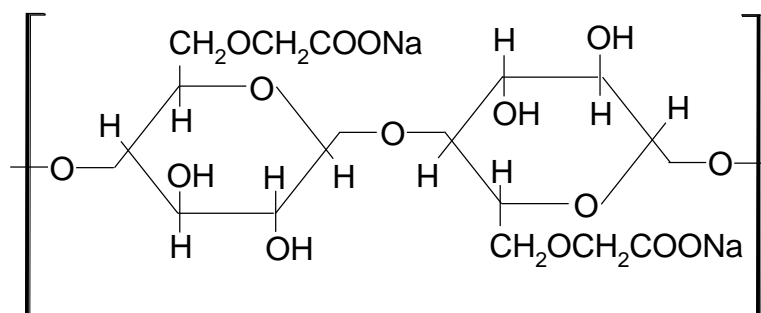


Figure 2.2 The repeat structure of carboxymethyl cellulose.

- Gelatine

Gelatine is a natural protein which is derived from the refinement of animal collagen. It is commonly used as a gel-forming agent within the food industry, but in hydrocolloid wound dressing materials it is dispersed within the PIB matrix for its gelling properties. The structure of gelatine (Figure 2.3) is based on its parent molecule, collagen.

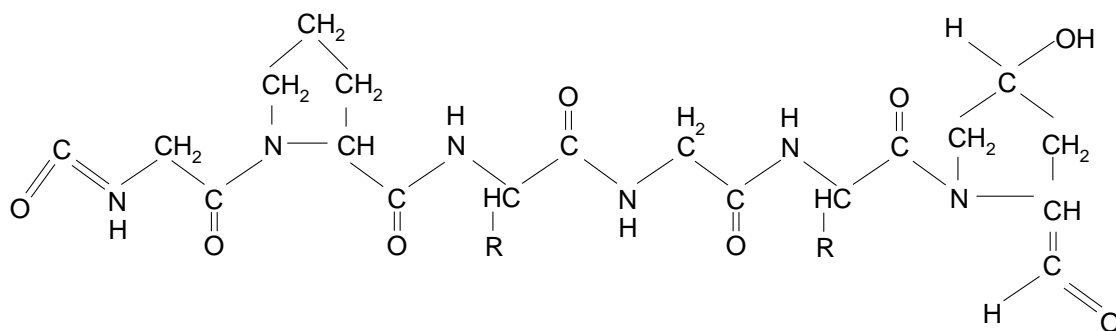


Figure 2.3 The structure of gelatine.

- Pectin

Pectins are natural polysaccharides, which can be extracted from the peel of many fruits and vegetables. Similarly to gelatine, pectin functions as a gel-forming agent in the hydrocolloid structure. Commercially produced pectin may be classified as either low methoxyl pectins (<50% methyl esterification) or high methoxyl pectins (>50% methyl esterification). The repeat unit of pectin is shown in Figure 2.4.

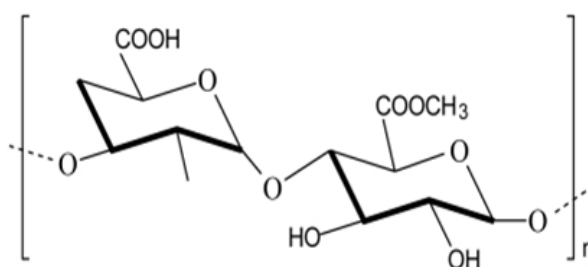


Figure 2.4 The repeat structure of pectin.

2.1.2.2 Other Skin Adhesive Materials

Table 2.5 lists all other skin adhesive wound dressing materials used in chapter five, which were not supplied by Salts Healthcare. This includes Ostomy Hydrocolloid Adhesives, ConvaTec Hydrocolloid Adhesives wound dressings, Commercial Medical Tapes and skin adhesive hydrogels that were synthesised in the laboratory.

Table 2.5 Commercial skin adhesive ostomy, hydrocolloid and medical tapes, and hydrogels prepared in the laboratory.

Product Type	Material Name	Thickness without release liner (mm)
Ostomy Hydrocolloid Adhesives	Coloplast ostomy	1.64
	ConvaTec ostomy	1.63
ConvaTec Hydrocolloid Adhesives	Granuflex	1.64
	Duoderm Extra Thin	0.51
Commercial Medical Tapes	3M microporous tape	1.93
	Boots microporous tape	1.89
Aston hydrogel adhesives*	Hydrogel 1*	1.57
	Hydrogel 2*	1.52

** The methodology for the preparation of the hydrogel adhesives is detailed fully in the Experimental Techniques section 2.2.3.*

2.2 Experimental Techniques

2.2.1 Cell Culture

A cell-based on-lens assay technique to detect the extent and locus of vitronectin on the surface of contact lenses is described.

2.2.1.1 Materials

Table 2.6 lists all chemicals and immunochemicals used for the cell culture work.

Table 2.6 Chemicals and immunochemicals used with name, abbreviation and supplier.

Name	Abbreviation	Supplier and Code
Dulbecco's modified Eagle medium	DMEM	Sigma-D6546
Fetal bovine serum	FBS	Sigma-F7524
Gluteraldehyde	-	Sigma-G6257
HEPES buffered saline	HBS	Sigma-H0887
Human Fibronectin	Fn	Sigma-F2006
Human Vitronectin	Vn	Sigma-V8379
L-glutamine	L-glu	Sigma-G7513
Magnesium chloride	MgCl ₂	Bioline-37026
Rabbit anti-Fibronectin antibody	Anti-Fn	Sigma-F3648
Rabbit anti-Vitronectin antibody	Anti-Vn	Merck-681125
Rabbit IgG	IgG	Sigma-I5006
Trypsin/Ethylenediaminetetraacetic acid	Trypsin/EDTA	Sigma-T4049

2.2.1.2 Isolation and Culture

An ampoule of frozen Mouse 3T3 Swiss Albino embryo fibroblasts cells was purchased from the European Collection of Cell Cultures (ECACC; Salisbury, UK). The ampoule was thawed and suspended in Dulbecco's modified Eagle medium (DMEM), supplemented with 10% fetal bovine serum (FBS) and 1% 200 mM L-glutamine solution. Cells were incubated in a Heracell 150 incubator at 37°C in 5% CO₂, and maintained for up to 10 passages. Cells were passaged upon reaching 80% confluency, as described below. All cell culture procedures were carried out in a laminar flow hood.

2.2.1.3 Determination of Cell Viability

Cell viability was determined by the standard trypan blue dye exclusion test. The test is based on the principle that dead cells with non-intact cell membranes uptake the dye to display a blue cytoplasm, whereas live viable cells do not. 250 µl of cell suspension was mixed with 100 µl of trypan blue dye in a bijou vial. The cell suspension/dye mixture was loaded onto a haemocytometer and ten separate counts were taken to determine cell viability.

2.2.1.4 Passage of Cells

The passage of cells involves the 'splitting' of a monolayer of cells and subsequent reseeding into a new cell flask. The Dulbecco's modified Eagle medium (DMEM) was prepared by adding 50 ml fetal bovine serum (FBS) and 5 ml of 200 mM L-glutamine solution. The medium and trypsin/EDTA were then pre-warmed to 37°C. When the cell flask had reached confluency, the medium was aspirated from the flask by means of a 25 cm³ pipette and discarded. Approximately 3 ml trypsin/EDTA was added to the monolayer of cells and the flask was gently shaken to remove any loose cells, which were then also discarded. A further 5 ml trypsin/EDTA was added to the flask and incubated at 37°C and 5% CO₂ for no longer than 5 minutes. After incubation the cells were seen to have detached from the bottom of the flask, turning the trypsin/EDTA solution slightly cloudy. The cells were observed under an inverted microscope to ensure detachment from the flask. 10 ml medium was added to the flask in order to neutralise the trypsin/EDTA. Of this solution, 10 ml was transferred to a centrifuge tube and centrifuged at 2000 rpm for 5 minutes, after which time a pellet of cells could be

seen. This 10 ml volume of trypsin/media supernatant was aspirated and discarded, and the pellet of cells was resuspended in either 10 ml medium (for further cell culture) or 10 ml HEPES buffered saline (HBS) (for the assay procedure). In order to reseed the cells at the required density, a small volume of suspended cells was placed in a haemocytometer slide to count the average number of cells. The density of cells to be reseeded was then calculated using the following calculations:

- a) Total no. cells in culture
= average cell count * vol. size of each square * vol. of cell suspension
= average cell count * 10^4 x 10
- b) Volume of cells to be reseeded
= (concentration required * vol. of flask) / total no. cells in culture

Medium was then added to a new cell flask together with the calculated volume of cell suspension and incubated at 37°C in 5% CO₂.

2.2.1.5 In Vitro Doping of Contact Lenses

Contact lenses were removed from packing solution and rinsed in phosphate buffered saline (PBS). Lenses were blotted, placed aseptically in polystyrene bijou vials and doped with specific solutions, which varied according to the requirements of each assay requirement. The individual bijou vials were placed on an orbital shaker for 24 hours at room temperature. Lenses were assayed in triplicate.

2.2.1.6 Ex Vivo Contact Lenses

Contact lenses were worn by asymptomatic subjects in either a daily wear modality, averaging 196 hours over 2 weeks, or an extended wear modality, averaging 168 hours over 1 week, as specified with each assay. Upon removal contact lenses were placed in PBS and stored at 4°C.

2.2.1.7 On-Lens Cell Attachment Assay Procedure

On-Lens Cell Attachment Assay Procedure: All solutions and analytes were pre-heated to 37°C. A magnesium chloride stock solution (MgCl₂, 50 mM), a rabbit IgG solution (300 µg/ml in HBS) and a 1% solution of glutaraldehyde in HBS were prepared. Each

assay procedure required the use of three controls; a vitronectin positive control, an antibody control and an anti-vitronectin control. The contact lenses, removed from either doping solution (control lenses and unworn lenses) or PBS (worn lenses), were placed individually into the appropriate test wells of a 24-well plate. Each well was rinsed with 1 ml HBS (x3). 1 ml HBS was added to the vitronectin positive control well, 1 ml of the prepared IgG solution was added to the antibody control well, and 100 μ l anti-human vitronectin diluted with 900 μ l HBS was added to the anti-vitronectin control well. Each 24-well plate was incubated for 60 minutes, at 37°C and 5% CO₂, and gently agitated every 10 minutes. After incubation, the solution from each contact lens was aspirated by means of a pipette taking care not to touch the lens. 1 ml of serum free HBS cell solution and 100 μ l of MgCl₂ stock were added to each well. The 24-well plate was then incubated for a further 60 minutes at 37°C and 5% CO₂. Following this second incubation period, the cell solution from each well was removed, and each well and contact lens was rinsed with 1 ml HBS three times. All contact lenses were moved to a new 24-well plate and rinsed once with 1 ml HBS. The cells were fixed in 1 ml of 1% glutaraldehyde stock solution ready for counting. A schematic diagram of the on lens - cell attachment assay is shown in Figure 2.5.

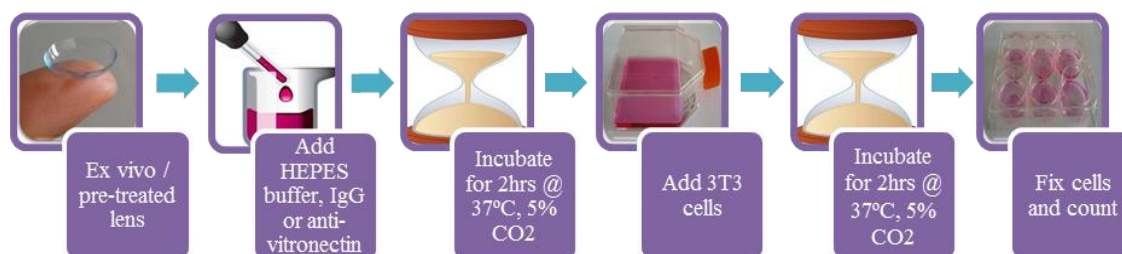


Figure 2.5 The on-lens cell attachment assay procedure for the location and quantification of surface-bound vitronectin on ex vivo or vitronectin-doped contact lenses.

Cell counts: In order to count the surface-located cells, each contact lens was notionally divided into two areas; the edge and the centre. The field of vision in which each individual count was taken was defined by an internal graticule in the eye piece of the microscope. The eye piece graticule measures 1 cm x 1 cm, which when read under a x10 magnification allowed a field of vision of 1 mm². Cell counts were taken at four areas on the edge of the lens and one area at the centre of the lens, as shown in Figure 2.6.

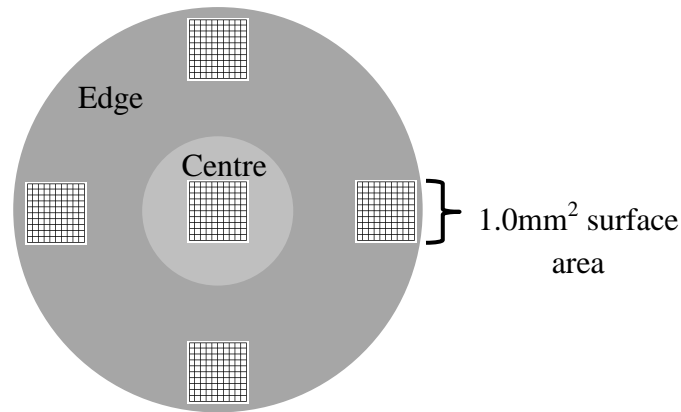


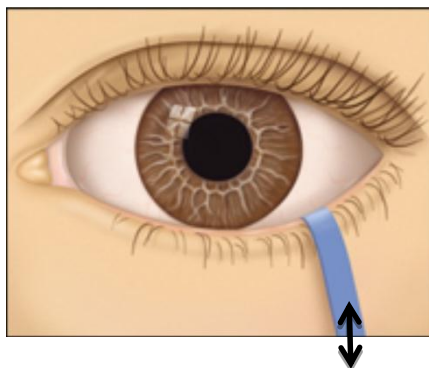
Figure 2.6 Five defined areas on the posterior contact lens surface for recording cell counts (zones not to scale).

2.2.2 Schirmer Test

The Schirmer test is a method for the measurement of tear secretions. It is one method of evaluating patients with dry eye symptoms. The test was first described by Schirmer in 1903 as a method to measure the amount of tears wetting a filter paper strip in 5 minutes [101]. A standardised filter paper strip is typically 35 mm by 5 mm. It is folded at one end to create a rounded lip, which is intended to reduce discomfort upon insertion in the eye.

Tests were performed on subjects who required the use of a bandage contact lens to manage an ophthalmic or corneal condition. The tests were carried out prior to bandage contact lens insertion. The end of the Schirmer strip with the folded lip was inserted into the lower eyelid, taking care not to touch the cornea (Figure 2.7). Subjects were asked to blink normally or to close their eyes as appropriate for the duration of the 5 minutes. The Schirmer strip was removed after the 5 minutes period using tweezers and the length of the wetted strip was measured to provide a Schirmer score. The following Schirmer scores are guidelines for tear secretion measurements [102]:

- ≥ 15 mm/5 minutes : normal
- 14 – 6 mm/5minutes : mild to moderate
- < 6 mm/5 minutes : severe



filter paper placed on the lower eyelid

Figure 2.7 The Schirmer test for sampling of tear secretions.

2.2.3 Preparation of Skin Adhesive Hydrogels

2.2.3.1 Materials

Anionic monomers:

- Sodium salt of 2-(acrylamido)-2-methyl propane sulfonate (NaAMPs)

Molecular weight: 229.23

[58% solution supplied by Lubrizol]

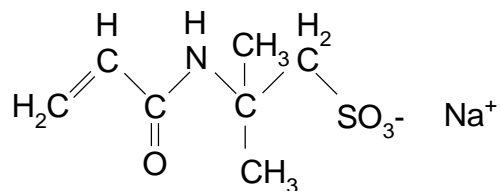


Figure 2.8 The structure of sodium salt of 2-(acrylamido)-2-methyl propane sulfonate (NaAMPs.)

- Potassium salt of 3-sulfopropyl acrylate (SPA)

Molecular weight: 232.29

[Supplied by Raschig]

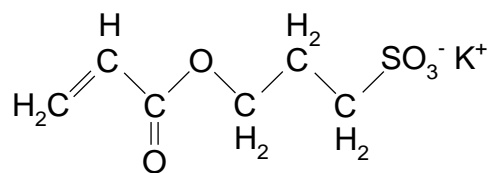
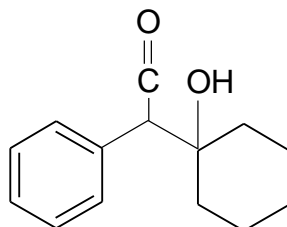


Figure 2.9 The structure of potassium salt of 3-sulfopropyl acrylate (SPA).

Initiator:

- 1-hydroxycyclohexyl phenyl ketone (Irgacure 184)

Molecular Weight: 204.27



[Supplied by CIBA]

Figure 2.10 The structure of Irgacure 184.

Crosslinker:

- Ebecryl 11

[Supplied by U.C.B – the structure of this poly(ethylene) diacrylate photo crosslinker is not available from its supplier]

Other Reagents:

- 1,2,3-propanetriol (Glycerol)

Molecular weight: 92.09

[Supplied by Sigma Aldrich]

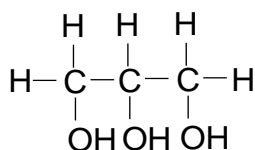


Figure 2.11 The structure of glycerol.

2.2.3.2 Preparation of Skin Adhesive Hydrogels Method

Skin adhesive hydrogels were prepared by photopolymerisation. This form of photopolymerisation has the following advantages:

- spatial and temporal control over thermal polymerisation
- fast curing rates

- minimal heat production

Two hydrogel compositions (Hydrogel 1 and Hydrogel 2) were prepared by using varying amounts of distilled water, glycerol, monomers and a photoinitiator/cross linker mixture, as shown in Table 2.7. The photoinitiator/cross linker mixture consists of a UV acrylated urethane crosslinker (Ebacryl 11) and a UV initiator (Irgacure 184). The photoinitiator/cross linker mixture was measured into a glass vial with a ratio of 10:3 (2.5:0.75g). The vial was placed onto an orbital shaker for 30 minutes to ensure the mixture had been adequately mixed. The vial was stored in darkness to prevent photodegradation of the initiator by stray light.

Table 2.7 Compositions of skin adhesive hydrogels – Hydrogel 1 and Hydrogel 2.

	Hydrogel 1	Hydrogel 2
Distilled Water (g)	1.1	10.0
Glycerol (g)	30.0	30.0
NaAMPs	68.9	40.0
SPA	0.0	20.0
Photoinitiator/cross linker mixture (g)	0.25	0.25

NaAMPs, 2-acrylamido-2-methyl-1-propanesulfonic acid, sodium salt, 50% wt solution in water; SPA, 3-sulfopropyl acrylate, potassium salt.

For each hydrogel composition, the water, glycerol and monomers were mixed in glass vessels and shaken gently to ensure thorough mixing. The photoinitiator/cross linker mixture (0.25 g) was added to the monomer mixture and the vessel was inverted three times. The mixture was poured immediately into a metal tray lined with release paper and then passed under a UV lamp (GEW Ultraviolet Lamp) at a speed of 5 m/mins, until the monomers had completely polymerised to form an adhesive gel. This typically took five passes on a moving conveyor under the UV lamp. To prevent contamination and dehydration, the hydrogels were covered with a paper release liner and stored in poly(ethylene) bags.

2.2.4 Surface Energy Measurements

Surface energy measurements were taken for the skin adhesive materials as listed in Table 2.4 and Table 2.5 using the sessile drop technique.

2.2.4.1 Materials

Water and diiodomethane were used as two separate probe liquids. These liquids were chosen because of their opposing polar components; water has a high polar component (51.0 mNm⁻¹) whereas diiodomethane in comparison has an extremely low polar component (2.3 mNm⁻¹). The surface free energy data for each probe liquid, which includes the polar component [$\gamma_{lv}(p)$], dispersive component [$\gamma_{lv}(d)$], surface tension [$\gamma_{lv}(T)$] and contact angle is provided in Table 2.8.

Table 2.8 The surface free energy data for water and diiodomethane.

Liquid	$\gamma_{s(p)}$	$\gamma_{s(d)}$	$\gamma_{s(T)}$	Contact Angle (°)
Water	51.0	21.8	72.8	60
Diiodomethane	2.3	48.5	50.8	40

2.2.4.2 The Sessile Drop Technique

Surface and interfacial behaviour of synthetic materials govern their biocompatibility with aqueous environments, such as the open wound. Surface energy is a concept that describes the potential energy of surface molecules. The cohesive forces of attraction between molecules at the centre of a liquid drop are the same in every direction. At the surface of the drop, however, the cohesive forces of attraction are unbalanced, giving rise to the spherical shape of the droplet. The molecules at the surface therefore possess energy known as surface energy or surface tension. Weak cohesive forces between molecules at the surface give rise to a lower surface energy and vice versa.

When a liquid comes into contact with a solid, forces of attraction between the two surfaces lead to the concept of interfacial tension. A lower interfacial tension will allow the liquid to spread over the surface. Interfacial tension is given by Equation 2:

$$\text{Equation 2} \quad \gamma_{1,2} = \gamma_1 + \gamma_2 - 2(\gamma_{1p} \cdot \gamma_{2p})^{1/2} - 2(\gamma_{1d} \cdot \gamma_{2d})^{1/2}$$

The sessile drop technique is a means of evaluating surface free energy of a solid by contact angle measurements. The technique was used to calculate the surface energy of a range of skin adhesive wound dressing materials and ostomy devices (as listed in Table 2.4 and Table 2.5). A GBX Digidrop instrument was used with the Windrop

software program. Adhesive materials were prepared to give 1cm² sized samples. The release liner was removed from the adhesive material and the sample was placed on the platform of the GBX. Two probe liquids were used: water and diiodomethane. The syringe component was filled with the probe liquid, taking care to ensure there were no air bubbles present. A separate syringe was used for each probe liquid to prevent any contamination. A droplet of probe liquid was then suspended from the needle of the syringe until an appropriate sized droplet was formed. The platform of the GBX instrument, with the sample in place, was raised automatically, causing the droplet to drop onto the sample (Figure 2.12). A contact angle is formed at the liquid-solid interface. The angle formed can give rise to wetting, partial wetting or non-wetting hysteresis owing to the adhesive and cohesive forces involved, as shown in Figure 2.13. A high contact angle (greater than 90°), or low/non-wetting surface, indicates a low surface energy. Conversely, a low contact angle (less than 90°), or high wetting surface, indicates a high surface energy. The integrated camera of the instrument photographed the droplet shape upon contact with the sample and simple on-screen integration allowed the contact angle to be recorded. Five contact angle measurements were taken for each adhesive to provide an average angle and the method was repeated for both probe liquids. Surface energies were determined using an Excel spreadsheet application.

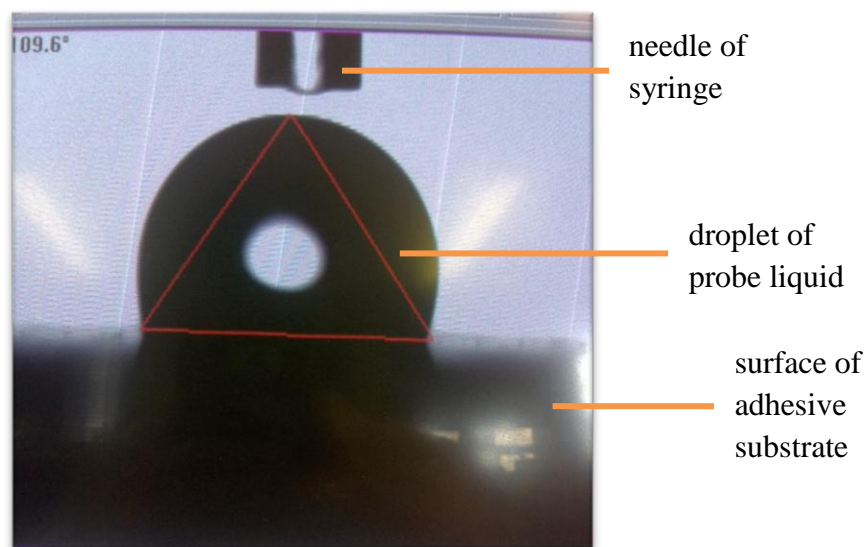


Figure 2.12 A droplet of probe liquid forming a contact angle with a solid surface.

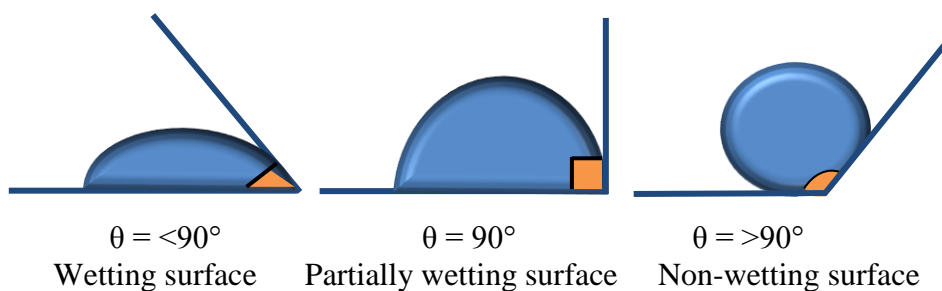


Figure 2.13 Contact angle hysteresis.

2.2.5 X-ray Photoelectron Spectroscopy

X-ray photoelectron spectroscopy (XPS), also referred to as electron spectroscopy for chemical analysis (ESCA), is a powerful surface sensitive chemical analysis technique to investigate the chemical composition of surfaces. The technique, which was developed in the mid 1960's by Siegbahn, is based upon the photoelectric effect whereby an X-ray source is used to ionise electrons from the surface of a solid sample. In this work, XPS was used to analyse the surface of Salts Hydrocolloid Adhesives S1, S2, S3 and S4 (listed in Table 2.4) with their respective release liners. Samples of 2 cm² were prepared and sent externally for analysis to Midlands Surface Analysis.

XPS irradiates the solid surface of a sample with mono-energetic X-rays, causing the electrons of atoms at the surface to become excited. Each element has a characteristic binding energy. If the electrons of an element have a binding energy less than the X-ray energy, photoelectrons will be emitted from the sample surface (as shown in Figure 2.14). Only photoelectrons at the extreme outer surface of the sample are ejected (at a penetration depth of 10 nm), thus XPS is sensitive surface analysis technique. The kinetic energies of photoelectrons relate to the speed at which they are emitted from the sample and can be measured from the simple Equation 3 which relates kinetic energy to the binding energy:

$$\text{Equation 3} \quad KE = h\nu - BE - e\Phi$$

where

KE: Kinetic Energy of ejected photoelectron

$h\nu$: Characteristic energy of X-ray photon

BE: Binding Energy of the atomic orbital from the electron

$e\Phi$: Spectrometer work function

The kinetic energy enables direct identification of elements in the sample from peaks in the photoelectron spectrum. The presence of a peak at a particular kinetic energy indicates the presence of a specific chemical element and the intensity under each peak is related to the concentration of the element.

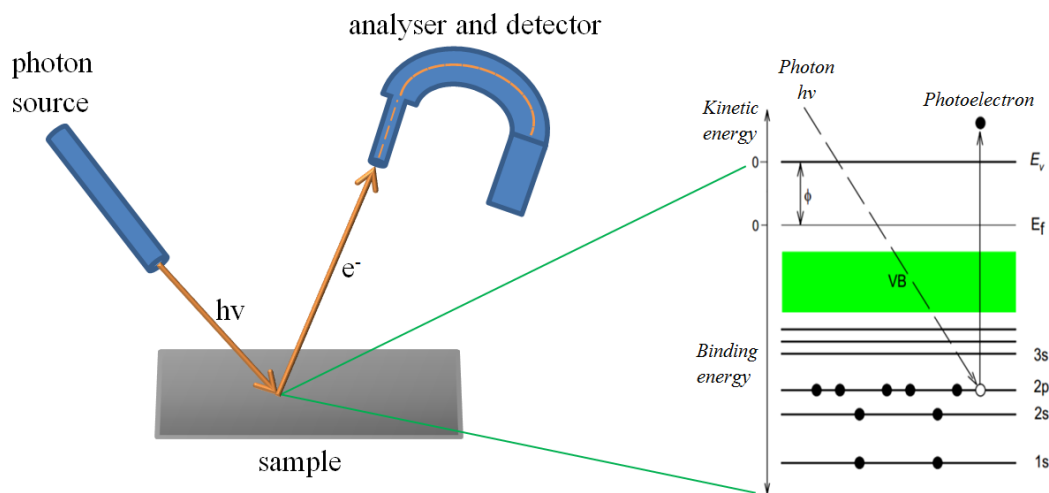


Figure 2.14 Photoelectron spectroscopy - excitation of electrons to emit photoelectrons by photoemission.

2.2.6 Peel Strength

The adhesive strength of a material, or the strength of an adhesive bond between two materials, may be measured by peel strength tests. As discussed in the main introduction to this work, the adhesive component of a dermal wound dressing has many functions. Amongst these, the adhesive must not fail cohesively during application and must not cause trauma upon removal from the wound site. Therefore, peel tests were performed for skin adhesive materials listed in Table 2.4 and Table 2.5 to determine adhesive strength and ease of removal from skin. Tests were performed at 90° on skin and a steel substrate and at 180° on steel using a Hounsfield Hti tensometer. The tests provided the average peel strength (N), the average peel strength per width (N/mm) and the maximum force of removal (N).

Adhesive materials samples were cut into strips measuring 12 cm by 2.5 cm, with the release liners in place. All samples were tested in triplicate.

90° Peel Test – Steel Substrate

The 90° peel test required a test fixture to create a 90° angle between the adhesive sample and the substrate. A wooden base with a sliding tray was placed directly underneath the tensometer grip. The steel substrate was positioned at the centre of the sliding tray so that the substrate was perpendicular to the grip (the substrate was held in place using tape). The release liner from the adhesive sample was then removed and the sample was applied to the steel substrate. A representation of the test set-up is shown in Figure 2.15A. A 1 kg weight was rolled over the length of the material to ensure adequate adhesion. The sample was left for 5 minutes before testing in order to keep adhesion times consistent between samples. A tensometer grip was attached to one end of the sample and the strip was peeled from the steel substrate at a peel speed of 500 mm/min using a 10 N load cell. The sliding tray was moved at a rate steady with the peel speed to ensure that the 90° angle between the adhesive and substrate remained consistent throughout the test.

90° Peel Test – Skin Substrate

The 90° peel test was conducted on skin to provide a comparison against steel. Tests were carried out in a similar method as described above for steel, but on the unbreached forearm skin of a healthy volunteer. The release liner of the adhesive was removed before sample application to the forearm and a 1 kg weight was rolled over the sample. Again, the sample was left for 5 minutes before the peel test was carried out. The arm was then placed on the sliding tray and the test was performed. The forearm was cleaned with methanol before and after each test to remove any dirt, lipids, or residual adhesive left from samples.

180° Peel Test – Steel Substrate

The 90° peel test on steel was modified to increase the angle between the adhesive sample and steel substrate from 90° to 180°. The wooden box was turned vertically underneath the tensometer grip and the tests were repeated as described for the 90° tests on steel (Figure 2.15B). Because of the difficulty in positioning the arm at 180°, it was not possible to conduct tests on skin as well.

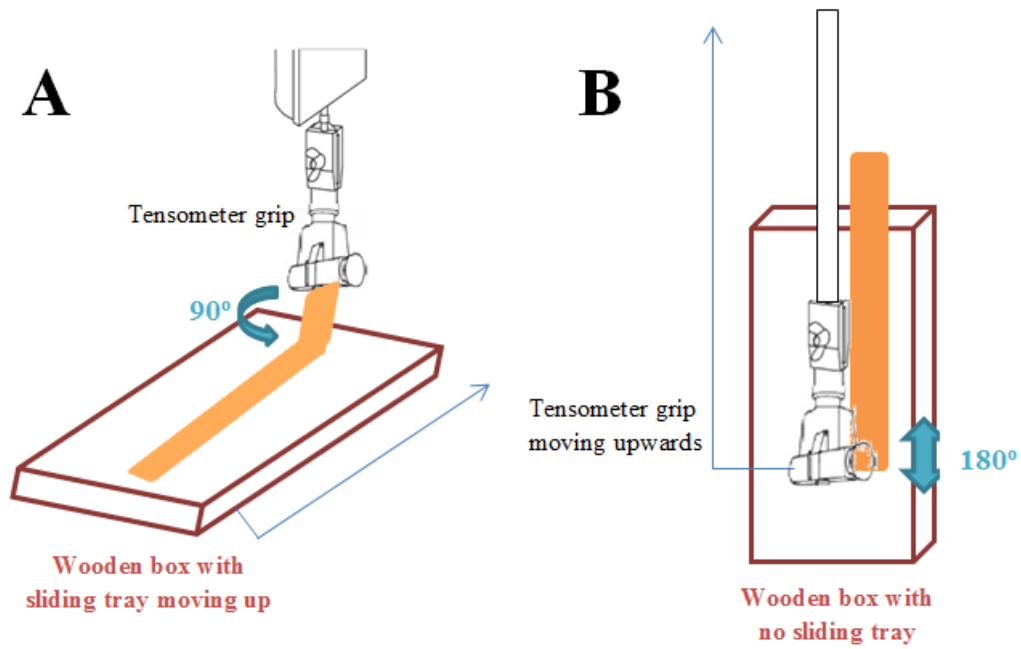


Figure 2.15 A representation of the peel test set-up at: A) 90° and B) 180°.

2.2.7 Tensile Strength

Tensile strength testing of adhesive materials provides an indication of the mechanical strength and elasticity of adhesives. Tests were conducted on skin adhesive wound materials listed in Table 2.4 and Table 2.5 using a Hounsfield Hti tensometer coupled with QMAT Testzone software. During a tensile test a load is applied to a sample until it stretches and breaks. Three values are provided from a typical tensile test:

- 1) tensile strength (T_s) - the maximum stress applied before the adhesive breaks

$$\text{Equation 4} \quad T_s = \text{load at break} / \text{cross-sectional area}$$

- 2) elongation at break (E_b) - percentage increase in length of adhesive before it breaks under tension

$$\text{Equation 5} \quad E_b = (\text{extension of gauge length} / \text{original gauge length}) * 100$$

- 3) the elastic modulus (E.mod) – also referred to as Young's modulus, this is a measure of rigidity

$$\text{Equation 6} \quad E.\text{mod} = \text{stress} / \text{strain}$$

where stress = load / cross-sectional area

strain = extension of gauge length / original gauge length

Samples were cut from the adhesive materials using a dumbbell shaped cutter to give dimensions of 8 mm gauge length and 3.3 mm width. The sample size is shown in Figure 2.16. Where samples had a woven backing on the non-contact side of the adhesive, the backing was removed using acetone. A few millilitres of acetone were used to dampen the backing to enable it to be peeled off. This did not appear to affect the integrity of the adhesive material itself. The thickness of each sample was determined using a micrometer.

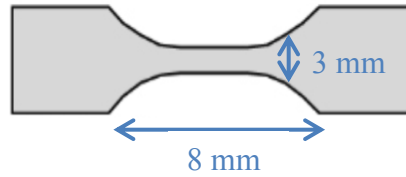


Figure 2.16 Dimensions of an adhesive samples for tensile testing.

The release liner was removed from the sample prior to testing and the sample was clamped vertically between the two grips of the tensometer. The sample was stretched at a test speed of 100 mm/min under a 10 N load cell and 30 mm extension range. A diagrammatic representation of the test set-up is shown in Figure 2.17. Each sample was tested in triplicate. The tensile strength at break, elongation at break and Young's modulus for each sample were recorded.

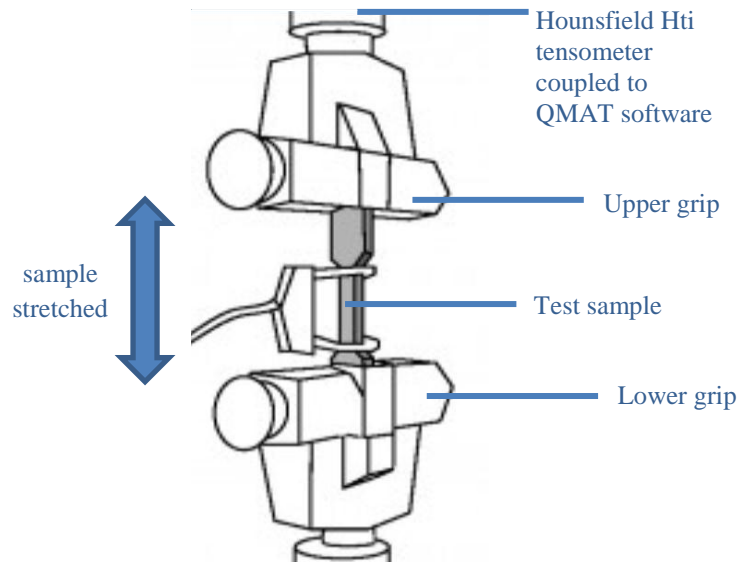


Figure 2.17 A representation of the tensile strength test set-up.

2.2.8 Dynamic Testing

Rheology testing was performed on skin adhesive materials listed in Table 2.4 and Table 2.5. Rheology is the study of deformation and flow of matter under the influence of an applied sheared stress. Material deformation behaviour may be described by two parameters. Elasticity describes the property that enables a material to return to its original undeformed state after a deforming stress is applied and removed. The energy that is used to cause the deformation is stored and then released once the stress is removed and relaxation has occurred. This is signified by the elastic, or storage, modulus (G'). Viscosity describes the non-recoverable linear deformation of a material. It is a measure of the resistance of a material to being deformed. This is described by the viscous, or loss, modulus (G'') and such behaviour is characteristic of liquids.

Most materials exhibit both elastic and viscous behaviour; hence these are viscoelastic materials. The viscoelastic behaviour of a material may be measured as a function of frequency by deforming the material with an applied stress to in turn cause a strain. An oscillation test, where an oscillating force is applied to the sample whilst the frequency is varied, generates a sinusoidal stress or strain. The difference between the stress and sine waves is the phase shift (δ). The $\tan \delta$ is a ratio of the viscous modulus (G'') to the elastic modulus (G'). $\tan \delta$ values below a certain value indicate elastic-dominant 'solid-like' behaviour, whereas values above this value indicate more viscous-dominant 'liquid-like' behaviour. The $\tan \delta$ values may be calculated by Equation 7:

$$\text{Equation 7} \quad \tan \delta = G''/G'$$

The viscoelastic behaviour of skin adhesive materials was measured using a Bohlin CVO Rheometer. 20 mm discs were cut from adhesive materials in their unhydrated form using a number 13 cork borer. All tests were performed at 37°C to represent body temperature conditions. The release liners were removed from the samples and the samples were then loaded individually onto the lower plate of the rheometer and subjected to an oscillating frequency of between 0.5 Hz and 25 Hz. The lower frequencies were chosen to represent the application of adhesive materials to skin, whereas the higher frequencies represent the removal of the materials from skin. All samples were repeated in triplicate. The elastic modulus (G') and viscous modulus (G'') were recorded for each sample.

2.2.9 Total Protein Method

2.2.9.1 Materials

The total protein content of biological fluids was detected and quantitated by a Micro BCA Protein Assay Kit purchased from Thermo Scientific (product code 23225). The kit consists of a Micro BCA Reagent A, Micro BCA Reagent B, Micro BCA Reagent C and Bovine Serum Albumin (BSA) Standard ampules.

2.2.9.2 Preparation of Diluted Albumin Standards

A set of protein standards was prepared from the BSA Standard, according to Table 2.9. The Albumin Standard was diluted with saline to give 7 vials (A-G) of protein concentrations from 1000 µg/ml to 0 µg/ml. A new set of standards was prepared for each test.

Table 2.9 Preparation of bovine serum albumin (BSA) standards.

Vial	Final Concentration (µg/ml)
A	1000
B	750
C	500
D	375
E	250
F	125
G	0 = Blank

2.2.9.3 Preparation of the Micro BCA Working Reagent (WR)

The Working Reagent (WR) was prepared from the three Micro BCA Reagents using the following calculation:

Volume of WR = (#standards + #unknowns) * (# replicates) * (volume of WR per sample)

i.e. to test 5 unknown samples in triplicate:

$$\begin{aligned}\text{Volume of WR} &= (7 + 5) * (3) * (1) \\ &= 36 \text{ ml}\end{aligned}$$

Micro BCA Reagent A (25 parts) was mixed with Micro BCA Reagent B (24 parts) and Micro BCA Reagent C (1 part). The WR reagent was mixed thoroughly to give a clear-green solution. The reagent was stored at room temperature and discarded after one day.

2.2.9.4 Total Protein Determination

1 ml of each BSA standard and unknown sample was pipetted into appropriately labelled test tubes. 1 ml of the WR was added to each tube and mixed well. The tubes were covered and incubated at 60° in a water bath for 1 hour. After this incubation period the tubes were cooled to room temperature to allow for colour development. The absorbance of all the standards and samples were measured on a SpectraMax M2 spectrophotometer at 562 nm. Colour development still occurs after the cooling period at a low rate, therefore, all absorbance measurements were made within a 10 minute time period. The average absorbance reading of the blank standard (0 µg/ml) was subtracted from the remaining standards and unknown samples to provide blank-corrected readings at 562 nm. A concentration curve was determined by plotting the blank-corrected reading for each standard versus its concentration in µg/mL. The total protein concentration of each unknown sample was determined by extrapolation of the concentration curve. An example of a curve is provided in Figure 2.18.

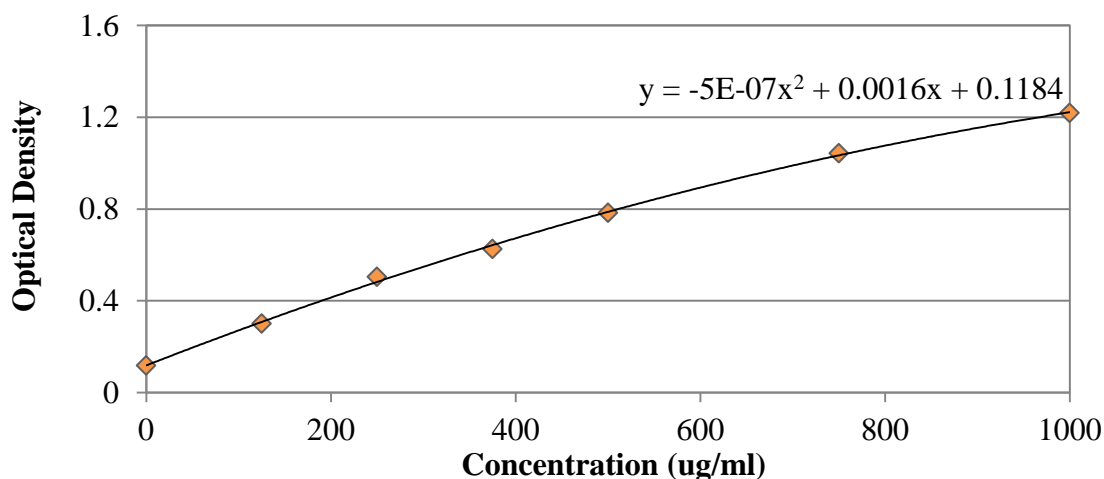


Figure 2.18 A concentration curve for bovine serum albumin standards at 0-1000 µg/mL.

2.2.10 Osmolarity Measurements

Osmolarity measurements were made on a micro-Digital CamLab osmometer. The osmometer was calibrated with a standard solution of known osmolarity, for example pH 7 phosphate buffered saline (300 mOsm/kg).

CHAPTER THREE

The Nature and Consequences of Vitronectin Interactions in the Non-Compromised Contact Lens- Wearing Eye

3.1 Aim

The main introduction to this thesis highlighted vitronectin as a very adhesive glycoprotein with a high affinity for hydrogel biomaterials. It is likely that this affinity extends to hydrogel contact lenses. The important roles of vitronectin as a cell adhesion molecule in the wound healing process have also been discussed. It is this cell-binding function that forms the basis of this work. Vitronectin was selected to investigate interactions with hydrogel contact lenses in the healthy non-compromised eye by the use of a novel on-lens cell attachment assay technique.

The aim of this chapter was to investigate the locus and extent of vitronectin-mediated cell adhesion on *ex vivo* contact lenses and to determine the influence of wear modality together with surface and bulk characteristics of the contact lens material. A cell-based vitronectin mapping technique was used to investigate vitronectin-mediated cell adhesion to a range of lens contact materials.

3.2 Introduction

3.2.1 Introduction

A contact lens has the potential to alter normal ocular function. Specifically, material composition has the propensity to affect local changes in tear biochemistry, particularly those encountered in the post-contact lens environment [103]. There is growing interest in the biomarkers related to inflammation and immunoregulation of the ocular environment in contact lens wear. One interesting candidate biomarker is vitronectin, a prominent inflammatory regulatory glycoprotein and adhesion molecule, which has been detected in tears [104, 105]. Section 1.3.5 emphasised vitronectin as an important inflammatory marker and very adhesive protein with a high affinity for natural and synthetic compositions – a feature that is of particular relevance to studies of lens-eye interactions. Additionally, due to the adhesive nature of vitronectin, once adsorbed to a surface it is very difficult to remove. This property enables the locus of specific physical interaction of the contact lens and the cornea to be determined. The purpose of this work was to determine the locus and the extent of maximum physical interaction of a range of contact lenses upon the cornea in the non-compromised eye, and to determine the influence of this on wear modality together with surface and bulk

characteristics of the contact lens material. A novel on-lens cell-based vitronectin mapping technique was used to quantify vitronectin-mediated cell adhesion on contact lenses doped *in vitro* and on *ex vivo* contact lenses, and therefore assess the potential upregulation of the plasmin protease which is found in the post-contact lens environment.

3.2.2 *Vitronectin in Tears*

The concentration of vitronectin in tears has been shown to be dependent on the tear state; the levels in reflex, open-eye, and closed-eye tear samples have been reported to be 0.08 ± 0.3 $\mu\text{g/ml}$, 0.75 ± 0.32 $\mu\text{g/ml}$, and 3.7 ± 2.2 $\mu\text{g/ml}$ respectively [104, 105]. Detection in tears can, however, be difficult because other proteins with similar molecular weights (e.g. albumin at 68 kDa, lactoferrin at 77 kDa) are often found in higher concentrations in tears and can therefore mask vitronectin. It has been proposed that the majority of vitronectin comes from conjunctival blood vessels [105], but more recently, vitronectin was found within the basement membrane of the corneal epithelium, which may indicate a possible endogenous source [106]. It has also been suggested that the overall elevation of protein levels during eye closure is due to an increase in vascular permeability in combination with the accumulation of leakage products resulting from a reduced tear turnover [104, 107]. The effect of vascular leakage on the ocular surface and the potential consequences of the altered overnight ocular environment are at present poorly understood. Although the parallel influx of certain components, including plasmin and complement proteins are likely to be related [108], the anti-inflammatory properties of vitronectin, such as the inhibition of complement lysis and plasmin-mediated inflammation, may be extremely important in controlling or co-controlling the closed eye environment.

The diverse list of functions of vitronectin and its involvement in many cascades generally relate to its interactions with plasma associated proteins and systems, suggesting its relevance in the eye may be less important. However, this cannot be the case with growing evidence of more and more plasma proteins 'invading' the tear film as a result of inflammation, ocular dysfunction, and diurnal variation and contact lens wear amongst others [109-111]. Contact lens wear can induce mild or acute red eye, involving vascularisation of the cornea, thus increasing the permeability of the blood/tear barrier and creating more susceptibility to plasma/serum leakage.

Consequently, the contact lens has the potential to alter normal ocular function. Specifically, material composition has the propensity to affect local changes in tear biochemistry, particularly those encountered in the post-contact lens environment [103].

3.3 Method Validation - *In Vitro* Demonstration of the On-Lens Cell Attachment Assay for the Detection of Vitronectin-Mediated Cell Adhesion

3.3.1 Assessment of the Contributory Role of Vitronectin

The cell attachment assay used in this work relies on the basis that vitronectin adheres to contact lens surfaces and that fibroblast cells with integrin receptors for vitronectin adhere to the contact lens using vitronectin as the binding ligand. An initial experiment was performed to prove that vitronectin adsorbed out of solution onto the contact lens surface and that it could be detected using the cell-based assay. Three Group I unworn polyHEMA contact lenses were doped for 24 hours *in vitro* with a 20 µg/ml solution of vitronectin, by the doping method described in section 2.2.1.5. A duplicate set of unworn, non-doped polyHEMA contact lenses (n=3) were assayed as a control. The choice of a Group I set of contact lenses in this assay was used to take the assay to the limits. Group I lenses are known to display lower levels of spoilation over various wear regimes compared to Groups II and IV, and thus could be classed as the lowest threshold for all contact lenses to be analysed. The cell assay involves the selective inhibition of the adhesion molecules, by the use of antibody blocking techniques, to validate the significance of vitronectin-mediated cell adhesion on the contact lens surface. An anti-vitronectin (anti-Vn) antibody control diluted to 1:100 in HBS was incorporated into the assay to block the action of vitronectin and used as a comparison against the vitronectin standard control wells in order to assess vitronectin-mediated cell adhesion to the lens. The use of an IgG antibody, at 300 µg/ml, as a control was to negate the action of an arbitrary antibody in the system. For *in vitro* assays human vitronectin diluted in PBS to give a range of concentrations was used as the positive vitronectin control (Vn positive control).

Figure 3.1 shows that the average cell count per field to doped contact lenses was greatest for the vitronectin positive control contact lenses (59 ± 3) and for the antibody control contact lenses (52 ± 3), whereas the contact lenses blocked with anti-vitronectin demonstrated low cell counts per field (4 ± 2), as expected. A set of four non-doped polyHEMA contact lenses was also assayed as a control group where an average background level of <5 cells was observed on all lenses; this is a similar cell count to the lenses treated with anti-vitronectin (also shown on Figure 3.1). The comparison of cell counts between the blank lenses and doped lenses shows a 20-fold increase in the average cell count per field.

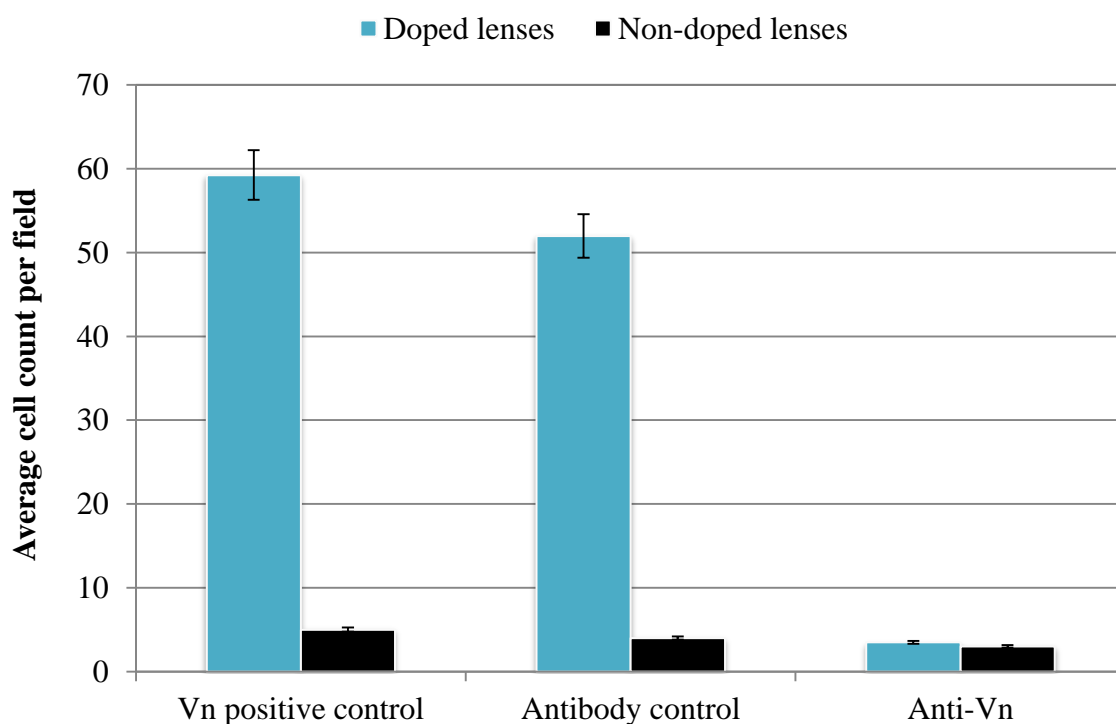


Figure 3.1 Cell counts on polyHEMA contact lenses doped with $20\ \mu\text{g/ml}$ vitronectin *in vitro*.

3.3.2 Assessment of the Contributory Role of Fibronectin

Fibronectin is an important adhesion protein which, in addition to vitronectin, has been reported in tears [112]. Both of these cell attachment-promoting proteins are immunologically unrelated and biochemically different, but due to the fact that their cell adhesive properties are similar, it was inadvisable to assume that vitronectin was solely responsible for both adsorption onto the contact lens and the cell-mediated adhesion. From a doubling dilution range of standards, a concentration of $12.5\ \mu\text{g/ml}$ of

fibronectin was selected - taking into account the requirement for a satisfactory cell count and cost effectiveness. This concentration, which was similar to those used for vitronectin doping experiments, but far greater than those found in tears, was selected to incorporate any extremes of fibronectin influx. Group IV etafilcon A contact lenses were doped in 12.5 $\mu\text{g}/\text{ml}$ of fibronectin for 24 hours (n=3). For all initial validation assays an anti-fibronectin (anti-Fn) antibody, at 1:100 in HBS, was also used as a direct comparison against the anti-Vn antibody and vitronectin standard controls. Again this was to either eliminate or accept the role of fibronectin as a competitive adhesion molecule in contact lens wear and/or to further validate the dominant adhesion of vitronectin onto the contact lens.

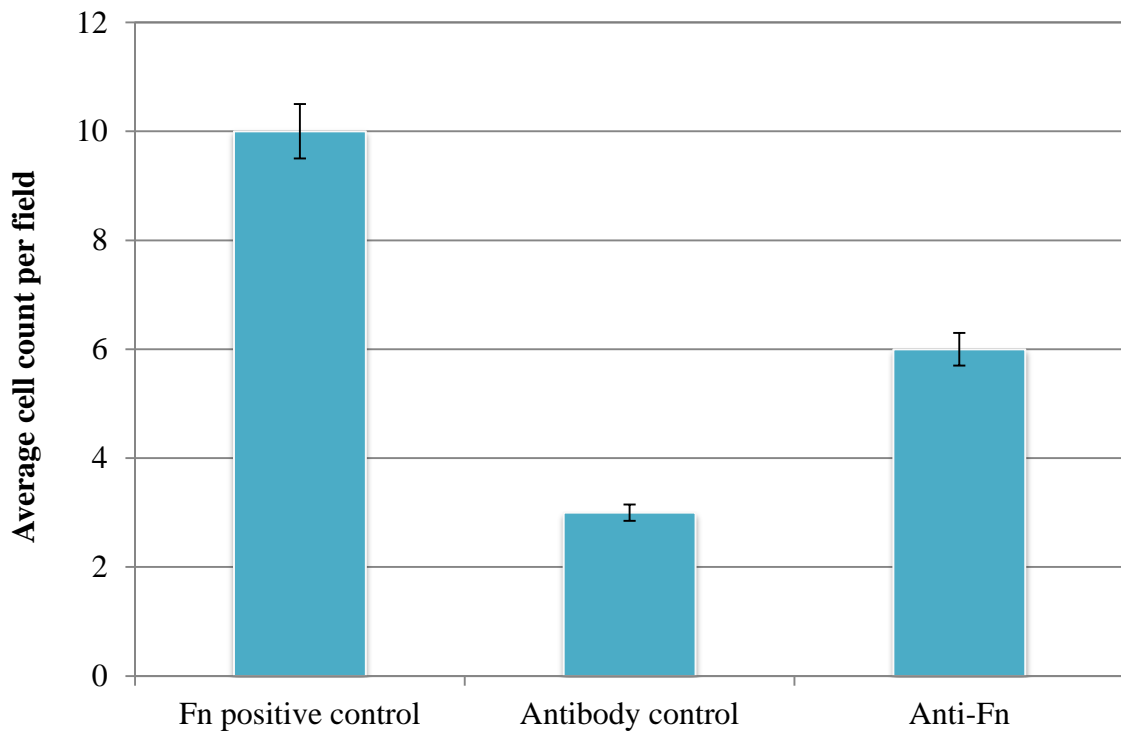


Figure 3.2 Cell counts on polyHEMA contact lenses doped with 20 $\mu\text{g}/\text{ml}$ fibronectin *in vitro*.

Figure 3.2. shows that fibronectin demonstrated poor adsorption out of doping solution onto the contact lens, displaying low cell counts per field (10 ± 2) in comparison to vitronectin-mediated adhesion (59 ± 3).

3.3.3 Discussion

In terms of method validation, the assay was verified using vitronectin doped polyHEMA contact lenses. The use of polyclonal anti-vitronectin antibodies as a control in the cell-based assay demonstrated the essential role of vitronectin-mediated mouse 3T3 Swiss Albino embryo fibroblasts cell adhesion, and thus validated the use of the cells as a means of detecting vitronectin presence. The negative control antibodies blocked the numerous exposed sites of vitronectin, preventing cell attachment; the level of adhesion to the contact lenses treated with anti-vitronectin was comparable with those on the blank contact lenses, indicating the effective inhibitory action of anti-vitronectin. These results verify vitronectin dependant adhesion of cell fibroblasts to contact lenses and demonstrate the use of a cell-based assay to detect vitronectin.

Additionally, it was shown that fibronectin, which also mediates cell adhesion, did not adversely interfere with the vitronectin dominated cell-based assay. Therefore, vitronectin was established as the dominant ligand involved for cell-mediated adhesion to the contact lens surface.

3.3.4 Key Points for Cell Assay Method Validation

- Vitronectin was shown to adsorb out of doping solution and onto the contact lens surface. This adsorption can be detected by vitronectin-mediated fibroblast cell adhesion.
- Fibronectin was demonstrated to show poor adsorption out of doping solution, as demonstrated by the low fibronectin-mediated cell counts. Therefore, the presence of fibronectin in solution does not interfere with the detection of vitronectin.

3.4 The Effect of Protein Concentration on Vitronectin-Mediated Cell Adhesion

3.4.1 *In Vitro* Doping Experiments – Varying Protein Concentration

The effect of vitronectin doping concentration on vitronectin-mediated cell adhesion to the contact lens surface was evaluated. PolyHEMA contact lenses (n=4) were used in

order to keep the contact lens type consistent with the initial experiment performed in section 3.3.1 and to reduce experiment parameter variability. The four concentrations of vitronectin used to dope the contact lenses were: 1 µg/ml, 5 µg/ml, 10 µg/ml and 20 µg/ml. Control non-doped contact lenses (n=3) were also analysed. No antibody controls were required for these assays. The results show that the higher the vitronectin concentration of the doping solution the higher the vitronectin-mediated cell adhesion. Increasing the vitronectin concentration from 1 µg/ml to 20 µg/ml gave an increase in the average cell count per field from 5±0.8 to 37±1.7 (Figure 3.3). All subsequent contact lenses doped with vitronectin were done so at a concentration of 10 µg/ml, as this was found to be the optimum concentration.

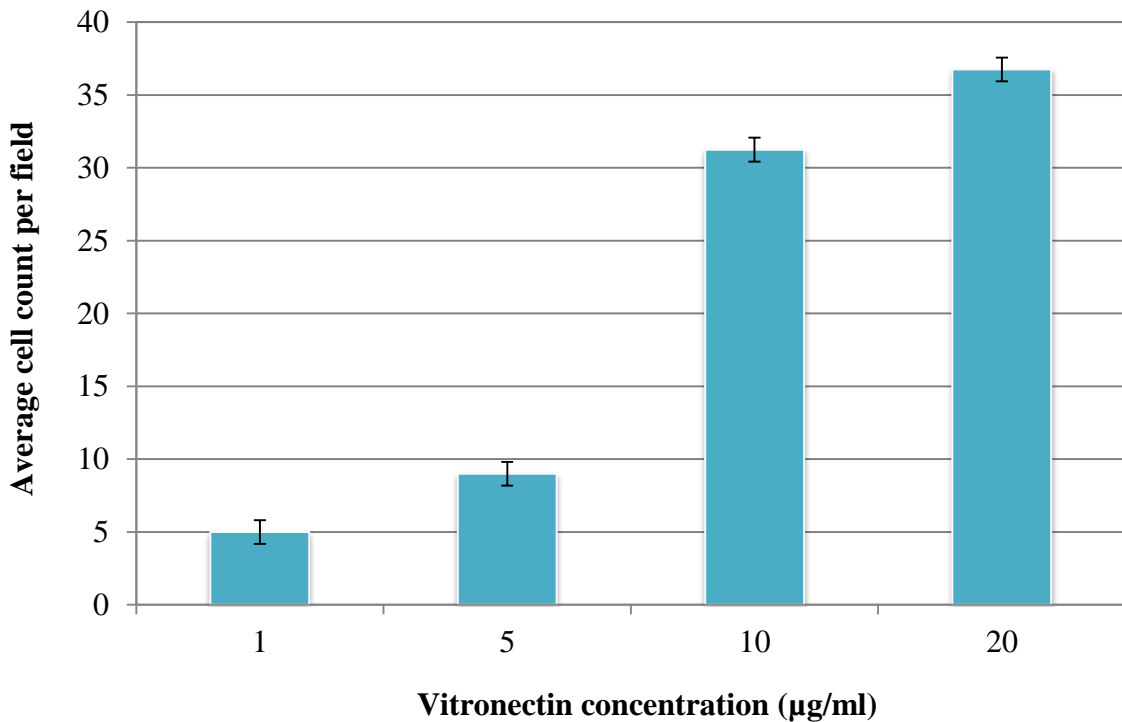


Figure 3.3 The relationship between vitronectin-mediated cell adhesion and concentration of the vitronectin doping solution.

3.4.2 Discussion

The *in vitro* doping of contact lenses with vitronectin at varying concentrations showed a direct correlation between an increase in vitronectin concentration and vitronectin-mediated cell adhesion to the contact lens. Although a plateau was not reached within the concentration levels studied, it can be expected that a limiting plateau would

ultimately be achieved after a gradual increase. However, as previously stated, vitronectin concentrations in the eye have been reported at $0.75 \pm 0.32 \mu\text{g/ml}$ in the open eye [104]. It is, therefore, extremely unlikely for vitronectin concentrations to exceed the *in vitro* experimental limits of $20 \mu\text{g/ml}$ in tears. These results demonstrate that cell adhesion is dependent upon vitronectin concentration in solution. However, it would be inadvisable to produce concentration curves to calculate vitronectin concentration against cell counts as each assay must be treated separately.

3.4.3 Key Points for the Effect of Protein Concentration on Vitronectin-Mediated Cell Adhesion

- Vitronectin-mediated cell adhesion is directly dependent upon vitronectin concentration in solution; the higher the concentration the higher the vitronectin-mediated cell adhesion to the contact lens surface.
- The optimum doping concentration for the purpose of initial experimentation was found to be $10 \mu\text{g/ml}$.

3.5 The Influence of Contact Lens Water Content and Ionicity on Vitronectin-Mediated Cell Adhesion

3.5.1 *In Vitro* Doping Experiments – Varying Contact Lens Water Content and Ionicity

Two separate assays were designed to assess the influence of the contact lens material on vitronectin-mediated cell adhesion. Firstly a contact lens water content assay was performed; the contact lenses used were all non-ionic lenses with water contents of 38%, 42%, 60%, and 75% (n=4). HEMA or HEMA/NVP lenses were chosen to evaluate the effect of contact lens water content on cell adhesion because the material is available in a range of water contents. The effect of contact lens water content on cell count showed the higher the water content of the contact lens the higher the vitronectin-mediated cell adhesion. The average cell count per field for contact lenses with water contents of 38% and 75% increased from 42 ± 0.8 to 58 ± 0.96 respectively (Figure 3.4A).

Secondly, a contact lens ionicity assay using non-ionic Group II (vasurfilcon A, n=2) versus ionic Group IV (etafilcon A, n=2) contact lenses (both are high water content

lenses) was performed. Both contact lens types were doped with vitronectin at a concentration of 10 $\mu\text{g/ml}$ for 24 hours. Only the vitronectin standard control and anti-vitronectin lenses were tested. Figure 3.4B reveals greater cell counts on the ionic Group IV contact lenses (73 ± 6) in comparison to the non-ionic Group II contact lenses (53 ± 9).

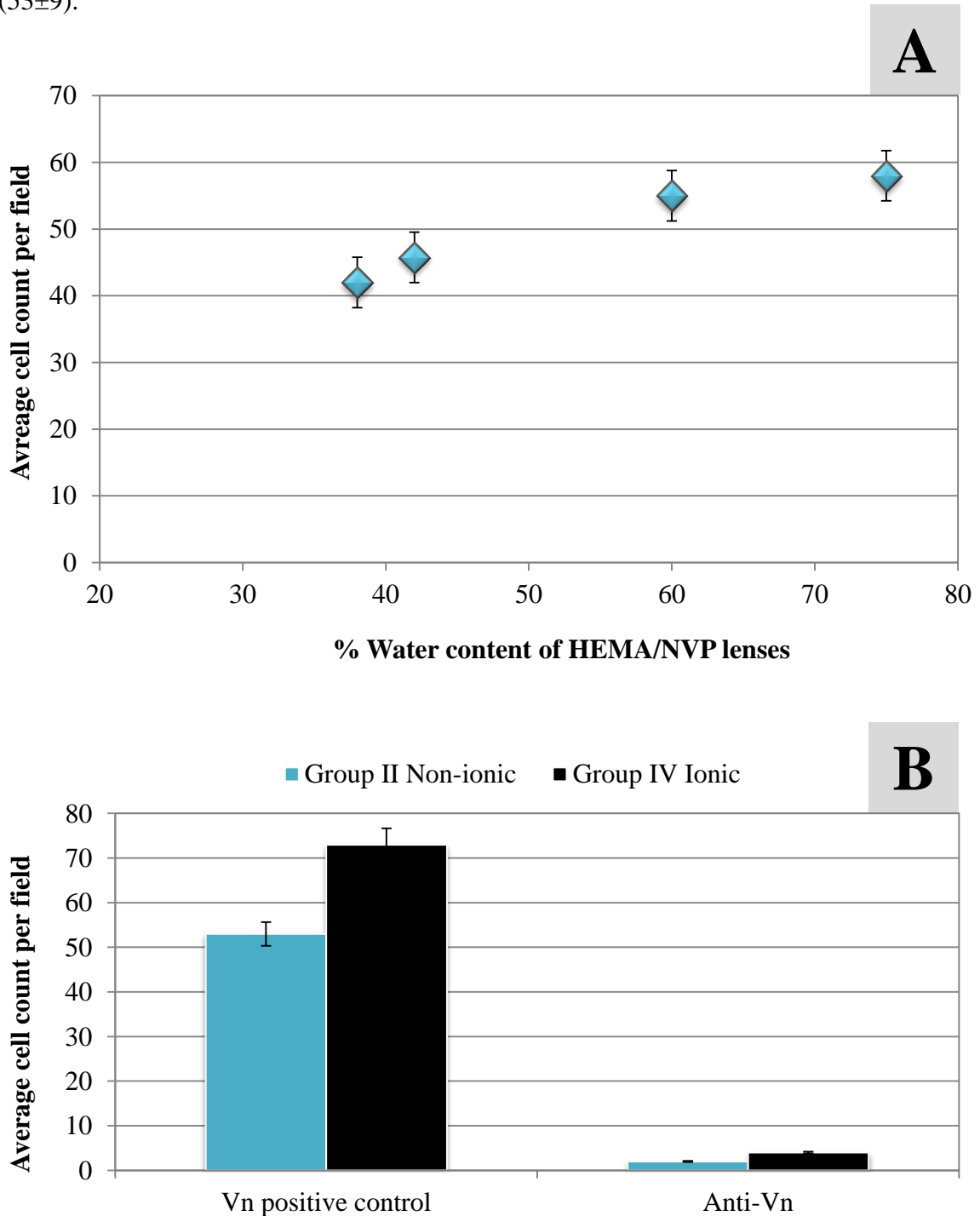


Figure 3.4 The relationship between vitronectin-mediated cell adhesion and: A) contact lens water content, B) contact lens ionicity.

3.5.2 Discussion

The results from Figure 3.4A illustrate the fact that the percentage water content of the contact lens material directly affects vitronectin-mediated cell adhesion; an increase in water content clearly exhibited a rise in the levels of vitronectin-mediated cell adhesion. Additionally, the ionicity of the contact lens also greatly influences cell adhesion, with greater cell counts on the ionic (Group IV) versus the non-ionic (Group II) contact lenses. In this work vitronectin-mediated cell adhesion to etafilcon A contact lenses (Group IV – 58% water content, ionic) was compared with adhesion to vasurfilcon A (Group II – 74% water content, non-ionic). Although vasurfilcon A has the higher water content of the two materials, cell adhesion was found to be greater to etafilcon A contact lenses. This suggests that the ionicity of the contact lens material is more important than the water content with regards to vitronectin-mediated cell adhesion.

3.5.3 Key Points for the Influence of Contact Lens Water Content and Ionicity on Vitronectin-Mediated Cell Adhesion

- Vitronectin-mediated cell adhesion is influenced by contact lens water content; the higher the water content the higher the vitronectin-mediated cell adhesion onto the contact lens surface.
- Vitronectin-mediated cell adhesion is also influenced by contact lens ionicity; in these investigations cell adhesion was found to be greater to an ionic lens material in comparison to a non-ionic material.
- It appears that ionicity is the greater contributing factor to vitronectin-mediated cell adhesion, as greater cell counts were detected on high water content ionic contact lenses (etafilcon A 58%) than high water content non-ionic lenses (vasurfilcon A 74%).

3.6 Vitronectin-Mediated Cell Adhesion to Anterior and Posterior Surfaces of *ex vivo* Contact Lenses in Daily Wear and Extended Wear Modalities

3.6.1 *Ex vivo* Contact Lenses - Anterior versus Posterior and Daily Wear versus Extended Wear

Cell counts on the anterior and posterior surfaces of Group IV etafilcon A contact lenses were analysed. Lenses from 8 subjects were worn on a daily wear basis (n=8) and on an extended wear basis (n=8). Figure 3.5 reveal that higher cell counts per field on the posterior surface of the contact lenses were determined in comparison to the anterior surface, irrelevant of the modality of wear, as average cell counts per field increased by 95% from the anterior to the posterior surface in both wear modalities. All further test lenses therefore analysed the posterior contact lens surface only. Greater cell counts were also detected on extended wear lenses than daily wear lenses, with an average increase in cell count of 46% for both the posterior and anterior surfaces of the lenses, as also shown in Figure 3.5.

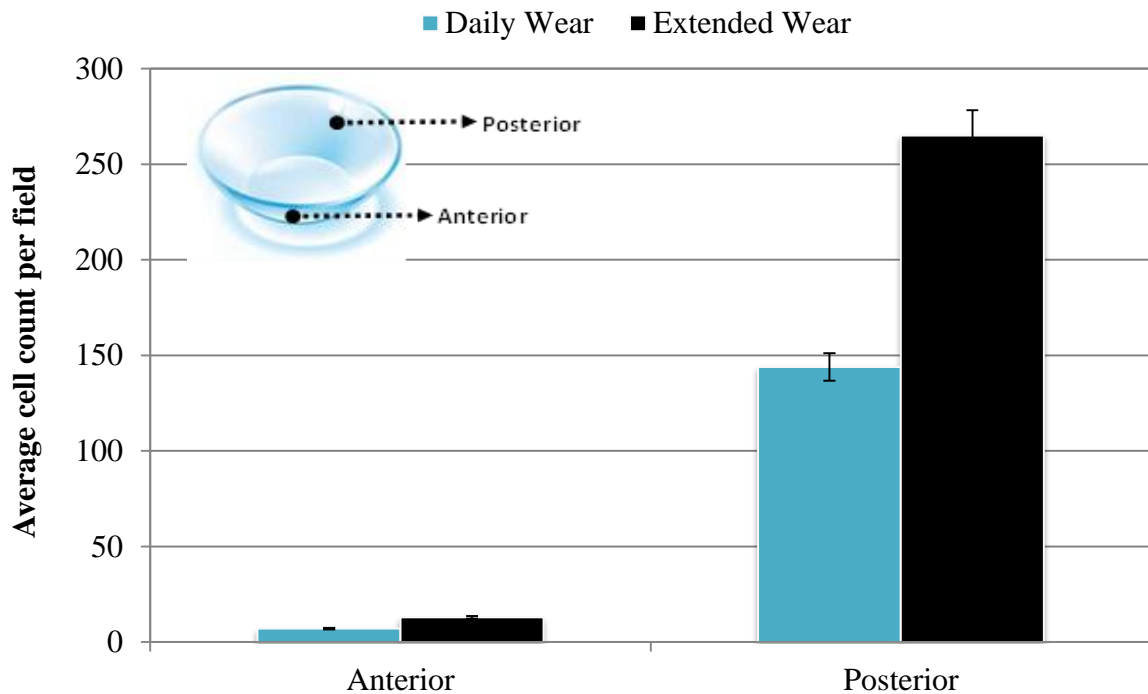


Figure 3.5 Cell counts on the anterior and posterior surfaces of etafilcon A contact lenses worn on both daily wear and extended wear basis.

3.6.2 Discussion

The analysis of vitronectin-mediated cell adhesion on both the anterior and the posterior surfaces of the contact lens revealed that adhesion was predominantly found to occur on the posterior surface of the lens. In contrast, very low levels were revealed on the anterior surface - resembling the levels of vitronectin in tears. The posterior surface presented greater accumulation of vitronectin-mediated cell adhesion, accounting for the majority of vitronectin detected. This accumulation at the posterior contact lens surface may reflect vitronectin moving out of the corneal tissue bed due to contact lens-tissue interactions, as opposed to being simply derived from tears. The aggregation of vitronectin on the posterior surface is thought to create a particular micro climate, which due to its multifunctional nature and ability to bind to numerous ligands and proteins, could lead to the initiation of, or assist in, a number of effector systems.

Greater vitronectin-mediated cell adhesion was also detected on extended wear contact lenses in comparison with daily wear lenses. Taking the total wear time and contact lens-tissue bed contact into consideration, the cell attachment was always greater for the extended wear lenses than the daily wear lenses. The cell attachment observed at the *in vitro* concentrations equivalent to those found in tears are much lower than those found on posterior surfaces of worn lenses. This may be explained by the interaction between the ocular tissue and contact lens, with the posterior microclimate favouring vitronectin attachment.

3.6.3 Key Points for the Analysis of Anterior versus Posterior and for Daily Wear versus Extended Wear on *Ex Vivo* Contact Lenses

- Greater vitronectin-mediated cell adhesion to the posterior surfaces of *ex vivo* contact lenses in comparison to the anterior surfaces strongly suggests that vitronectin deposits as a result of contact lens-tissue mechanical interaction as opposed to adsorption from tears.
- Vitronectin-mediated cell adhesion was found to be greater on *ex vivo* extended wear contact lenses than *ex vivo* daily wear lenses on the lenses studied in this work.

3.7 Vitronectin-Mediated Cell Adhesion to *ex vivo* Daily Wear Contact Lenses - Centre versus Edge

3.7.1 *Ex Vivo* Contact Lenses – Centre versus Edge

It was noted that there was a difference in the locus of vitronectin-mediated cell adhesion to the posterior contact lens surface. Therefore, a comparison of cell adhesion at the centre and edge of the contact lenses was performed. The location of cell adhesion was analysed for Group II (vasurfilcon A, n=8) daily wear and Group IV (etafilcon A, n=8) daily wear lenses (n=16). Greater vitronectin-mediated cell adhesion was observed at the contact lens edge compared to the centre, irrespective of the contact lens material type. Average increases in cell counts per field from centre to edge (on the posterior contact lens surface) of 68% and 65% were observed for Group II contact lenses and Group IV contact lenses respectively (Figure 3.6). The results revealed a greater cell attachment on the Group IV ionic material in comparison to the Group II non-ionic material, both for the contact lens centre with an average cell count increase of 30%, and the contact lens edge with an average increase of 25%. Figure 3.7 illustrates cells on the contact lens edge of an *ex vivo* etafilcon A lens under an inverted microscope.

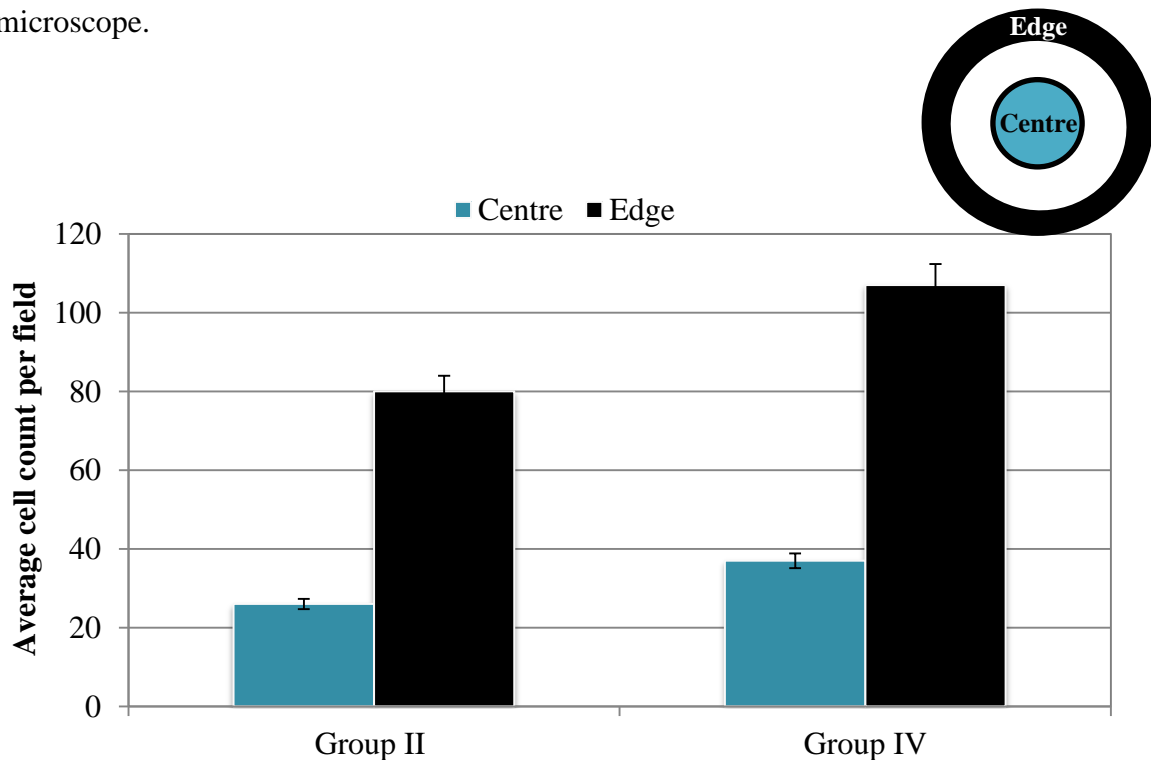


Figure 3.6 Cell counts on the centre and edge areas of the posterior surface of *ex vivo* Group II and Group IV contact lenses worn on a daily wear basis.

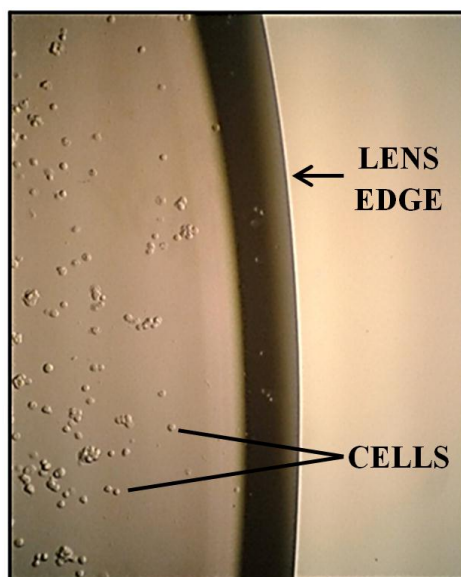


Figure 3.7 Cells on the posterior surface of the contact lens edge of a Group IV *ex vivo* etafilcon A material. High cell counts at the lens edge are apparent.

3.7.2 Discussion

Vitronectin-mediated cell adhesion was significantly greater to *ex vivo* contact lenses in comparison to lenses doped with vitronectin *in vitro*. Centre versus the edge of the contact lens analysis revealed interesting differences in vitronectin-mediated cell adhesion. There was a marked increase in cell adhesion at the edge of the contact lens in contrast to the centre of the lens. This phenomenon was evident in both the daily and extended wear regimes. The fact that this preferential adhesion was evident for both wear modalities is very significant. As the name suggests, daily wear contact lenses are inserted and removed on a daily basis, the effect of daily handling of the lens, varying insertion and removal parameters and cleaning would be expected to change the characteristics of the deposition of vitronectin. However, this was not the case and the adhesion profiles resembled that of the extended wear modality. Both wear modalities appeared to create a vitronectin rich micro-climate at the edge of the lens, which may be the site of localised inflammatory mediation.

A comparison of vitronectin-mediated cell adhesion levels for the central and peripheral regions of Group II and Group IV contact lenses was performed. Greater cell adhesion to Group IV materials in contrast with Group II materials demonstrated that cell attachment is markedly dependent upon material type, highlighting the potential for materials effects in influencing vitronectin deposition on the lens surface and the nature

of the post-contact lens microclimate. Again, an evaluation of the centre versus the edge of the contact lens revealed that greater vitronectin-mediated cell adhesion resulted at the edge. The locus of vitronectin deposition is significant, as this may influence the locus of plasmin regulation. Localised plasmin at the edge has the potential to escape into the tear film, whereas plasmin regulated at the centre of the contact lens may become “trapped” in that region.

3.7.3 Key Points for Vitronectin-Mediated Cell Adhesion to the Contact Lens Centre versus the Lens Edge

- Vitronectin-mediated cell adhesion was found to be greater at the edge of lens than at the centre of the lens.

3.8 Investigating Contact Lens Material Variation

3.8.1 The Effect of Contact Lens Modulus on Vitronectin-Mediated Cell Adhesion

The study was extended to include one conventional hydrogel contact lens material (etafilcon A) and three silicone hydrogel contact lens materials (lotrafilcon A, lotrafilcon B and balafilcon A). Each contact lens type (n=4) was worn by the same asymptomatic subject on a daily wear basis and stored in saline solution after removal. Four contact lenses of each material type were assayed and the average cell count per field calculated. Figure 3.8 reveals that the highest levels of vitronectin-mediated cell adhesion were determined on the etafilcon A material (117 ± 4), with lotrafilcon B, balafilcon A and lotrafilcon A showing decreasing cell counts at the contact lens edge (115 ± 4 , 107 ± 5 , 88 ± 6 respectively). Figure 3.9 shows the relationship between vitronectin-mediated cell adhesion and contact lens modulus - the lower the modulus, the greater the cell adhesion at the contact lens edge. It was demonstrated that a low water content high modulus material, such as lotrafilcon A, has a lower edge:centre ratio of 1.3:1, whereas a high water content low modulus material, such as etafilcon A, has a higher edge:centre ratio of 3.3:1. The modulus and centre:edge ratios are summarised in Table 3.1.

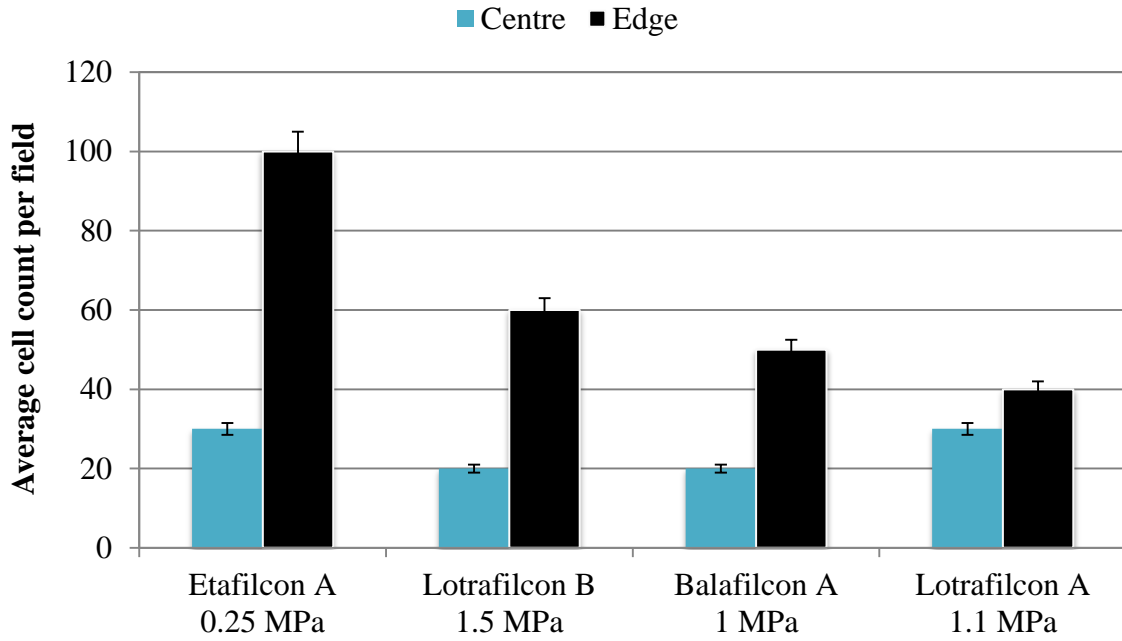


Figure 3.8 Vitronectin-mediated cell adhesion to ex vivo contact lenses worn on a daily wear basis averaging 8 hours over 1 day, where $n=8$.

Table 3.1 The relationship between edge:centre ratio and contact lens modulus.

Material	Water Content (%)	Modulus (MPa)	Edge:Centre Ratio
Etafilcon A	58	0.25	3.3 : 1
Lotrafilcon B	33	1	3 : 1
Balafilcon A	36	1.1	2.5 : 1
Lotrafilcon A	24	1.5	1.3 : 1

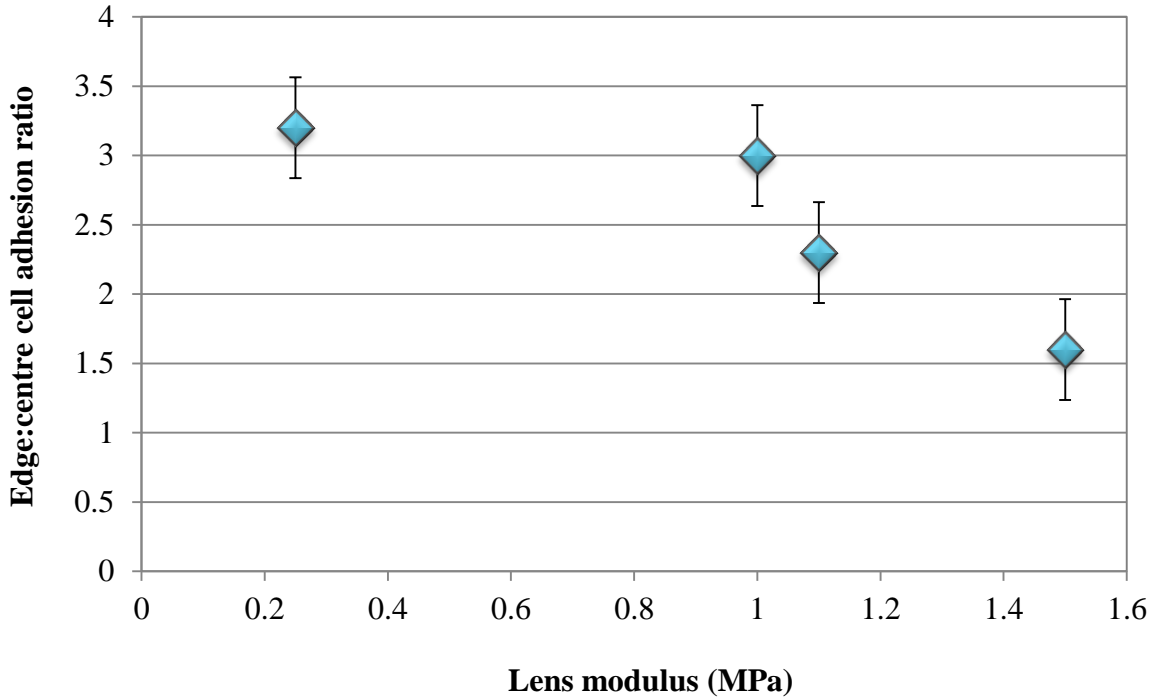


Figure 3.9 The relationship between vitronectin-mediated cell adhesion and contact lens modulus; the lower the material modulus the greater the cell adhesion at the lens edge.

3.8.2 Discussion

Interaction of the contact lens edge with the cornea was further demonstrated using a range of materials with varying moduli. The modulus of a contact lens describes its resistance to deformation, where modulus is equal to stress/strain. An edge:centre cell count ratio was calculated for each material. The edge:centre cell count ratio is clearly material dependent and one important aspect of this appears to be modulus – above a certain value a more even distribution of vitronectin-mediated cell adhesion is found, and overall cell adhesion levels are lower. It must be noted that it is difficult to decouple the effect of lens water content and the effect of lens modulus on vitronectin-mediated cell adhesion. The effect of the contact lens material modulus on the edge:centre ratio was, however, further demonstrated with two similar contact lens materials; lotrafilcon A and lotrafilcon B. Both lens materials are FDA group I materials (low water content and non-ionic). However, lotrafilcon B with a lower modulus of 1.0 MPa revealed a much greater edge:centre ratio in comparison to lotrafilcon A with a higher modulus of 1.5 MPa. Lotrafilcon B, the softer material,

allows more drape of the contact lens over the cornea, thus contact lens-tissue interaction is emphasised at the edge.

3.8.3 Key Points for the Influence of Contact Lens Modulus on Vitronectin-Mediated Cell Adhesion

- The locus and extent of vitronectin-mediated cell adhesion is largely influenced by material modulus.
- Lower modulus materials exhibit greater cell adhesion at the contact lens edge, whereas higher modulus materials give a more even distribution of vitronectin-mediated cell adhesion over the lens surface.

3.9 Concluding Discussion

3.9.1 Vitronectin-Mediated Cell Adhesion Due to Contact Lens-Tissue Interaction

This study has shown that, in general, the high levels of vitronectin-mediated cell adhesion detected on *ex vivo* contact lenses cannot be reproduced with *in vitro* doping experiments at similar concentrations of vitronectin in tears. This suggests that vitronectin adsorption from the tear film alone cannot explain the levels detected on *ex vivo* contact lenses; deposition arising from mechanical contact of the contact lens with the corneal tissue bed, rather than out of solution, is highly likely. This is further demonstrated by the comparison of vitronectin-mediated cell adhesion between the anterior and posterior surface of the lens. There is a significant difference between cell adhesion levels on both surfaces, and the low levels of vitronectin-mediated cell adhesion detected on the anterior surface resemble the vitronectin levels found in tears.

The sliding motion of the eyelid over the contact lens surface will bring about friction-mechanical stimulation. This movement might be expected to stimulate a biochemical response with the potential to generate an upregulation of particular components or to activate additional pathways in response to the physical trauma of the eyelid-contact lens interaction – modest though that might be. The diminished tear flow at the posterior surface of the lens, in addition to a reduction in the dynamic interaction with the tissue bed, would be expected to produce a quite different level of response with the potential adsorption of specific biochemical components from the more ‘closed’

environment. This difference is typified by the fact that dramatically higher (greater than tenfold) levels of vitronectin deposition have been reported on posterior, relative to anterior contact lens surfaces [46].

3.9.2 Vitronectin and Tear Plasmin Activity

The emerging patterns are clear - the presence of a contact lens concentrates vitronectin in close proximity to the ocular tissue bed, and thus the preferential adsorption of vitronectin onto the contact lens surface highlights the fact that post-contact lens micro climate, particularly towards the edge, is rich in vitronectin to a degree that is capable of influencing localised inflammation and upregulation of plasmin. Vitronectin is involved in the regulation of fibrinolysis, a consequence of the fact that it binds and stabilises plasminogen activator inhibitor-1 (PAI-1), which thereby allows PAI-1 to inhibit the action of tissue plasminogen activator (tPA) and the fibrinolysis process as a whole. If vitronectin is localised on a surface adjacent to the cellular site, the somatomedin B homology region of the protein binds to the active site of PAI-1, thereby generating plasminogen activator and resulting in the upregulation of plasmin [113]. Tear plasmin activity has been observed in tear fluid of subjects with corneal disorders, for example an increase in tear plasmin in corneal ulcers has been demonstrated [114]. This leads to the implication that elevated plasmin levels are important in the pathogenesis of ocular infection and dysfunction. The view is that it is an important potential trigger of additional events, leading in extreme cases to pathology in an otherwise healthy tissue. Plasmin, for example, can cleave fibronectin (an important adhesion molecule involved in corneal re-epithelisation), which is significant as fibronectin degradation is associated with impaired wound healing [115, 116].

Levels of tear plasmin have been shown to increase progressively in the sequence: no contact lens control group, daily wear soft, extended wear soft [117], and it has been proposed that the proteolytic activity of plasmin may contribute to corneal epithelial abnormalities associated with contact lens wear [113]. Vitronectin localised on the contact lens surface adjacent to the corneal surface [46] may remove PAI-1 leading to local upregulation of plasmin in the posterior tear film. Plasminogen is synthesised in the cornea and can be activated by plasminogen activator to produce plasmin, this in

turn activates latent collagenase which can result in collagen degradation implicated in corneal ulceration [118]. The physical contact between the contact lens and tissue bed can potentially remove vitronectin together with PAI-1, thus plasmin is found in the post-contact lens environment [119]. Studies also suggest a link between high plasminogen activator levels and the pathogenesis of persistent corneal defects [120]. To parallel this observation in the eye, chronic wound fluid from venous ulcers often shows complete degradation of vitronectin and fibronectin into smaller peptides that prevent local cell adhesion to the wound bed, therefore preventing closure [121]. If vitronectin is localised on a (synthetic) surface adjacent to the cellular site (such as a chronic wound) it removes PAI-1 from the reaction by fixing it, creating an imbalance in favour of plasminogen activator. This can result in a local upregulation of plasmin formation, thereby controlling an important regulatory mechanism in wound repair; an increase in degradative proteolysis which may then result in a state of non-healing and excessive inflammation.

The potential for materials to affect vitronectin deposition from the corneal tissue bed will affect the locus of plasmin generation and thus influence lens-induced inflammatory processes. The clinical implications of this are yet to be determined, and further studies are required in order to comment on the ideal properties of a contact lens when considering the connection between contact lenses and the consequential inflammatory process. It can be said, however, that an ideal contact lens is one that minimises protein interaction at the surface and that allows more exchange of protein at the edge. The unique conformational flexibility and multidomain structure of vitronectin which allows it to bind to a large repertoire of ligands makes its potential interactions with biomaterials all the more intriguing. The versatile binding capabilities and receptor functions of vitronectin could, in the future, be used in the characterisation of structure-function properties and importantly in the design of new biomaterials.

3.9.3 Potential for Further Work

The significance of this body of research must lie in the area of wound healing and the compromised anterior eye. Bandage contact lenses (BCLs) are regularly used to protect the compromised cornea from further ocular insult, to enable the relief of pain and to improve the ability of the corneal epithelium to heal. However, the use of contact lenses

in therapeutics as bandage lenses is in its infancy. Lens choice appears to be influenced by convenience and availability rather than specific knowledge of their biochemistry of the healing process. Little is known about the interaction of specific materials with corneal conditions and the way in which materials can promote/inhibit the healing process. The importance of contact lens choice is therefore apparent when evaluating the effect of material on the inflammatory process. *Ex vivo* contact lenses worn in the non-compromised eye only were analysed in this work. The study may therefore be expanded to include contact lenses worn for bandage use in the compromised eye.

3.10 Chapter Summary

The aim of this work was to investigate vitronectin-mediated cell adhesion to the surface of *ex vivo* contact lenses worn in the healthy non-compromised eye. It is the exploitation of two specific properties of vitronectin which enabled its presence on hydrogel and silicone hydrogel contact lenses to be detected. Firstly, vitronectin has a high affinity for hydrogel materials and is not easily removed from the surface. Secondly, vitronectin possesses cell-binding properties. Therefore, the development and optimisation of a novel on-lens fibroblast cell-based assay has enabled the locus and distribution of vitronectin-mediated cell adhesion to be measured directly on the contact lens surface. The work presented here shows that the adhesive nature of vitronectin enables it to adsorb to a range of contact lens materials. Importantly, the influence of the contact lens on vitronectin deposition out of solution and from the corneal tissue bed was established. Vitronectin-mediated cell adhesion to contact lenses is influenced by material water content, ionicity and modulus. Cell adhesion was shown to be greater on the posterior surface than the anterior surface, and greater at the edge than at the centre of the lens.

The technique used in this chapter can be extended to contact lenses worn in the compromised eye.

CHAPTER FOUR

The Investigation of the Locus and Extent of Vitronectin Deposition on Bandage Contact Lenses

4.1 Aim

The locus and extent of vitronectin-mediated cell adhesion to a range of contact lens materials worn in the non-compromised eye was studied in chapter three. Following these baseline experiments with the non-injured cornea, the aim of the research described in this chapter was to investigate the quantity and locus of vitronectin-mediated cell adhesion to the posterior surfaces of *ex vivo* bandage contact lenses (BCLs) worn under hospital conditions. This was to provide a comparison against the healthy eye. Lenses in this study were worn by symptomatic subjects with various ocular disorders, and examined using the cell-based on-lens vitronectin assay.

4.2 Introduction

Principles regarding silicone hydrogel (SiHy) contact lenses for therapeutic bandage applications were discussed in the main introduction of this work (section 1.6). SiHy contact lenses with enhanced oxygen permeability allow for longer periods of wear, including nominally safe extended wear, in comparison to conventional hydrogel contact lenses [90]. This, together with the fact that SiHy contact lenses generally produce less protein deposition [94-96], enables SiHy contact lenses to offer advantages over conventional hydrogels for bandage contact lens (BCL) applications. The work presented in chapter three shows that vitronectin readily deposits onto SiHy contact lenses. This deposition on lenses can potentially result in the upregulation of plasmin. Tear plasmin activity has been observed in tear fluid of subjects with corneal disorders [122]; it was therefore logical to investigate vitronectin-mediated cell adhesion on SiHy BCLs worn in the compromised eye and thus potential plasmin upregulation.

Many studies have investigated the efficacy of various SiHy contact lenses for therapeutic use [75, 80, 91, 123], in particular lotrafilcon A (Air OptixNight & Day) has been shown to be an effective BCL for improving the ocular condition and comfort in bullous keratopathy patients [91] and photorefractive keratectomy patients [80]. However, no study has yet reported the specific interaction of contact lenses with the compromised corneal tissue bed in terms of deposition of biomarkers. Consequently, the work described in this chapter represents the first systematic attempt to understand this interaction, with a particular focus on the consequences of vitronectin deposition on BCLs. Subjects diagnosed with a variety of corneal and ocular surface disorders and

who required BCLs to manage these conditions were included in this work. BCLs were examined in the context of vitronectin-mediated cell adhesion as a mediator for plasmin generation. These contact lenses were assayed according to the novel on-lens assay technique described in chapters two and three.

4.3 Methods

4.3.1 Contact Lens Materials

The two contact lens materials used within this controlled study were: Biofinity (comfilcon A- approved for seven days continuous wear) and UltraWave SiH (Filcon V 3 - approved for four weeks continuous wear). A brief overview of each contact lens type is provided in Table 4.1. The full properties of each contact lens can be found in section 2.1.1.

Table 4.1 Properties and characteristics of the two contact lens materials studied: Biofinity and UltraWave SiH.

Contact Lens Material		
Commercial Name	Biofinity	UltraWave SiH
USAN Nomenclature	Comfilcon A	Filcon II 3
FDA Group	I	IV
Water Content (%)	48	58
Modulus (MPa)	0.75	0.5

4.3.2 Study Population for Bandage Contact Lens Wearers

Subjects with a variety of corneal and ocular surface disorders presenting at the Leicester Royal Infirmary UK (LRI) and Warwick Hospital UK (WK) who required the long term use of a BCL were included in this work. All subjects required a BCL in one eye only.

The subject population comprised fifteen subjects (seven men and eight women) with an average age of 66 ± 16 (range 32-86). Of this total subject population, eleven subjects were from Leicester Royal Infirmary UK and received a Biofinity contact lens in the affected eye. These subjects are referred to with a patient ID of LRI. The ocular/corneal conditions for these subjects included band keratopathy, bullous keratopathy, Sjögren's

syndrome and a corneal graft. The remaining four subjects of the total subject population were from Warwick Hospital and received an UltraWave SiH contact lens in the affected eye. These subjects are referred to with a patient ID of WK. Conditions for these subjects included trichiasis corneal scarring, corneal ulcers and epithelial disruption. Information for each patient in the study is provided in Table 4.2. This information is also shown as a flowchart in Figure 4.1. BCL wear time ranged from one day to eight weeks depending upon the subject's condition and individual requirement. No care solutions were used. Contact lenses were removed aseptically from the eye and stored in 0.9% saline solution at 4°C.

Six healthy CL-wearers (non-compromised eye, n=6) were also included as controls to provide a comparison against BCL-wearers (compromised eye) and wore Biofinity contact lenses. Contact lenses from the non-compromised eye were worn for eight hours on a daily wear schedule. The same healthy contact lens wearers then wore Biofinity lenses on a daily wear schedule over five days. These lenses were removed overnight and stored in care solutions before reinsertion the following day.

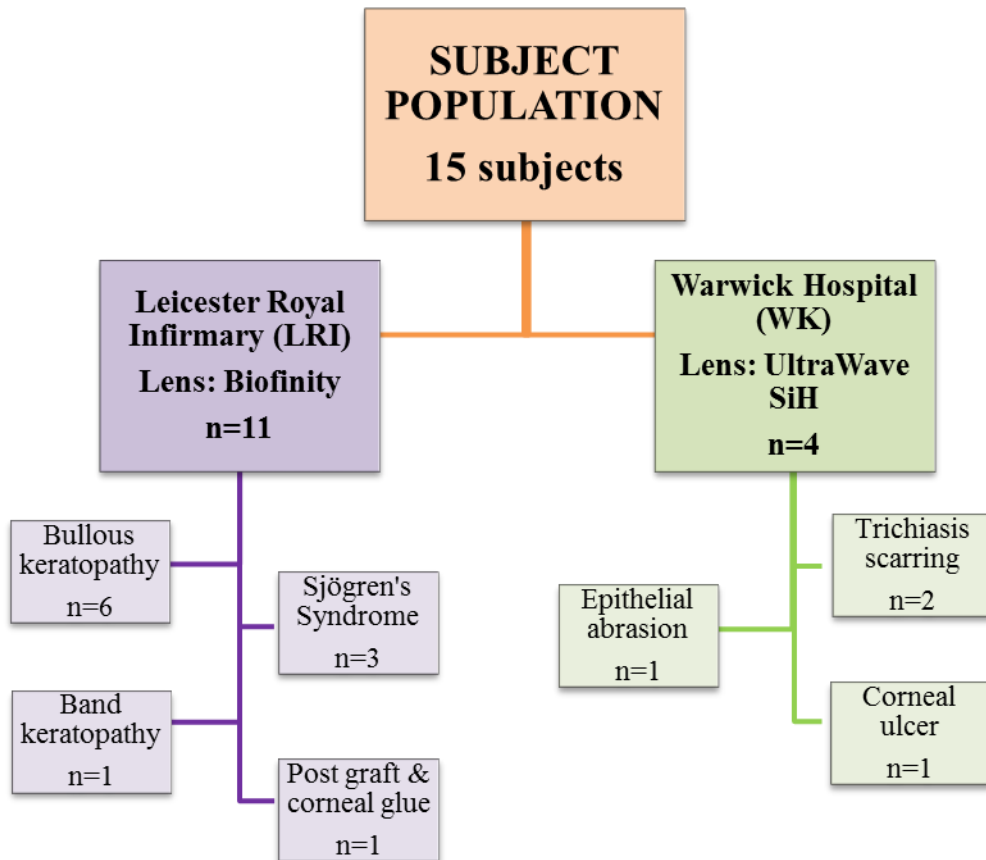


Figure 4.1 A flowchart to show contact lens material and clinical condition information for the study population of bandage contact lens wearers.

Table 4.2 Patient information for the subject population of bandage contact lens wearers (n=15).

Patient ID	Gender	Age	Corneal/Ocular Condition	Contact Lens Type	Wear Duration (weeks)
Subjects from Leicester Royal Infirmary (LRI)					
LRI-1	F	63	Bullous keratopathy	Biofinity	2
LRI-2	F	78	Bullous keratopathy	Biofinity	4
LRI-3	M	76	Bullous keratopathy	Biofinity	4
LRI-4	M	63	Bullous keratopathy	Biofinity	4
LRI-5	F	60	Bullous keratopathy	Biofinity	4
LRI-6	F	83	Bullous keratopathy	Biofinity	4
LRI-7	F	64	Sjögren's syndrome	Biofinity	3
LRI-8	F	62	Sjögren's syndrome	Biofinity	3
LRI-9	F	77	Sjögren's syndrome	Biofinity	6
LRI-10	F	86	Band keratopathy	Biofinity	4
LRI-11	M	37	Post graft & corneal glue	Biofinity	6
Subjects from Warwick Hospital (WK)					
WK-1	M	73	Trichiasis corneal scarring	UltraWave SiH	8
WK-2	M	73	Trichiasis corneal scarring	UltraWave SiH	8
WK-3	M	30	Epithelial abrasion	UltraWave SiH	0.14
WK-4	M	72	Corneal ulcer	UltraWave SiH	1.4

4.3.3 Assay Procedure

All *ex vivo* contact lenses were assayed according to the on-lens cell-based vitronectin assay, as described fully in section 2.2.1, whereby cell attachment to the contact lens surface is indicative of the quantity and locus of vitronectin-mediated cell adhesion on the contact lens surface.

4.4 A Comparison between Vitronectin-Mediated Cell Adhesion to *ex vivo* Contact Lenses Worn in the Healthy Contact Lens-Wearing Eye and the Bandage Contact Lens-Wearing Eye

4.4.1 Non-Compromised versus Compromised Eye

The aim of this section was to draw an initial comparison between vitronectin-mediated cell adhesion to lenses worn in the healthy-CL wearing eye (contact lenses in the non-compromised eye) versus lenses worn in the BCL-wearing eye (bandage contact lenses in the compromised eye).

All contact lenses from the BCL study population (n=15, as defined in Figure 4.1) were assayed. Lenses from healthy CL-wearers (n=6) were also assayed for a comparison. Figure 4.2 presents an average of cell count data for five fields on the posterior surface of:

- Biofinity BCL (n=11)
- UltraWave SiH BCL (n=4)
- Biofinity contact lenses in the normal lens-wearing eye (n=6)

Greater vitronectin-mediated cell adhesion was detected to both BCL materials worn in the compromised eye (average cell count per field: Biofinity 90 ± 5 , UltraWave SiH 78 ± 5) in comparison to the non-compromised healthy CL-wearing eye (14 ± 1). Various parameters that could contribute towards the large difference in cell adhesion seen here, such as duration of contact lens wear, lens material type and ocular condition, are studied in further depth in sections 4.5 - 4.7.

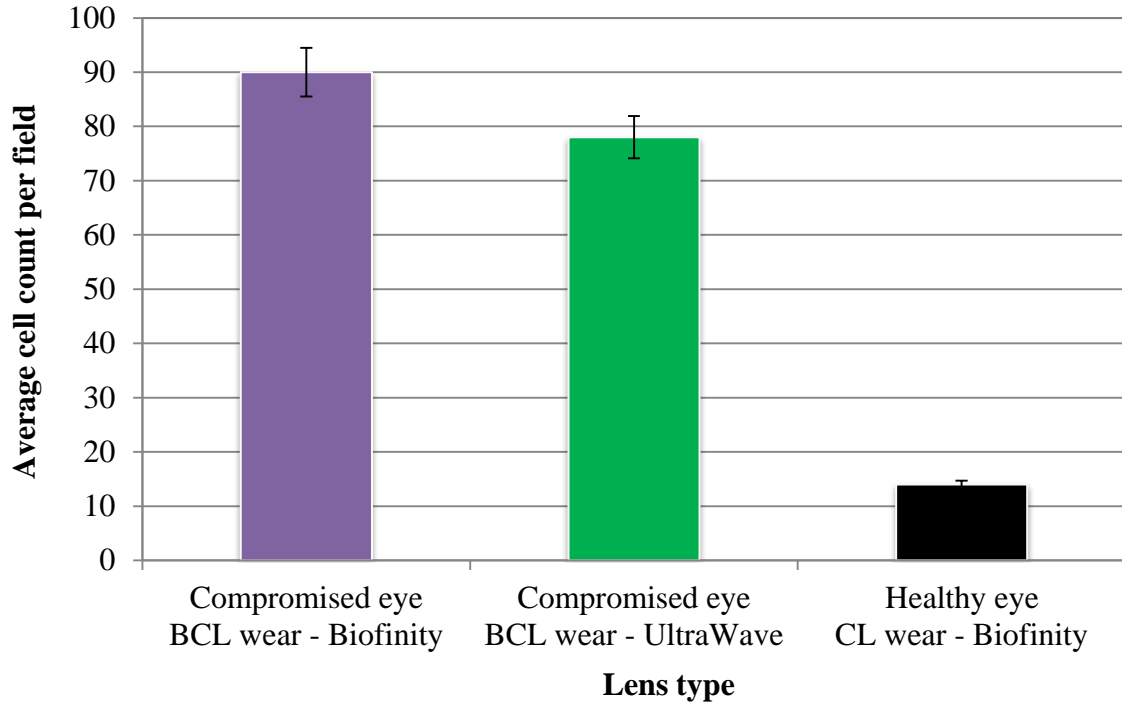


Figure 4.2 A comparison of cell counts on ex vivo Biofinity bandage contact lenses (BCLs) (n=11) and UltraWave SiH BCLs (n=4) worn in the compromised eye. Biofinity lenses (n=6) worn by a subgroup of healthy contact lens-wearers (CL wear) are also shown for comparison.

4.4.2 Discussion

As previously discussed in chapter three, vitronectin deposition on the contact lens surface is believed to arise from contact lens-tissue interaction as opposed to from the tear film. The results presented here suggest that vitronectin-mediated cell adhesion is greater on contact lenses worn in the compromised eye than on lenses worn in the non-compromised eye (Figure 4.1). As stated in the methods section, the lenses studied here were not worn for the same wear duration. The BCLs were worn for up to eight weeks of continuous wear, whereas contact lenses for the healthy eye were worn for eight hours. It is, therefore, highly likely that varying wear durations contributed to the large difference in cell adhesion seen between contact lenses worn for bandage use in the healing eye and for contact lenses worn in the healthy eye. The following section aims to examine the effect of wear duration on vitronectin-mediated cell adhesion on BCLs worn in the compromised eye.

4.5 The Influence of Wear Duration on Vitronectin-Mediated Cell Adhesion

4.5.1 The Effect of Wear Duration on Vitronectin-Mediated Cell Adhesion to *ex vivo* Contact Lenses Worn in the Healthy Contact Lens-Wearing Eye

The effect of wear duration on vitronectin-mediated cell adhesion to contact lenses was investigated in the healthy CL-wearing eye (non-compromised). Biofinity contact lenses were worn by three healthy subjects in both eyes (n=6). Two wear schedules were employed:

- 1 day wear (n=6) - daily wear regime of eight hours. Contact lenses were worn for 8 hours and then removed to be stored in saline solution.
- 5 days wear (n=6) - five day daily wear regime. Contact lenses were worn for forty hours over five days. Care solutions were used to store the lenses overnight.

Cell counts were taken over five fields on the posterior surface of each contact lens to give an average cell count per field. Figure 4.3 shows that overall cell adhesion levels were found to be significantly greater on contact lenses worn for the five day daily wear regime (25 ± 1 average cell counts per field) in comparison to contact lenses worn for one day disposable wear (14 ± 1 average cell counts per field). The average cell count per field increased from one day to five days by 44%.

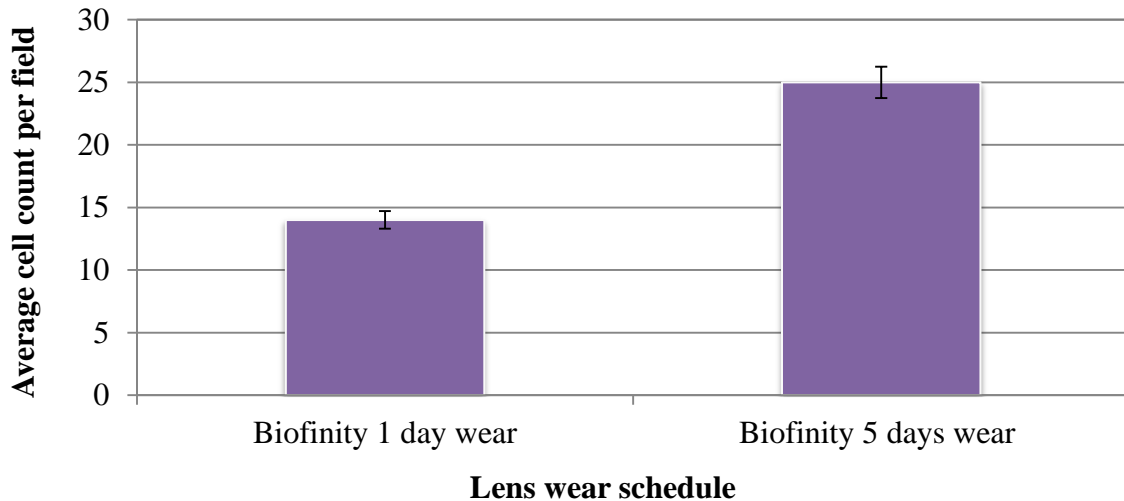


Figure 4.3 Comparative average cell count data on the posterior surface of *ex vivo* Biofinity contact lenses (1 day wear schedule, n=6) and *ex vivo* Biofinity contact lenses (5 day daily wear schedule, n=6) in the healthy contact lens-wearing eye.

4.5.1.1 Discussion

The study of wear duration in the healthy CL-wearing eye revealed that as contact lens wear duration is increased from 1 day to 5 days, vitronectin-mediated cell adhesion to the contact lens surface also significantly increases (Figure 4.3). This shows that the cell adhesion detected on contact lenses worn in the healthy eye is a progression effect over five days wear. In order to determine whether the same trend of increasing vitronectin-mediated cell adhesion levels with wear duration is observed on contact lenses worn in the compromised eye, the next logical step was to investigate vitronectin-mediated cell adhesion to *ex vivo* bandage contact lenses (BCLs).

4.5.2 The Effect of Wear Duration on Vitronectin-Mediated Cell Adhesion to *ex vivo* Contact Lenses Worn in the Bandage Contact Lens-Wearing Eye

The effect of wear duration on vitronectin-mediated cell adhesion on contact lenses was then investigated in the BCL-wearing eye. All Biofinity (n=11) and UltraWave SiH (n=4) lenses from the BCL study population described in section 4.3.2 were assayed. Cell counts were taken for five fields on the posterior surface of each contact lens to give an average cell count per field. Figure 4.4 shows the average cell count per field for each subject in relation to the contact lens wear duration. The shortest wear duration (1 day subject WK-1) showed the lowest cell adhesion. Conversely, the longest wear

durations (8 weeks subjects WK-3 and WK-4) showed the highest cell counts. All BCLs worn after 10 days had average cell counts higher than 60.

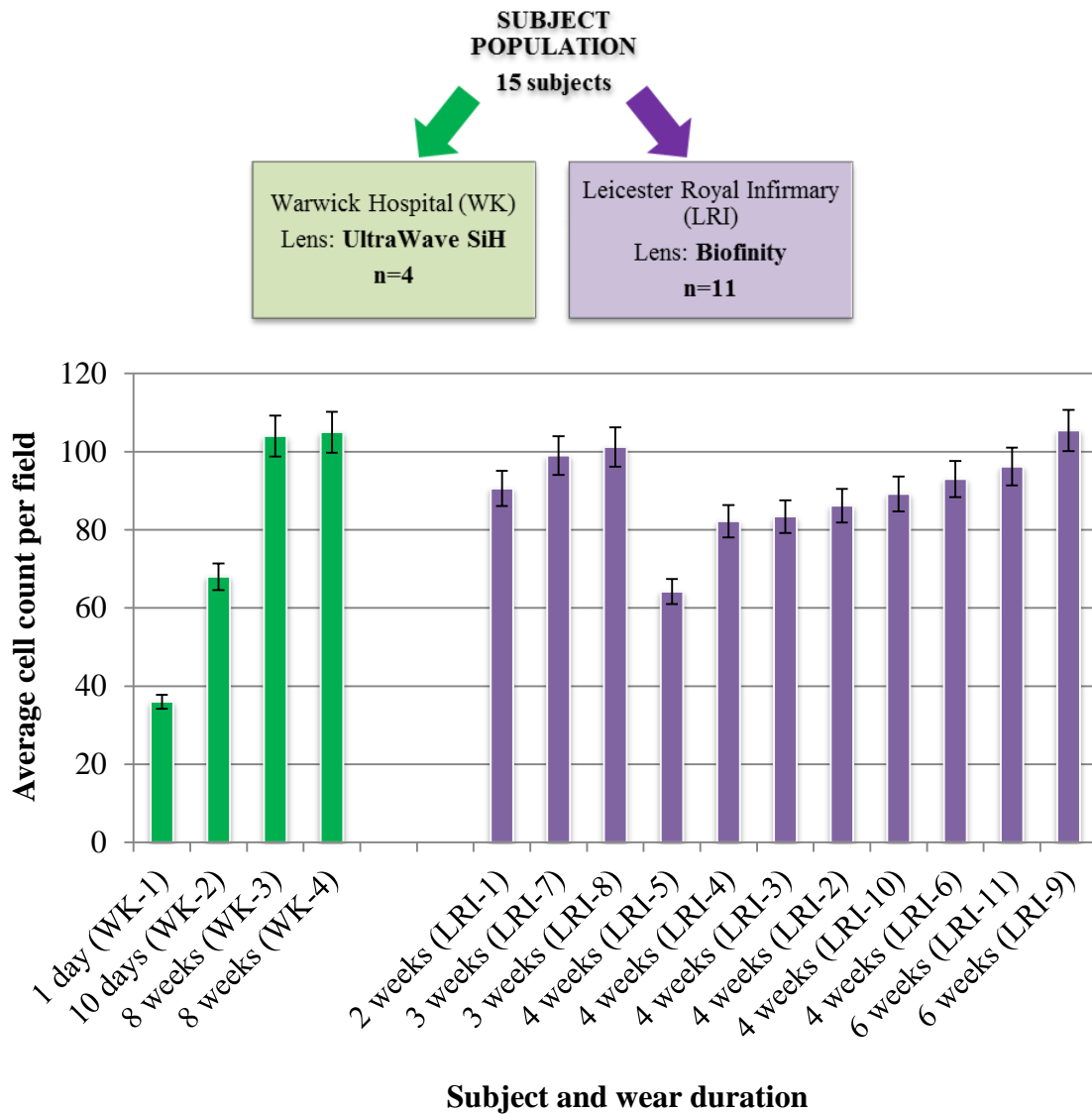


Figure 4.4 Comparative average cell count data from 5 fields for ex vivo UltraWave SiH bandage contact lenses (n=4) and Biofinity bandage contact lenses (n=11). Lenses were worn for durations ranging from 1 day daily wear to 8 weeks continuous wear.

In order to determine a correlation between wear duration and cell counts, the cell count data from Figure 4.4 is presented in scatter form for both Biofinity and UltraWave SiH contact lenses (Figure 4.5). For the Biofinity contact lenses, there is a positive trend; as wear duration increases, the cell counts also increase (Figure 4.5A). For the UltraWave

SiH contact lenses, the results also show an increase in cell counts, with an apparent plateau effect after circa 1 week (Figure 4.5B).

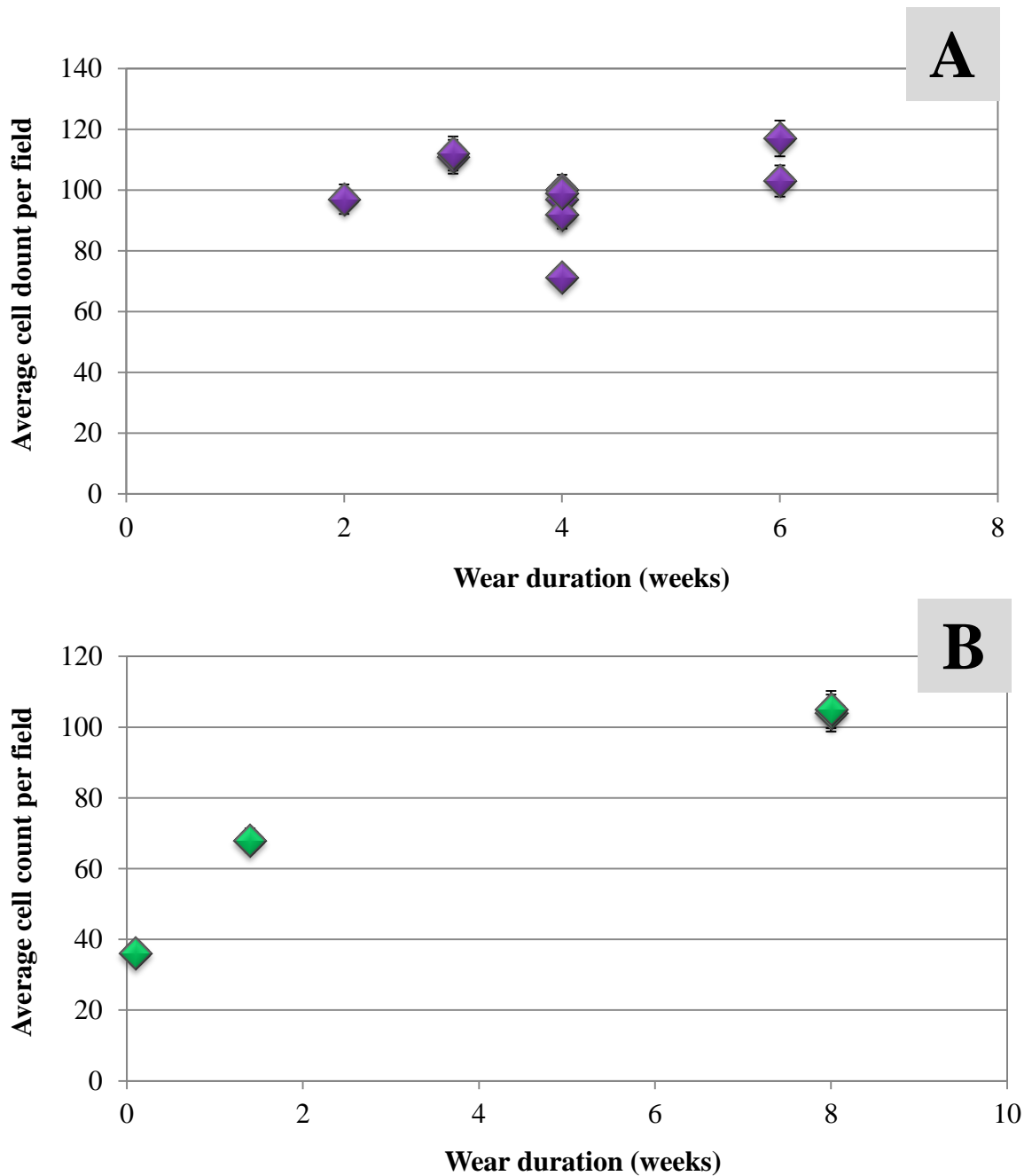


Figure 4.5 The effect of wear duration of bandage contact lenses on cell counts to:

A) Biofinity lenses (n=11) and B) UltraWave SiH lenses (n=4).

Bandage contact lenses were worn by subjects over differing wear durations ranging from 1 day to 8 weeks.

4.5.2.1 Discussion

From the BCL-wearing study population (n=15), a range of Biofinity contact lenses (n=11) and UltraWave SiH contact lenses (n=4) were worn from one day daily wear to eight weeks continuous wear. One contact lens from this study (WK-1) was worn for a short duration of one day. Lens WK-1 showed the lowest average cell count per field of all the contact lenses assayed (36 ± 2). In comparison, two BCLs worn for the maximum eight weeks continuous wear (WK-3 and WK-4) showed the highest average cell count per field (104 ± 5 and 105 ± 5 respectively). These results initially suggest that as wear duration is increased in the BCL-wearing eye, the extent of vitronectin-mediated cell adhesion to the contact lenses also increases, regardless of contact lens type.

Further examination of the results presented in Figure 4.4 show that cell counts on two BCLs worn for the maximum eight weeks continuous wear (WK-3: 104 ± 5 and WK-4: 105 ± 5) are comparable with BCLs worn for three weeks and four weeks. For example, contact lens LRI-8 was worn for three weeks continuous wear and showed an average cell count per field of 99 ± 5 , and contact lens LRI-8 was worn for four weeks and showed a comparable average cell count per field of 101 ± 5). These results suggest that the intensity of vitronectin deposition from the corneal bed does not continually increase with time, more rather there is initially a rapid increase in deposition followed by an apparent plateau effect after approximately one week, as shown in Figure 4.5B. The sensitivity of the assay technique must also be accounted for - it is possible that beyond a certain period the technique may lose sensitivity. Assuming that vitronectin deposits in layers, it is unknown whether the technique sensitivity remains for several protein layers.

It is known that the cornea has the ability to heal rapidly, thus it would be highly unusual for the healing process in the compromised eye to be active for eight weeks. These results suggest that the BCL serves to protect the eye from further insult rather than aid in healing during extended wear. On average, the cell counts seen on BCLs in the compromised eye are significantly higher than contact lenses worn in the regular non-compromised eye. BCLs in this work were worn on a longer continuous wear schedule than lenses worn on a daily basis in the healthy eye and therefore a direct comparison between lenses worn for the same wear duration in the compromised and non-compromised eye is required.

4.5.3 The Effect of Wear Duration on Vitronectin-Mediated Cell Adhesion: One Day Healthy CL-wearing Non-Compromised Eye versus One Day BCL-wearing Compromised Eye

Biofinity contact lenses worn in the healthy non-compromised eye (n=6) for one day are compared with one Biofinity contact lens worn in the BCL-wearing compromised eye (n=1, subject WK-1 treated for epithelial abrasion) also worn for one day. All contact lenses were worn for 8 hours. Cell counts were taken over five fields on the posterior surfaces to obtain an average cell count per field. (Figure 4.6) reveals significantly higher cell counts on the contact lens worn in the compromised eye (36 ± 2) in comparison to cell counts on the lenses worn in the healthy non-compromised eye (14 ± 1).

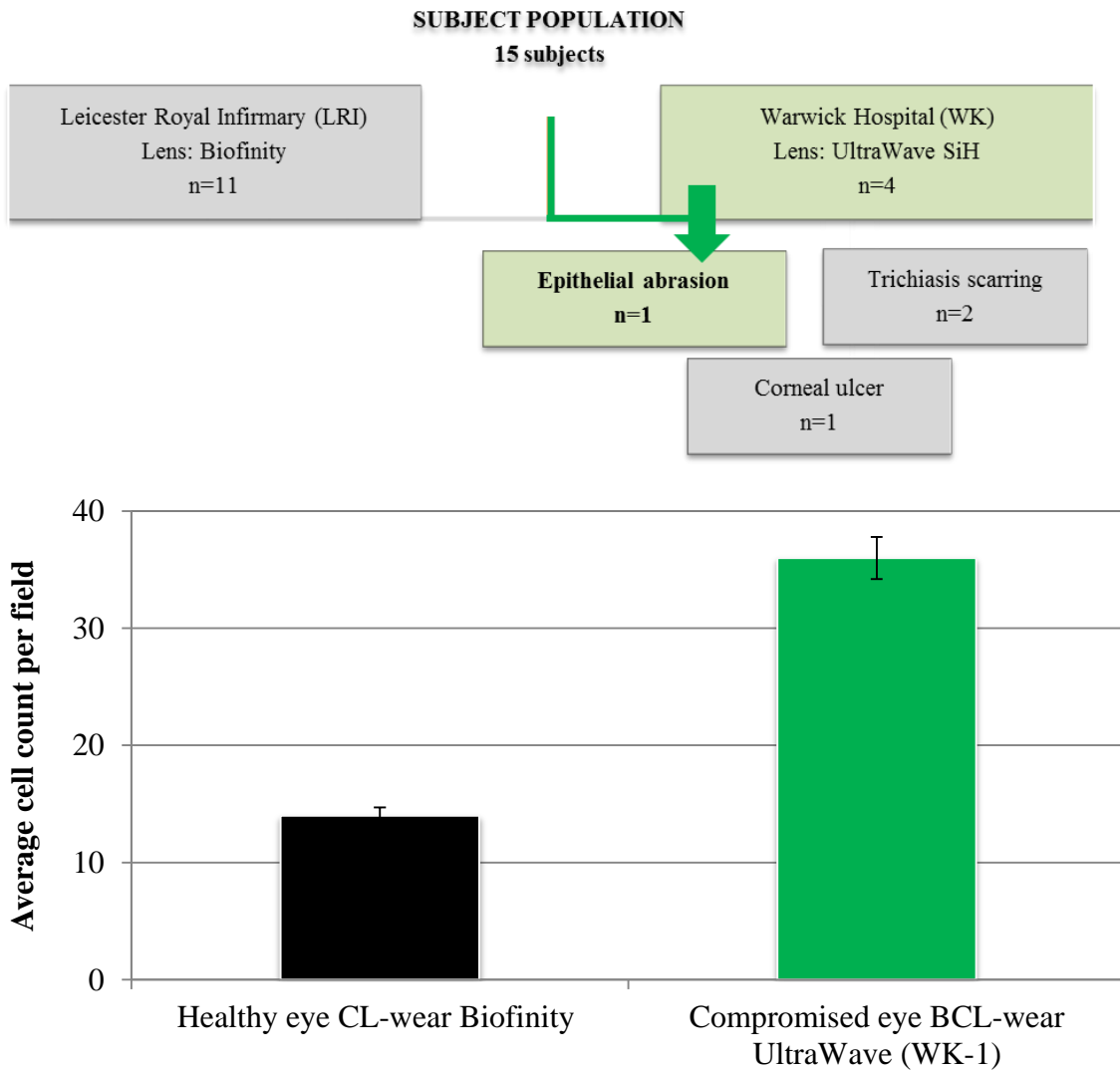


Figure 4.6. A comparison of average cell counts on Biofinity contact lenses worn in the non-compromised eye (n=6) with a Biofinity bandage contact lens worn in the compromised eye (n=1). All contact lenses were worn for 8 hours.

4.5.3.1 Discussion

In the BCL study population, the shortest duration of contact lens wear was a one day Biofinity lens for the management of a corneal abrasion (subject WK-1). The comparison of the average cell count per field on lens WK-1 (36 ± 2) with the average for contact lenses worn for one day in the non-compromised eye (14 ± 1) reveals significant differences. Because vitronectin deposition on the contact lens surface results from mechanical interaction between the contact lens and the cornea, the results presented in Figure 4.6 strongly suggest that vitronectin is more readily deposited on the contact lens posterior surface from the compromised cornea than from the non-compromised cornea.

The nature of the abrasion in subject WK-1 must be considered in greater depth. Due to the propensity of the corneal epithelium to heal rapidly for superficial injuries, it is feasible that the abrasion on the cornea partially healed during the time lapse between the damage to the cornea and the BCL application. Although the BCL would have provided instant pain relief, it would not have greatly influenced the healing process. If the BCL was applied immediately after the injury occurred, the extent of vitronectin deposition to this contact lens may potentially have been higher than the actual levels observed.

4.5.4 The Effect of Wear Duration on Vitronectin-Mediated Cell Adhesion: Four Week Wear Duration

A subset of the BCL study population includes five subjects who were prescribed with Biofinity contact lenses for the management of bullous keratopathy. All contact lenses ($n=5$) were worn for a period of four weeks continuous wear. An average cell count per field was obtained for the posterior surface of each lens. Figure 4.7 shows that despite the isolation of wear duration, contact lens type and clinical condition, the average cell count per field ranges largely from 64 ± 3 to 86 ± 4 . In particular, the average cell count per field on the contact lens worn by patient LRI-5 (64 ± 3) is significantly lower than the other four contact lenses in the same sub-group.

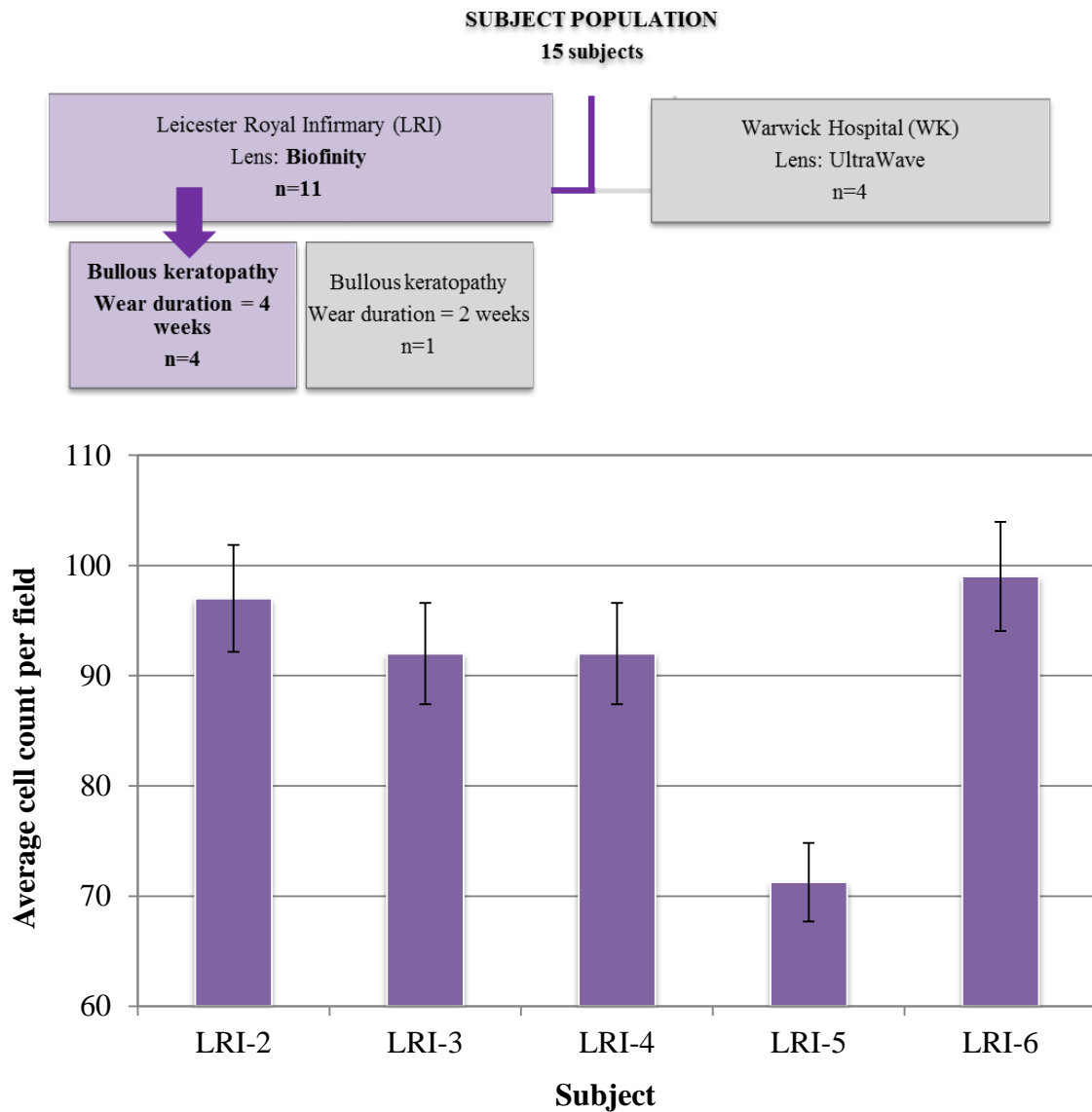


Figure 4.7 Cell count data for ex vivo Biofinity bandage contact lenses worn by five subjects for the management of bullous keratopathy (n=5). All lenses were worn for four weeks.

4.5.4.1 Discussion

Comparison of cell counts on BCLs of the same contact lens materials type (Biofinity), worn for the same wear duration (four weeks continuous wear) and clinical condition (bullous keratopathy) reveal significant differences between contact lenses. These results highlight that wear duration in the compromised eye is not the overriding influential factor on vitronectin-mediated cell adhesion and that the effect of ocular clinical condition and patient-to-patient variation must also be accounted for.

4.5.5 Key Points for the Influence of Wear Duration on Vitronectin-Mediated Cell Adhesion

- In the healthy CL-wearing eye, overall vitronectin-mediated cell adhesion was found to be significantly greater on contact lenses worn for five days extended wear in comparison to contact lenses worn for one day disposable wear. This shows that as wear duration is increased in the non-compromised eye, the extent of vitronectin-mediated cell adhesion also increases.
- In the BCL-wearing eye, cell adhesion appears to increase with wear duration, reaching a plateau after approximately 1 week, regardless of contact lens material type.
- The comparison of contact lenses worn in the compromised eye and the non-compromised eye reveals significant differences; it appears that vitronectin is more readily deposited from the impaired corneal tissue bed than the intact healthy corneal tissue bed.
- Vitronectin-mediated cell adhesion to contact lenses varied significantly between bullous keratopathy subjects, despite contact lenses being worn for the same wear duration. This suggests that wear duration alone does not determine the extent of vitronectin deposition levels from the corneal tissue bed.

4.6 The Influence of Contact Lens Material on Vitronectin-Mediated Cell Adhesion in the Bandage Contact Lens-Wearing Eye

4.6.1 Biofinity versus UltraWave SiH

In chapter three it was demonstrated that the locus and extent of vitronectin-mediated cell adhesion is largely influenced by contact lens modulus. It was therefore logical to determine whether this effect is also seen with *ex vivo* BCLs. Two types of *ex vivo* BCLs were compared in order to investigate the influence of contact lens material type upon vitronectin-mediated cell adhesion. The contact lenses included Biofinity and UltraWave SiH.

Analysis of the contact lenses reveals that Biofinity with a higher modulus of 0.75 MPa gave a more even distribution of cell adhesion on the lens surface (1.9:1 edge:centre ratio), whereas UltraWave SiH with a lower modulus of 0.5 MPa shows greater cell adhesion at the edge (2.7:1 edge:centre ratio). Figure 4.8 shows that although both materials show greater vitronectin-mediated cell adhesion at the edge of the contact lens than at the centre as expected, there is a significant difference in the distribution over the lens surface. This difference in contact lens material behaviour is also demonstrated in Figure 4.9, where the relationship between wear duration and the edge:centre cell count ratio for each contact lens in this study is provided.

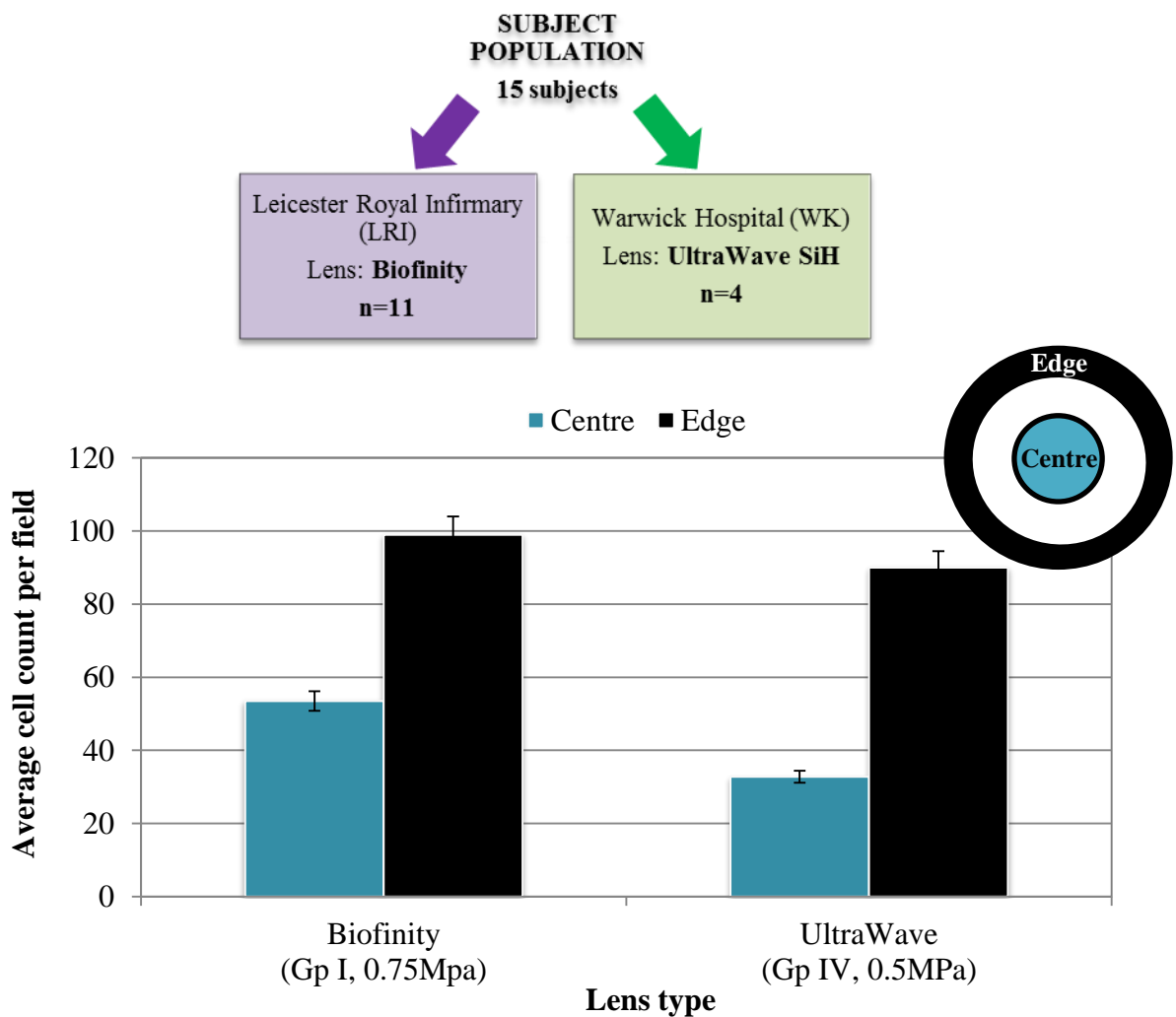


Figure 4.8 The effect of contact lens material type on the locus of vitronectin mediated-cell adhesion. The locus of cell adhesion (contact lens centre and lens edge) is shown for ex vivo Group II Biofinity bandage contact lenses (n=11) and for ex vivo Group IV UltraWave SiH bandage contact lenses (n=4).

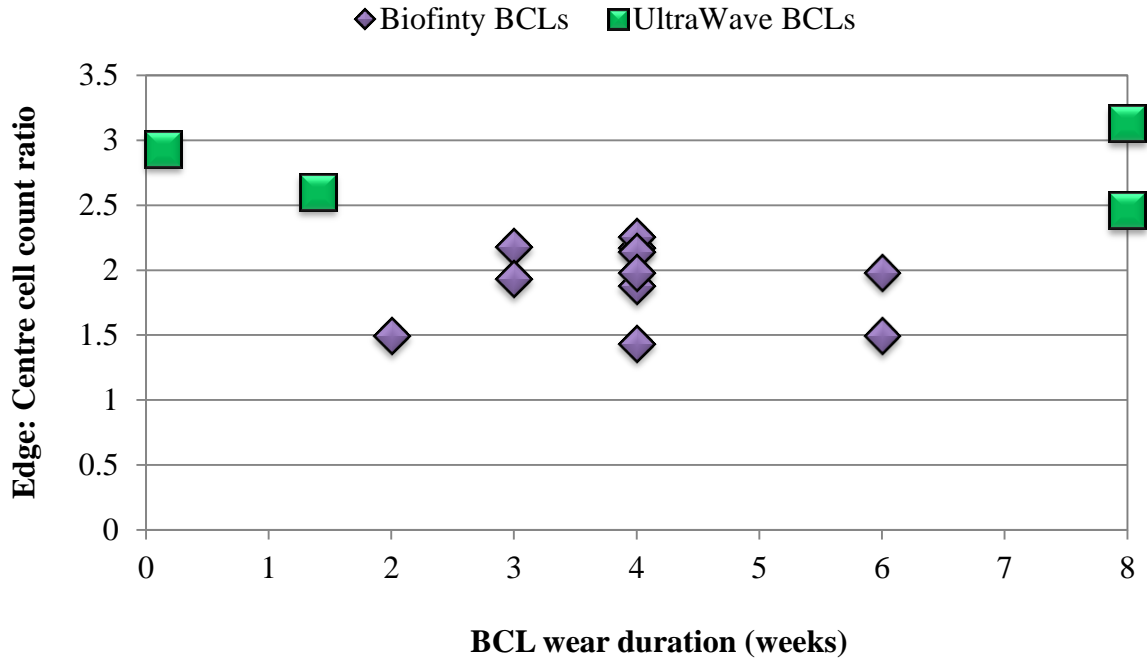


Figure 4.9 The relationship between bandage contact lens (BCL) wear duration and the edge:centre cell count ratio. Data is provided for Biofinty contact lenses ($n=11$) and UltraWave SiH contact lenses ($n=4$).

4.6.2 Discussion

It was shown in chapter three that:

- the higher the contact lens water content the higher the vitronectin-mediated cell adhesion (section 3.5).
- the higher the contact lens modulus the lower the edge:centre cell count ratio (section 3.8).

In this study two materials of similar water contents, but differing moduli were examined. Inspection of Figures 4.8 and 4.9 show that UltraWave SiH contact lenses (0.5 MPa) gave greater vitronectin-mediated cell adhesion at the edge of the contact lens than at the centre. Biofinty contact lenses (0.75 MPa) also showed greater cell adhesion at the edge of the lens, but in comparison to UltraWave SiH, this edge/centre effect was less pronounced. Increased cell adhesion at the contact lens edge may be due to a number of factors. Firstly, the contact lens is constantly rotating to give mechanical contact lens-tissue interaction with the cornea. As the eyelid moves over the anterior

contact lens surface, the lens edge will firstly be compressed followed by the centre. This contact lens-tissue interaction is greatly influenced by material modulus; the effect at the edge is more pronounced with lower modulus contact lenses which tend to drape over the cornea. Therefore, a comparison of the two materials studied shows that a material such as UltraWave SiH with a low modulus (0.5 MPa) is shown to have greater vitronectin-mediated cell adhesion at the contact lens edge. The radial movement of the contact lens means that the contact lens-tissue contact in rotation is greater at the contact lens edge than at the lens centre. As Biofinity has a higher modulus (0.75 MPa), the stiffer material produces more contact with the cornea at the centre of the lens. Secondly, progressive dehydration of any contact lens material in the eye during wear may affect the radius of curvature, allowing greater contact and interaction with the contact lens edge. This accounts for greater vitronectin-mediated cell adhesion at the edge, a trend which is seen throughout each assay performed.

The locus of vitronectin-mediated cell adhesion on the posterior surface of the contact lens is significant because this will in turn influence the locus of plasmin upregulation. As discussed in section 3.9, vitronectin binds and stabilises plasminogen activator inhibitor-1 (PAI-1). The specific localised removal of vitronectin from the corneal tissue bed, together with PAI-1, leads to the specific localised upregulation of plasmin. In this work, assuming that the BCL is constantly rotating as usual during wear, plasmin generated at the contact lens edge is likely to be removed from the contact lens surface and escape into the tear film. Conversely, plasmin generated at the centre of the contact lens has a lower chance of removal, regardless of the extent of contact lens rotation.

When comparing the two materials studied here, UltraWave SiH appears to be the favourable contact lens material for BCL wear because it shows less vitronectin-mediated cell adhesion at the centre of the contact lens. This may potentially give less plasmin generation. In terms of mechanical properties, the advantage of a soft contact low modulus contact lens for therapeutic use is evident; such a material can offer minimal vitronectin build-up at the contact lens centre.

4.6.3 Key Points for the Influence of Contact Lens material Type on Vitronectin-Mediated Cell Adhesion

- Material modulus greatly influences the locus of vitronectin-mediated cell adhesion.
- Biofinity with a higher modulus of 0.75 MPa gave a more even distribution of cell adhesion on the posterior surface of the lens, whereas UltraWave SiH with a lower modulus of 0.5 MPa gave greater vitronectin-mediated cell adhesion at the contact lens edge than at the lens centre.
- The locus of vitronectin-mediated cell adhesion on the posterior surface of the contact lens may influence the locus of plasmin upregulation.

4.7 A Comparison Between Vitronectin-Mediated Cell Adhesion to *ex vivo* Biofinity Contact Lenses Worn for the Management of Bullous Keratopathy or Sjögren's Syndrome

4.7.1 Bullous Keratopathy versus Sjögren's Syndrome

Vitronectin-mediated cell adhesion was compared for BCLs worn for the two treatment of two different ocular conditions: bullous keratopathy and Sjögren's syndrome.

Bullous Keratopathy

Bullous keratopathy is a condition of corneal oedema due to endothelial dysfunction. Impaired endothelial cells are unable to remove fluid entering the cornea at a sufficient rate, thus causing persistent oedema to the cornea. The epithelium separates from Bowman's layer to result in areas of separation termed bullae, which are pushed towards the surface of the cornea to appear as fluid-filled blisters (figure 4.10). The bullae can rupture to cause extreme pain because of exposed nerve endings, and a reduction/loss of visual acuity is typically experienced. There are potentially many causes for bullous keratopathy, including Fuch's endothelial dystrophy (a genetic disorder causing endothelial loss), infection and trauma. However, bullous keratopathy commonly occurs as a complication following cataract surgery or intraocular lens implantation; the onset of the condition is often due to endothelium trauma caused by

contact from the implanted intraocular lens or surgical instrumentation. The condition may be managed by:

- surgical intervention. Procedures such as excimer laser phototherapeutic keractomy and penetrating keratoplasty offer treatment for bullous keratopathy. However, surgery is not suitable in many cases.
- the use of hypertonic agents to reduce oedma. Sodium chloride (5%) eye drops or ointment can be effective in reducing oedema.
- medications to reduce intraocular pressure. The intraocular pressure must be controlled to prevent further compromise to endothelial function.
- contact lenses for bandage applications.

A bandage contact lens may offer instant pain relief for patients suffering with bullous keratopathy. The BCL protects the exposed nerves of the bullae on the corneal surface, which can consequently reduce the level of pain experienced. Additionally, the BCL may increase visual acuity [124]. The symptoms of bullous keratopathy may also reduce with the use of long term BCL wear [125].



Figure 4.10 Corneal oedema and the formation of bullae in bullous keratopathy [126].

Sjögren's Syndrome

Sjögren's Syndrome is a chronic autoimmune disease, which mainly affects the lacrimal and salivary glands, resulting in dry eyes (keratoconjunctivitis sicca) and dry mouth (xerostomia). The etiology of Sjögren's Syndrome is currently unknown, but the condition may be classified as primary Sjögren's Syndrome, when the condition develops by itself, or secondary Sjögren's Syndrome, when the condition develops in association with another autoimmune disease such as rheumatoid arthritis. The intensity of ocular symptoms may vary from patient to patient, but include decreased tears, inability to tear, intolerance to light and foreign body sensation. Further ocular

complications also include persistent corneal infections due to irritation caused by dry eyes. Oral symptoms include inflammation of the oral mucosa and salivary glands, dry oral mucosal surfaces and dental decay. Figure 4.11 indicates how the disease can affect the body. Diagnosis is confirmed by physical examination and a variety of tests, such as the Schirmer test (described in chapter two) to determine tear production, saliva tests to determine the volume of saliva production and blood tests for the presence of certain antibodies indicative of Sjögren's Syndrome. The condition is not curable, but topical eye drops and artificial saliva can help to lubricate the dry body sites. BCLs may be used to protect the corneal surface.

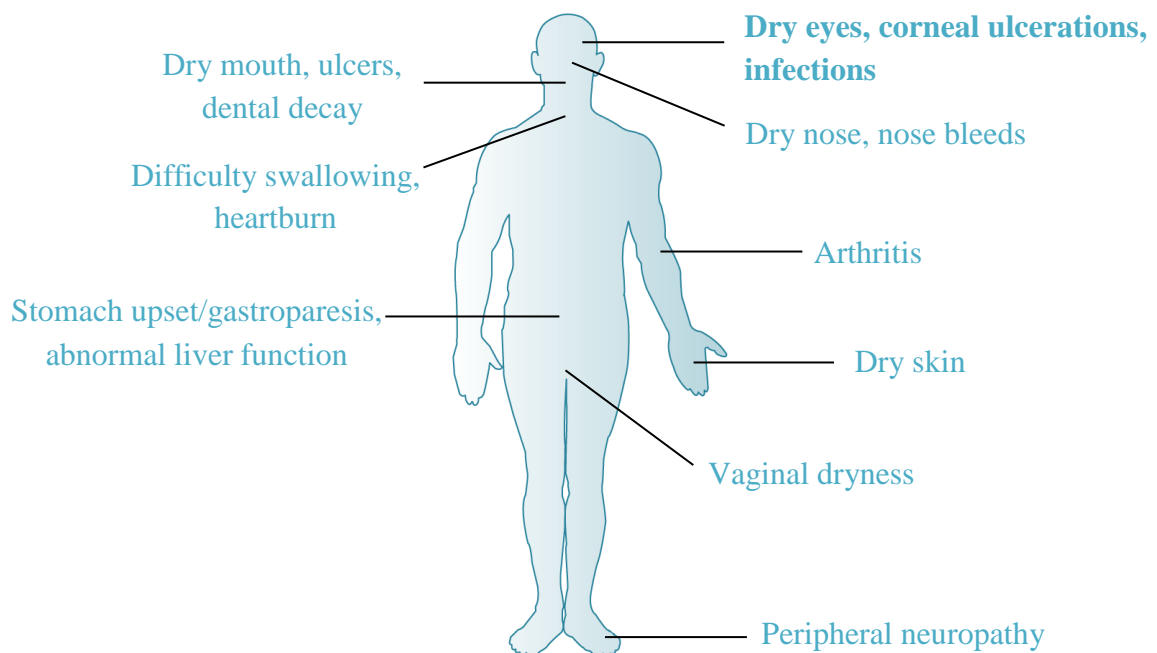


Figure 4.11 Possible symptoms of Sjögren's Syndrome.

Of the entire patient population in this study, six subjects wore Biofinity contact lenses for the management of bullous keratopathy (LRI-21 – LRI-6) and three subjects wore Biofinity contact lenses for the management of Sjögren's syndrome (LRI-7 - LRI-9). A brief summary of each subject's ocular history is provided in Table 4.3 for bullous keratopathy and Table 4.4 for Sjögren's syndrome. All contact lenses were worn for a duration greater than 2 weeks, beyond the point at which a plateau of vitronectin-mediated cell adhesion is reached. Additionally, the same contact lens material type (Biofinity) was worn in all cases. Therefore, by isolating wear duration and material effects, the influence of clinical condition (bullous keratopathy versus Sjögren's syndrome) on vitronectin-mediated cell adhesion could be compared.

Table 4.3 Patient information for subjects requiring Biofinity bandage contact lenses for the management of bullous keratopathy (BK).

Patient ID	Gender	Age	Ocular History	Lens exchange every 4-6 weeks?
LRI-1	F	63	Cataract surgery in 2008, leading to further ocular disruptions. Developed BK in 2010 - BCL fitted immediately.	Yes
LRI-2	F	78	Retinal detachment surgery in 2005, leading to chronic inflammation in one eye. Developed band keratopathy in 2009 leading to BK - BCL fitted in 2012.	Yes
LRI-3	M	76	Developed glaucoma in both eyes in 1969, but treated surgically in 1980s. Cataract surgery in 2004. Developed BK in RE in 2004 - BCL fitted in 2012.	Yes
LRI-4	M	63	Surgery to treat corneal laceration of RE in 2009, leading to cataracts and surgery. Developed BK in 2009 - BCL fitted in 2013. RE left with scarred cornea, amniotic membrane transplant and aphaikic.	No, BCL management stopped
LRI-5	F	60	Chronic uveitis treated with steroids in 1970s, leading to cataracts and secondary glaucoma in both eyes. Developed BK and corneal decomposition in 2007 - BCL fitted in 2010. Registered blind.	Yes
LRI-6	F	83	Cataract surgery in 2002, leading to ocular disruptions and retinal bleeding. BK in 2010 - BCL fitted immediately.	Yes

LRI, Leicester Royal Infirmary; BK, bullous keratopathy; BCL, bandage contact lens; RE, right eye.

Table 4.4 Patient information for subjects requiring Biofinity bandage contact lenses for the management of Sjögren's syndrome (SS).

Patient ID	Gender	Age	Ocular History	Schirmer Strip Data (mm/5 minutes)	Lens exchange every 4-6 weeks?
LRI-7	F	64	Diagnosed with primary SS in 2002, unassociated with any other condition - BCL fitted in 2009.	1	Yes
LRI-8	F	62	Diagnosed with primary SS in 2008, unassociated with any other condition - BCL fitted in 2010.	5	Yes
LRI-9	F	77	Diagnosed with rheumatoid arthritis in 1995 and then secondary SS. Developed glaucoma in RE (unconnected to SS). Recurring filamentary keratitis – BCL fitted in 2003.	1	Yes

LRI, Leicester Royal Infirmary; SS, Sjögren's Syndrome; BCL, bandage contact lens; RE, right eye.

Figure 4.12 shows that vitronectin-mediated cell adhesion to the contact lenses studied is consistent with the trend seen thus far in terms of locus on the posterior surface of the lens, regardless of the clinical condition or wear duration involved. Greater cell adhesion was also found on the surface of contact lenses worn by Sjögren's syndrome subjects (102 ± 5) in comparison to contact lenses worn in bullous keratopathy cases (83 ± 4).

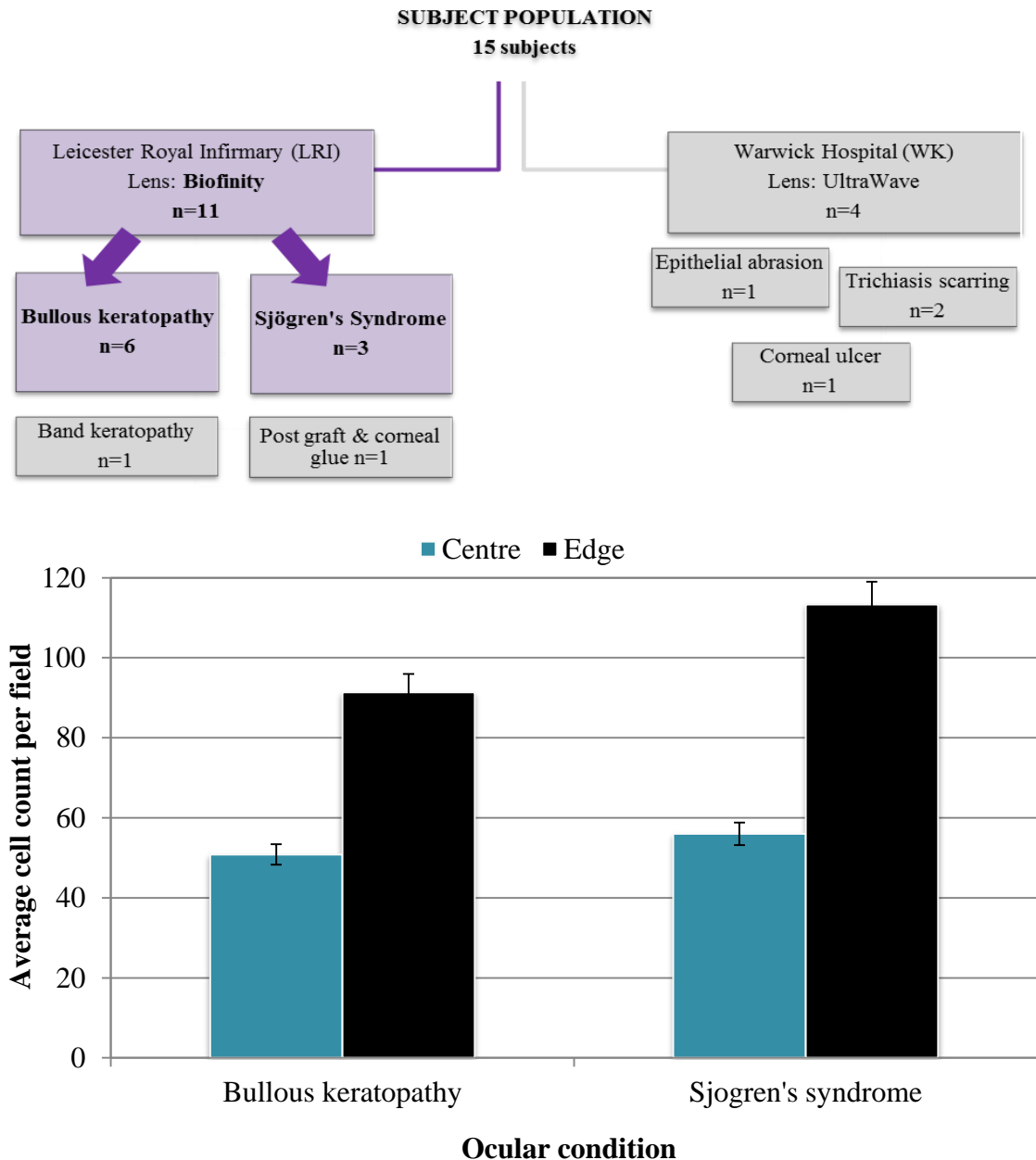
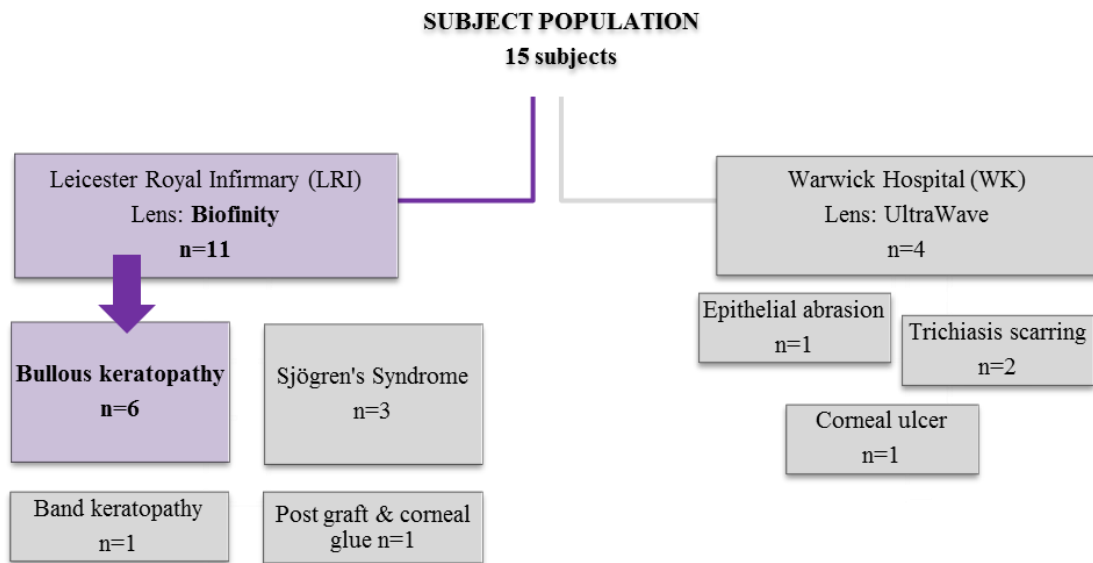


Figure 4.12 A comparison of the locus of cell adhesion on ex vivo Biofinity bandage contact lenses worn for the management of Sjögren's Syndrome ($n=3$, contact lens wear duration: 3-6 weeks) and for the management of bullous keratopathy ($n=6$, contact lens wear duration: 2-4 weeks).

Bullous Keratopathy Subjects

A breakdown of the subject data for the bullous keratopathy group reveals interesting observations and differences between subjects. Figure 4.13 shows the locus of cell adhesion on each BCL worn for bullous keratopathy management. It can be seen that subject-to-subject variability is relatively modest within this clinical sub-group. However, it is interesting to note that subject LRI-5 shows a noticeably reduced gross level of vitronectin-mediated cell adhesion in comparison to the other contact lenses analysed in this sub-group. The aggregated (centre + edge) value for all other bullous keratopathy subjects lies between 135 and 168 cell counts per field, whereas LRI-5 has a much lower aggregate value of 105, which is a statistically significant difference. Additionally, there does not appear to be a relationship between the edge:centre cell count ratio and overall vitronectin-mediated cell adhesion, as shown in Figure 4.14.



(the key to Figures 4.13 and 4.14)

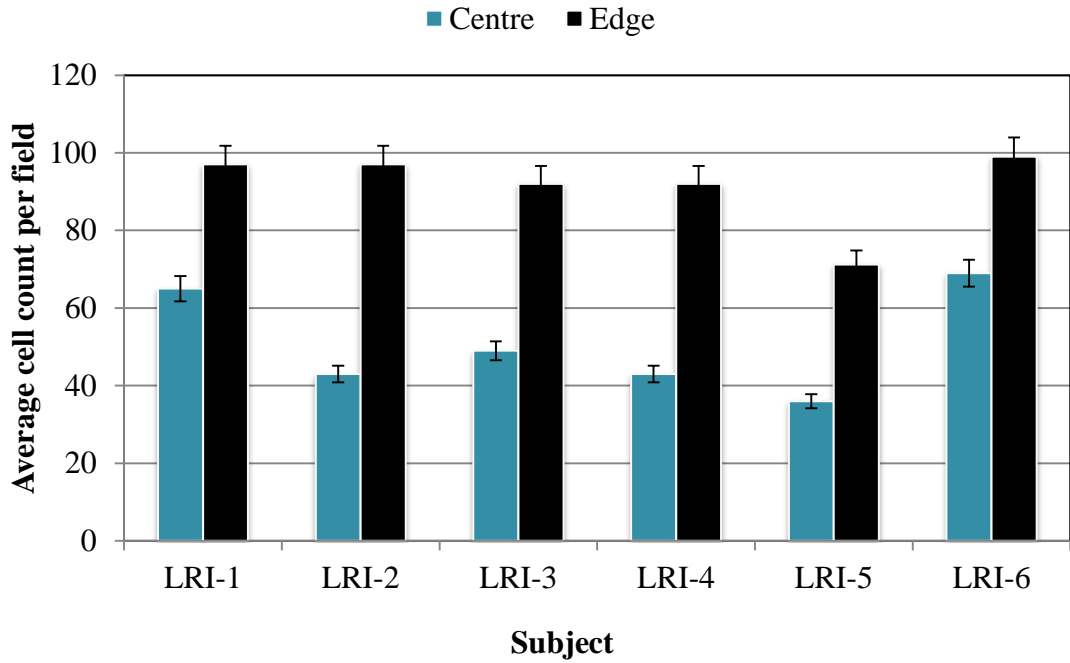


Figure 4.13 The locus of cell adhesion (contact lens centre and lens edge) on ex vivo Biofinity bandage contact lenses worn for the management of bullous keratopathy (n=6). Lenses were worn from 2-6 weeks.

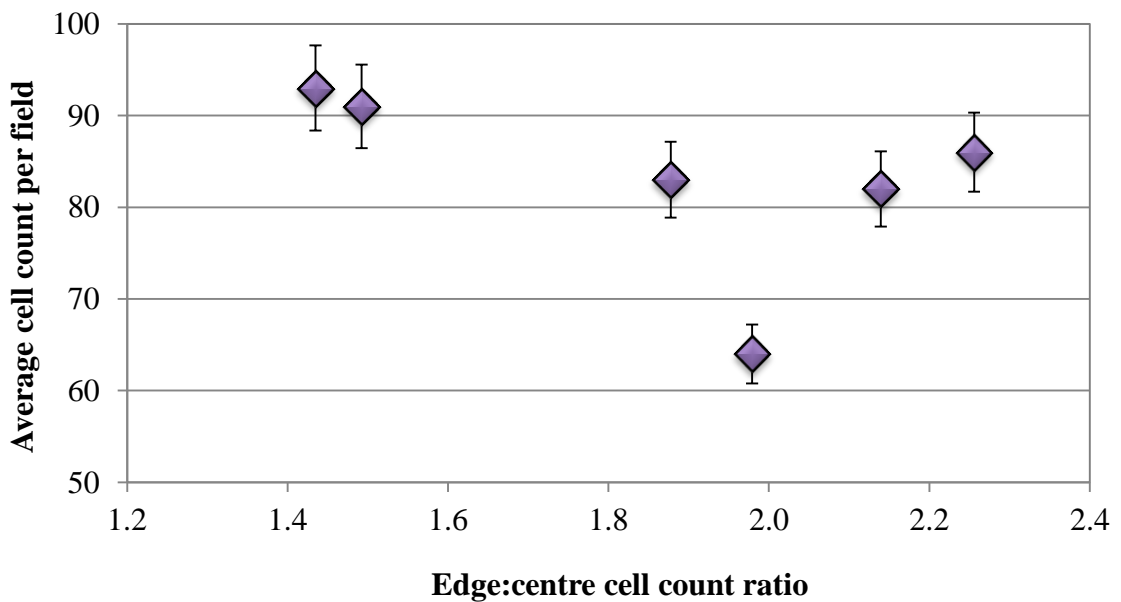


Figure 4.14 The relationship between vitronectin-mediated cell adhesion and the edge:centre cell count ratio for ex vivo Biofinity bandage contact lenses worn for the management of bullous keratopathy (n=6).

Sjögren's Syndrome Subjects

A comparison of vitronectin-mediated cell adhesion between subjects for the Sjögren's syndrome group reveals little variability, as shown in Figure 4.15. All subjects had a poor tear flow and demonstrated higher levels of cell adhesion relative to the bullous keratopathy subjects shown in Figure 4.13. The edge:centre cell count ratios are fairly similar for Sjögren's syndrome subjects LRI-7, LRI-8, and LRI-9 at 2.2:1, 1.9:1 and 2.0:1 respectively.

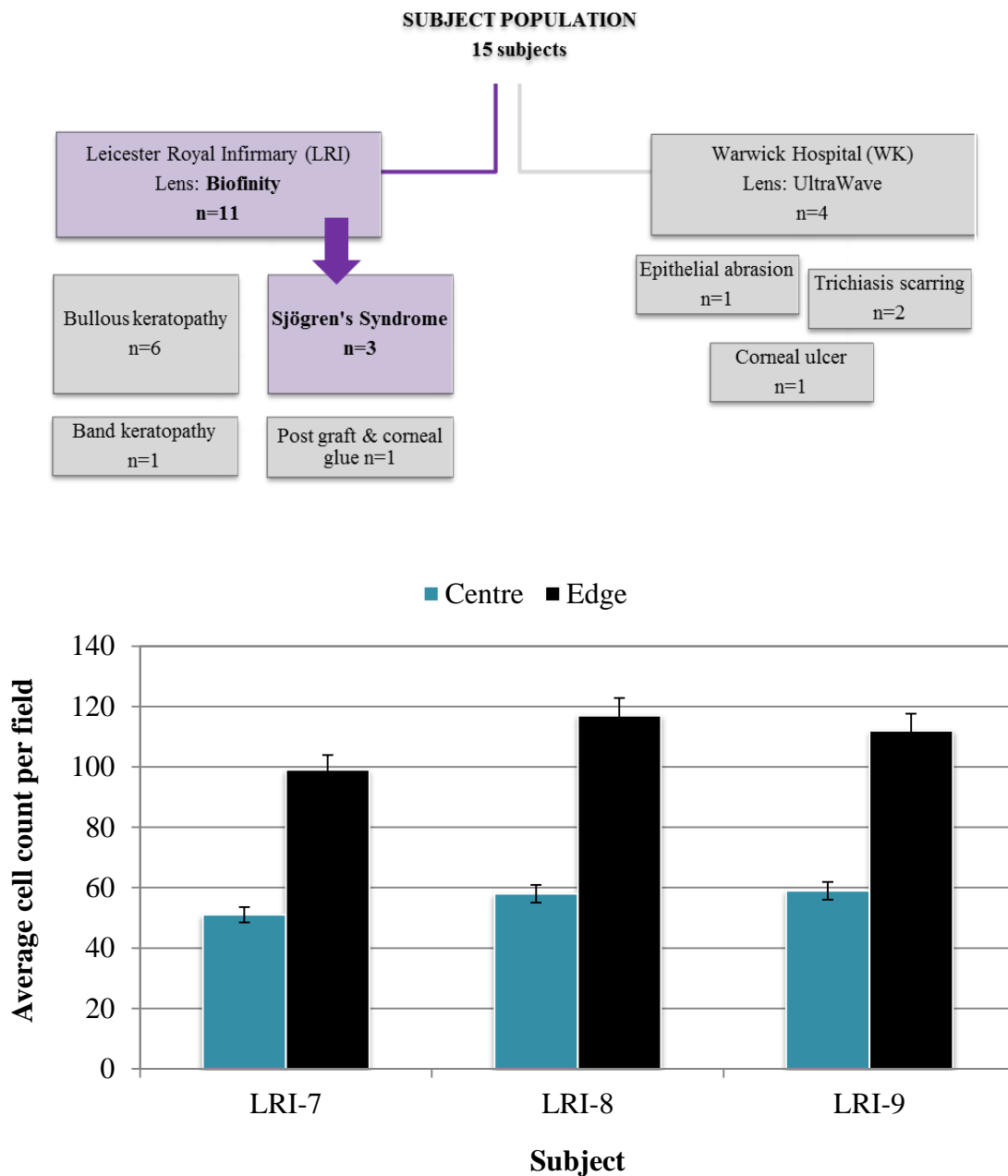


Figure 4.15 The locus of cell adhesion (contact lens centre and lens edge) on ex vivo Biofinity bandage contact lenses worn for the management of Sjögren's Syndrome (n=3). Lenses were worn from 3-6 weeks.

4.7.2 Discussion

It has been shown that a significant difference in vitronectin-mediated cell adhesion exists between bullous keratopathy and Sjögren's syndrome; there is a general observation that Sjögren's syndrome subjects produce greater vitronectin-mediated cell adhesion to the BCL surface. Although vitronectin deposition on the lens surface arises from direct contact of the contact lens with the tissue bed, this difference may be described by the measure of the subject's tear flow. In Sjögren's syndrome, inflammation of the tear glands results in chronic dry eye. It is therefore expected for the tear flow to be considerably diminished or effectively non-existent in Sjögren's syndrome patients. Artificial tears are used to replace natural tears and thus keep the cornea hydrated and lubricated. A Schirmer test, as described in section 2.2.2, is a simple measure of tear deficiency for patients presenting with dry eye symptoms. In patients with Sjögren's syndrome, the Schirmer test is one type of test typically undertaken at the time of diagnosis, but it is not continually repeated during treatment because the tear flow is expected to deteriorate as the condition progresses. Therefore, successive tests to determine the tear flow levels would be unnecessary (Prof Martin Rubinstein, personal communication, 27th November 2013). It is widely accepted that a Schirmer score of ≥ 15 mm/5 minutes is considered normal for the healthy eye, a score of 14-6 mm/5 minutes is mild to moderate and a score of less than 5 mm/5 minutes is considered severe [102]. The average Schirmer score for the Sjögren's syndrome group studied here was 4mm/5 minutes, indicating that all subjects had a severely compromised tear flow. It seems highly likely that the deficient tear film enables greater contact lens-tissue mechanical interaction and, therefore, greater vitronectin deposition on the posterior surface of the lens. Tear flow measurements were not collected for any of the bullous keratopathy subjects because they did not present symptoms relating to dry eye and were assumed in clinic to have sufficient tear flow. The results presented for the bullous keratopathy group suggest that a more regular tear flow in these cases could enable less abrasive contact lens-tissue interaction, thus explaining one possible difference in vitronectin-mediated cell adhesion in comparison to the Sjögren's syndrome subjects.

When considering the bullous keratopathy clinical sub-group, although there is a degree of uniformity in cell counts within these subjects, it is possible that any variations that

do occur are tear flow dependant. Assuming that there was no unreported interruption in wear, and that contact lens fit is comparable in all cases, the data suggest that subject LRI-5 has a more coherent posterior tear film in comparison to the other subjects analysed. Potentially, tear flow measurements could be beneficial for all long term BCL wearers, to include bullous keratopathy patients, and not just for dry eye or Sjögren's syndrome patients. It is apparent that the condition of the tear flow may affect vitronectin-mediated cell adhesion and overall vitronectin deposition, which is then likely to affect plasmin upregulation in a sequential process.

It is evident from the subject histories detailed in Tables 4.2 and 4.3 that in several of these cases the first instance of BCL application occurred many years after the initial clinical diagnosis. For instance, subject LRI-4 was diagnosed with bullous keratopathy in 2007, but was fitted with a BCL four years later. This may be due to the advances of contact lens materials for extended wear. Due to the propensity of the cornea to heal rapidly, it is unlikely for any of the corneas in these cases to have been in an actively healing state at the time of the first BCL insertion. It appears that the BCL does not aid the healing process in such cases, as ascertained in experiments investigating wear duration in section 4.5, and the tear film plays a protective role in conjunction with the BCL device. An adequate tear flow is therefore imperative in order to sustain the healthy corneal surface. Nevertheless, the BCL serves in other roles, such as mechanical protection from eyelid blinking, pain relief, maintaining corneal hydration and the protection from other injuries. It is accepted that regular contact lens wearers with a low tear flow find contact lens wear to be difficult; this factor should be taken into consideration when selecting an appropriate contact lens material. The choice of BCL material is ever more vital in patients requiring the long term use of contact lenses for the management of conditions such as Sjögren's syndrome and may influence the success and outcome of BCL wear.

4.7.3 Key Points – Bullous Keratopathy versus Sjögren's Syndrome

- Greater vitronectin-mediated cell adhesion was observed to contact lenses worn in Sjögren's syndrome cases in comparison to bullous keratopathy cases. All Sjögren's syndrome subjects exhibited a poor tear flow.

- Vitronectin deposition on the contact lens surface arises from contact lens-tissue mechanical interaction. It appears that the deficient tear film enables greater interaction and, therefore, greater vitronectin deposition on the posterior surface of the lens.
- The substantivity of the tear flow may affect vitronectin deposition and in turn affect plasmin upregulation.

4.8 Concluding Discussion

From the work described in this chapter it is evident that vitronectin, an extremely adhesive glycoprotein, adheres strongly to the BCL posterior surface. It is often argued that SiHy materials minimise protein adsorption, but due to the “sticky” nature of vitronectin, this protein has been detected on *ex vivo* BCLs. The development of a novel on-lens cell-based assay rather than an extraction technique has enabled this detection. The consequences of vitronectin deposition and the potential effect of plasmin upregulation in the compromised eye must not be overlooked.

In this study comparisons were drawn between vitronectin-mediated cell adhesion on contact lenses worn in the non-compromised eye and compromised eye. It was demonstrated in chapter three that vitronectin deposition on contact lenses results from the mechanical interaction of the contact lens with the cornea. Evidence presented from the study in this chapter strongly suggests that vitronectin is more readily deposited from the impaired corneal surface than from the healthy intact cornea. Additionally, the contact lens material type has a significant influence on the locus of vitronectin-mediated cell adhesion; lower modulus contact lenses deposit greater levels of cell adhesion at the edge of the lens.

Furthermore, comparisons between vitronectin-mediated cell adhesion on contact lenses worn for bullous keratopathy and contact lenses worn for Sjögren’s syndrome were made by isolating material variation and wear period. A measurable overall difference in the levels of cell adhesion was observed and these appear to be associated with the nature of the tear flow. It is important to note that these levels of vitronectin-mediated cell adhesion are high in comparison to those of contact lens wear in the healthy eye. The recognised link between contact lens wear and plasmin generation means that

increased vitronectin may result in greater plasmin levels. The success of a BCL for the management of Sjögren's syndrome in particular appears to be dependent upon the tear flow of the contact lens wearer. Greater success and comfort with a contact lens may be achieved if it is more suited to the wearer's tear film. As a result, addressing the state of the tear flow first and improving the lubrication of the eye as a whole may reduce vitronectin build up on the contact lens surface. A contact lens material with a more useful ability to sustain a sufficient tear flow would be useful. It is arguable that some contact lenses are viewed as more favourable for dry eye patients than others. Currently the only contact lens available with a clinical indication for dry eye is Proclear, with a maximum wear time of thirty days, but it is not frequently selected as a bandage lens (Prof Martin Rubinstein, personal communication, 27th November 2013). There is clearly a shortfall in appropriate contact lens materials which can potentially minimise vitronectin deposition during extended periods of wear.

Plasmin is the key component of the plasminogen activator system, and is also involved in the degradation of the extracellular matrix and plasma proteins during pathological processes. Although plasmin activity is essential to the inflammation process, a balance is required to prevent the negative effects of plasmin over activity. The centre and edge of the lens, depending upon material mechanical properties, have different levels of vitronectin sorption. If plasmin generation is a progressive effect of vitronectin removal from the corneal tissue bed, these mechanical properties of the contact lens will determine the extent of active plasmin accumulation in the eye. As links between increased tear plasmin activity and corneal disease, due to contact lens wear or trauma, have been reported [122], and over activity of plasmin has been shown to inhibit wound healing, the upregulation of plasmin is potentially a considerable problem in the compromised eye. The majority of subjects studied in this chapter were non-surgical cases, thus the presence of active plasmin would be unlikely to adversely inhibit the healing process because the corneal wound would have healed by the time of the first BCL insertion. Nevertheless, the disturbed cornea is undoubtedly in a compromised state and understanding what is occurring behind the contact lens is vitally important for the ocular health of the subject. There is also the possibility of plasmin interaction with the cornea to generate more vitronectin, resulting in further corneal compromise.

In this study, BCLs were supplied by two hospitals. The selection of a BCL should ideally be dependent upon the type of corneal defect presented by a subject and the nature of their ocular health. It appears that the choice of Biofinity and UltraWave SiH contact lenses for therapeutic uses, however, was influenced by convenience and availability rather than specific knowledge of their healing capacity or suitability for each individual subject. The Biofinity or UltraWave SiH BCLs studied in this chapter were worn from between one day to eight weeks of continuous extended wear. Biofinity has a recommended wear duration of just seven days, thus it is highly abnormal that contact lenses harvested for this work were worn excessively beyond this period. It may be argued that the reasonable oxygen permeability of Biofinity (128 Dk) justifies exceeding the recommended wear duration of seven days. The lower oxygen permeability of UltraWave SiH (86 Dk), however, is comparable to that of conventional hydrogel materials. Hence, the risk of continuous wear for over thirty days as worn by some UltraWave SiH subjects appears to be irrational. The impact of this upon the compromised eye must be taken into account when selecting a contact lens material. In particular, consideration should be given to what is specifically required from the BCL in terms of protein interaction. From the majority of cases studied here, it is evident that the BCL is required as a protective corneal shield for extended wear use rather than to aid healing. Vitronectin deposition on the contact lens is inevitable due to its strong affinity for contact lens surface. The contact lens most certainly has a protective power, but is not biomimetic, thus it is able to remove vitronectin from the corneal tissue site. The “best” contact lens material choice would provide minimal interaction with the cornea, resulting in less vitronectin deposited central to the cornea and less vitronectin deposition overall. Deposition is influenced greatly by material modulus and a lower modulus material has been shown to minimise vitronectin deposition.

This work has shown that levels of vitronectin-mediated cell adhesion to the posterior contact lens surface are higher in persistent BCL wear in comparison to healthy contact lens-wear. It appears that contact lens manufacturers are generally more concerned with the anterior surface of the lens, in terms of movement of the eyelid and initial comfort for example, rather than the posterior contact lens surface. However, understanding posterior surface interactions is as equally important if we are to consider the health of the cornea in persistent contact lens wearers. The link between plasmin and contact lens wear means that there is a strong argument that the design of specific BCLs with greater

ocular compatibility and lower levels of vitronectin deposition appears to be an excellent target for maintaining the ocular health of long term BCL wearers.

4.9 Chapter Summary

Following baseline experiments in chapter three, the aim of this chapter was to investigate the quantity and locus of vitronectin-mediated cell adhesion to the posterior surfaces of *ex vivo* bandage contact lenses (BCLs) worn in the compromised eye. Optimisation of the on-lens cell-based assay technique is undoubtedly an important method to investigate the interaction of a contact lens biomaterial with the compromised cornea. The findings presented in this work reveal that vitronectin-mediated cell adhesion is significantly influenced by:

- *wear duration*: in the non-compromised eye, cell adhesion increases with wear duration of a five day period. In the compromised eye, adhesion increases with wear duration until it reaches a plateau at approximately one week.
- *contact lens material modulus*: a higher contact lens modulus will give a lower centre:edge cell count ratio (i.e. a more even distribution over the contact lens surface), whereas a lower lens modulus will give a higher centre:edge cell count ratio (i.e. a more vitronectin-mediated cell adhesion at the edge of the contact lens than at the centre).
- *clinical condition and nature of the patient's tear film*: where the tear film is severely low in volume, contact lens-corneal interaction will be increased and, therefore, may result in greater levels of vitronectin-mediated cell adhesion.

The consequences of deposition in the BCL wearing eye in terms of potential plasmin upregulation must not be overlooked.

CHAPTER FIVE

Surface and Mechanical Properties of Skin Adhesive Wound Healing Materials

5.1 Aim

Chapters three and four demonstrated how mechanical interactions of the contact lens with the cornea can stimulate a biochemical response to potentially generate an upregulation of plasmin. In a similar manner, the success of a dermal wound dressing material lies in its surface and mechanical properties. The work presented in this chapter focusses on the biophysical properties of human skin and the corresponding properties of skin adhesive materials used in medical devices, such as wound dressings and ostomy devices, which are designed to function in direct contact with breached and unbreached skin. The important properties that directly influence behaviour of the skin adhesive interface, that include the mechanical properties (static and dynamic moduli) and surface properties of both skin and adhesive, are investigated.

5.2 Introduction

There are many studies that investigate the efficacy of skin adhesive wound healing materials for medical device applications in acute/chronic dermal wound and ulcer environments. The vast majority of these studies focus on the comparison of adhesive materials for the management of wounds [127-129], for the efficacy of materials on wound healing rates [130], and for the comparison of materials for fluid management and retention [131, 132]. In an industry where an extensive range of skin adhesive materials are available, such studies enable a platform for appropriate material selection. For example, Thomas and Loveless [131] compared twelve commercial hydrocolloid dressings in order to distinguish between performance in fluid handling, fluid retention, moisture vapour permeability and conformation. The authors found significant differences between these properties for different dressings that initially appear to be similar in appearance and function, and thus proposed a grading system to enable effective dressing selection.

Although studies that critically compare adhesive materials provide an essential basis for material selection, a review of the literature shows that there is very little known regarding the biophysical properties of skin adhesive wound dressings and the direct impact that these properties have upon material performance. The important properties that will directly influence behaviour of the skin adhesive interface are the surface energies and mechanical properties of skin adhesive materials. This chapter recognises

the fact that there is a gap in information within this field and consequently addresses the important biophysical properties of human skin and the corresponding biomaterials (skin adhesive wound dressings and ostomy devices) that function with skin. These biomaterials have direct contact with skin and act as a physically protective barrier against the external environment, thus biocompatibility with skin is a primary requirement. As with any biomaterial, the surface and interfacial behaviour of skin adhesive materials governs their biocompatibility with the host body site. To promote a compatible skin adhesive interface, the synthetic adhesive material should ideally possess similar surface properties to that of the skin surface. Therefore, the first stage of this investigation was to study the surface properties of a range of skin adhesive materials.

5.3 Materials

5.3.1 Skin Adhesive Materials

5.3.1.1 Overview of Skin Adhesive Materials

The skin adhesive materials studied in this chapter are listed in section 2.1.2 and are of three sorts; adhesive hydrocolloids, adhesive hydrogels and medical tapes. For the purpose of the investigations carried out in this chapter, these materials may then be grouped further to give five groups, with twelve variables in total:

- Salts Hydrocolloid Adhesives for wound dressings (n=4)
- ConvaTec Hydrocolloid Adhesives wound dressings (n=2)
- Commercial Hydrocolloid Adhesives for ostomy devices (n=2)
- Aston hydrogels synthesised in-house (n=2)
- Commercial Medical Tapes (n=2)

Table 5.1 provides a brief overview of the five skin adhesive material groups used within this chapter. A description of each adhesive material is provided in the following sub-sections. Compositions of adhesives are detailed where available.

Table 5.1 Five skin adhesive material groups used for investigations.

Product Type	Material Name/Code
Salts Hydrocolloid Adhesives	S1
	S2
	S3
	S4
ConvaTec Hydrocolloid Adhesives	Granuflex
	Duoderm Extra Thin
Ostomy Hydrocolloid Adhesives	Coloplast ostomy
	ConvaTec ostomy
Aston Hydrogel Adhesives	Hydrogel 1
	Hydrogel 2
Commercial Medical Tapes	3M microporous tape
	Boots microporous tape

5.3.1.2 Hydrocolloids

Hydrocolloids are absorptive, occlusive and generally adhesive materials. They typically consist of sodium carboxymethyl cellulose (NaCMC) for absorptive and fluid management properties, poly(isobutylene) (PIB) for the provision of an adhesive matrix, and gelatine and pectin which act as ‘gum-like’ gel forming agents [54]. Thus, hydrocolloids may be described as a continuous phase of PIB with a particulate dispersed phase of NaCMC, gelatine and pectin. The structure of each hydrocolloid component and the overall properties and functions of the material are provided in (section 1.4.3 – Skin Adhesive Hydrocolloids).

The application of hydrocolloids in biomaterials may be classified for two purposes. Firstly, hydrocolloids may be fabricated for skin adhesive wound dressings. These materials are able to absorb low to moderate levels of wound exudate by undergoing a phase inversion to form a hydrophilic gel. This hydrophilic gel supports a moist wound environment and the occlusive nature of the material aids autolytic debridement. The absorptive capacity of the material is determined by its composition. Secondly, hydrocolloids may be used for ostomy devices. These medical devices are designed to collect discharged bodily waste through a surgically created ostomy. A more detailed

description of the function of ostomy devices can be found in section 1.4.3. Ostomy devices consist of two components; a pouch or bag that collects fluid discharged from the body and an adhesive component that adheres to the peri-ostomy area. The adhesive, commonly referred to as a skin barrier or wafer, is typically a hydrocolloid material. Devices are available as a one-piece system, in which the pouch and wafer are attached together to form one unit, or devices are available as two-piece system, in which the pouch and wafer are detachable.

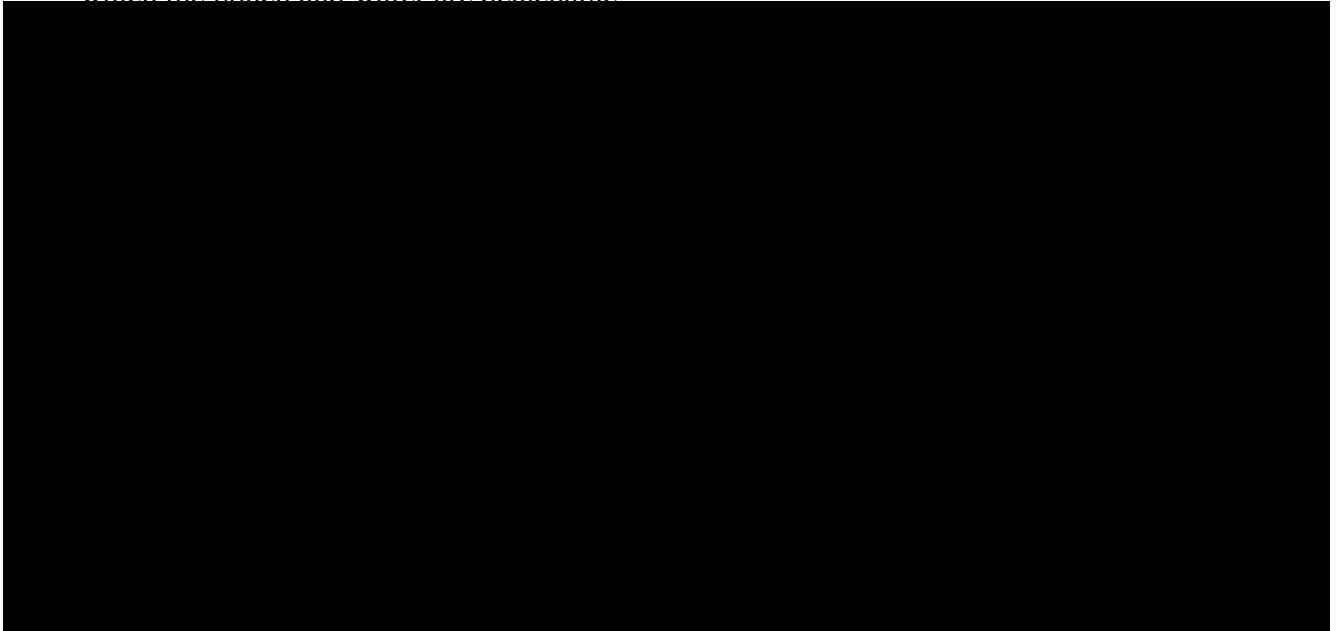


Table 5.2 Compositions of the Salts Hydrocolloid Adhesives group for wound

PIB, poly(isobutylene); CMC, carboxymethyl cellulose.

- 2) **ConvaTec Hydrocolloid Adhesives*** - Two hydrocolloid adhesives for wound dressings were purchased from ConvaTec UK. ConvaTec is a competitor manufacturer to Salts Healthcare and one of the leaders of wound care and ostomy products. Granuflex and Duoderm were selected as two leading hydrocolloid adhesives products for comparison against the Salts Healthcare Adhesives. Both examples of the ConvaTec Hydrocolloid Adhesives were supplied with paper release liners on the adhesive surface.

- **Granuflex**

- **Duoderm Extra Thin**

- 3) **Ostomy Hydrocolloid Adhesives*** – Hydrocolloid adhesives for ostomy devices were purchased from two leading commercial manufacturers – Coloplast ostomy from Coloplast and ConvaTec ostomy from ConvaTec. Both ostomy adhesives were supplied with paper release liners on the adhesive surface.

- **Coloplast ostomy**

- **ConvaTec ostomy**

*The compositions of the ConvaTec Hydrocolloid Adhesives and Ostomy Hydrocolloid Adhesives were not available from the manufacturers. The compositions of commercial skin adhesive materials are generally not advertised with the products. The adhesives chosen for this work were selected as examples of leading products in the market.

5.3.1.3 Hydrogels

Hydrogel are networks of cross-linked water-swollen polymers [51]. Hydrogel adhesives are used in many biomedical applications such as bioelectrodes and transdermal drug-delivery patches. However, the ability of adhesive hydrogels to absorb fluid makes them ideal for skin adhesive wound dressing applications. Additionally, absorptive hydrogels are able to maintain a moist wound healing environment by providing moisture to the wound.

The hydrogel skin adhesive materials studied in these investigations were synthesised in-house. Two materials of different compositions were prepared – Hydrogel 1 and

Hydrogel 2. The full protocol for the preparation of these two materials is provided in section 2.2.3. The compositions of each hydrogel material are provided in Table 5.3.

Table 5.3 Compositions of skin adhesive hydrogels synthesised in-house: Hydrogel 1 and Hydrogel 2.

	Hydrogel 1	Hydrogel 2
Distilled Water (g)	1.1	10.0
Glycerol (g)	30.0	30.0
NaAMPs (g)	68.9	40.0
SPA (g)	0.0	20.0
Photoinitiator/cross linker mixture (g)	0.25	0.25

NaAMPs, 2-acrylamido-2-methyl-1-propanesulfonic acid, sodium salt, 50% wt solution in water; SPA, 3-sulfopropyl acrylate, potassium salt.

5.3.1.4 Medical Tapes

Medical tapes, or surgical tapes, are designed to secure a wound dressing to the peri-wound area. Such tapes are known as pressure sensitive adhesives because they form a bond with a substrate when applied with pressure. Activation by heat, solvent or water is not required. A typical medical tape is made of a thin sheet of polymer, such as poly(ethylene terephthalate), coated with an adhesive. The majority of tapes currently available are made from microporous materials.

Two commercial brands of medical tape were purchased for the investigations in this chapter:

- **3M Microporous Tape**
- **Boots Microporous Tape**

5.3.2 Release Liner Materials

The skin adhesive hydrocolloid and hydrogel materials described in section 5.3.1 all require the use of release liner materials. Release liners provide effective release from an adhesive substrate. They are either paper or plastic based, of which one side is coated with a release agent. Silicon derivatives, such as poly(dimethylsiloxane), are commonly used as release agents. The structure of poly(dimethylsiloxane) is provided

in Figure 5.1. Release agents serve numerous functions, from the initial time of formulation of the adhesive, to up until the application of the adhesive to skin. During the formulation stage, temporary liners are applied to the adhesive materials in order to transport the adhesives from process to process. The temporary liner prevents the adhesive surface from adhering to other surfaces. Liners may be applied and removed several times during the formulation stage. The adhesive is then fabricated into a biomaterial device, such as a wound dressing or ostomy device. After the device fabrication, a permanent liner is applied to the adhesive, which protects the surface of the device during storage. This permanent liner is only removed from the adhesive immediately before the device is to be applied.

Paper and plastic release liners with siliconised surfaces were supplied by Salts Healthcare. For the purpose of this work the paper release liner is referred to as **RL1-paper** and the plastic release liner is referred to as **RL2-plastic**.

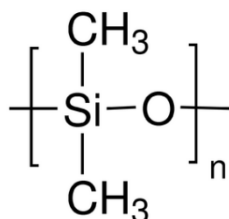


Figure 5.1 The structure of poly(dimethylsiloxane).

5.4 Surface Properties of Skin Adhesive Materials

5.4.1 Surface Energy Measurements for a Range of Skin Adhesive Materials

Surface energy (SE) measurements were taken for a range of skin adhesive materials, as listed in Table 5.1. All adhesives had different compositions, with the exception of Salts Adhesive Hydrocolloids S1 and S3 (refer to Table 5.2 for Salts Adhesive Hydrocolloid compositions).

SE measurements were taken for each adhesive material using the sessile drop technique. This technique is commonly used to evaluate the surface free energy of a solid by contact angle measurements. The full protocol for the technique, which used GBX Digidrop instrumentation, can be found in section 2.2.4. The release liner was

removed from the adhesive immediately before measurements were taken. Five contact angle measurements were taken for each adhesive material to provide an average SE. An average SE for each adhesive group was then calculated.

From Table 5.4 it can be observed that there are significant differences in SE between the groups of materials. The Ostomy Hydrocolloid Adhesives group and Salts Hydrocolloid Adhesives group exhibited similar average SEs (21.3 mNm^{-1} and 23.8 mNm^{-1}), whereas the ConvaTec Hydrocolloid Adhesives group in comparison gave a significantly higher average SE (33.6 mNm^{-1}). The in-house Aston Hydrogel Adhesives group had an average SE of 29.5 mNm^{-1} .

Table 5.4 Average surface energy measurements (derived from contact angle measurements with water and diiodomethane probe liquids) for a range of commercial and non-commercial skin adhesive materials.

Skin Adhesive Material	Av. Contact Angle (°) Water	Av. Contact Angle (°) Diiodomethane	Av. Surface Energy (mNm^{-1})
Ostomy Hydrocolloid Adhesives n=2	90.6	77.9	21.3 (± 0.1)
Salts Hydrocolloid Adhesives n=4	94.0	69.4	23.8 (± 7.6)
Aston Hydrogel adhesives n=2	92.1	58.6	29.5 (± 3.5)
ConvaTec Hydrocolloid Adhesives n=2	101.7	52.5	33.6 (± 0.4)

5.4.1.1 Discussion

The sessile drop technique measures the contact angle formed between a probe liquid and substrate. Measurements enable the SE of the substrate to be determined. In order to evaluate the SE values of the hydrocolloid skin adhesive materials in Table 5.4, the structure of hydrocolloids must be considered. A typical hydrocolloid consists of a mixture of sodium carboxymethylcellulose (NaCMC), gelatine and pectin particles dispersed in a matrix of poly(isobutylene) (PIB). Figure 5.2 shows a representation of the particle dispersion within the polymer matrix.

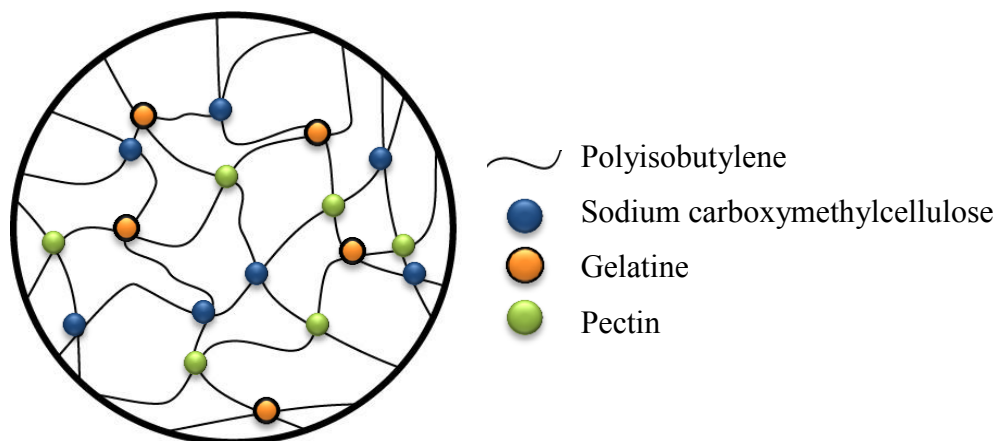


Figure 5.2 A representation of the hydrocolloid system.

The NaCMC, gelatine and pectin particles are embedded within the PIB matrix, thus the presence of these particles at the surface of the hydrocolloid is generally low. PIB forms the supporting polymer matrix and thus it is generally the most visible component at the surface in terms of SE. Therefore, the SE of a hydrocolloid is governed by the SE of PIB. The SE of PIB is approximately 33 mNm^{-1} [133].

From the initial SE values of the various adhesive groups in Table 5.4, it can be observed that the ConvaTec Hydrocolloid Adhesives group gave on average a SE value of 33.6 mNm^{-1} , which is comparable to the SE of PIB (33 mNm^{-1}). This suggests that the PIB component of the ConvaTec Hydrocolloid Adhesives is unmodified at the adhesive surface. However, the Salts Hydrocolloid Adhesives group and the Ostomy Hydrocolloid Adhesives group gave on average lower SEs (23.8 mNm^{-1} and 21.3 mNm^{-1} respectively) in comparison to the ConvaTec Hydrocolloid Adhesives group (33.6 mNm^{-1}). It is plausible that the surfaces of the Salts Hydrocolloid Adhesives and Ostomy Hydrocolloid Adhesives were contaminated with an agent that could lower the SE of these adhesives by such a considerable extent. One obvious candidate is contamination from the siliconised release liners. The SE of silicone oil is approximately 21 mNm^{-1} (value measured in lab). A low SE is an essential requirement for a release agent in order to prevent it from adhering to the substrate, which in this case is the hydrocolloid adhesive.

It was observed that the difference between the adhesives with high SEs and the adhesives with low SEs was possibly due to the choice of release liner applied to the adhesives. The Ostomy Hydrocolloid Adhesives group and two adhesives from the

Salts Hydrocolloid Adhesives group with plastic release liners had 'low' SEs, whereas the ConvaTec Hydrocolloid Adhesives group with 'high' SEs were supplied with paper release liners. Because the choice of release liner appears to have some influence on the SE of the adhesive surface, it was therefore rational to further investigate these liner materials, which were provided by Salts Healthcare.

5.4.2 A Comparison Between Release Liners and Their Effect on Hydrocolloid Adhesive Surface Properties – Paper versus Plastic

Two types of siliconised release liners (as described in section 5.3.2) form the basis of this investigation:

- Salts paper release liner: RL1-paper
- Salts plastic release liner: RL2-plastic

Surface energy (SE) measurements of both samples, prior to application to hydrocolloid adhesives, were taken by the sessile drop technique (described in chapter two). Measurements were taken five times for each surface to obtain an average SE value. Both sides of the liners, to include the contact (siliconised surface) and the non-contact side (non-siliconised surface), were assessed to determine any differences between the opposing surfaces.

Table 5.5 reveals that both RL1-paper and RL2-plastic showed similar SEs for the contact sides (15.3 mNm^{-1} and 18.2 mNm^{-1} respectively). Similarly, the SE values for the non-contact sides of RL1-paper and RL2-plastic were also of the same order (31.7 mNm^{-1} and 38.4 mNm^{-1} respectively). It is important to note that the SEs for the contact sides of both the paper and plastic release liners are comparable. Although both release liner materials are of different substrates, the contact sides for both liners are coated with silicone to provide non-adherent surfaces. Therefore, the high ($>30 \text{ mNm}^{-1}$) SEs for the contact side of the release liners are lowered ($<20 \text{ mNm}^{-1}$) when the surfaces are coated with silicone.

Table 5.5 Surface energy values for the contact side and non-contact side of release liners RL1-paper and RL2-plastic before application to adhesives.

Surface	RL1-paper	RL2-plastic
Prior to liner application: Surface energy of release liner – non-contact side (mNm^{-1})	31.7 (± 1.6)	38.4 (± 1.9)
Prior to liner application: Surface energy of release liner – contact side (mNm^{-1})	15.3 (± 2.8)	18.2 (± 3.9)

In order to determine whether the release liner material type influences the surface properties of the adhesives that they are applied to, two Salts Hydrocolloid Adhesives with the same composition, but with different release liners were compared (S1 and S3). The compositions of S1 and S3 were detailed in Table 5.2 in section 5.3.1 of this chapter. Table 5.6 reveals clear differences between the two adhesives; S1 with a paper release liner had a SE value of 29.9 mNm^{-1} , whereas adhesive S3 with a plastic release liner had a statistically lower SE of 16.8 mNm^{-1} . These results suggest that silicone is transferred from the Salts plastic release liner to the adhesive, but not from the Salts plastic release liner to the adhesive.

Table 5.6 A comparison between surface energy values of two Salts Hydrocolloid Adhesives with the same composition, but different release liner materials: S1 and S3.

Material	Av. Surface Energy (mNm^{-1})
Adhesive S1 with release liner removed	29.9 (± 1.8)
Paper release liner removed from S1	19.9 (± 4.8)
Adhesive S3 with release liner removed	16.8 (± 5.1)
Plastic release liner removed from S3	23.7 (± 4.5)

5.4.2.1 Discussion

Initial measurements for a range of hydrocolloid adhesives in section 5.4.1 suggested that the release liner material may influence the SE of the adhesive surface. This speculation was investigated further by taking measurements of the liner materials prior

to application to adhesives. Analysis of both sides of the paper and plastic release liner materials showed that both release liners had similar SEs for the contact side.

In order to determine whether the liner material influences the surface properties of adhesives, a direct comparison was made between two adhesives of the same composition, but with different liners (S1 and S3). This comparison between adhesives S1 and S3 showed that although both adhesives were of the same composition, adhesive S3 with the plastic liner had a significantly lower SE adhesive S1 with the paper liner. These results strongly suggest that the plastic release liner transfer silicone to the adhesive during adhesive-liner contact and, therefore, lowers the SE of the adhesive closer to that of silicone oil (approximately 21 mNm^{-1}). Conversely, silicone transfer from the paper release liner to the adhesive material appears to have a minimal effect, if any at all. Before fully considering the implications of any possible silicone transfer, it was rational to confirm the presence of silicon on the adhesive surfaces. This was performed by X-ray photoelectron spectroscopy, as reported in the following section.

5.4.3 Quantifying Silicon on the Adhesive Surface – X-Ray Photoelectron Spectroscopy

X-ray photoelectron spectroscopy (XPS) was adopted as a sensitive spectroscopic technique for the detection of silicon on specific regions of four different Salts Hydrocolloid Adhesives materials; S1, S2, S3 and S4. The full protocol for XPS methodology can be found in section 2.2.5. The release liners were removed from the four individual adhesives prior to analysis, and both the liners and the adhesives were analysed. Additionally, a Salts paper release liner (RL1-paper) and a Salts plastic release liner (RL2-plastic), which had not been applied to adhesives, were analysed separately as reference points. Table 5.7 provides the percentage of each element detected at the surface of materials from the spectroscopy analysis. Carbon was the main element detected on all materials, ranging from 45.8% to 98.4%. Oxygen was detected on the surface of all materials, ranging from 1% to 25.6%. Silicon was also detected on all material surfaces, but the value detected was dependent upon the material type. Nitrogen was detected on adhesives S3 and S4 at 0.2 and 0.3% respectively, whereas sodium was only detected on adhesive S4 at 0.2%. The spectroscopic analysis did not detect calcium on the surface of any material.

Figure 5.3 shows the lower levels of silicon detected on the surface of adhesives S1 and S2 after siliconised paper release liners had been removed. This is in contrast to the higher levels of silicon detected on the surfaces of adhesives S3 and S4 after siliconised plastic release liners had been removed. Figure 5.4 shows silicon detected on surface of the release liners removed from the corresponding adhesives.

Table 5.7 Photoelectron spectroscopy results for the detection of silicon on the surface of Salts Hydrocolloid Adhesives (S1-S4) after the release liners are removed. Values for the paper (RL1) and plastic (RL2) release liners are also provided.

Material	% Element Detected					
	Carbon	Oxygen	Silicon	Nitrogen	Sodium	Calcium
Paper liner on S1	45.8	25.4	28.9	-	-	-
S1 adhesive	98.4	1.0	0.7	-	-	-
Paper liner on S2	46.8	25.1	28.0	-	-	-
S2 adhesive	97.0	1.8	1.2	-	-	-
Plastic liner on S3	48.6	25.6	25.8	-	-	-
S3 adhesive	79.3	12.0	8.6	0.2	-	-
Plastic liner on S4	49.4	24.9	25.7	-	-	-
S4 adhesive	78.5	13.0	8.1	0.3	0.2	-
RL1 (paper liner)	69.1	6.6	24.3	-	-	-
RL2 (plastic liner)	48.6	25.1	26.3	-	-	-

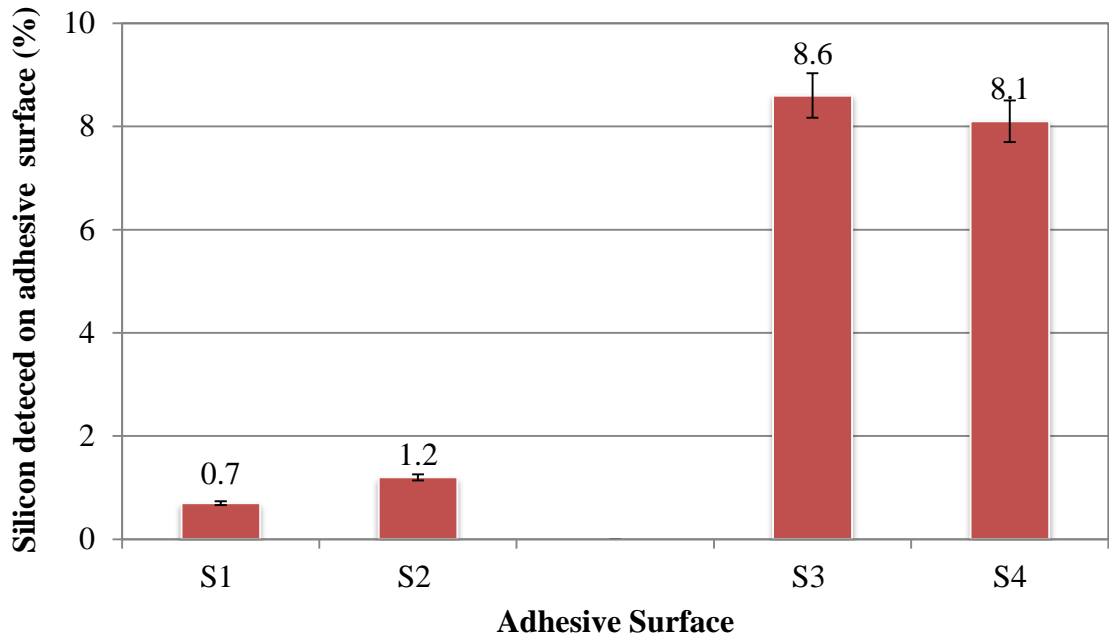


Figure 5.3 Silicon detected on the surface of adhesives S1 and S2 that had paper release liners and of Salts Hydrocolloid Adhesives S3 and S4 that had plastic release liners.

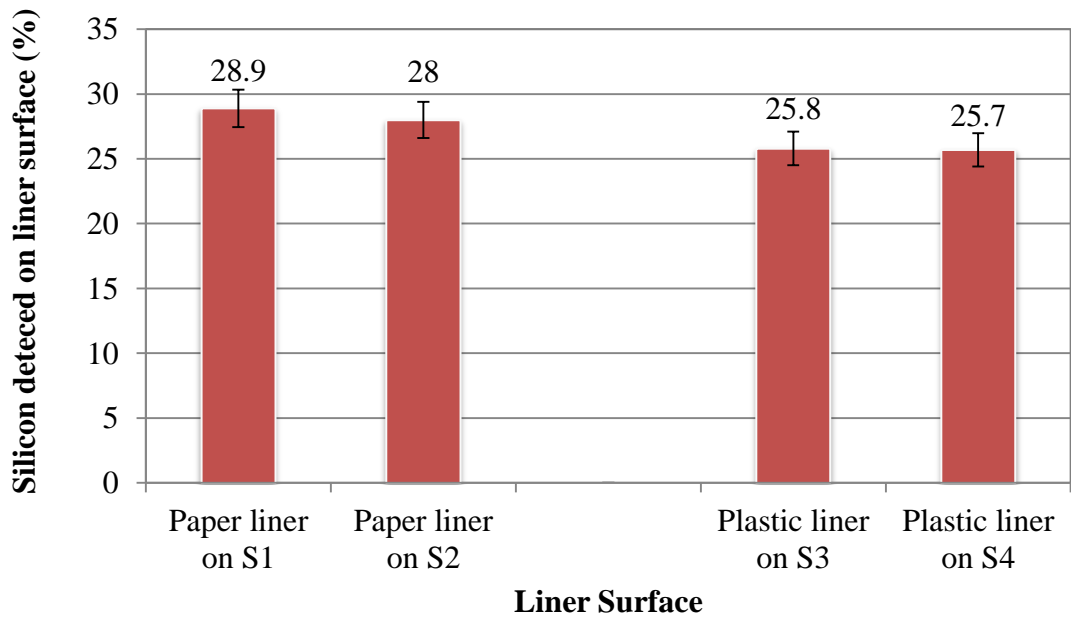


Figure 5.4 Silicon detected on the surface of paper and plastic release liners removed from Salts Hydrocolloid Adhesives.

The results revealed:

- similar levels of silicon were detected on the contact sides of the release liners RL1-paper and the RL2-plastic at 24.3% and 26.3% respectively. Comparable levels of silicon on both release liners were to be expected because both the paper and plastic liners were coated with silicone for its use as a release agent.
- similar silicon levels were detected for both the paper (28.9% and 28.0%) and plastic (25.8% and 25.7%) release liners that were in contact with adhesives and then removed.
- a significant difference in the silicon levels on adhesives with different release liners. Adhesives with paper release liners (S1 and S2) had lower levels of silicon on the surfaces (0.70% and 1.20% respectively) in comparison to adhesives with plastic release liners (S3 and S4) which had significantly higher levels of silicon detection in comparison (8.60% and 8.10% respectively).
- the levels of silicon detected on the paper release liners after contact with adhesives increased from 24.30% to 28.45%. This may be due to disturbance of the silicon monolayer on the liner surface.

The results show that silicone transfer from plastic release liners is significantly higher than from paper release liners.

5.4.3.1 Discussion

XPS was performed on Salts Hydrocolloid Adhesives (S1-S4) and Salts liner materials (RL1-paper and RL2-plastic) to detect silicon on the material surfaces. Table 5.7 shows that the technique successfully verified on average higher levels of silicon on the surface of two hydrocolloid adhesives with Salts plastic release liners (8.6% and 8.1%), in great contrast to hydrocolloid adhesives with Salts paper release liners (0.7% and 1.2%).

A large difference between transfer of silicone from the paper and plastic release liners to the adhesives is clearly apparent from Table 5.7; both liners have a similar silicon surface composition, yet the plastic release liner transfers approximately three times as

much silicone to the adhesive surface than the paper alternative. The transfer of silicone from a release liner to the hydrocolloid surface is not entirely a surprising phenomenon. The SE of silicone oil is approximately 21 mNm^{-1} and the SE of poly(isobutylene) (PIB) at the surface of the hydrocolloid adhesive is approximately 33 mNm^{-1} . When a liquid has a lower SE than the substrate, the liquid will spread over or 'wet' the surface [51]. From the findings in this investigation, it is evident that silicon from the release liner surface with a lower SE than PIB spreads over the PIB surface of the hydrocolloid. Silicon transfer from liner to adhesive is dependent upon contact adhesion – silicon will only transfer at points of adhesive-liner contact. This factor is influenced by the properties of the release liner materials. In particular, the two liner materials studied here have different surfaces. For instance, the siliconised fibrous paper release liner has a porous surface. The silicon is bound to the fibres of the porous surface and is unlikely to detach easily, which results in less effective contact transfer. Conversely, the siliconised plastic release liner possesses a smooth regular surface, whereby contact with the adhesive enables high silicon transfer. Silicone is known for its spreading behaviour, and it is likely to spread to form a thin molecular monolayer on the plastic liner surface. The extent of adhesive siliconisation by either liner material may also be affected by storage conditions to include time, temperature and pressure.

The results presented suggest that the paper liner has a significant advantage over the plastic liner in relation to transfer of silicon to the adhesive. In turn this could affect the surface properties of the adhesive and potentially affect other factors such as the peel strength or adhesivity of the adhesive material.

5.4.4 Removal of Silicone from the Adhesive Surface

Surface energy (SE) measurements for Salts Hydrocolloid Adhesives, which had not been in contact with release liners, would have proved valuable for this investigation. However, due to the nature of the manufacturing process, adhesives are only available with the release liners already applied. Therefore, attempts were made to remove the silicone detected from the surface of Salts Hydrocolloid Adhesives in order to obtain more accurate SE measurements for the adhesive materials. Two Salts Hydrocolloid Adhesives, S1 and S3, were treated with acetone immediately after the release liners had been removed with the purpose to eradicate any silicone from the surfaces. This was performed by blotting 1cm^2 adhesive samples with acetone for 1 minute. Table 5.8

shows that the treatment of adhesive S3 with acetone increased the SE measurement by 27%, whereas the treatment of adhesive S1 with acetone showed only a 0.5% increase in SE.

Table 5.8 Surface energy values for Salts Hydrocolloid Adhesives S1 and S3, before and after the treatment of acetone to remove silicone from the adhesive surfaces.

Adhesive	Initial Surface Energy (mNm ⁻¹)	Surface Energy After Acetone Treatment (mNm ⁻¹)	% Increase in SE
S1	29.9 (±1.8)	30.05 (±5.5)	0.5%
S3	16.8 (±5.1)	21.4 (±5.3)	27%

5.4.4.1 Discussion

Following the detection of silicon on the surface of adhesive materials by X-ray photoelectron spectroscopy (XPS) in section 5.4.3, attempts were made to remove the silicone by the treatment of adhesive surfaces with acetone. Adhesive S3, which had 8.60% levels of silicon detected on its surface by XPS, saw a large increase in SE of 29% following acetone treatment. This SE after acetone treatment is more representative of the surface properties of the adhesive before it had been influenced by the siliconised plastic release liner and of PIB (with a SE of approximately 33 (mNm⁻¹) at the hydrocolloid adhesive. In contrast, adhesive S1 saw just a 0.5% increase in SE. This small increase was to be expected as the adhesive had a significantly low level of silicon detection on the surface of 0.7% by XPS.

5.4.5 Key Points for the Surface Properties of Skin Adhesive Materials

- Silicon was detected by X-ray photoelectron spectroscopy on the surface of hydrocolloid adhesives, thus verifying that silicone is transferred from the release liner to the adhesive by direct contact. This ‘siliconisation’ of the adhesive is dependent upon the nature of the release liner material; plastic release liners transfer significant levels of silicone to the adhesive surface, whereas paper release liners in comparison transfer small quantities of silicone, if any at all.

- Silicone transfer by liner-adhesive contact has a direct effect upon the surface energy of the adhesive surface, regardless of the adhesive composition.
- Paper release liner materials do not alter the surface energy of the adhesive. The SE of the adhesive remains unchanged and correlates to the SE of PIB (approximately 33 mNm^{-1}). Conversely, siliconisation by plastic release liner materials lowers the surface energy of the adhesive closer to that of silicone rubber (approximately 21 mNm^{-1}).
- The findings from this investigation suggest that the siliconised paper release liner is a favourable material liner choice in comparison to the plastic release liner. Although both release liner materials have silicone coated surfaces, the surface of the porous paper liner does not transfer silicone as effectively as the smooth plastic surface. Therefore, the paper release liner does not significantly change the SE of the skin adhesive wound care products.
- The altered surface properties of the hydrocolloid adhesive materials in contact with plastic release liners could potentially affect material performance in terms of adhesivity. Materials are required to provide adherence upon application and for the duration of wear. Factors that could potentially affect adhesivity, such as silicone on the adhesive surface, could have implications for overall material performance. The adhesive properties of the materials studied thus far shall be investigated in the following sections.

5.5 Peel Strength Analysis of Skin Adhesive Materials

5.5.1 Peel Strength Measurements of Skin Adhesive Wound Dressing and Medical Tape Materials

Chapter two described peel strength tests as a method for adhesive strength assessment and an indication of the effectiveness of removal from skin. Peel tests on selected skin adhesives, outlined in Table 5.1, were performed. The peel test method described in section 2.2.6 was used to determine any correlation between the adhesive strength and the surface properties of materials recorded in the previous section 5.4. Measurements were performed for all materials at 90° and 180° on a steel substrate and at 90° on unbreached skin of a healthy volunteer, whereby the test site was the forearm. Each material was tested in triplicate.

The results for each adhesive material are provided in Table 5.9. Of all materials tested on skin, both Hydrogel 1 and Hydrogel 2 adhesives showed the highest maximum force (9.77 and 9.61 N) and peel strength (0.29 and 0.25 N/25mm) required to remove from the test substrates. The measurements for the 180° steel test on the two hydrogel materials exceeded the 10N force limit. The Commercial Medical Tapes (3M and Boots) showed the lowest maximum force (1.89 and 0.93 N) and peel strength (0.05 and 0.04 N/25mm). The Commercial Ostomy Hydrocolloid Adhesives, Salts Hydrocolloid Adhesives and ConvaTec Hydrocolloid Adhesives all showed comparable data.

Table 5.9 Peel strength measurements of skin adhesive wound dressings and medical tapes at 90° and 180° on steel and skin test substrates.

Adhesive Material	Angle (°) and Surface	Av. Max. Force (N)	Av. Peel Strength (N/25mm)
Coloplast Ostomy	90 Steel	2.80 (±0.12)	0.11 (±0.01)
	180 Steel	4.84 (±0.57)	0.19 (±0.02)
	90 Skin	1.70 (±0.23)	0.07 (±0.01)
ConvaTec Ostomy	90 Steel	2.66 (±0.24)	0.10 (±0.01)
	180 Steel	4.52 (±0.59)	0.19 (±0.02)
	90 Skin	1.51 (±0.16)	0.07 (±0.01)
Salts Hydrocolloid S1	90 Steel	2.22 (±0.27)	0.12 (±0.01)
	180 Steel	4.74 (±0.50)	0.22 (±0.05)
	90 Skin	1.76 (±0.57)	0.07 (±0.01)
Salts Hydrocolloid S3	90 Steel	3.64 (±0.20)	0.15 (±0.01)
	180 Steel	4.27 (±0.44)	0.17 (±0.03)
	90 Skin	1.93 (±0.61)	0.08 (±5.5)
Granuflex	90 Steel	3.49 (±0.11)	0.14 (±0.01)
	180 Steel	4.43 (±0.41)	0.59 (±0.06)
	90 Skin	2.65 (±0.32)	0.11 (±0.01)
Duoderm Extra Thin	90 Steel	2.77 (±0.38)	0.11 (±0.01)
	180 Steel	4.84 (±0.82)	0.19 (±0.02)
	90 Skin	2.13 (±0.67)	0.09 (±0.01)
Hydrogel 1	90 Steel	9.82 (±0.15)	0.39 (±0.03)
	180 Steel	>10	>10
	90 Skin	9.77 (±0.24)	0.29 (±0.1)
Hydrogel 2	90 Steel	9.86 (±0.12)	0.39 (±0.02)
	180 Steel	>10	>10
	90 Skin	9.61 (±0.15)	0.25 (±0.05)
3M Microporous Tape	90 Steel	0.87 (±0.12)	0.03 (±0.01)
	180 Steel	2.60 (±0.30)	0.10 (±0.02)
	90 Skin	1.89 (±0.35)	0.05 (±0.01)
Boots Microporous Tape	90 Steel	1.78 (±0.19)	0.07 (±0.01)
	180 Steel	3.66 (±0.44)	0.15 (±0.02)
	90 Skin	0.93 (±0.30)	0.04 (±0.01)

Figure 5.5 shows a typical trace generated from the peel test method. The trace was obtained from the peel test of Coloplast Ostomy at 90° on a skin test substrate. The maximum force of peel strength after an extension of 9.4 mm can be read at 1.6 N. Additionally, the average maximum force of peel strength data for each adhesive material tested at 90° and 180° on a steel substrate and at 90° on skin is shown in Figure 5.6.

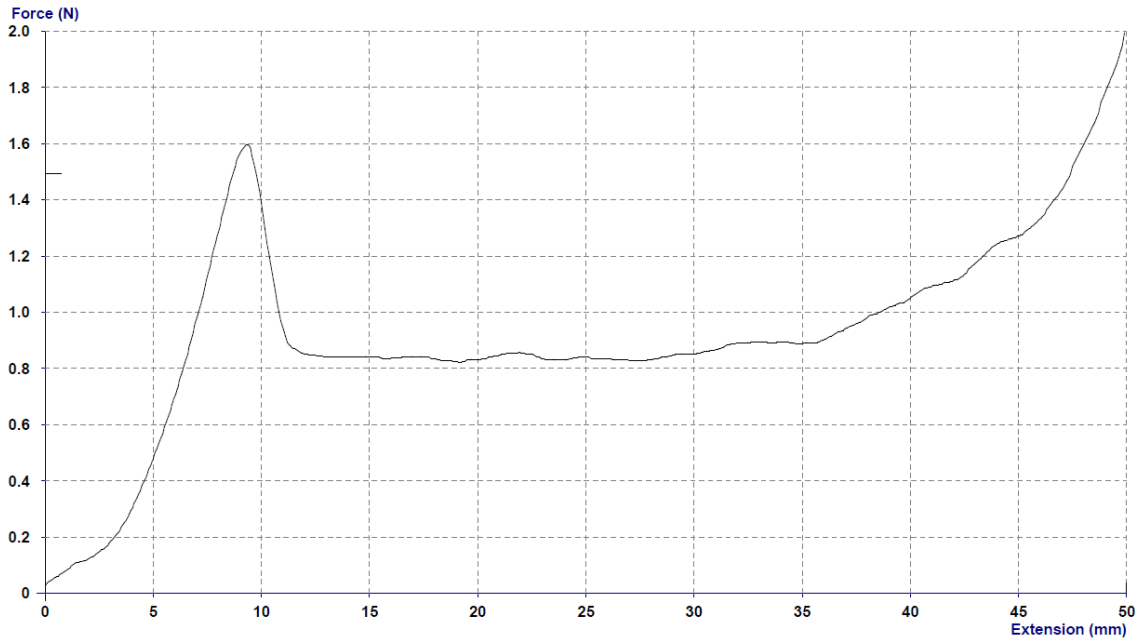


Figure 5.5 The peel strength trace for Coloplast Ostomy at 90° on a skin test substrate, showing the maximum force of peel strength at 1.6 N.

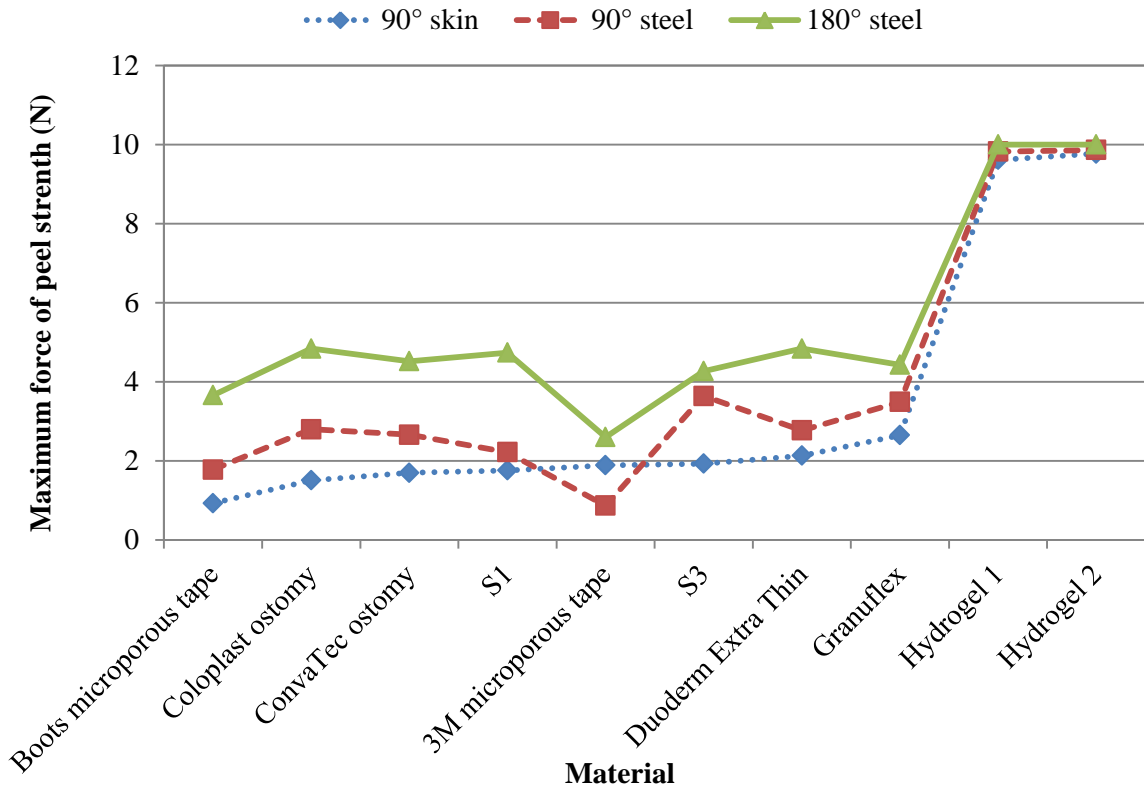


Figure 5.6 Average maximum forces of peel strength (N) for various skin adhesive materials for three substrates - 90° skin, 90° steel and 180° steel.

5.5.1.1 Discussion

From Figure 5.6 it can generally be seen that a strong correlation does not exist between the 90° and 180° peel tests on steel - the maximum force required to peel adhesives from steel at 180° was always greater than the force required at 90° on the same steel substrate, but not always by a factor of two. There also does not appear to be a significant correlation between 90° tests on steel and skin. In all cases the skin measurements at 90° were lower than equivalent measurements on steel, but not by a measurable factor. The correlation must, therefore, depend upon numerous factors, such as nature of the adhesive, adhesive composition and adhesive thickness. Consequently, peel strengths for adhesive removal from skin cannot be predicted directly from measurements made on steel.

5.5.2 Pain Scores for Skin Adhesive Wound Dressing and Medical Tape Materials

Peel tests were performed on human skin and therefore a pain scale was also devised to determine any possible correlation between peel strength of the adhesives and pain caused from removal. For each test material, the volunteer was asked to score the material based on three categories: pain/discomfort, redness and residue left on skin after removal of adhesive from the forearm. Each category was scored from one to five, with one being the least painful/red and five being the most painful/red. The scores for each material were then totalled to provide an overall pain score, as shown in Table 5.10, together with the peel strength data. It must be noted that pain is a completely subjective experience and therefore the pain scores in Table 5.10 are subjective data. The Aston Hydrogel Adhesives were scored as the most painful (scores of 11/15) with redness and bruising occurring immediately after the tests. The Commercial Medical Tapes had the next highest scores (2.5/15 and 4/15), whereas the remainder of the hydrocolloid materials all scored less than 2/15.

Table 5.10 Pain scores for skin adhesive wound dressing and medical tape materials.

Adhesive	Pain /5	Redness /5	Residue /5	Overall Score /15
Coloplast Ostomy	0	0	0.5	0.5
ConvaTec Ostomy	0	0	0.5	0.5
Salts Hydrocolloid S1	1	0	0.5	1.5
Salts Hydrocolloid S3	1	0	0.5	1.5
Granuflex	1	0	0.5	1.5
Duoderm Extra Thin	1	0	0	1
Hydrogel 1	5	4	2	11
Hydrogel 2	5	4	2	11
3M Microporous Tape	0.5	2	0	2.5
Boots Microporous Tape	1	3	0	4

5.5.3 Correlations Between Adhesive Peel Strengths, Pain Scores and Surface Energies

Table 5.11 shows collated data for the peel tests, pain scales and surface energy tests. Little correlation was found between the surface energies of adhesives and their respective peel strengths. For example, adhesive S1 (high SE of 28.5 mNm^{-1}) had a comparable average peel strength per width of 0.07 N with adhesive S3 (low SE 19.6 mNm^{-1}) with an average peel strength per width of 0.08 N. However, it can be seen that the higher the peel strength, the higher the overall pain score (Figure 5.7). Hydrogel 1, which was the most painful adhesive to remove from skin (pain score of 11/15), also showed the highest average maximum force (9.77 N) and the highest average peel strength per width (0.29 N). Conversely, Coloplast Ostomy device was the least painful to remove of all materials tested (pain score of 0.5/15) and had the lowest average maximum force (0.07 N) and lowest average peel strength per width (0.29 N).

Table 5.11 The correlation between adhesive peel strengths on skin at 90° , corresponding pain scores and surface energy data.

Adhesive	Peel Tests		Pain Scale	Surface Tests
	Av. Max. Force (N)	Av. Peel Strength (N/25mm)	Overall Pain Score /15	Surface Energy (mNm^{-1})
Coloplast Ostomy	1.70 (± 0.23)	0.07 (± 0.01)	0.5	21.4 (± 0.1)
ConvaTec Ostomy	1.51 (± 0.16)	0.07 (± 0.01)	0.5	21.2 (± 0.1)
Salts Hydrocolloid S1	1.76 (± 0.57)	0.07 (± 0.01)	1.5	29.9 (± 1.8)
Salts Hydrocolloid S3	1.93 (± 0.61)	0.08 (± 0.01)	1.5	16.8 (± 5.1)
Granuflex	2.65 (± 0.32)	0.11 (± 0.01)	1.5	36.3 (± 0.4)
Duoderm Extra Thin	2.13 (± 0.67)	0.09 (± 0.01)	1	36.8 (± 0.4)
Hydrogel 1	9.77 (± 0.24)	0.29 (± 0.01)	11	27.0 (± 3.5)
Hydrogel 2	9.61 (± 0.15)	0.25 (± 0.05)	11	32.0 (± 3.5)
3M Microporous Tape	1.93 (± 0.35)	0.11 (± 0.35)	2.5	22.3 (± 5.2)
Boots Microporous Tape	1.89 (± 0.30)	0.09 (± 0.30)	4	24.1 (± 5.7)

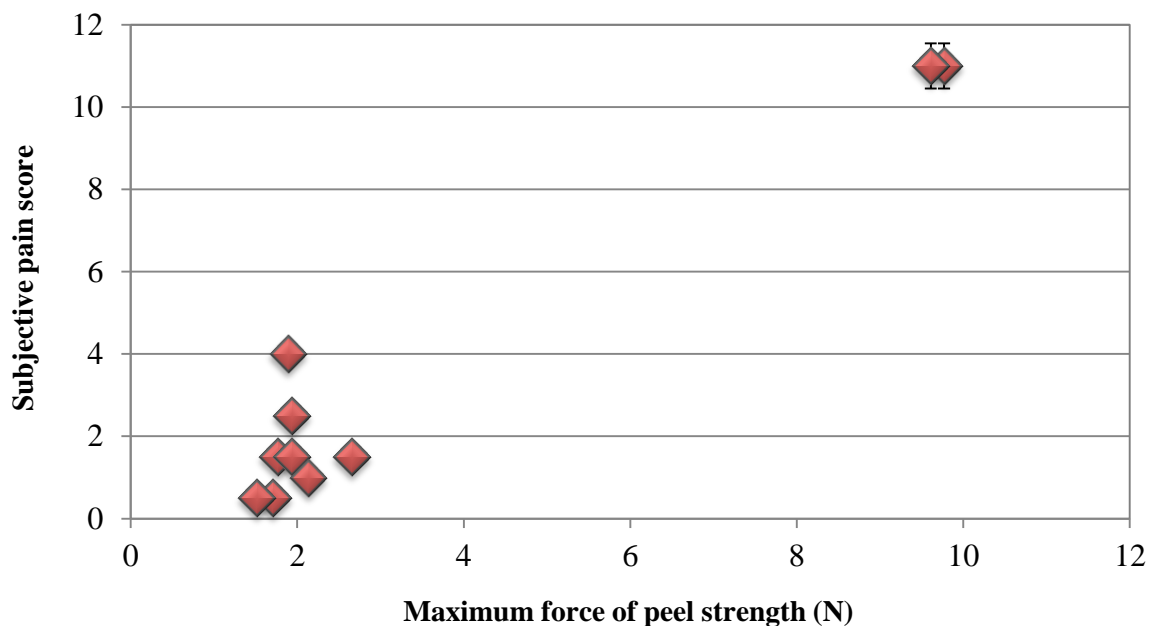


Figure 5.7 The relationship between maximum force of peel strength (N) and pain scores.

5.5.3.1 Discussion

The Aston adhesive hydrogel materials caused the most pain upon removal from skin. These materials also showed the highest peel strengths. From Figure 5.7 it generally appears that pain is related to the average maximum force measurements – the higher the maximum force, the higher the pain experienced. Many adhesives with a maximum force of around 2 N varied in pain from scores of 1/15 to 4/15.

Additionally, these peel tests were also carried out to determine whether siliconisation of the adhesives by adhesive-release liner contact affected the adhesive strength. This was not found to be the case, with little correlation between the two properties. The peel tests in this work were performed as part of an idealised system on the forearm skin of a healthy volunteer. The skin was cleaned with methanol before and after adhesive application. However, in real life applications, skin adhesives are required to function at different body sites. Adhesives are applied to the outer layer of skin – the stratum corneum of the epidermal layer. The stratum corneum consists of corneocytes and extracellular lipid membranes (ceramides, cholesterol and free fatty acids), that together build the barrier function of skin. The surface of skin varies at different parts of the body and also from person-to-person. The lipid composition of skin will, therefore, also vary from person-to-person. Because lipids and silicone are miscible, a high lipid

composition has the potential to detach silicone from the surface of the adhesive material. The *in vitro* peel tests were performed under idealised conditions and no correlation was found with peel measurements. In real life systems, however, the lipid composition of skin has the potential to interact with silicone on adhesive material surfaces and affect material performance in terms of adhesion.

5.5.4 Key Points for the Peel Strength Analysis of Skin Adhesive Materials

- Peel strength measurements on a steel substrate cannot be used effectively to predict values on skin. Thickness and adhesive composition must also be considered.
- The maximum force measurements during peel tests may contribute to the ‘pain factor’ experienced in the removal of adhesives from skin (rather than peel strength per width values). The results suggest that the higher the maximum force, the higher the pain experienced.
- Although silicone was detected on the surface of hydrocolloid adhesives, this contaminant does not appear to affect peel strength measurements under laboratory conditions. The influence of silicone on the adhesive material surface in real life applications, however, has the potential to affect adhesion between the adhesive and skin host site. Skin with a high lipid composition may detach silicone from the adhesive surface more easily than skin with a low lipid composition.

5.6 Tensile Strength Analysis of Skin Adhesive Materials

5.6.1 Tensile Strength Measurements of Skin Adhesive Wound Dressing and Medical Tape Materials

The function of skin adhesive wound dressings is to provide an adhesive and absorbent material of sufficient tensile strength. Tensile measurements were taken for the skin adhesive materials listed in Table 5.1 according to the mechanical testing method as described in section 2.27. The Commercial Medical Tapes group and Aston Hydrogel Adhesives were not tested because the material widths were insufficient to provide

samples sizes consistent with the testing protocol. All release liners from the contact side of the samples were peeled off and all woven backings were removed from the non-contact side of the samples prior to testing. All samples were repeated in triplicate. Table 5.12 reveals that the Commercial Hydrocolloid Adhesives Granuflex and Duoderm had the highest tensile strengths of all materials tested at 0.76 and 0.90 MPa respectively. The tensile strengths of Coloplast ostomy and ConvaTec ostomy were slightly lower at 0.68 and 0.59 MPa. In comparison, the Salts Hydrocolloid Adhesives S1 and S3 had extremely low tensile strengths at 0.04 and 0.03 MPa respectively.

Table 5.12 Tensile strength measurements for a range of skin adhesive materials.

Adhesive	Av. Thickness (mm) without release liner	Av. Elongation at Breaking Point (%)	Av. Initial Modulus (MPa)	Av. Tensile Strength (MPa)
Coloplast Ostomy	1.64	87 (± 16)	0.56 (± 0.06)	0.68 (± 0.14)
ConvaTec Ostomy	1.63	88 (± 15)	0.54 (± 0.05)	0.59 (± 0.12)
Salts Hydrocolloid S1	0.93	15 (± 5)	0.04 (± 0.01)	0.04 (± 0.02)
Salts Hydrocolloid S3	1.08	13 (± 4)	0.05 (± 0.01)	0.03 (± 0.02)
Granuflex	1.64	100 (± 24)	0.96 (± 0.1)	0.76 (± 0.15)
Duoderm Extra Thin	0.51	97 (± 25)	1.18 (± 0.1)	0.90 (± 0.18)

5.6.1.1 Discussion

The results for the Salts Hydrocolloid Adhesives S1 and S3 from Table 5.12 may initially seem erroneous because these results indicate that the materials have an extremely low tensile strength. However, the extremely low values may be described by the sample treatment prior to testing. Adhesive S1 and S3 were supplied with woven backings on the non-contact sides of the adhesives. These were removed by blotting with acetone before the tensile strength tests were conducted in order to gain accurate measurements for the hydrocolloid adhesives without any backing support. However, without the woven backing, adhesives S1 and S3 were extremely difficult to handle. It was observed that these two adhesives broke immediately in the grips of the tensometer

machine when a force was applied. In comparison, the commercial materials Granuflex and Duoderm, and ostomy materials, Coloplast and ConvaTec, were not supplied with a woven backing. These materials were observably easier to handle.

The tensile properties of a hydrocolloid adhesive material cannot be correlated to the surface properties of the material. Mechanical testing studies the bulk properties of the material. In an isotropic hydrocolloid system, the bulk consists of a dispersed phase of particles within a continuous phase of poly(isobutylene). Therefore, the surface is different to the bulk.

In these mechanical tests, materials were tested in their unhydrated form. The assessment of materials once partially and fully hydrated, however, would provide better indication for material performance at the exuding wound site. It would then be useful to perform wet tensile tests. A suitable wound fluid model, to mimic the moist wound environment, would prove useful for such testing conditions.

5.6.2 Key Points for the Tensile Analysis of Skin Adhesive Materials

- Accurate tensile measurements of adhesives S1 and S3 could not be carried out because of the woven backings applied to the materials during the manufacturing process. In contrast, tensile testing for commercial hydrocolloids for wound and ostomy applications without woven backings was successful.
- Tensile measurements cannot be related to surface properties of hydrocolloid materials due to the nature of their formulation.
- Wet tensile testing of materials may be a useful method to assess material tensile behaviour in their hydrated forms.

5.7 Dynamic Testing of Skin Adhesive Materials

5.7.1 Rheology Measurements of Skin Adhesive Wound Dressing and Medical Tape Materials

Section 2.2.8 described the importance of rheological properties, such as elasticity and viscoelasticity, for the characterisation of adhesive materials. The elastic modulus (G')

describes the ability of a material to return to its original undeformed state after a deforming stress is applied and removed. The viscous modulus (G'') describes the resistance of a material to being deformed.

Rheology measurements were taken for the range of skin adhesive materials listed in Table 5.1, with the exception of Salts Adhesives S2 and S4 and the Commercial Medical Tapes which were not tested. A Bohlin CVO Rheometer was used according to the method described in chapter two. For each dry adhesive sample, the viscous modulus, elastic modulus and $\tan \delta$ (where $\tan \delta = \text{viscous modulus/elastic modulus}$) were recorded. Table 5.13 reveals that the $\tan \delta$ values for the hydrocolloid materials fall in the range of between 0.65-0.80. The hydrogel adhesives, however, exhibited the lowest $\tan \delta$ values of the adhesives studied (Hydrogel 1 – 0.38 and Hydrogel 2 - 0.25).

Figure 5.8 presents the relationship between $\tan \delta$ values and the maximum force of peel strength (N) from the peel strength data in section 5.5. It can be observed that the hydrogel adhesives with a $\tan \delta$ value below 0.6 had a high maximum force of removal (greater than 9 N), whereas hydrocolloid adhesives with a $\tan \delta$ value greater than 0.6 had a low maximum force of removal (less than 3 N).

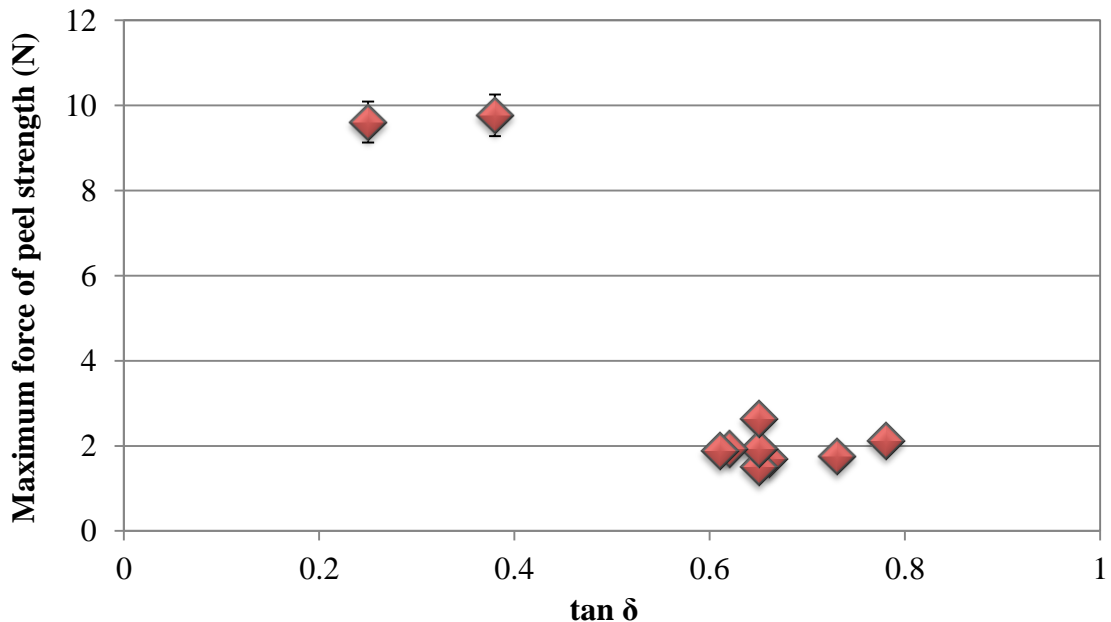


Figure 5.8 The relationship between $\tan \delta$ and the maximum force of peel strength (N).

Table 5.13 Rheological measurements for skin adhesive materials tested at 0.5-25 Hz.

Adhesive Material	G' Elastic Modulus (MPa)	G'' Viscous Modulus (MPa)	tan δ (viscous/elastic)
Coloplast Ostomy	0.75	0.49	0.65
ConvaTec Ostomy	0.74	0.48	0.65
S1	0.34	0.24	0.71
S3	0.31	0.20	0.65
Granuflex	0.42	0.28	0.67
Duoderm Extra Thin	0.15	0.12	0.80
Hydrogel 1	1.830	0.69	0.38
Hydrogel 2	2.644	0.66	0.25

5.7.1.1 Discussion

Table 5.13 shows the elastic modulus and viscous modulus for the range of skin adhesive materials. The two hydrogel materials, Hydrogel 1 and Hydrogel 2 exhibited the highest viscous moduli (0.694 and 0.661 MPa respectively). A relatively high viscous modulus equates to relatively high rigidity – a rigid adhesive material may be less comfortable than a lower modulus more flexible material. Such rheological tests may also be made on hydrogel contact lens materials. Although contact lenses are designed for application to one bodily site only, skin adhesive wound dressing materials may be applied to various skin sites. High viscosity may, therefore, restrict a material in performance at different host sites. Ideally a skin adhesive material should have a high modulus upon application and a low modulus upon removal.

From the elastic modulus and viscous modulus measurements, the tangent of the phase shift ($\tan \delta$) values can be evaluated. The $\tan \delta$ describes the ratio of viscous modulus to

elastic modulus, where $\tan \delta = \text{viscous modulus/elastic modulus}$. $\tan \delta$ values below a certain value indicate ‘solid-like’ behaviour, whereas values above this value indicate more viscous ‘liquid-like’ behaviour. From the above data it can be observed that the majority of materials tested had $\tan \delta$ values of approximately 0.65. The exceptions to this were Hydrogel 1 and Hydrogel 2 with lower values of 0.38 and 0.25. From the peel strength data and pain scores in section 5.5, it was noted that these hydrogels had significantly higher maximum peel forces and pain scores in comparison to the commercial and non-commercial hydrocolloids tested. Therefore, it may be suggested that materials with $\tan \delta$ values lower than 0.6, such as the hydrogels, have high maximum forces of peel removal and thus cause the most pain to detach.

5.7.2 Key Points for the Dynamic Testing of Skin Adhesive Materials

- All hydrocolloid skin adhesives studied gave $\tan \delta$ values of ~ 0.65 .
- The hydrogel skin adhesives tested gave \tan values of ~ 0.3 . These hydrogels had extremely high peel strengths and were the most painful to remove from skin.
- $\tan \delta$ values below ~ 0.6 may correlate with the maximum force of peel removal.

5.8 Concluding Discussion

The aim of this chapter was to study the properties of skin adhesive materials used in wound healing applications in relation to the biophysical properties of skin. The focus of this work was principally on the properties of hydrogel and hydrocolloid skin adhesives for wound applications, and hydrocolloid adhesives for ostomy devices, which are applied directly to breached skin.

It was shown that inadvertent modifications to the surface properties of adhesive hydrocolloids have the potential to affect the material performance. In particular, the comparison of two hydrocolloid adhesives (S1 and S3) revealed considerable differences in surface properties. Both adhesives, from different batches, have the same hydrocolloid composition and were manufactured by the same company, process and at similar processing times. It was shown that the choice of release liner material, has the ability to alter the surface energy of the material – the siliconised plastic release liner

transferred silicone to the S3 adhesive surface by adhesive-liner contact during storage, whereas the siliconised paper release liner performed as a more inert material on adhesive S1. The transfer of silicone by the plastic release liner was shown to significantly lower the surface energy of adhesive S3. In contrast the surface properties of adhesive S1 remained unchanged.

The measure of bulk properties shows that material properties are interdependent. Best success of a material may be achieved if mechanical properties are above a certain minimum, rather than the material exceeding in one test alone. The surface and mechanical properties of skin adhesive wound dressing materials is not a widely studied area, but investigations into these properties demonstrate how they can influence behaviour of the skin-adhesive interface. Although *in vivo* work is always the final testing point for materials that are designed to come into contact with biological tissue, it is not always possible to examine *in vivo* all aspects of material behaviour. The gross functionality of the material, that includes all of the material properties, is important.

The difficulty in the design of an ideal adhesive wound dressing materials most certainly lies in the variability of skin. The surface and mechanical properties of skin vary widely depending upon numerous factors which include: the location of the body, the treatment or washing of skin, the texture and age of skin, the lipid or moisture content, and general patient-to-patient variation. Table 5.14 highlights the variable surface properties of skin under different conditions. It can be noted that the surface energies vary largely from 25.3 mNm⁻¹ to 57 mNm⁻¹ depending upon the temperature, relative humidity and treatment of skin.

Table 5.14 Surface properties of human skin [51].

	Surface Energy (mNm ⁻¹)
Human skin (23°C, 34% relative humidity)	38
Human skin (36°C, 50% relative humidity)	57
Human skin (untreated)	38.9
Human skin (cleaned)	25.3
Human skin (high lipid)	42

Consequently, a ‘one size fits all’ dressing, such as a hydrogel, hydrocolloid or ostomy product, must therefore function over a range of properties and interact with complex biological fluids. Hydrocolloids, which consist of gelatine/pectin, carboxymethylcellulose and poly(isobutylene) components, are suitable for this purpose because the composition results in extremely responsive materials. Hydrocolloids are unique in that not only can they adhere to unbreached clean dry skin, they can also provide adequate adherence to moist surfaces, such as the wound bed environment, thus covering a range of substrate surface properties.

Tests in this chapter were performed on various adhesive materials as received; they had not been in contact with breached or unbreached skin. During application, however, the adhesive materials come into contact with skin under different conditions. Elements such as skin moisture, sweat, lipid content and dirt, for example, can affect material performance. These materials used in contact with biological tissue do not have one single purpose. Accordingly, the applications considered within this thesis involve the material in multiple purposes – skin adhesive wound dressings must be protective, occlusive and provide adherence to the wound/peri-wound area. Perhaps a more substantial point of interest is that materials are designed to absorb and manage wound fluid, often in large volumes, from exuding wounds. Just as the study of surface and mechanical properties of materials is beneficial to further understanding of material behaviour, the study of material interactions with wound fluid is also a valuable field. Because the actual wound environment is extremely difficult or impractical to study, the design of an artificial wound fluid model would be ideal to investigate material interactions with the dermal wound.

5.8 Chapter Summary

There is clearly a gap within the literature for information on the surface and mechanical properties of skin adhesive materials for wound applications. This chapter used various techniques, including surface energy probes, peel testing, tensile testing and dynamic testing to investigate the surface and bulk properties of materials. One major finding of this work was that the siliconised release liner applied to adhesives during the fabrication process affects the surface properties of the adhesive. Greater silicone levels were detected on the surface of skin adhesives after contact with plastic

release liners than after contact with paper release liners. Although this finding did not correlate with peel test measurements under laboratory conditions, the implications of silicone on the adhesive material surface could potentially affect material and adhesivity performance in real life applications. The peel testing and mechanical testing of adhesive materials showed that materials do not perform to their maximum ability in every test. It appears that it is better for a material to exhibit the minimum values in a range of tests (peel, tensile, dynamic), rather than exceed in one particular area.

CHAPTER SIX

Towards the Design of an Artificial Wound Fluid Model

6.1 Aim

The eye provides an excellent site to examine specific interactions between a synthetic biomaterial (the contact lens) and a complex biological fluid (tear fluid). Chapters three and four of this thesis have shown that a cell-based technique to determine the interaction between the non-compromised eye/contact lens and the compromised eye/bandage contact lens have proved successful. Access to acute and chronic dermal wounds, however, is far more challenging because of ethical considerations. The concept for the development of synthetic biological wound fluid models is attractive in order to facilitate biochemical interaction studies. The aim of this chapter was to work towards considerations for the design of a standard chronic wound fluid model. The use of such a model provides a rational basis to aid material design and selection, and further the understanding of biomaterials-related processes that influence dermal wound healing. In addition, this chapter is concerned with the interaction of biological fluids with materials used for wound healing applications.

6.2 Introduction

Section 1.2 of this thesis introduced the analogy between the ocular wound healing and dermal wound healing environments. In summary, the human cornea shares several structural and biochemical similarities to the moist dermal wound bed environment. Specific comparisons may be drawn between: the cornea and wound bed, tear fluid and wound fluid, and contact lens materials and wound dressing materials.

Tear fluid ↔ Wound fluid
Cornea ↔ Wound bed
Bandage contact lens ↔ Wound dressing

Tear fluid/Wound fluid: The natural tear film is the liquid layer that bathes the surface of the cornea. It consists of three distinct layers shown in Figure 6.1; the overlying lipid layer prevents evaporation of the tear film; the intermediate aqueous layer forms 98% of the fluid and contains proteins, electrolytes, and metabolites; and the mucous layer anchors the tear film to the underlying epithelial cells of the cornea [67]. A more comprehensive description of each layer of the tear film can be found in the main introduction of this thesis (section 1.5.1.2). Wound fluid, or wound exudate, is produced

after injury in all wounds as an inflammatory response. Originating from blood plasma, the fluid may vary in colour, consistency and odour. Comparisons may be drawn between tear fluid and wound fluid. Both are complex biological fluids that contain proteins, electrolytes, proteases and growth factors.

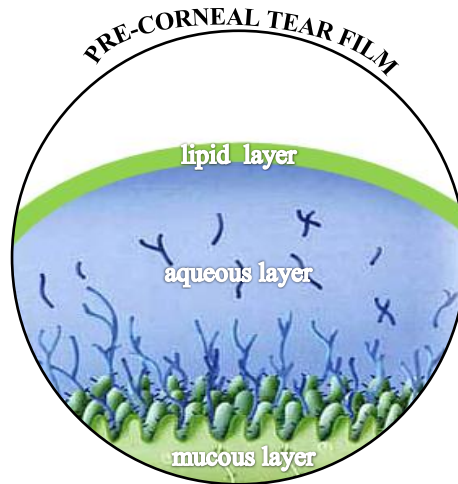


Figure 6.1 Cross-section of the tear film.

The interaction between the tear film and a contact lens results in protein and lipid deposition onto the contact lens surface, which in turn affects contact lens material performance. Likewise, the tear film is also affected as it is denuded of vital biochemical components which are deposited on the lens. In order to study the compositional changes of the tear fluid, tear sampling methods such as microcapillary, Schirmer strip and microsponges can be used to collect the fluid. Tear sampling methods are generally considered to be non-invasive and pose few ethical concerns. However, whereas the eye is easily accessible and the collection of tear fluid is a reasonably straightforward task, sampling of wound fluid from the wound bed is far more complicated. Accessing the wound may be difficult and aspiration of fluid from beneath dressings is difficult [134]. Additionally ethical considerations must be taken into account for *in vivo* human studies. Various collection techniques exist for wound fluid collection which include: aspiration with a syringe from under an occlusive dressing, blunt end glass capillaries, closed suction drains and extraction from swabs. However, although there are many collection techniques available, there is a lack of a single standardised collection procedure.

- *lubricious role*: the tear film sustains a moist surface which is essential for providing lubricity between the corneal surface and the upper eyelid. This ensures comfort during the blinking mechanism.
- *protective barrier role*: it acts as a barrier to the hostile external environment.
- *antibacterial role*: the antibacterial activity of tear proteins, such as lysozyme, provide antibacterial defence.
- *transport role*: since the cornea is an avascular tissue, the tear film acts as a transport medium for oxygen and nutrients. It also provides a pathway for the removal of metabolic waste products.

The composition of tear fluid consists of serum electrolytes, protein, immunoglobulins and lipids. Different types of tear, such as basal, reflex and emotional, have different compositions. Table 6.1 lists the major tear components (electrolytes, lipids, immunoglobulins and sugar) and concentrations of tear fluid, with average values obtained from a survey of over 100 studies [135].

Table 6.1 Composition of the human tear fluid [135].

	Tear Component	Average Concentration (mg/100ml) and Range
<i>Electrolytes</i>	Chloride	470 (85-512)
	Sodium	338 (327-354)
	Calcium	3.9 (1.2-8)
	Potassium	101 (58-137)
<i>Lipid</i>	Total lipid	206 (180-240)
	Cholesterol	64 (8-190)
<i>Immunoglobulins</i>	IgA	29 (4-85)
	IgG	13 (0-79)
	IgM	1.4 (0-5)
	IgE	0.0017 (0.003-0.025)
<i>Sugar</i>	Glucose	11 (0-65)

A varying number of proteins have also been determined in tears. A recent study by Zhou reported 1543 individual proteins in tears from the analysis of samples taken from four healthy subjects [136]. Figure 6.2 shows the comparison between proteins in human tears and blood plasma. The protein concentrations range from mg/l to pg/ml. It can be observed that a number of the same proteins are found in tears and plasma, but at different concentrations; proteins are generally found at higher concentrations in tears than in healthy blood plasma.

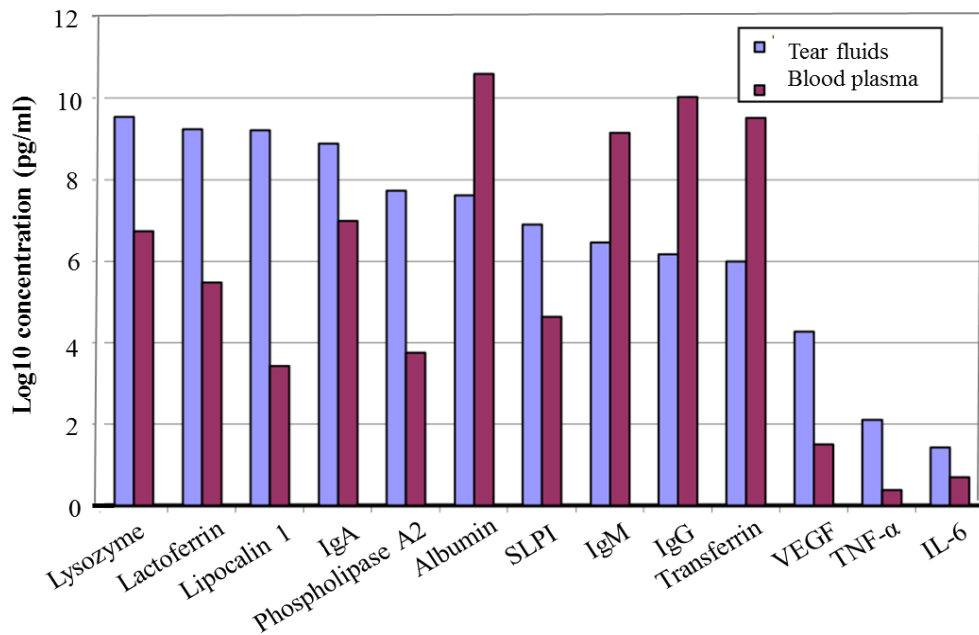


Figure 6.2. A comparison between proteins concentrations of tear fluid and blood plasma of healthy subjects. Protein concentrations range from pg/ml to mg/l. (Adapted from Zhou et al [136]).

6.3.2 Artificial Tear Fluid Models

There are two types of tear fluid models which exist; the first is artificial tears or tear substitutes for clinical use and the second is artificial tear fluid models for *in vitro* experimental work. Both types of models and their purposes shall be discussed.

6.3.2.1 Tear Substitutes

Dry eye syndrome is a condition which may be defined as “a disorder of the tear film due to tear deficiency or excessive evaporation, which causes damage to the interpalpebral ocular surface and is associated with symptoms of ocular discomfort”

[137]. Symptoms may include a short tear break-up time and a sensation of irritation and grittiness. Artificial tears are commonly used to replace the natural tear film in order to lubricate the corneal surface, thus reducing discomfort and acting towards maintaining a healthy ocular environment. Substitute fluids also smooth the ocular surface, which can subsequently increase optical resolution. Artificial tears may be produced from different bases such as [138]:

- *water* – the aqueous phase of tear film forms 98% of its structure.
- *saline solutions*: sodium chloride is most commonly used to maintain the osmolarity of the tear film which is approximately 300 mOsm/l, but solutions can include potassium chloride, calcium chloride, magnesium chloride or zinc chloride.
- *glycerol*: acts as a humectant to retain moisture.
- *polysaccharides*: mucilages, such as hydroxypropyl methylcellulose (hypromellose) and carboxymethylcellulose (carmellose) are commonly used to provide adequate viscosity to tears.
- *synthetic polymers*: poly(vinyl alcohol) and poly(ethylene glycol) derivatives are used for solubility and tear-stabilisation properties.

Preservatives are added to artificial tears designed for multiple use to prevent bacterial growth in the bottled container. If artificial tears are designed for single use then the addition of preservatives is generally not required.

The healthy ocular environment and compromised dermal wound environment share a similarity in that both tissue sites must be kept moist and well lubricated. In the ocular environment, as described in section 6.3.1, the tear film serves many functions to maintain the health of the cornea. The use of artificial tears when the tear film becomes dysfunctional, such as in the case of dry eye syndrome, is well documented within academic literature. This has been highlighted by Moshirfar *et al*, who reviewed studies and clinical trials for the use of commercially available artificial tears for one method of dry eye syndrome therapy [139]. In the compromised dermal wound, it has been shown that a moist wound healing environment facilitates the wound healing process [47].

Although topical ointments may be applied to dermal wounds to prevent infection and promote a moist wound environment, the application of an artificial fluid to substitute wound fluid would be inappropriate. This is because wound fluid represents the condition of the underlying granulation tissue [140]. The colour, odour and consistency of wound fluid provide an indication of the state of healing. Therefore, altering the exudate from a wound, in any capacity, would interfere with direct observations of the wound health.

6.3.2.2 *The Need for Artificial Tear Fluid Models to Study in vitro Biomaterial*

Interactions with Biological Fluids

Artificial tear fluid models may be implemented for a variety of *in vitro* research purposes. Models must reflect the composition of the tear film, whilst taking into account patient to patient variation. The use of real tears for *in vitro* tear models would be impractical for several reasons. Firstly, tear sampling techniques, such as microcapillaries, are only able to collect a few microliters at a time (approximately 1-7 μ l from one sample) [141]. The stimulation of tears would increase the volume collected, however, the composition of reflex tears differs to that of basal tears. Secondly, tear compositions vary from person to person. Therefore, the need for the design of a standard artificial tear fluid model is appealing.

There is a significant amount of work on the use of artificial tear fluids, which vary in complexity from single protein mixtures, to more complex mixtures that involve lipids and mucins. A general approach for the formulation of a multi-component tear model is to use saline as a base to mix various proteins, such as lysozyme and lactoferrin, at concentrations found in tears. The shortcoming of this approach, however, often lies in the solubility of the lipid components added to saline. The resulting models rarely mimic tear fluid to an accurate degree and, consequently, such models are limited to the components that may be included. Vital non-water soluble species that are found in tears, such as lipids and phospholipids, are often excluded.

The Aston Tear Model, developed by Franklin [142], takes a different approach to the average saline-based artificial tear model because it is based on an animal serum (fetal bovine serum, FBS). The FBS base is diluted with phosphate buffered saline (PBS) for the tear solution (1:2 ratio of FBS:PBS), to which additional lipid and protein

components, as detailed in Table 6.2, are introduced. The serum-based model provides a composition which is more comparable to tear fluid than saline-based models.

Table 6.2 The composition of the Aston Serum-based Tear Model developed by Franklin [142].

<i>Aston fetal bovine serum-based tear model</i>	
Proteins (all at 0.004 w/v)	Lysozyme
	Lactoferrin
	Albumin
Lipids (all at 0.004 w/v)	Fatty acid standards
	Triglyceride mixtures
	Phospholipids

Animal serum, such as FBS, as a base for artificial tear models offers greater advantages over water or saline bases. Firstly, the compositions of tear fluid and FBS are broadly similar. Secondly, in practical terms, FBS is readily available at a relatively low cost. Thirdly, and perhaps the most valuable property of FBS, is that it is a stable solution containing an array of solubilised proteins and lipids. The major limitation of water or saline-based artificial tear models is that the inclusion of non-water soluble lipid components is difficult or impossible. FBS, on the other hand, already contains many of the proteins and lipids found within tear film, but also provides a suitable base for the inclusion of other additional components. Although the total composition of FBS is not completely understood, FBS as a base for biological fluid models appears to be a more compositionally accurate alternative to water or saline.

Although much work has reported the use of artificial tear fluid models, there is little parallel work on wound fluids. Exudate from wounds often represents different states of health, for example, those associated with healing acute wounds and with chronic non-healing wounds. In order to develop an artificial model that represents chronic wound fluid, the approach for the use of an animal serum base, as implemented in tear models, was expanded.

6.4 Artificial Wound Fluid Models

In order to work towards an artificial wound fluid model, the functions, compositions and requirements of wound fluid must first be understood in greater depth.

6.4.1 Wound Fluid – Function and Composition

Traditional ideologies for successful wound healing include the notion that wounds must be kept dry, free from excess wound fluid and, therefore, free from infection. Moist wound healing was first described around 120 AD, but it was not until 1962 when George Winter [47] demonstrated that wounds sustained in a moist state showed faster rates of healing, leading to an evolution of wound dressing materials. The role of the moist wound environment and bacterial infection was reported by Cutting [143], who expressed that although pathogens such as staphylococcus aureus (gram positive) and Pseudomonas aeruginosa (gram negative) flourish in the moist wound, neutrophils also thrive in these conditions. As a result, wound fluid has an important role in suppressing infection.

The composition of wound fluid is patient-dependent, with numerous reasons giving rise to the biochemical differences found between wound fluid samples, including: [144]

- general health of the patient
- nutritional status of the patient
- state/condition of the wound including wound type, wound size and phase of healing
- prior wound bed management

Additionally, the technique for fluid sampling may also influence the fluid composition:

- method/procedure of wound fluid collection
- time of sampling
- assay used for sample analysis

Wound fluid is a complex soup of electrolytes, proteins, lipids, growth factors and proteases. Very few studies have analysed wound fluid on a biochemical level [121,

140, 143, 145, 146]. The significance of wound fluid must not be overlooked, as it provides an insight into the healing condition of the wound. As mentioned above, the many variables occurring between patients, wounds and sampling techniques all have the propensity to affect the wound fluid composition and state/fate of the complex dermal wound healing process. Nonetheless, key differences between the compositions of healing wound fluid from acute wounds and non-healing wound fluid from chronic wounds are known. The following sections discuss these compositions in further detail.

6.4.1.1 Acute Wound Fluid versus Chronic Wound Fluid

The differences between acute and chronic wounds were outlined in section 1.3.4. Whilst acute wounds heal within a timely and well-defined healing process, chronic wounds fail to proceed through the orderly process and become trapped in a phase of inflammation and non-healing.

It is, therefore, unsurprising that the compositions of fluids from acute healing wounds and non-healing chronic wounds differ, as shown in Table 6.3. The information presented in Table 6.3 is drawn from a study by Trengove *et al* [145], where wound fluid samples were collected from eight patients with healing or non-healing leg ulcers. Biochemical analysis from the two types of fluids reveals higher levels of bicarbonate, glucose, total protein, albumin, gamma globulin and cholesterol in the healing phase [145]. Both acute healing fluid and chronic non-healing fluids have similar levels of growth factors. It can be observed from Table 6.3 that C-reactive protein, a marker for inflammation, is found in greater concentrations in chronic wound fluid (13 mg/l) than in acute wound fluid (5 mg/l). This significant difference in C-reactive protein concentration highlights the measurable difference in inflammation between healing and non-healing wounds. Additionally, the functions of fibronectin were described in chapter three; as a similar protein to vitronectin, it is an adhesive glycoprotein that mediates cell adhesion. Wysocki *et al* [147] found that fibronectin is readily degraded into smaller molecular weight proteins in chronic wound fluid, but remains intact within acute wound fluid.

Table 6.3 The compositional comparison of healing wound fluid from acute wounds and non-healing wound fluid from chronic wounds [145].

Biochemical Component	Function	Healing Wound Fluid: Acute Wounds	Non-healing Wound Fluid: Chronic Wounds
Bicarbonate (mmol/l)	Alkaline component	19	17.5
Glucose (mmol/l)	Cellular energy source	2	1.2
Total protein (mg/l)	Support tissue repair	41	34
Albumin (g/l)	Support tissue repair	23	19
C-reactive protein (mg/l)	Inflammation protein	5	13
Gamma globulin (g/l)	Antibody functions	6	4.5
Cholesterol (mmol/l)	Supports cell renewal	1.8	1.6

Remodelling of the extracellular matrix (ECM) in the wound healing process is regulated by the antagonistic mechanism between matrix metalloproteinases (MMPs) and tissue inhibitors of metalloproteinases (TIMPs). MMPs are extracellular proteinases that belong to the metzincin protease family and are regulated by the inhibitory action of TIMPs [148]. They function to degrade components of the ECM such as collagen, fibronectin, laminin, proteoglycan and elastin [22] and are involved in various aspects of wound repair and healing. The timely action of MMPs allows not only for the removal of damaged matrix, but also for cellular migration and angiogenesis. There is, however, evidence to support the over expression of MMPs in chronic wound fluid [22, 147]. Trengove *et al* [22] reported a 30-fold increase of MMPs in chronic wounds compared with acute wounds. The raised level of MMPs in chronic wound fluid is a result of the increased production by proinflammatory cytokines, which also exhibit a decreased production of TIMPs. Subsequently, the crucial MMP/TIMP balance is disturbed and, therefore, causes the compositions of acute wound fluid and chronic wound fluid to be vastly different from each other [149]. As

the wound progresses from a non-healing to healing state, however, the levels of MMP activity decrease [22].

Another important component of wound fluid is growth factors. Growth factors are released by inflammatory cells during the second stage of wound healing, with roles within the regulation of extracellular matrix degradation and synthesis, angiogenesis, coagulation, chemotaxis, epithelialisation and cell proliferation [150]. It has been suggested that growth factors, such as epidermal growth factor (EGF), platelet-derived growth factor (PDGF) and vascular endothelial growth factor (VEGF), amongst others, are deficient within chronic wound fluid as opposed to within acute wound fluid [22]. Accordingly, the application of exogenous growth factors to chronic wounds and ulcers to accelerate healing has been studied, but with varied results. This is demonstrated by the fact that at present, the only singly approved growth factor for topical application is PDGF [151]. However, it has also been argued that the exogenous application of growth hormones to chronic wounds may be without success. It has been suggested that the higher than normal levels of inflammatory proteins in chronic wounds are an overriding factor in unsuccessful healing, rather than due to the lower than normal levels of growth factors present [152].

Table 6.4 provides a broad overview of a comparison between the acute healing wound fluid and chronic non-healing wound fluid.

Table 6.4 A comparison of acute wound fluid and chronic wound fluid in relation to healthy human serum [22, 143, 145-147, 152].

Component	Healing Wound Fluid: Acute Wounds	Non-healing Wound Fluid: Chronic Wounds
Serum components i.e. Na ⁺ , K ⁺ , Cl ⁻	Present	Present
Bicarbonate	Present	Lower than AWF and serum
Glucose	Lower than serum values	Lower than AWF and serum
Total Protein	44 g/l Lower than serum values of 73g/l	30 g/l Lower than AWF and serum
Albumin	25 g/l Lower than serum values of 73g/l	17 g/l Lower than AWF and serum
C-reactive protein	Same as serum values	Raised levels - denotes inflammatory phase
Cytokines	Present	At increased levels (in particular IL-6 and TNF-a)
Matrix metalloproteinases	Present	Increased levels (in particular MMP-2 and MMP-9)
Tissue inhibitors of metalloproteinases	Present	Absent or low levels
Growth factors	Present	Degraded or completely absent
Vitronectin and Fibronectin	Present in their usual forms	Degraded into lower molecular weight proteins
Urea	8.4 mmol/l Similar to serum values of 73g/l	10.3 mmol/l Lower than AWF and serum
Free radicals	Low levels	Raised levels

6.4.2 An Overview of Artificial Wound Fluid Models in Literature for Biomaterial Design and Investigations

A literature search was conducted to investigate the availability and compositions of existing artificial wound fluid models. Few models have been produced by authors for different purposes and no review has attempted to collate information in a bid to compare the different designs. This section discusses existing artificial wound fluid models, with a view to consider the design of a standard artificial wound fluid.

Water-based fluids: A simple water-based fluid was produced by Lindsay *et al* [153] for *in vitro* studies to evaluate wound dressing performance. Various components were added to de-ionised water: 2% bovine albumin, 0.02 M calcium chloride dihydrate, 0.4 M sodium chloride and 0.08 M tris methylamine. The overall pH of the fluid was pH 7.5. Although this simple isotonic salt solution is more representative of wound fluid than unmodified water or saline, which are often used in such studies, many important components of wound fluid are missing. These include vital proteins and lipids.

Saline-based fluids: Hobson *et al* have also produced what may be considered a simple artificial wound fluid, but from a phosphate buffered saline (PBS) base. The components that were dissolved in PBS at pH 7.5 included: 0.2% w/v fatty acids, 4.0% w/v albumin, 2.5% w/v globulins and 0.05% w/v triglycerides. This fluid was designed in order to test the characteristics of a novel wound dressing material pending a patent; the importance of such artificial fluids is therefore apparent. Although this fluid contains more constituents than the water-based fluid produced by Lindsay *et al* it is still not fully representative of actual wound fluid.

3M Health Care has developed a more compositionally accurate artificial wound fluid from saline to mimic human extracellular fluid [154]. The saline-based wound fluid consists of proteins, electrolytes and nutrients as found in extracellular fluid. The composition of the fluid is shown in Table 6.5. A study by Campbell *et al* used the 3M artificial wound fluid to mimic exuding wounds in order to assess fluid absorption, fluid retention and wear duration of two selected wound dressings. Although the artificial fluid did not reproduce the composition of wound fluid, it was found to be sufficient to test fluid handling properties of the dressings.

Table 6.5 The composition of artificial wound fluid produced by 3M Health Care [154].



A study by Lutz *et al* [155] used a different approach to develop an artificial wound fluid from PBS for investigations in material fluid handling characteristics. PBS was adjusted with; whey protein isolate for a high protein concentration; vegetable oil for a lipid content; sodium bicarbonate; simethicone for an anti-foaming agent and dextrose/sucrose for a sugar content. The authors obtained a reasonably accurate composition of artificial wound fluid by using the protein, lipid and sugar values of human extracellular fluid and chronic wound fluid determined by Trengove *et al* [145] as a guide, as shown in Table 6.6. The use of a preservative system (Germaben® II) was also incorporated to prevent microbial growth and reduce odour of the fluid. This appears to be the most developed artificial wound fluid reported, but still lacks essential growth factors and matrix metalloproteinases.

Table 6.6 The composition of artificial wound fluid produced by Lutz *et al* in comparison to extracellular fluid and chronic wound fluid [155].

Component	Human Extracellular Fluid*	Human Chronic Wound Fluid*	Artificial Wound Fluid by Lutz <i>et al</i> [155]
Sodium (g/l)	3.30	3.24	3.24
Potassium (g/l)	0.20	0.17	0.56
Calcium (g/l)	0.10	0.09	0.05
Magnesium (g/l)	0.04	0.02	0.01
Chloride (g/l)	3.70	3.69	3.40
Protein (g/l)	20.30	39	40.06
Lipids (g/l)	5.00	2.3	2.32
Sugars (g/l)	0.90	1.30	1.05
* The compositional values of human extracellular fluid and human chronic wound fluid were obtained from a study by Trengove <i>et al</i> [145]			

Serum based fluids: An animal serum-based model has been produced by Parsons *et al* [156] in a study investigating the antibacterial, physical and chemical characteristics of a silver containing wound dressing materials. The wound fluid consisted of fetal bovine serum (FBS) diluted with maximum recovery diluent (in a 1:1 ratio). FBS provides a solid basis for the design of artificial fluid as it already contains serum components, albumins, other proteins, immunoglobulins, lipids, minerals, vitamins and possibly growth factors. In this study two pathogens (*Staphylococcus aureus* and *Pseudomonas aeruginosa*) were also introduced to the artificial wound fluid in order to test the antibacterial properties of the dressing materials. Maximum recovery diluent was added to the fluid as it contains a low level of peptone, which reduces osmotic shock to the bacterial pathogens. Therefore, the artificial fluid was tailored towards the requirements of this particular study and thus it is not suitable as a standard wound fluid model.

Conclusions: As very few artificial wound fluid models have been formulated, substantial comparisons cannot be made to determine which model accurately represents wound fluid from exuding wounds, or to determine which model is reliable for interactions with biomaterials. Many of the models form the basic foundation of an artificial wound fluid, but do not include many important components found in chronic wound fluid. An ideal artificial chronic wound fluid model should ideally contain representative levels of proteins, lipids and sugars to that of chronic wound fluid, and additionally should contain low/absent levels of growth factors and TIMPs, and high levels of proteases and MMPs.

6.4.3 Fetal Bovine Serum for Preliminary Considerations of an Artificial Chronic Wound Fluid Model

As the functions and compositions of wound fluid have been discussed in preceding sections, and synthetic fluids by other authors have been identified, the preliminary design of an ideal artificial chronic wound fluid may now be considered. As previous tear fluid models have been based successfully on animal serum, the same approach has been taken to propose a standard wound fluid model based on animal serum.

Animal serum provides a rational basis for the design and development of chronic wound fluid models. In general, animal serum is less expensive to purchase than human serum and poses fewer ethical considerations. Many animal sera already contain proteins, electrolytes, trace elements and lipids found at similar concentrations to that of chronic wound fluid. Therefore, using serum as a basis eradicates the need to spike water or saline with many biological components. Table 6.7 compares the biochemical compositions of seven various animal sera [fetal bovine serum (FBS), cow, horse, pig, sheep, goat and rabbit] with human chronic wound fluid. All animal sera data was obtained from Merck Manuals [157] with the exception of FBS data which was obtained from Sigma Aldrich (Appendix 1 – FBS Specification). It can be observed from Table 6.7 that the specifications of all the animal sera are comparable to human chronic wound fluid in terms of serum components, osmolality and pH. The total protein content of FBS (30-45 g/l) is most similar to chronic wound fluid (39 g/l), whereas the total protein contents for the remaining animal sera range from 54-83 g/l. Therefore, FBS was determined as the most similar in composition to chronic wound fluid from the range of animal sera compared. As FBS is also fairly inexpensive and

more easily attainable in comparison to other animal sera, it was used as a basis for an artificial chronic wound fluid in this work.

Table. 6.7 The comparison of compositions of different animal sera with human chronic wound fluid.

	<i>Animal Sera</i>							
	Chronic Wound Fluid* [145]	Fetal Bovine** (Appendix 1)	Cow [157]	Horse [157]	Pig [157]	Sheep [157]	Goat [157]	Rabbit [157]
Sodium mMol/L	141	138	136-144	128-142	139-153	142-160	137-152	131-155
Potassium mMol/L	4.4	11.1	3.6-4.9	2.9-4.6	4.4-6.5	4.3-6.3	3.8-5.7	3.6-6.9
Chloride mMol/L	104	100	99-107	98-109	97-106	101-113	100-112	92-112
Total Protein Content (g/l)	39	30-45	67-75	56-76	58-83	59-78	61-75	54-83
Osmolality (mOsm/kg)	287	260-340	260-340	260-340	260-340	260-340	260-340	260-340
pH	7.15-8.9	6.7-8	6-8	6-8	6-8	6-8	6-8	6-8

* The values of human chronic wound fluid were obtained from Trengove *et al* [145].

** The values of fetal bovine serum were obtained from Sigma Aldrich and may be found in Appendix 1.

6.5 Proposals for the Design of Standard Artificial Wound Fluid Models

Based upon the findings in section 6.4, a simple FBS-based artificial wound fluid model is proposed in this section. FBS was filtered using 13 mm cellulose acetate syringe filters to remove any impurities. The same batch of FBS was always used to ensure that the biochemical specification of the model was kept constant. The pH of the fluid model was determined at pH 7.4. No other components were added to the fluid.

The model was implemented to test the performance of a hydrocolloid skin adhesive wound material before and after contact with the artificial fluid. For the purpose of these *in vitro* tests, materials of size 2cm² were immersed in 5 ml volume of the artificial fluid. The composition of the hydrocolloid adhesive was: 20% sodium carboxylethyl cellulose (NaCMC), 20% gelatin, 20% pectin and 40% poly(isobutylene) (PIB). The hydrocolloid was compared with two contact lens materials (etafilcon A and lotrafilcon A), in order to highlight the differences between material behaviour.

Total Protein Measurements: A sample of the hydrocolloid material (2cm²), one etafilcon A contact lens and one lotrafilcon contact A lens were immersed in 5 ml of FBS-based artificial fluid model for 90 minutes. Total protein measurements were taken for the artificial fluid model soak solution at 0, 30, 60 and 90 minutes. Measurements were made by the total protein method, as described in section 2.2.9. Readings were measured at 750 nm on a Spectramax M2. Figure 6.3 shows the total protein measurements of the artificial fluid model soak solution for the three different material types at the four time intervals. It can be seen that when the hydrocolloid adhesive was submerged in the FBS solution, the total protein concentration of the soak solution rose sharply from 0-30 minutes before levelling off. The adhesive hydrocolloid wound dressing is designed to absorb a large volume of fluid; the absorption rate of a 2 cm² sample of adhesive was determined as 1.3 ml over 90 minutes. This uptake of water from the FBS-based model excludes larger sized protein molecules. As a result the soak solution of the hydrocolloid material showed an increase in total protein concentration with time. Unlike the wound adhesive, the two contact lenses studied, etafilcon A and lotrafilcon A, are not designed to absorb water and differences in interaction with the artificial model can be seen between the two contact lens types. Etafilcon A, a Group

IV contact lens, shows a general decrease with time in total protein concentration of the soak solutions. Its anionic surface creates an electrostatic attraction with positively charged proteins, such as lysozyme in the tear fluid model. Lotrafilcon A, however, a Group I contact lens with a plasma coated surface, has a maximum protein adsorption of 5 µg/ml per lens. This contact lens showed no significant difference in total protein absorbance.

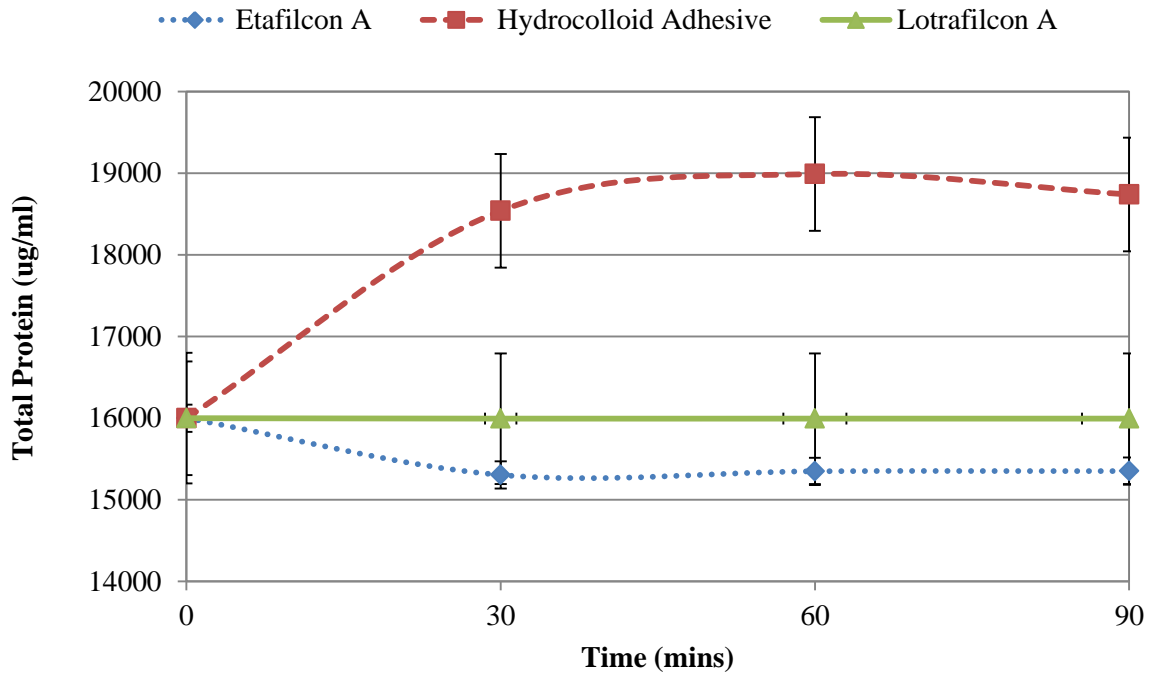


Figure 6.3 Changes in total protein concentration after material interaction with the fetal bovine serum-based artificial chronic wound fluid model.

Osmolarity Measurements: The hydrocolloid material (2 cm²), one etafilcon A contact lens and one lotrafilcon A contact lens were immersed in 5ml of FBS-based artificial fluid model for up to 90 minutes. Osmolarity measurements were taken for the artificial fluid model soak solutions at 0, 30, 60 and 90 minutes. Measurements were made on a Camlab Micro-Osmometer. Figure 6.4 shows the osmolarity measurements for the artificial fluid model soak solutions for the three different material types over the 90 minutes. The osmolarity of the artificial wound fluid was initially determined at 299 mOsm/kg. It can be observed that the adhesive hydrocolloid material absorbed a small concentration of ions in addition to water, as demonstrated by the increase in osmolarity with time. The two contact lens materials, however, show little or no change in

osmolarity as they were stored in contact lens solution containing sodium chloride, which results in an extremely small ion adsorption, if any at all.

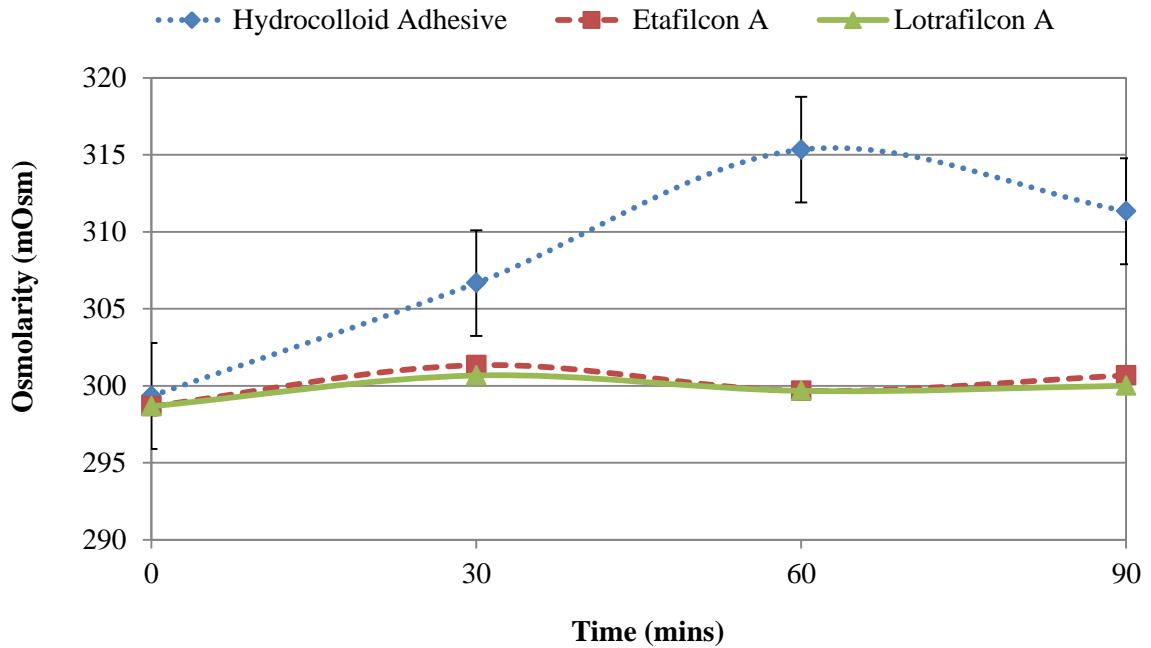


Figure 6.4 Changes in osmolarity after material interaction with the fetal bovine serum-based artificial chronic wound fluid model.

The premise for the use of animal serum as a base for the design of a standard artificial wound fluid model is appealing. The preliminary FBS-based model proposed here is a relatively simple, but effective suggestion; the properties and composition of the serum are very similar to that of acute wound fluid. However, the disturbance of the critical balance between TIMPs and MMPs is the difference between acute wound fluid and chronic wound fluid. Therefore, in order to simulate chronic wound fluid to a more accurate standard, the presence of MMPs is required within the model. To elaborate upon the FBS-based model for chronic wound fluid, it may be suggested that the addition of MMPs would further develop the model. In particular, MMP-2 and MMP-9 are found at significantly higher concentrations in chronic wound fluid than acute wound fluid [147]. Both of these MMPs are widely available from chemical suppliers, in addition to MMP assay detection kits.

The aim of this chapter was to work towards preliminary considerations for the design of a standard chronic wound fluid model. As the composition of wound fluid varies

greatly from acute wounds to chronic non-healing wounds (as discussed in section 6.4.1.1), it is valuable to suggest a standard artificial acute wound fluid model in addition to a standard chronic wound fluid model:

- Artificial acute wound fluid model:
 - 1) FBS with no additional components
 - or
 - 2) FBS with TIMPs and GFs present at similar concentrations to that of serum
- Artificial chronic wound fluid model:
 - 1) FBS with high concentrations of MMP-2 and MMP-9

6.6 Overall Discussion

This thesis concerns the investigation of biomaterial interactions with host tissue sites. Studies of material interactions with compromised sites should ultimately lead to the improvement of material design and selection. The ocular surface is an easily accessible tissue site and the study of material interactions with the compromised and non-compromised eye is well documented within the literature. In great contrast to the eye, it is virtually impossible to study *in vivo* the way in which biomaterials, such as wound dressings and ostomy devices, can influence the impaired dermal environment. This is because of the diverse characteristics of different wounds types and wound fluids (acute healing fluid versus chronic non-healing fluid). Consequently, this chapter recognises the growing need for a standard artificial wound fluid model to facilitate material interaction studies.

The work contained within this chapter demonstrated preliminary attempts to assemble synthetic biological fluids to study material/fluid interactions for the compromised wound healing environment. An approach was taken founded upon the similarities between the ocular and dermal environments. The comparisons between these two tissue sites (as described in section 6.2) and the significant amount of work documenting the use of artificial tear fluids within the literature enabled the ocular environment to be chosen as a starting basis. Literature reports the well-documented use of various artificial tear models for contact lens material studies on wettability, mechanical properties and spoilation phenomenon. However, very little parallel work

exists on artificial wound fluids, in particular those that would accurately represent different states of wound health. Primarily, the difficulties of simulating wound fluid lie in the marked differences between the complex compositions of acute healing wound fluid and chronic non-healing wound fluid. Therefore, existing knowledge from artificial tear fluid models was applied to the design of artificial wound fluids. Specifically, the use of an animal serum base for the formulation of tear fluid was extended to artificial wound fluid. Tear fluid and wound fluid share many similarities; both are complex biological fluids. It was, therefore, rational to consider animal serum for the design of a standard artificial wound fluid model.

A more developed *in vitro* wound fluid based upon animal serum could ultimately be used to study one particular aspect of material-tissue interaction, and that is the extent to which the material disturbs active components of the wound fluid. Within this work, unmodified, filtered fetal bovine serum (FBS) was used as a simple wound fluid model to demonstrate how the fluid composition and properties change when exposed to a biomaterial. It was shown in Figure 6.2 that the total protein content of the FBS fluid increased after an adhesive material was submerged in the fluid for 90 minutes. This suggests that the material only absorbed water from the FBS fluid during this time frame and excluded the uptake of protein molecules. The concentration of protein within the fluid was, therefore, observed to rise. Such experiments using an animal serum-based wound fluid model could be extended to the study of more complex components of wound fluid. For instance, it is recognised that non-healing wound fluid from the chronic wound differs largely in its composition in comparison to healing wound fluid from the acute wound. Chronic wound fluid exhibits higher levels of matrix metalloproteinases (MMPs) than acute wound fluid, with an imbalance between levels of proteins, growth factors, proteases and cytokines [22, 145]. Therefore, incorporation of MMPs and growth factors into the FBS-based model would enable the study of these components with material interaction.

This work forms the preliminary basis of an important aspect for future *in vitro* biointeraction studies. The study of active components within complex biological fluids, which have an essential role in wound healing, and the influence of the presence of the wound biomaterial on these is critical if the understanding of biomaterials-related processes is to progress. Although there are fewer challenges encountered in the study of material interactions with the ocular environment, the design of a standardised tear

fluid model would similarly be beneficial for biochemical interaction studies. Biomaterial interactions with artificial models of tear fluid reported within the literature show that no single tear fluid model adequately represents all modes of contact lens wear. Likewise, the significant differences in wound fluid composition between the healing and non-healing wound mean that no single wound fluid model represents all types of wound health. Accordingly, the concept to have an appropriate number of standard tear fluid models and wound fluid models, and a means of varying these is useful. There are many improvement that can be made for the design of biomaterials that are used in contact with healing tissue sites. The design of artificial fluids brings together *in vitro* measurements of material behaviour and the considerations for the design and selection of materials for wound applications.

CHAPTER SEVEN

Conclusions and Suggestions for Further Work

7.1 Introduction

From the outset, the purpose of this thesis was to investigate the nature of biomaterial interactions with non-compromised and compromised ocular and dermal tissue sites. The clear analogies between the two tissue sites provided a novel approach to study material-tissue interactions. Compelling similarities may be drawn between the cornea/dermal wound bed, tear fluid/wound fluid and materials for contact lens/wound dressings. These similarities have not previously been studied and were explored in this work to gain a better understanding of material-tissue interactions in the ocular and dermal environments.

7.2 Interactions of Vitronectin with the Non-Compromised Eye

The eye was chosen as an initial platform to study material-tissue interactions for two reasons. Firstly, unlike the dermal wound, the eye is an easily accessible tissue site, whether it is in a non-compromised or compromised state. Secondly, contact lenses are extensively studied and well-documented biomaterial devices within both academic literature and clinical settings.

The first aim of this work was to investigate the interactions of one particular biomarker, vitronectin, with the non-compromised lens-wearing eye. Vitronectin was described in chapter one as a prominent glycoprotein present in both tear fluid and wound fluid. This glycoprotein has many important functions within wound healing, but its cell adhesion properties and role within fibrinolysis were of particular interest. It is also well-recognised that vitronectin has a strong affinity for hydrogel materials [46]. Vitronectin was, therefore, selected for investigations of contact lens-corneal interactions in the healthy non-compromised eye. A novel on-lens cell-based assay technique was used to detect vitronectin-mediated cell adhesion on a range of contact lenses doped *in vitro*, and on *ex vivo* contact lenses. The assay exploited two specific properties of vitronectin to detect its presence by vitronectin-mediated cell adhesion on the contact lens surface, the first being its adhesive nature and the second being its cell binding property. The key findings from this investigation are discussed within this section.

In vitro investigations using the cell-based assay revealed that vitronectin adsorbs out of doping solution and onto the contact lens surface. Fibronectin is another important cell-adhesion glycoprotein. Although vitronectin and fibronectin are biochemically unrelated, fibronectin also possesses cell-binding properties which had the potential to interfere with vitronectin-mediated cell adhesion detection. The adsorption of fibronectin was, therefore, also investigated. Fibronectin demonstrated poor adsorption out of doping solution and thus, it was concluded that vitronectin was the dominant protein involved in cell adhesion.

Several assays were performed to understand in greater depth the interaction of vitronectin with contact lenses. Vitronectin-mediated cell adhesion to contact lenses *in vitro* was found to be influenced by material properties. The effect of contact lens water content was firstly studied. It was found that the higher the water content of the contact lens material, the higher the vitronectin-mediated cell adhesion to the contact lens surface. Secondly, the influence of contact lens ionicity was studied. Vitronectin-mediated cell adhesion from doping solution was greater on ionic contact lens materials than non-ionic materials. Additionally, cell adhesion counts were significantly higher on high water content ionic contact lenses (etafilcon A 58%) in comparison to high water content non-ionic lenses (vasurfilcon A 74%). This suggested that contact lens ionicity is the overriding factor for the influence on vitronectin-mediated cell adhesion rather than contact lens water content.

The investigation was extended to the study of *ex vivo* contact lenses worn in the non-compromised eye, where key findings were determined. In comparison to the contact lenses doped *in vitro*, the extent of vitronectin-mediated cell adhesion observed on *ex vivo* contact lenses was observed to be significantly higher, regardless of wear modality. It was shown that *in vitro* doping experiments at similar concentrations of vitronectin in tears cannot reproduce the high levels of deposition detected on *ex vivo* lenses. Furthermore, a comparison between cell adhesion levels on the anterior and posterior surface of the contact lens revealed significantly greater levels on the posterior surface. Together, these findings strongly suggest that vitronectin deposition on the contact lens surface arises from the mechanical interaction of the contact lens with the corneal tissue bed, rather than from adsorption out of tears. The potential implications of this finding are immense. The antagonistic actions of plasminogen activator inhibitor-1 (PAI-1) and

tissue plasminogen activator (tPA) equilibrate the conversion of plasminogen to plasmin. One of the functions of vitronectin is to bind plasminogen activator inhibitor-1 (PAI-1) in the fibrinolysis process and thereby modulate the conversion of plasminogen to plasmin. If, however, vitronectin is removed from the corneal tissue bed by the contact lens-corneal interaction, it is also likely to bind and remove PAI-1. This may then result in the upregulation of plasmin [113]. Because tear plasmin activity has been observed in the tear film of patients with corneal disorders [114, 122], a post-contact lens microclimate abundant with vitronectin has the potential to influence inflammation.

Analysis of the locus of vitronectin-mediated cell adhesion to *ex vivo* contact lenses showed that cell adhesion is always greater at the edge of the contact lens in comparison to the centre of the lens. This finding was true for all contact lenses studied, regardless of wear modality or contact lens material type. The material type, however, was found to influence the locus of cell adhesion to the posterior surface of the lens. Hydrogel contact lenses and silicone hydrogel (SiHy) contact lenses of varying moduli were analysed; lower modulus lenses (for example etafilcon A, 0.25 MPa) were shown to exhibit greater cell adhesion at the edge of the contact lens in comparison to higher modulus lenses (for example lotrafilcon A, 1.1 MPa). The material influence on the locus of vitronectin-mediated cell adhesion has the potential to consequently influence the locus of plasmin upregulation. Additionally, although protein adsorption to SiHy contact lenses is believed to be lower than to conventional hydrogel contact lenses [91, 94-96], this investigation determined that the very adhesive nature of vitronectin means that it readily adsorbs to SiHy lenses.

These investigations of vitronectin interactions in the non-compromised eye highlighted the potential consequences of vitronectin deposition from the corneal tissue bed on contact lenses and, therefore, provided an excellent basis to extend the study of the interactions of this particular protein to the compromised bandage lens-wearing eye.

7.3 Interactions of Vitronectin with the Compromised Bandage Contact Lens-Wearing Eye

The second aim of this thesis was to investigate vitronectin as a specific biomarker in lens-cornea interactions within the compromised ocular environment. Due to the

consequences of localised vitronectin deposition on the posterior contact lens surface and the potential upregulation of plasmin, it was vital to study vitronectin interactions in the compromised bandage contact lens-wearing (BCL) eye. A search of the literature showed that very little is known regarding the interaction of BCLs with the impaired corneal surface. In fact, the majority of contact lenses selected for therapeutic bandage lens use are actually designed for conventional use. BCLs are often worn for extended continuous wear durations, which exceed the recommended wear duration provided by the manufacturers. The choice of a BCL for the compromised cornea appears to be based upon convenience and availability; a contact lens is not often chosen because of its healing capacity or suitability for the impaired cornea. Therefore, vitronectin-mediated cell adhesion to BCLs worn in the compromised eye was investigated using the on-lens cell-based assay. Fifteen subjects with various ocular conditions were included as part of the investigation. Regular contact lens wearers were also included to provide a comparison against the compromised eye. The influence of BCL wear duration, material type (Biofinity versus UltraWave SiH) and clinical condition (bullous keratopathy versus Sjögren's Syndrome) on vitronectin-mediated cell adhesion to BCLs revealed interesting outcomes.

The direct comparison of a Biofinity contact lens worn for conventional use in the non-compromised eye and a Biofinity contact lens worn as a BCL in the compromised eye detected significantly higher vitronectin-mediated cell adhesion to the BCL. Both contact lenses were worn for the same duration (one day). The comparison of these two contact lenses suggested that vitronectin is more readily deposited from the injured corneal tissue bed than from the healthy intact corneal tissue. Importantly, vitronectin deposition to BCLs and the effect of plasmin upregulation in the compromised eye could potentially interfere with the ocular wound healing process and result in further corneal compromise.

The influence of material modulus on the locus of vitronectin-mediated cell adhesion to contact lenses studied in the non-compromised showed that lower modulus contact lenses exhibited higher levels of cell adhesion at the edge of the contact lens in comparison to the centre of the lens. This modulus effect was also apparent for the two BCL material types studied. Both materials, Biofinity and Ultrawave SiH, gave greater cell adhesion at the edge of the contact lens than at the centre, but this effect was found

to be to a greater extent with lower modulus UltraWave SiH contact lenses (0.5 MPa) than higher modulus Biofinity contact lenses (0.75 MPa). The locus of vitronectin deposition from the corneal tissue bed could lead to localised plasminogen activator inhibitor and, therefore, localised plasmin upregulation.

The nature of the corneal condition, more specifically the nature of the tear film as a result of the condition, was also found to influence the extent of vitronectin-mediated cell adhesion. BCLs worn by Sjögren's syndrome subjects with a severely low tear flow (Schirmer scores <5 mm/5minutes) exhibited high cell adhesion levels. This was in comparison to contact lenses worn by bullous keratopathy subjects with a sufficient tear flow. The results suggested that a deficient tear flow may enable greater interaction of the BCL with the already compromised corneal tissue bed and, therefore, greater vitronectin-mediated cell adhesion and greater vitronectin deposition from the tissue bed. Conversely, the presence of a more substantial tear flow may assist to reduce this effect and the levels of vitronectin deposition on the BCL.

It is apparent that the choice of BCL material for the management of an ocular condition is highly likely to have an impact on the health of the cornea. However, BCLs are not generally selected with the knowledge of their healing capacity in mind. Understanding the interactions of the posterior contact lens surface with the impaired cornea is vitally important to aid material design and selection. The link between plasmin and contact lens wear, and the link between plasmin levels in tears of patients with corneal disorders, mean that the design of specific BCLs with greater compatibility would be desirable. Such contact lenses should ultimately lower the levels of vitronectin deposition to accordingly reduce levels of plasmin upregulation.

7.4 Investigation of the Surface and Mechanical Properties of Skin Adhesive Materials

In order to consider biomaterial interactions with non-compromised and compromised dermal tissue sites, an examination of the physical properties of skin adhesive materials for wound care was required. A scan of the literature showed that many studies had reported the use and efficacy of skin adhesives for wound healing devices. These studies commonly included the comparison of material performance in terms of fluid handling and retention, and the effect on the rate of wound healing. However, it was

determined that very little is known regarding the properties of adhesive materials and how this relates to the corresponding properties of skin. The characterisation of skin adhesives based upon their properties is in its infancy. A third aim of this thesis was then to investigate the properties of skin adhesive materials in relation to the biophysical properties of skin, and to investigate material interactions with unbreached, healthy skin.

Biocompatibility of materials with the host tissue site is influenced by the surface and interfacial behaviour of the materials. Skin adhesive materials come into direct contact with both breached (wound area) and unbreached (peri-wound) skin, yet knowledge regarding of the surface properties of materials is sparse. In contrast, the surface properties of contact lenses are well-reported. Therefore, the first stage of material investigations in the dermal environment was to study the surface properties of a range of skin adhesive materials. These adhesives included; examples of hydrocolloid adhesives for both wound and ostomy devices obtained from leading wound care product manufacturers (Salts Healthcare, ConvaTec UK and Coloplast); hydrogels synthesised in-house by photopolymerisation; and examples of medical tapes by leading manufacturers used to secure wound dressings in place. Materials were supplied with either a siliconised paper or plastic release liner attached to the adhesive surface.

It was convenient to organise the adhesive materials into five groups in order to enable comparisons to be made:

- 1) Salts Healthcare Hydrocolloid Adhesives (paper and plastic release liners)
- 2) ConvaTec Hydrocolloid Adhesives (paper release liners)
- 3) Commercial Hydrocolloid Ostomy adhesives (plastic release liners)
- 4) Aston Hydrogel Adhesives (paper release liners)
- 5) Commercial Medical Tapes (no release liner)

Initial surface energy measurements of the adhesive material groups revealed significant differences between the hydrocolloid adhesives groups. It was observed that the Commercial Hydrocolloid Adhesives group and specific materials from the Salts Hydrocolloid Adhesives group with siliconised plastic release liners exhibited a lower surface energy in contrast to other materials from the Salts Hydrocolloid Adhesives group and ConvaTec Hydrocolloid Adhesives with siliconised paper release liners. It

was hypothesised that silicone was being transferred from the plastic release liners to the hydrocolloid adhesives. This assumption was verified by the detection of silicon on the adhesive surfaces by X-ray photoelectron spectroscopy (XPS). Silicon was detected at significantly higher levels on the adhesives with plastic release liners (on average 8.35% silicon at the surface) in comparison to lower levels detected on the adhesive with paper release liners (on average 0.95%).

Hydrocolloids may be described as a continuous phase of poly(isobutylene) (PIB) with a particulate dispersed phase of sodium carboxymethyl cellulose, gelatine and pectin. Thus, PIB with a surface energy of 33 mNm^{-1} is at the surface of the hydrocolloid, rather than the particles of the dispersed phase. Silicone oil, with a fairly low surface energy of approximately 21 mNm^{-1} will effectively spread over PIB at the surface of the hydrocolloid adhesive after liner-adhesive contact. This is because particles with a lower surface energy than the substrate will spread or wet the surface. Silicone transfer from release liner to adhesive surface is dependent upon liner-adhesive contact; silicone will only transfer at points of contact. The 'rough' porous surface of the siliconised paper liner transfers less silicone to the adhesive, whereas the smooth surface of the siliconised plastic release liner transfers higher levels due to greater contact with the adhesive. These findings suggest that siliconised paper is the favourable material choice in comparison to siliconised plastic. Altering the surface properties of the hydrocolloid could potentially affect the adhesivity of the materials.

The adhesive properties of materials were investigated by peel test measurements on skin and on a steel substrate. The average maximum force of removal appeared to correlate to the pain caused by adhesive removal from skin; the higher the maximum force, the greater the pain experienced. Furthermore, dynamic testing revealed that materials with a $\tan \delta$ value below approximately 0.60 were the most painful to remove. The presence of silicone on the adhesive surface did not appear to affect adhesion of the material to skin or to a steel substrate. However, this is not to say that silicone on the hydrocolloid adhesive surface will not affect adhesion properties in real life applications. Peel tests performed within this idealised adhesion system were carried out on the forearm of a healthy volunteer. The forearm was cleaned with methanol prior to adhesive application. In real life systems, the lipoidal composition of skin will vary greatly from person-to-person. A high lipid composition has the potential to dissolve

silicone from the hydrocolloid surface and, therefore, affect the overall adhesion performance of the hydrocolloid.

Additionally, comparative data for the tensile behaviour of adhesives revealed that the Commercial Hydrocolloid Ostomy group had the highest tensile strength (average of 0.64 MPa) of the adhesive materials tested. A high tensile strength is a desirable property for a wound care product, whether it is a dressing or an ostomy device. These adhesive products are applied to different parts of the body and should be able to bear stresses of bodily contours at different body sites.

The ideal skin adhesive material for successful wound applications should have a good hydrophobic interaction with skin, a high tensile strength, but a low modulus on application and a high modulus on removal. The benefits of investigating material properties are conducive for the design and selection of materials. From these investigations it was determined that no adhesive material performs well in every test; the best success is achieved when material properties are above a minimum level for each test, rather than performing exceptionally well in one particular area.

7.5 Considerations for the Design of an Artificial Wound Fluid Model

Investigations of material interactions with the non-compromised and compromised ocular environment are feasible because the cornea is a readily accessible tissue site. Interactions between the contact lens and cornea bathed in tear fluid were successfully studied in this thesis by investigating the deposition activity of vitronectin in both the regular contact lens-wearing eye and the bandage contact lens-wearing eye. The study of the dermal environment, however, is far more complex. In order to further *in vitro* studies of material-tissue interactions, suggestions for artificial wound fluid models were proposed.

Parallels between the ocular and dermal environments were considered in order to work towards an ideal wound fluid model. Studies of artificial tear fluid models are well-established within the literature and it was apparent that lessons could be learnt from the ocular environment and applied to the dermal environment. In particular, the use of animal sera as a base for synthetic tear fluids appeared to be an excellent starting point for the development of an artificial wound fluid model. Animal sera (such as fetal

bovine serum, FBS) offer substantial advantages over water or saline bases that are modified with additional components. FBS contains many proteins at similar concentrations to that of chronic wound fluid. Furthermore, the problem of the inherent lack of solubility of non-polar lipids is overcome by the use of a biological fluid such as FBS.

The compositional differences between wound fluid from acute healing wounds and wound fluid from chronic non-healing wounds were highlighted. Acute wound fluid contains all the components of healthy serum at normal or lower concentrations to that of serum [145]. These include: serum components, total protein, C-reactive proteins, cytokines, matrix metalloproteinases (MMPs) and tissue inhibitors of metalloproteinases (TIMPs) [145]. In contrast, chronic wound fluid contains significantly increased levels of MMPs and low or absent levels of TIMPs [22, 147]. Consequently, it was logical to propose artificial models for both acute wound fluid and chronic wound fluid:

Artificial acute wound fluid model:

- 3) FBS base with no additional components
- 4) FBS with TIMPs and growth factors present at similar concentrations to that of serum.

Artificial chronic wound fluid model:

- 2) FBS with high concentrations of MMP-2 and MMP-9.

These preliminary designs for artificial wound fluid models would very importantly provide a platform for the study of *in vitro* material interactions with fluid.

7.6 Suggestions for Further Work

The area of bandage contact lens (BCL) interactions with the impaired cornea is ripe for further investigations. Within this thesis, the contact lenses worn for therapeutic use by subjects with corneal conditions were supplied by two large hospitals in the UK. The contact lenses were silicone hydrogel materials that are designed for conventional contact lens use rather than for therapeutic use. There are very few purposely designed BCLs and it appears that although these do exist, their lack of availability makes them

less desirable as a material choice within the hospital setting. Nonetheless, it would be extremely interesting to compare vitronectin-mediated cell adhesion to contact lenses designed for conventional use that are worn in the compromised eye against vitronectin-mediated cell adhesion to contact lenses purposely designed for bandage use in the compromised eye. For example, in this study UltraWave SiH monthly contact lenses produced by UltraVision were analysed by a cell-based assay technique for the detection of vitronectin on the contact lens surface. However, UltraVision also produce a bandage lens named UltraWave Bandage, which is suitable for three months extended wear. Because UltraWave SiH can be used for both conventional and bandage lens use, it is a practical choice for hospitals when selecting contact lens materials in comparison to UltraWave Bandage. However, the comparison of these two contact lens types could prove very useful. If it appears that overall vitronectin deposition is lower on UltraWave Bandage, there could be a strong argument for this contact lens as a better choice for wear in the compromised eye. This is just one example of comparisons between contact lenses for therapeutic use that could be studied further.

Additionally, it would be interesting to study vitronectin-mediated cell adhesion to BCLs worn over a period in the compromised eye, from the time of initial injury to the end of the corneal wound healing process. It was suggested from this work that vitronectin is more readily deposited from the impaired corneal tissue bed than from the healthy intact cornea. Therefore, are vitronectin deposition levels on BCLs higher immediately after injury? Do these deposition levels on BCLs decrease as the cornea heals? These questions may be difficult to answer in the eye which has been injured by accident; due to the propensity of the cornea to heal rapidly following injury, the corneal tissue bed may reach a certain degree of healing by the time a contact lens is inserted into the eye. However, this type of study could be feasible in the eye following surgery. In elective surgery procedures, such as laser-assisted *in situ* keratomileusis (LASIK), a contact lens is normally inserted in the eye immediately after the surgical process. Harvesting such contact lenses immediately after surgery and then replacing them after appropriate time intervals could further determine the link between vitronectin deposition on contact lenses and corneal healing. This could potentially provide a further insight into the negative consequences of vitronectin deposition in terms of plasmin upregulation in the ocular environment.

With respect to material-tissue interactions in the dermal environment, further work is required for the development of a standard artificial wound fluid model. Preliminary suggestions were made for compositions of acute and chronic wound fluids using animal serum as a base. The development and optimisation of such artificial fluids is not without difficulty; the composition of wound fluid varies tremendously from wound-to-wound and from patient-to-patient. However, an artificial wound model, which can be modified accordingly to represent different states of healing, would provide a premise to study wound dressing material interactions with a biological fluid. In this work the surface and mechanical properties of skin adhesive materials were studied in their undisturbed unhydrated form. Material properties, such as the surface energies, peel strengths, tensile strength and dynamic moduli, will inevitably change once a material is subjected to fluid and becomes hydrated. The investigation of material properties after contact with artificial wound fluid would logically be the next step for understanding material-tissue interactions.

In the ocular environment, a great deal is known about how the contact lens can influence the composition of the tear film in the lens-wearing eye. However, the way in which materials influence and disturb the composition of wound fluid is not an area that is widely studied. Further work in this area could importantly aid in material design and selection for wound care products.

REFERENCES

- References -

1. Sullivan, D.A., *Lacrimal Gland, Tear Film, and Dry Eye Syndromes*. Vol. 1. 1994, Plenum Press: New York.
2. Falanga, V., *The Chronic Wound: Failure to Heal*. Cutaneous Wound Healing. 2001, Martin Dunitz: London.
3. Posnett, J. and Franks, P.J., *The burden of chronic wounds in the UK*. Nursing Times, 2008. **104**(3): p.44-45.
4. Farrar, D., *Advanced Wound Repair Therapies*. 2011, Woodhead Publishing Limited: Cambridge.
5. Hess, C.T., *Skin and Wound Care*. 6th ed. 2008, Lippincott Williams & Wilkins: Pennsylvania.
6. Walter, K.A. and Roberts, M.A., *The Structure and Function of Skin*, in *Dermatological and Transdermal Formulations*, K.A. Walter, Editor. 2002, Marcel Dekker: New York.
7. Segura, S. and Requena, L., *Anatomy and histology of normal subcutaneous fat, necrosis of adipocytes, and classification of the panniculitides*. Dermatologic Clinics, 2008. **26**(4): p.419-424.
8. Shuster, S.A.M., Black, M.M. and McVitie, E.V.A., *The influence of age and sex on skin thickness, skin collagen and density*. British Journal of Dermatology, 1975. **93**(6): p.639-643.
9. Zaidi, Z. and Walton, S., *A Manual of Dermatology*. 2013, Jaypee Brothers: New Dehli.
10. Livesley, N.J. and Chow, A.W., *Infected pressure ulcers in elderly individuals*. Clinical Infectious Diseases, 2002. **35**(11): p.1390-1396.
11. Bennett, G., Dealey, C. and Posnett, J., *The cost of pressure ulcers in the UK*. Age and Ageing, 2004. **33**(3): p.230-235.
12. Margolis, D.J., Bilker, W., Santanna, J. and Baumgarten, M., *Venous leg ulcer: incidence and prevalence in the elderly*. Journal of the American Academy of Dermatology, 2002. **46**(3): p.381-386.
13. NHS. *Venous leg ulcer*. Available from: <http://www.nhs.uk/conditions/Leg-ulcer-venous/Pages/Introduction.aspx>. 2014.
14. Gosain, A. and DiPietro, L.A., *Aging and wound healing*. World Journal of Surgery, 2004. **28**(3): p.321-326.
15. Gilchrest, B.A., Garmyn, M. and Yaar, M., *Aging and photoaging affect gene expression in cultured human keratinocytes*. Archives of Dermatology, 1994. **130**(1): p.82-86.
16. Diridollou, S., Vabre, V., Berson, M., Vaillant, L., Black, D., Lagarde, J.M., Grégoire, J.M., Gall, Y. and Patat, F., *Skin ageing: changes of physical*

- properties of human skin in vivo*. International Journal of Cosmetic Science, 2001. **23**(6): p.353-362.
17. Whitton, J.T. and Everall, J.D., *The thickness of the epidermis*. British Journal of Dermatology, 1973. **89**(5): p.467-476.
 18. Eming, S.A., Krieg, T. and Davidson, J.M., *Inflammation in wound repair: molecular and cellular mechanisms*. The Journal of Investigative Dermatology, 2007. **127**(3): p.514-525.
 19. Levenson, S.M., Geever, E.F., Crowley, L.V., Oates, J.F., Berard, C.W. and Rosen, H., *Healing of rat skin wounds*. Annals of Surgery, 1965. **161**(2): p.293-308.
 20. Mustoe, T.A., O'Shaughnessy, K. and Kloeters, O., *Chronic wound pathogenesis and current treatment strategies: a unifying hypothesis*. Plastic and Reconstructive Surgery, 2006. **117**(7): p.35S-41S.
 21. Stadelmann, W.K., Digenis, A.G. and Tobin, G.R., *Impediments to wound healing*. The American Journal of Surgery, 1998. **176**(2, Supplement 1): p.39S-47S.
 22. Trengove N, J., Stacey, M.C., MaCauley, S.M., Bennett, N., Gibson, J., Burslem, F.G., Murphy, G. and Schultz, G., *Analysis of the acute and chronic wound environments: The role of proteases and their inhibitors*. Wound Repair and Regeneration, 1999. **7**(6): p.442-452.
 23. Homans, J., *The etiology and treatment of varicose ulcer of the leg*. Surgery, Gynecology & Obstetrics, 1917. **24**: p.300-311.
 24. Pratt, G.H., *Arterial varices; a syndrome*. American Journal of Surgery, 1949. **77**(4): p.456-60.
 25. Browse, N.L. and Burnand, K.G., *The cause of venous ulceration*. Lancet, 1982. **2**(8292): p.243-245.
 26. Falanga, V. and Eaglstein, W.H., *The "trap" hypothesis of venous ulceration*. Lancet, 1993. **341**(8851): p.1006-1008.
 27. Coleridge Smith, P.D., Thomas, P., Scurr, J.H. and Dormandy, J.A., *Causes of venous ulceration: a new hypothesis*. British Medical Journal, 1988 **296**(6638): p. 1726-1727.
 28. Bjarnsholt, T., Kirketerp-Moller, K., Jensen, P.O., Madsen, K.G., Phipps, R., Kroghfelt, K., Hoiby, N. and Givskov, M., *Why chronic wounds will not heal: a novel hypothesis*. Wound Repair and Regeneration, 2008. **16**(1): p.2-10.
 29. Jang, Y.C., Tsou, R., Gibran, N.S. and Isik, F.F., *Vitronectin deficiency is associated with increased wound fibrinolysis and decreased microvascular angiogenesis in mice*. Surgery, 2000. **127**(6): p.696-704.

30. Holmes, R., *Preparation from human serum of an alpha-one protein which induces the immediate growth of unadapted cells in vitro*. The Journal of Cell Biology, 1967. **32**(2): p.297-308.
31. Barnes, D.W. and Silnutzer, J., *Isolation of human serum spreading factor*. The Journal of Biological Chemistry, 1983. **258**(20): p.12548-12552.
32. Preissner, K.T., Wassmuth, R. and Muller-Berghaus, G., *Physicochemical characterization of human S-protein and its function in the blood coagulation system*. Biochemical Journal, 1985. **231**(2): p.349-355.
33. Schwartz, I., Seger, D. and Schaltiel, S., *Molecules in focus: Vitronectin*. The International Journal of Biochemistry & Cell Biology 1999. **31**: p.539-544.
34. Buzza, M.S., Zamurs, L., Sun, J., Bird, C.H., Smith, A.I., Trapani, J.A., Froelich, C.J., Nice, E.C. and Bird, P.I., *Extracellular matrix remodeling by human granzyme B via cleavage of vitronectin, fibronectin, and laminin*. The Journal of Biological Chemistry, 2005. **280**(25): p.23549-23558.
35. Preissner, K.T., *The role of vitronectin as multifunctional regulator in the hemostatic and immune systems*. Blut, 1989. **59**(5): p.419-431.
36. Underwood, P.A. and Bennett, F.A., *A comparison of the biological activities of the cell-adhesive proteins vitronectin and fibronectin*. Journal of Cell Science, 1989. **93**(Pt 4): p.641-649.
37. Horton, M.A., *The avp3 integrin "vitronectin receptor"*. The International Journal of Biochemistry & Cell Biology, 1997. **29**(5): p.721-725.
38. Sheehan, M., Morris, C.A., Pussell, B.A. and Charlesworth, J.A., *Complement inhibition by human vitronectin involves non-heparin binding domains*. Clinical & Experimental Immunology, 1995. **101**(1): p.136-141.
39. Podack, E.R., Kolb, W.P. and Muller-Eberhard, H.J., *The SC5b-7 complex: formation, isolation, properties, and subunit composition*. The Journal of Immunology, 1977. **119**(6): p.2024-2029.
40. Fabrizio-Homan, D.J. and Cooper, S.L., *A comparison of the adsorption of three adhesive proteins to biomaterial surfaces*. Journal of Biomaterials Science. Polymer Edition, 1991a. **3**: p.27-47.
41. Fabrizio-Homan, D.J. and Cooper, S.L., *Competitive adsorption of vitronectin with albumin, fibrinogen, and fibronectin on polymeric biomaterials*. Journal of Biomedical Materials Research, 1991b. **25**(8): p.953-971.
42. Steele, J.G., Dalton, B.A., Johnson, G. and Underwood, P.A., *Polystyrene chemistry affects vitronectin activity: an explanation for cell attachment to tissue culture polystyrene but not to unmodified polystyrene*. Journal of Biomedical Materials Research, 1993. **27**(7): p.927-940.
43. Steele, J.G., Dalton, B.A., Johnson, G. and Underwood, P.A., *Adsorption of fibronectin and vitronectin onto PrimariaTM and tissue culture polystyrene and*

- relationship to the mechanism of initial attachment of human vein endothelial cells and BHK-2 1 fibroblasts.* *Biomaterials*, 1995. **16**(14): p.1057-1067.
44. Saika, S., Yamanaka, A., Tanaka, S.-I., Ohmi, S., Ohnishi, Y. and Ooshima, A., *Extracellular matrix on intraocular lenses.* *Experimental Eye Research*, 1995. **61**(6): p.713-721.
 45. Linnola, R.J., Sund, M., Ylonen, R. and Pihlajaniemi, T., *Adhesion of soluble fibronectin, vitronectin, and collagen type IV to intraocular lens materials.* *Journal of Cataract & Refractive Surgery*, 2003. **29**(1): p.146-152.
 46. Tighe, B.J., Jones, L., Evans, K. and Franklin, V., *Patient-dependent and material-dependent factors in contact lens deposition processes.* *Advances in Experimental Medicine and Biology*, 1998. **438**: p.745-751.
 47. Winter, G.D., *Formation of the scab and the rate of epithelisation of superficial wounds in the skin of the young domestic pig.* *Nature*, 1962. **193**: p.293 - 294.
 48. Jolly, S., *Dry Wound Healing Concept Using Spray-on Dressings for Chronic Wounds*, in *Advanced Wound Repair Therapies*, D. Farrar, Editor. 2011, Woodhead Publishing: Cambridge.
 49. Gethin, G., *The significance of surface pH in chronic wounds.* *Wounds UK*, 2007. **3**(3): p.52-56.
 50. Kloth, L.C., Berman, J.E., Dumit-Minkel, S., Sutton, C.H., Papanek, P.E. and Wurzel, J., *Effects of a normothermic dressing on pressure ulcer healing.* *Advances in Skin & Wound Care*, 2000. **13**(2): p.69-74.
 51. Tighe, B.J. and Mann, A.M., *Adhesive and interfacial phenomena in wound healing*, in *Advanced Wound Repair Therapies* D. Farrar, Editor. 2011, Woodhead Publishing Limited: Cambridge.
 52. Helfman, T., Ovington, L. and Falanga, V., *Occlusive dressings and wound healing.* *Clinics in Dermatology*, 1994. **12**(1): p.121-127.
 53. Baranoski, S. and Ayello, E.A., *Wound Care Essentials: Practice Principles.* 2nd ed. 2008, Lippincott Williams & Wilkins: Pennsylvania.
 54. Eaglstein, W.H., *Effect of occlusive dressings on wound healing.* *Clinics in Dermatology*, 1984. **2**(3): p.107-111.
 55. Baxter, A. and Salter, M., *Stoma care nursing.* *Nursing Standard*, 2000. **14**(19): p.59.
 56. McBain, J.W. and Hopkins, D.G., *On adhesives and adhesive action.* *The Journal of Physical Chemistry*, 1925. **29**(2): p.188-204.
 57. Hollinworth, H., *The management of patients' pain in wound care.* *Nursing Standard*, 2005. **20**(7): p.65-73.

58. Malhotra, A., Minja, F.J., Crum, A. and Burrowes, D., *Ocular anatomy and cross-sectional imaging of the eye*. Seminars in Ultrasound, CT and MRI, 2011. **32**(1): p.2-13.
59. Smerdon, D., *Anatomy of the eye and orbit*. Current Anaesthesia & Critical Care, 2000. **11**(6): p.286-292.
60. Kiely, P.M., Smith, G. and Carney, L.G., *The mean shape of the human cornea*. Journal of Modern Optics, 1982. **29**(8): p.1027-1040.
61. Freegard, T.J., *The physical basis of transparency of the normal cornea*. Eye, 1997. **11**(4): p.465-471.
62. Kiely, P.M., Carney, L.G. and Smith, G., *Diurnal variations of corneal topography and thickness*. American Journal of Optometry and Physiological Optics, 1982. **59**(12): p.976-982.
63. Sheardown, H. and Cheng, Y.L., *Mechanisms of corneal epithelial wound healing*. Chemical Engineering Science, 1996. **51**(19): p.4517-4529.
64. Dua, H.S., Faraj, L.A., Said, D.G., Gray, T. and Lowe, J., *Human corneal anatomy redefined: a novel pre-Descemet's layer (Dua's layer)*. Ophthalmology, 2013. **120**(9): p.1778-1785.
65. Chang, J.H., Gabison, E.E., Kato, T. and Azar, D.T., *Corneal neovascularization*. Current Opinion in Ophthalmology, 2001. **12**(4): p.242-249.
66. Denniston, A.K.O. and Murray, P.I., *Oxford Handbook of Ophthalmology*. 2nd ed. 2009, Oxford University Press: Oxford.
67. Ohashi, Y., Dogru, M. and Tsubota, K., *Laboratory findings in tear fluid analysis*. Clinica Chimica Acta, 2006. **369**(1): p.17-28.
68. Craig, J.P. and Tomlinson, A., *Importance of the lipid layer in human tear film stability and evaporation*. Optometry & Vision Science, 1997. **74**(1): p.8-13.
69. Wilson, S.A. and Last, A., *Management of corneal abrasions*. American Family Physician, 2004. **70**: p.123-132.
70. NHSBT. *Cornea transplantation*. Available at: http://www.organdonation.nhs.uk/newsroom/fact_sheets/cornea_transplantation_fact_sheet.asp. 2011.
71. Digest, R., ed. *Medical Breakthroughs*. ed. R.W. Chadd. 2004, Reader's Digest Association: New York.
72. Stocum, D.L., *Regenerative Biology and Medicine*. 2nd ed. 2012, Elsevier Inc: China.
73. Steele, C., *Corneal wound healing: a review*. Optometry Today, 1999. **24**: p.28-32.

74. Jackson, A.J., Sinton, J.E., Frazer, D.G. and Morrison, E., *Therapeutic contact lenses and their use in the management of anterior segment pathology*. Journal of the British Contact Lens Association, 1996. **19**(1): p.11-19.
75. Arora, R., Jain, S., Monga, S., Narayanan, R., Raina, U.K. and Mehta, D.K., *Efficacy of continuous wear PureVision contact lenses for therapeutic use*. Contact Lens and Anterior Eye, 2004. **27**(1): p.39-43.
76. Ruben, M., *Soft contact lens treatment of bullous keratopathy*. Transactions of the Ophthalmological Societies of the United Kingdom, 1975. **95**(1): p.75-78.
77. Kok, J.H. and Visser, R., *Treatment of ocular surface disorders and dry eyes with high gas-permeable scleral lenses*. Cornea, 1992. **11**(6): p.518-522.
78. Gemoules, G., *Therapeutic effects of contact lenses after refractive surgery*. Eye and Contact Lens, 2005. **31**(1): p.12-22.
79. Hovding, G., *Hydrophilic contact lenses in corneal disorders*. Acta Ophthalmologica, 1984. **62**(4): p.566-576.
80. Engle, A.T., Laurent, J.M., Schallhorn, S.C., Toman, S.D., Newacheck, J.S., Tanzer, D.J. and Tidwell, J.L., *Masked comparison of silicone hydrogel lotrafilcon A and etafilcon A extended-wear bandage contact lenses after photorefractive keratectomy*. Journal of Cataract & Refractive Surgery, 2005. **31**(4): p.681-686.
81. Lemp, M.A. and Yamamoto, G.K., *The role of bandage lenses in the management of recurrent erosions of the cornea*. Eye & Contact Lens, 1977. **3**(2): p.28-33.
82. Arrington, G.E., *A History of Ophthalmology*. 1959, MD Publications: New York.
83. Ridley, F., *Therapeutic uses of scleral contact lenses*. International Ophthalmology Clinics, 1962. **2**(3): p.687-716.
84. Wichterle, O., *Hydrophilic gels for biological use*. Nature, 1960. **185**: p.117-118.
85. Gasset, A.R. and Kaufman, H.E., *Therapeutic uses of hydrophilic contact lenses*. American Journal of Ophthalmology, 1970. **69**(2): p.252-259.
86. Lindahl, K.J., DePaolis, M.D., Aquavella, J.V., Temnycky, G.O. and Erdey, R.A., *Applications of hydrophilic disposable contact lenses as therapeutic bandages*. Contact Lens Association of Ophthalmologists, 1991. **17**(4): p.241-243.
87. Gruber, E., *The Acuvue disposable contact lens as a therapeutic bandage lens*. Annals of Ophthalmology, 1991. **23**(12): p.446-447.
88. Srur, M. and Dattas, D., *The use of disposable contact lenses as therapeutic lenses*. Contact Lens Association of Ophthalmologists, 1997. **23**(1): p.40-42.

89. Holden, B.A., Mertz, G.W. and McNally, J.J., *Corneal swelling response to contact lenses worn under extended wear conditions*. Investigative Ophthalmology & Visual Science, 1983. **24**(2): p.218-226.
90. Dumbleton, K., *Adverse events with silicone hydrogel continuous wear*. Contact Lens and Anterior Eye, 2002. **25**(3): p.137-146.
91. Ambroziak, A.M., Szaflik, J.P. and Szaflik, J., *Therapeutic use of a silicone hydrogel contact lens in selected clinical cases*. Eye and Contact Lens, 2004. **30**(1): p.63-67.
92. Kim, J.H. and Yoon, J.Y., *Protein adsorption on polymer particles.*, in *Encyclopedia of Surface and Colloid Science.*, A. Hubbard, Editor. 2002, Marcel Dekker: New York. p. 4373-4381.
93. Thevenot, P., Hu, W. and Tang, L., *Surface chemistry influences implant biocompatibility*. Current Topics in Medicinal Chemistry, 2008. **8**: p.270-280.
94. Senchyna, M., Jones, L., Louie, D., May, C., Forbes, I. and Glasier, M.A., *Quantitative and conformational characterization of lysozyme deposited on balafilcon and etafilcon contact lens materials*. Current Eye Research, 2004. **28**(1): p.25-36.
95. Jones, L., Senchyna, M., Glasier, M.A., Schickler, J., Forbes, I., Louie, D. and May, C., *Lysozyme and lipid deposition on silicone hydrogel contact lens materials*. Eye and Contact Lens, 2003. **29**(1 Suppl): p.S75-S79.
96. McNally, J. and McKenney, *A clinical look at a silicone hydrogel extended wear lens*. Contact Lens Spectrum, 2002. **17**(1): p.38-41.
97. Stone, R.P., Mowrey-McKee, M.F. and Kreutzer, P., *Protein: a source of lens discoloration*. Contact Lens Forum 1984(9): p.33-41.
98. Green-Church, K.B. and Nichols, J.J., *Mass spectrometry-based proteomic analyses of contact lens deposition*. Molecular Vision, 2008. **14**: p.291-297.
99. Jones, L., Franklin, V., Evans, K., Sariri, R. and Tighe, B., *Spoilation and clinical performance of monthly vs. three monthly Group II disposable contact lenses*. Optometry & Vision Science, 1996. **73**(1): p.16-21.
100. Holden, B.A. and Mertz, G.W., *Critical oxygen levels to avoid corneal edema for daily and extended wear contact lenses*. Investigative Ophthalmology & Visual Science, 1984. **25**(10): p.1161-1167.
101. Schirmer, O., *Studies on the physiology and pathology of tear secretion and tear dissipation*. Graefe's Archive for Clinical and Experimental Ophthalmology, 1903. **56**(2): p.197-291.
102. van Bijsterveld, O.P., *Diagnostic tests in the Sicca syndrome*. Archives of ophthalmology, 1969. **82**(1): p.10-14.

- References -

103. Mann, A. and Tighe, B., *Contact lens interactions with the tear film*. Experimental Eye Research, 2013. **117**: p.88-98.
104. Sack, R.A., Underwood, P.A., Tan, K.O., Sutherland, H. and Morris, C.A., *Vitronectin: Possible contribution to the closed-eye external host-defense mechanism*. Ocular Immunology and Inflammation, 1993. **1**(4): p.327-336.
105. Sack, R.A., Underwood, P.A., Tan, K.O. and Morris, C.A., *Vitronectin in human tears--protection against closed eye induced inflammatory damage*. Advances in Experimental Medicine and Biology, 1994. **350**: p.345-349.
106. Xiao, J., Natarajan, K., Rajala, M.S., Astley, R.A., Ramadan, R.T. and Chodosh, J., *Vitronectin: a possible determinant of adenovirus type 19 tropism for human corneal epithelium*. American Journal of Ophthalmology, 2005. **140**(3): p.363-369.
107. Willcox, M.D., Morris, C.A., Thakur, A., Sack, R.A., Wickson, J. and Boey, W., *Complement and complement regulatory proteins in human tears*. Investigative Ophthalmology & Visual Science, 1997. **38**(1): p.1-8.
108. Tan, K.O., Sack, R.A., Holden, B.A. and Swarbrick, H.A., *Temporal sequence of changes in tear film composition during sleep*. Current Eye Research, 1993. **12**(11): p.1001-1007.
109. Acera, A., Vecino, E., Rodríguez-Agirretxe, I. and Aloria, K.L., *Changes in tear protein profile in keratoconus disease*. Eye, 2011. **25**(9): p.225-233.
110. Gupta, A.K., Sarin, S., Mathur, M.D. and Ghosh, B., *α 1-Antitrypsin and serum albumin in tear fluids in acute adenovirus conjunctivitis*. British Journal of Ophthalmology, 1988. **72**(5): p.390-393.
111. Sack, R.A., Tan, K.O. and Tan, A., *Diurnal tear cycle: evidence for a nocturnal inflammatory constitutive tear fluid*. Investigative Ophthalmology & Visual Science, 1992. **33**: p.626-640.
112. Jensen, O.L., Glud, B.S. and Eriksen, H.O., *Fibronectin in tears following surgical trauma to the eye*. Acta Ophthalmologica, 1985. **63**(3): p.346-350.
113. Vaheri, A., Salonen, E.-M., Tapiovaara, H., Sirén, V., Myöhänen, H., Stephens, R.W. and Bizik, J., *Regulation of the pericellular activation of plasminogen and its role in tissue-destructive processes*. Acta Ophthalmologica, 1992. **70**(S202): p.34-41.
114. Salonen, E.M., Tervo, T., Torma, E., Tarkkanen, A. and Vaheri, A., *Plasmin in tear fluid of patients with corneal ulcers: basis for new therapy*. Acta Ophthalmologica, 1987. **65**(1): p.3-12.
115. Ghosh, K., Ren, X.D., Shu, X.Z., Prestwich, G.D. and Clark, R.A., *Fibronectin functional domains coupled to hyaluronan stimulate adult human dermal fibroblast responses critical for wound healing*. Tissue Engineering, 2006. **12**(3): p.601-613.

116. Agren, M.S. and Werthen, M., *The extracellular matrix in wound healing: a closer look at therapeutics for chronic wounds*. The International Journal of Lower Extremity Wounds, 2007. **6**(2): p.82-97.
117. Tervo, T., van Setten, G.B., Andersson, R., Salonen, E.M., Vaheri, A., Immonen, I. and Tarkkanen, A., *Contact lens wear is associated with the appearance of plasmin in the tear fluid--preliminary results*. Graefe's Archive for Clinical and Experimental Ophthalmology, 1989. **227**(1): p.42-44.
118. Farooqui, S., Z, Foster, C., S and Ma, J. *Central Sterile Corneal Ulceration*. Available at: <http://emedicine.medscape.com/article/1196936-overview>. 2008.
119. Vannas, A., Sweeney, D.F., Holden, B.A., Sapyska, E., Salonen, E.M. and Vaheri, A., *Tear plasmin activity with contact lens wear*. Current Eye Research, 1992. **11**(3): p.243-251.
120. Hayashi, K., Berman, M., Smith, D., el-Ghatit, A., Pease, S. and Kenyon, K.R., *Pathogenesis of corneal epithelial defects: role of plasminogen activator*. Current Eye Research, 1991. **10**(5): p.381-398.
121. Grinnell, F., Ho, C. and Wysocki, A., *Degradation of fibronectin and vitronectin and vitronectin in chronic wound fluid: Analysis by cell blotting, immunoblotting, and cell adhesion assays*. Journal of Investigative Dermatology, 1992. **98**: p.410-416.
122. Tervo, T., Salonen, E.M., Vaheri, A., Immonen, I., van Setten, G.B., Himberg, J.J. and Tarkkanen, A., *Elevation of tear fluid plasmin in corneal disease*. Acta Ophthalmologica, 1988. **66**(4): p.393-399.
123. Gil-Cazorla, R., Teus, M.A., Hernandez-Verdejo, J.L., De Benito-Llopis, L. and Garcia-Gonzalez, M., *Comparative study of two silicone hydrogel contact lenses used as bandage contact lenses after LASEK*. Optometry and Vision Science, 2008. **85**(9): p.884-888.
124. Bartlett, J.D. and Jaanus, S.D., *Clinical Ocular Pharmacology*. 5th ed. 2008, Elsevier Inc: Missouri.
125. Andrew, N.C. and Woodward, E.G., *The bandage lens in bullous keratopathy*. Ophthalmic and Physiological Optics, 1989. **9**(1): p.66-68.
126. Lang, G., *Ophthalmology A Pocket Textbook Atlas*. 2nd ed. 2007, Thieme Stuttgart: New York.
127. Bowszyc, J., Bowszyc-Dmochowska, M., Kazmierowski, M., Ben-Amer, H.M., Garbowska, T. and Harding, E., *Comparison of two dressings in the treatment of venous leg ulcers*. Journal of Wound Care, 1995. **4**(3): p.106-110.
128. Thomas, S., Banks, V., Bale, S., Fear-Price, M., Hagelstein, S., Harding, K.G., Orpin, J. and Thomas, N., *A comparison of two dressings in the management of chronic wounds*. Journal of Wound Care, 1997. **6**(8): p.383-386.

129. Charles, H., Callicot, C., Mathurin, D., Ballard, K. and Hart, J., *Randomised, comparative study of three primary dressings for the treatment of venous ulcers*. British Journal of Community Nursing, 2002. **7**(6 Suppl): p.48-54.
130. Margolis, D.J., Gross, E.A., Wood, C.R. and Lazarus, G.S., *Planimetric rate of healing in venous ulcers of the leg treated with pressure bandage and hydrocolloid dressing*. Journal of the American Academy of Dermatology, 1993. **28**(3): p.418-421.
131. Thomas, S. and Loveless, P. *A comparative study of the properties of twelve hydrocolloid dressings: Available at: <http://www.worldwidewounds.com/1997/july/Thomas-Hydronet/hydronet.html>*. 1997.
132. Thomas, S., Fear, M., Humphreys, J., Disley, L. and Waring, M.J., *The effect of dressings on the production of exudate from venous leg ulcers*. Wounds UK, 1996. **8**(5): p.145-150.
133. Benedek, I. and Feldstein, M.M., *Technology of Pressure-Sensitive Adhesives and Products*. 2008, Taylor & Francis: Florida.
134. Schmohl, M., Beckert, S., Joos, T.O., Konigsrainer, A., Schneiderhan-Marra, N. and Loffler, M.W., *Superficial Wound Swabbing*. Diabetes Care, 2012. **35**(11): p.2113-2120.
135. Bright, A.M., *Towards an Improved Ocular Drug Delivery System*. 1992, Aston University: UK.
136. Zhou, L., Zhao, S.Z., Koh, S.K., Chen, L., Vaz, C., Tanavde, V., Li, X.R. and Beuerman, R.W., *In-depth analysis of the human tear proteome*. Journal of Proteomics, 2012. **75**(13): p.3877-3885.
137. Lemp, M.A., *Report of the National Eye Institute/Industry workshop on Clinical Trials in Dry Eyes*. Contact Lens Association of Ophthalmologists, 1995. **21**(4): p.221-232.
138. Sullivan, D.A., Sullivan, D.D., Dartt, D.A. and Meneray, M.A., *Lacrimal Gland, Tear Film, and Dry Eye Syndromes 2: Basic Science and Clinical Relevance* Vol. 438. 1998, Plenum Press: New York.
139. Moshirfar, M., Pierson, K., Hanamaikai, K., Santiago-Caban, L., Muthappan, V. and Passi, S.F., *Artificial tears potpourri: a literature review*. Journal of Clinical Ophthalmology, 2014. **8**: p.1419-1433.
140. Schmidtchen, A., *Chronic ulcers: A method for sampling and analysis of wound fluid*. Acta Dermato-Venereologica, 1999. **79**: p.291-295.
141. Tighe, B.J. and Mann, A.M., *Wound Healing Studies and Interfacial Phenomena: Use and Relevance of the Corneal Model.*, in *Advanced Wound Repair Therapies*, D. Farrar, Editor. 2011, Woodhead Publishing Limited: Cambridge (UK). p. 284-320.

142. Franklin, V.J., *Lipoidal species in ocular spoilation processes*. 1990, Aston University, UK.
143. Cutting, K.F., *Wound exudate: composition and functions*. Journal of Community Nursing, 2003. **9**(9 Suppl): p.4-9.
144. Staiano-Coico, L., Higgins, P., Schwatz, S., Zimm, J. and Goncalves, J., *Wound fluids: A reflection of the state of healing*. Ostomy/Wound Management, 2000. **46**(1A Suppl): p.85S-93S.
145. Trengove, N., *Biochemical analysis of wound fluid from non healing and healing chronic leg ulcers*. Wound Repair and Regeneration, 1996. **4**(2): p.234-239
146. James, T.J., Hughes, M.A., Cherry, G.W. and Taylor, R.P., *Simple biochemical markers to assess chronic wounds*. Wound Repair and Regeneration, 2000. **8**(4): p.264-269.
147. Wysocki, A.B., *Wound fluids and the pathogenesis of chronic wounds*. Journal of Wound Ostomy & Continence Nursing, 1996. **23**(6): p.283-290.
148. Madlener, M., Parks, W.C. and Werner, S., *MMPs and TIMPs are differentially expressed during excisional skin wound repair*. Experimental Cell Research, 1998. **242**(1): p.201-210.
149. Stojadinovic, A., *Topical advances in wound care*. Gynecologic Oncology, 2008. **111**(2 Suppl): p.S70-S80.
150. Barrientos, S., Stojadinovic, O., Golinko, M.S., Brem, H. and Tomic-Canic, M., *Growth factors and cytokines in wound healing*. Wound Repair and Regeneration, 2008. **16**(5): p.585-601.
151. Goldman, R., *Growth factors and chronic wound healing: past, present, and future*. Advances in Skin & Wound Care, 2004. **17**(1): p.24-35.
152. Trengove, N.J., Bielefeldt-Ohmann, H. and Stacey, M.C., *Mitogenic activity and cytokine levels in non-healing and healing chronic leg ulcers*. Wound Repair and Regeneration, 2000. **8**(1): p.13-25.
153. Lindsay, S., DelBono, M., Stevenson, R., Stephens, S. and Cullen, B. *Standardizing In Vitro Evaluations when Determining the Silver Release Profile of Antimicrobial Wound Dressings*. Available at: [http://www.systagenix.com/cms/uploads/final_Wounds_UK_2010_Silver_release_SL_\(2\)_002.pdf?phpMyAdmin=9cd5555e14577e170a20d1977060e8cb](http://www.systagenix.com/cms/uploads/final_Wounds_UK_2010_Silver_release_SL_(2)_002.pdf?phpMyAdmin=9cd5555e14577e170a20d1977060e8cb). 2014.
154. Campbell, K.E., Keast, D., Woodbury, G. and Houghton, P., *Wear time in two hydrocolloid dressings using a novel in-vivo model*. Wounds UK, 2003. **15**(2): p.1-11.
155. Lutz, J.B., Zehrer, C.L., Solfest, S.E. and Walters, S., *A new in vivo test method to compare wound dressing fluid handling characteristics and wear time*. Ostomy Wound Management, 2011. **57**(8): p.28-36.

- References -

156. Parsons, D., Bowler, P.G., Myles, V. and Jones, S., *Silver antimicrobial dressings in wound management: A comparison of antibacterial, physical, and chemical characteristics*. *Wounds*, 2005. **17**(8): p.222-232.
157. Merck. *Serum Biochemical Reference Ranges*. Available at: http://www.merckmanuals.com/vet/appendixes/reference_guides/serum_biochemical_reference_ranges.html. 2012.

APPENDICES

APPENDIX 1 – Fetal Bovine Serum Specification

SIGMA-ALDRICH®		sigma-aldrich.com
Second Avenue, Heatherhouse Industrial Estate, Irvine, Ayrshire KA12 8NB, Scotland		Tel: 00 44 (0) 1294 312222 Fax: 00 44 (0) 1294 313355
		CERTIFICATE OF ANALYSIS
Foetal Bovine Serum, Heat Inactivated		
Product No. F9665		
Lot No: 010M3395		
Expiry Date: Jan 2014		
Page 1 of 2		
	SPECIFICATION	OBSERVED RESULT
Source	Not of USA-Origin	Paraguay*
Appearance	Clear straw to amber liquid	PASS*
pH @ RT	6.7 - 8.0	7.21*
Osmolality	260 - 340 mOsm/Kg	303*
Sterility	Sterile	Sterile*
Endotoxin	≤10 EU/ml	0.65*
Haemoglobin	≤20 mg %	13.13*
Total protein	3.0 - 4.5 g %	3.62*
Mycoplasma	None detected	Negative*
Virus (BVD, IBR, PI3)	None Detected	Negative*
Cell culture testing	PASS	PASS*
Cell lines: MRC5, Sp2/0-Ag14, L929, HeLa		
Cloning assay	PASS	PASS*
Cell line: Sp2/0-Ag14		
* Supplier information		
Biochemical Profile: See attached.		
		
<hr/> ppJane Findlay PhD Quality Manager		
<hr/> 12 February 2010 Date		
SIGMA warrants that its products conform to the information contained in this and other Sigma publications. Purchaser must determine the suitability of the product for its particular use. See reverse side of invoice or packing slip for additional terms and conditions of sale.		
Accelerating Customers' Success through Leadership in Life Science, High Technology and Service		

CERTIFICATE OF ANALYSIS

Foetal Bovine Serum, Heat Inactivated
Product No: F9665
Lot No: 010M3395
Expiry Date: Jan 2014

Page 2 of 2

BIOCHEMICAL PROFILE	SPECIFICATION	OBSERVED RESULT
Sodium	Report result	138 mM/L*
Potassium	Report result	11.1 mM/L*
Chloride	Report result	100 mMol/L*
Uric Acid	Report result	2 mg%*
Calcium	Report result	13.9 mg%*
Phosphorous	Report result	10.3 mg%*
Alkaline Phosphatase	Report result	428 IU/L*
LDH	Report result	645 IU/L*
SGOT	Report result	46 IU/L*
SGPT	Report result	<6 IU/L*
Gamma GT	Report result	7 IU/L*
Cholesterol	Report result	32 mg%*
Bilirubin	Report result	0.2 mg%*
Glucose	Report result	71 mg%*
Urea	Report result	40 mg%*
Creatinine	Report result	3.5 mg%*
Total Triglycerides	Report result	55 mg%*
Albumin	Report result	1.73 g%*
Alpha Globulins	Report result	1.020 g%*
Beta Globulins	Report result	0.780 g%*
Gamma Globulins	Report result	0.080 g%*
Iron	Report result	160 µg%*

* Supplier information

Alison Donald

ppJane Findlay Ph.D, B.Sc.
Quality Manager

12 February 2010
Date